Investigation of the molecular mechanism of Paclitaxel-induced apoptosis in cultured-human cells

Thesis submitted for the degree of Doctor of Philosophy at the University of Leicester

by

Omeed Darweesh

Department of Molecular and Cell Biology

College of Medicine, Biological Sciences, and Psychology

University of Leicester

March 2019

Declaration

The accompanying thesis sybmitted for the degree of Doctor of Philosophy, entitiled '' Investigation of the mechanism of Paclitaxel-induced apoptosis in human cells'' is based on work conducted by author in the Department of Molecular and Cell Biology at the University of Leicester mainly during the period between July 2015 and March 2019. All the work recorded in this thesis is original unless otherwise acknowledged in the text or by references. None of the work has been submitted for another degree in this or any other university.

Signed:

Date:

Department of Molecular and Cell Biology

University of Leicester

Lancaster Road

LE1 9HN

Summary

Paclitaxel (Taxol) is a microtubule-targeting drug. It binds to the β-tubulin subunit of microtubules and interferes with microtubules disassembly in cell division. This prevents microtubule-kinetochore attachments and causes activation of the spindle assembly checkpoint (SAC). Prolonged activation of the SAC induces mitotic arrest by inhibiting the inactivation of Cdk1, and results in mitochondrial-mediated cell death. It is known that the key effector pro-apoptotic proteins, Bax and Bak, commit mitotically arrested cells to undergo apoptosis by inducing mitochondrial outer membrane permeabilization. However, the molecular signal that links SAC activation to the induction of apoptosis remains far from clear.

In this thesis, I show that both Bak and Bax are required for Taxol-induced apoptosis in HeLa cells as siRNA-mediated depletion of either Bak or Bax individually or in combination caused a significant decrease in Taxol-induced apoptosis. My data also demonstrate that Bak and Bax form a complex in the mitochondria with Mitochondrial Permeability Transition Pore components such as VDAC and ANT2 in the Taxol-arrested mitotic cells. Furthermore, I show here that inactive Cdk1 exists as two independent complexes with Bak and Bax in normal healthy interphase cells. In Taxol-arrested cells, a complex comprising activated Cdk1, cyclin B1, Bak and Bax is present in the mitochondrial membrane. In an *in vitro* assay, I demonstrate a direct interaction between recombinant Cdk1 and Bax. In functional assays, I show that the phosphorylation of the anti-apoptotic proteins Bcl-2 and Bcl-xL is dependent on the activated Cdk1/Bak and activated Cdk1/Bax complexes suggesting that Bak and Bax clearly mediate the transfer of activated Cdk1 to the MOM. My results lead me to predict that the Bax/Cdl1/cyclin B1 complex is the cytoplasmic signal that links SAC activation to the mitochondrial-mediated cell death.

Acknowledgments

Firstly, I would like to express my sincere gratitude to my supervisor Dr. Raj Patel for his great support, motivation and immense knowledge. His guidance helped me throughout my research and writing of this thesis. I would like to deeply thank you for giving me your time, patience and skills. I have really enjoyed the time that I have spent with you during my project. Many thanks to my co-supervisor Dr. Sally Prigent for her encouragement and advice through the time of my PhD. I would like to thank my committee members Professor lan Epron, Dr. Ildiko Gyori and Dr. Meike Vogler for all their guidance; helpful ideas, interesting discussions and feedbacks through the time of my project. My truly thankful to all the members of the Lab 2/38 and 2/42 for their help and advice during this project, in Particular Naif, Azim, Atiqah, Song, Anita, Tara, Laura, and Emily.

I'm very thankful to all my family members for the love, encouragement and support. To the most beautiful thing in this world, Dear Mum and Dad, I would like to say thank you for what you did for me without expecting anything but love from me, and there is no way of repaying you. I'm grateful for you every day and thankful for your love ''my champions''. To my incredible wife, thank you for your unconditional help and support during my study. You have always believed in me and my abilities. Thank you for the love that you keep awarding me, thank you for being part of my journey. The last words of thanks go to my lovely daughters Daniah, Dilveen and Arevan and my baby son Adam, the flowers of my heart and garden. I love you all and thank you for your patience during my study. Finally, I would like to say to my amazing wife and lovely kids sorry for almost all the weekends that I have been in the Lab '' Dad's house'' looking for exciting results and novelty rather than looking after you. You deserve more than just a thank you! You deserve a special place in my heart. This thesis is dedicated to my lovely family.

Table of Contents

List of figures

List of tables

Abbreviations

ADP	Adenosine diphosphate
ANT	Adenine nucleotide translocase
Apaf-1	Apoptosis protease activating factor-1
APC/C	Anaphase- promoting complex/cyclosome
APS	Ammonium persulphate
As_2O_3	Arsenic trioxide
ATP	Adenosine triphosphate
Asp	Aspartic Acid
Bad	BCL-2 antagonist of cell death
Bak	Bcl-2-associated killer
Bax	Bcl-2-associated X protein
Bcl-2	B cell lymphoma 2
Bcl-w	Bcl-2-like protein 2
Bcl-xL	B-cell lymphoma extra-large protein
Bid	BH3-interacting domain death agonist
Bim	BCL-2-interacting mediator of cell death
BOK	BCL-2 - related ovarian killer protein
BSA	Bovine serum albumin
Ca	Calcium
Cdc20	Cell division cycle protein 20

Cdks	Cyclin dependent kinases
Cdk1	Cyclin dependent kinase1
c-FLIP	Cellular FLICE-like inhibitory protein
CHAPS	3-[(3-cholamidopropyl) dimethylammonio]-1-propanesulfonate
CKII	Casein Kinase II
C-Mad2	Closed Mad2
CO2	Carbon dioxide
C-terminal	Carboxyl terminal
CypD	Cyclophilin D
DISC	Death-inducing signalling complex
DKO	Double knock-out
DMEM	Dulbecco’s modified Eagle’s medium
DNA	Deoxyribonucleic acid
DPBS	Dulbecco's Phosphate Buffered Saline
DSP	Dithiobis (succinimidyl propionate)
EDTA	Ethylenediaminetetraacetic acid
EGFP	Enhanced Green Fluorescent Protein
EGTA	Ethylene glycol tetraacetic acid
FACS	Fluorescence-activated cell sorting
FBS	Foetal bovine serum

FDA	Food and Drug Administration
g	Gram
G1	Gap 1
G2	Gap 2
GDP	Guanosine diphosphate
GFP-Bax	Green fluorescent protein-Bax
GST	glutathione-s-transferase
GTP	guanosine triphosphate
HCl	Hydrochloric acid
HeLa	Henrietta Lacks
His	Histidine
IP	Immunoprecipitation
JNK	C-Jun N-terminal kinase
kDa	kilo Daltons
M-phase	Mitotic-phase
Mad2	Mitotic arrest deficient protein 2
MCC	Mitotic checkpoint complex
MCF-7	Michigan Cancer Foundation-7
Mcl-1	Myeloid cell leukaemia sequence 1
MDA MB 231	M.D. Anderson (Texas) Metastasis Breast cancer
MEFs	Mouse embryonic fibroblasts

MIM	Mitochondrial inner membrane
ml	Millilitres
mM	Millimolar
MOM	Mitochondrial outer membrane
MOMP	Mitochondrial outer membrane permeabilization
MPS 1	Monopolar spindle kinase 1
MPT	Mitochondrial permeability transition
MPTP	Mitochondrial Permeability Transition Pore
mRNA	Messenger RNA
MS	Mass spectrometry
MTAs	Microtubule-targeting agents
N- terminal	NH2 terminal
nM	Nanomolar
NP40	Nonyl phenoxypolyethoxylethanol 40
ns	Not significant
O-Mad2	Open Mad2
PAK-Alpha	Serine/threonine-protein kinase PAK 1
PARP	Poly (ADP-ribose) polymerase
PBS	Phosphate Buffered Saline
PI	Propidium iodide
PiC	Phosphate carrier protein

PLK	Polo-like kinase
PMSF	Phenylmethylsulphonly fluoride
PP1	Protein phosphatases 1
PP2A	Protein phosphatase 2A
Puma	P53 upregulated modulator of apoptosis
RIPA	Radio-immunoprecipitation assay buffer
RNA	Ribonucleic acid
RNAse	Ribonuclease A
RPE1	Retinal pigment epithelial 1 cell line
rpm	Revolution per minute
RT	Room temperature
S-phase	Synthesis-phase
S	Serine
SAC	Spindle assembly checkpoint
SD	Standard deviation
SDS	Sodium dodecyl sulphate
SDS-PAGE	Sodium dodecyl sulphate polyacrylamide gel electrophoresis
shRNA	Small hairpin ribonucleic acid
siRNA	Small interfering ribonucleic acid
STS	Staurosporine

T	Threonine
Temed	Tetramethylethylenediamine
tBid	Truncated Bid
TM	Transmembrane domain
TNF	Tumour necrosis factor
TST	Tris-saline tween 20
U2OS	Human Bone Osteosarcoma Epithelial cell line
USA	United States of America
V	Voltage
v/v	Volume in volume ratio
VDAC	Voltage-dependent anion channel
WT	Wild type
w/v	Weight in volume ratio
α	Alpha
β	Beta
µ	Micron
µg	Microgram
µl	Microliter
µm	Micrometre
µM	Micromolar

Chapter 1. Introduction

1.1 Antimitotic drugs

Antimitotic drugs induce mitotic arrest and inhibit chronic cellular proliferation, which is one of the hallmarks of cancer cells (Hanahan, 2000, Pasquier and Kavallaris, 2008). There are two main classes of antimitotic drugs, Taxanes and Vinca alkaloids (see Table 1-1). Taxanes have been successfully used for the management of different types of solid cancers for over 25 years (Tischer and Gergely, 2018). Taxanes, such as Paclitaxel and Docetaxel, interact with the β-tubulin subunit to stabilize the microtubules (Abal et al., 2003). Vinca alkaloids, such as Vincristine, Vinblastine and Vinflunine, are mostly used for haematological malignancies, such as lymphomas and leukemias (Moudi et al., 2013). Vinca alkaloids interact with the β-tubulin subunit of the α/β-tubulin heterodimer and inhibit polymerization of microtubules (Zhou and Giannakakou, 2005). Both microtubule stabilising and depolymerising agents interfere with microtubule dynamics and cause long term mitotic arrest. The cells arrest in mitosis because of spindle assembly checkpoint activation and then undergo cell death, which ultimately inhibits tumour cell proliferation (Jordan and Wilson, 2004).

Microtubules are the active component of the cytoskeleton that play an essential role in various cellular functions including cell division, motility, maintaining cell shape and intracellular trafficking (Desai and Mitchison, 1997). Microtubules are cylindrical tubes composed of α and β-tubulin heterodimers. Microtubules are highly dynamic structures that alternate between periods of assembly and disassembly within the cell. This dynamic behaviour is crucial for accurate segregation of the replicated chromosomes into two daughter cells during mitosis (Mitchison et al., 1986, Jordan and Wilson, 2004). Polymerization of microtubules occurs when the nucleotide exchangeable site (E-site) of β-tubulin

and nucleotide non-exchangeable site (N-site) of α-tubulin bind to the GTP molecule (Nogales et al., 1998). The binding of α-tubulin to GTP is irreversible, whereas GTP reversibly binds to β-tubulin and is hydrolyzed to GDP during or shortly after polymerization (Nogales et al., 1998, Honore et al., 2005). The binding affinity of tubulin for adjacent molecules is reduced by GTP hydrolysis. As a result, microtubule depolymerisation is favoured, with the release of α and β-tubulin heterodimers into the cytoplasm (McGrogan et al., 2008). Therefore, the hydrolysis of GTP results in the dynamic behaviour of microtubules, in which microtubules undergo cycles of growth and shrinkage (Panda et al., 2002). Microtubule-binding drugs are known to affect microtubule dynamics and impeded their function. Attenuation of microtubule dynamics arrests cell division in mitosis and ultimately induces apoptotic cell death (Singh et al., 2008). Thus, microtubules are pharmaceutically validated targets for cancer therapy due to their importance in mitosis as shown by the variety of available antimitotic drugs (Table 1-1).

Microtubule stabilizing agents: Taxanes and Epothilones		Microtubule destabilizing agents: vinca alkaloids and Eribulin	
Paclitaxel	Breast, ovarian, lung cancer and Kaposi's sarcoma	**Vinblastine**	Breast and testicular cancer, lymphomas, Kaposi's sarcoma
Docetaxel	Head and neck, breast, lung, prostate, and stomach cancer	**Vincristine**	Neuroblastoma, lymphomas, soft tissue sarcoma and leukemia
Nab-Paclitaxel /Abraxane	Breast, pancreatic and lung cancer	**Vincristine Liposome**	Acute lymphoblastic leukemia (ALL)
Cabazitaxel	Prostate cancer	**Vindesine**	Lung, breast, colorectal cancer, lymphomas and ALL
Ixabepilone	Breast cancer	**Vinorelbine**	Breast, lung and ovarian cancer
Estramustine	Prostate cancer	**Vinflunine**	Bladder cancer
		Eribulin	Breast cancer and soft tissue sarcoma

Table 1-1: Antimitotic drugs can be divided into two main classes Taxanes and Vinca alkaloids.

Antimitotic drugs exert dose-dependent effects on microtubule dynamics. At high concentration, Taxanes block depolymerization of the microtubules, Vinca alkaloids inhibit polymerization of the microtubules, and both suppressing microtubule dynamics at low concentrations (Tischer and Gergely, 2018).

1.1.1 Paclitaxel (Taxol)

Taxol was originally isolated from the bark of *Taxus brevifolia* yew tree by Mansukh Wani and Monroe Wall in the United States (Wani et al., 1971). Taxol was renamed paclitaxel once it was commercially developed by the drug company Bristol-Myers Squibb USA (Zhang et al., 2014). Taxol is a microtubule-stabilizing drug that has potent chemotherapeutic effects against several cancer

types, including ovarian cancer (McGuire et al., 1989, Jeong et al., 2013), breast cancer (Holmes et al., 1991, McGrogan et al., 2008), non-small cell lung cancer (Sandler et al., 2006) and other malignancies (Wang et al., 2016, Jeong et al., 2013). Indeed, it has been approved by the Food and Drug Administration (FDA) for the treatment of ovarian, breast, non–small cell lung cancer and Kaposi's sarcoma (Weaver, 2014). It is also used clinically as a drug in coated balloons for the treatment of coronary artery disease (Cannon et al., 2018). Taxol binds to the β-tubulin subunit via hydrogen bonds and hydrophobic interaction (Snyder et al., 2001). Furthermore, structural studies of the microtubule revealed that the N-terminus of the polymerized β-tubulin, His 227 and Asp 224, is the critical site for the binding of Taxol (Nogales et al., 1999). Elie-Caille and colleagues reported that Taxol acts by binding to GDP-bound β-tubulin and that results in the formation of more stable GTP-bound β-tubulin (Elie-Caille et al., 2007). During mitosis more tubulin heterodimers incorporate into the spindle microtubules and binding of Taxol to the polymerized β-tubulin inhibits depolymerization of microtubules and blocks cell division (Abal et al., 2003, Jordan and Wilson, 2004).

It is well known that Taxol induces mitotic arrest in both cultured-cells and animal tumour models (Schiff and Horwitz, 1980, Weaver, 2014). Taxol induces mitotic arrest by inhibiting microtubule dynamics, which then triggers activation of the spindle assembly checkpoint (SAC) (Manchado et al., 2012). SAC activation prevents chromosome segregation until all sister chromatids achieve bipolar attachment to microtubules. Sister chromatids attach to spindle microtubules via their kinetochores (Chao et al., 2012). The SAC is activated by unattached kinetochores that inhibit cell cycle progression by preventing the anaphase-promoting complex/cyclosome (Foley and Kapoor, 2013). Sustained SAC activation keeps the cells arrested in mitosis which then either undergo apoptotic cell death, exit from mitosis to produce tetraploid G1 cells and subsequent survival (an abnormal exit from mitosis is called mitotic slippage) or mitotic slippage and death in the subsequent interphase (Brito and Rieder, 2006, Kienitz

et al., 2005). The determinants that control the fate of mitotically arrested cells remain unclear (Weaver, 2014).

1.1.2 How Taxol induces apoptosis

The mechanism of Taxol-induced cell death has been the subject of intense study for almost five decades (Zhang et al., 2014). Several studies, however, have shown that Taxol causes changes in the expression of Bcl-2 family members. Cancer cell lines treating with 10 nM Taxol led to the up-regulation of Bak and down-regulation of the anti-apoptotic protein Bcl-xL (Liu and Stein, 1997). Taxol treatment is also reported to up-regulate the expression of Bax and some BH3-only proteins such as Bad and Puma (Tudor et al., 2000, Yamaguchi et al., 2004). The sensitization of cancer cells to Taxol is clearly increased by over-expression of Bax or Bad (Hidehikosawa et al., 2000). Li and colleagues revealed that cancer cell lines with higher expression of the BH-3-only protein Bim are more sensitive to apoptosis when treated with Taxol (Li et al., 2005). Taxol-induced cell death is increased by forced expression of Bim in cells that have low levels of Bim.

The p53 tumour suppressor has a central role in the regulation of DNA damage responses (Kruiswijk et al., 2015). Orth and colleagues demonstrated that p53 is upregulated in Taxol or Nocodazole-arrested mitotic cells (Orth et al., 2012). Consequently, the expression of BH3-only proteins Puma and Noxa is increased in response to an apoptotic stimulus that activate P53. In addition to Puma and Noxa, Bax is also transcriptionally upregulated by P53. Therefore, P53 activity can impact on cell fate in the presence of microtubule-interfering agents (Batchelor et al., 2011, Orth et al., 2012, Michalak et al., 2005).

Other mechanisms of Taxol-induced apoptosis exist, such as inactivation of the anti-apoptotic proteins (Haschka et al., 2018). Anti-apoptotic Bcl-2 proteins are defined substrates of Cdk1 kinase and become heavily modified after treatment with microtubule poisons (Chu et al., 2012). Cdk1-mediated phosphorylation of

anti-apoptotic proteins reduces the apoptotic threshold, in which their anti-apoptotic function is inhibited or promoted for degradation by the proteasome (Sakurikar et al., 2012, Harley et al., 2010). Phosphorylation and proteasomal degradation of anti-apoptotic proteins shift the balance, favouring Bak and Bax activation. Several studies have concluded that phosphorylation of Bcl-2 antagonises its anti-apoptotic function (Scatena et al., 1998, Yamamoto et al., 1999, Eichhorn et al., 2013). In support of the current model that phosphorylation of Bcl-2 can trigger apoptosis, overexpression of Bcl-2 clearly reduced mitotic cell death in Taxol-treated MCF-7 cells (Kutuk and Letai, 2010). However, others reported that phosphorylation of Bcl-2 is a consequence of sustained mitotic arrest rather than apoptosis, and enhances its anti-apoptotic function (Roth et al., 1998, Zhou et al., 2014). The exact role of Bcl-2 phosphorylation in the regulation of Taxol-induced apoptosis remains controversial (Wang et al., 2000).

Terrano and colleagues proposed that sustained phosphorylation of Bcl-2 and Bcl-xL connects the signalling pathways between Taxol-induced microtubule perturbation and mitochondrial outer membrane permeabilization (MOMP) (Terrano et al., 2010). Specific phosphorylation of Bcl-xL at S62 in Taxol-arrested cells reduces its interplay with Bax, resulting in high levels of free Bax and the induction of apoptosis (Bah et al., 2014). Another recent study demonstrated that inhibition of the most prominent anti-apoptotic protein, Bcl-xL, effectively restores apoptosis when exposed to low-dose of Taxol in Myc-deficient cells. Myc plays a critical role in determining the fate of mitotically arrested cells as it increases the expression of certain BH3-only proteins such as Bim, Bid, and Noxa (Topham et al., 2015).

Of note, Bcl-w also contributes to the threshold of anti-apoptotic activity during Taxol-induced apoptosis. siRNA depletion of Bcl-w in HeLa cells increased mitotic cell death induced by Taxol, indicating a prosurvival role of Bcl-w (Huang et al., 2016). Without doubt, Mcl-1 seems to be particularly important in determining the apoptotic threshold of mitotically-arrested cells. By reducing Mcl-1 levels

using RNAi, the cells become highly sensitive to Taxol and mitotic cell death is significantly increased (Sloss et al., 2016).

The phases of the cell-cycle are closely monitored by cell cycle checkpoints to ensure that DNA replication and segregation are completed with high accuracy (Elledge, 1996). Interphase is controlled by three checkpoints during the cell cycle, whereas the transition from metaphase to anaphase is tightly controlled by the SAC (Barnum and O'Connell, 2014). In the presence of the microtubule poisons, microtubule dynamic behaviour is perturbed, inducing activation of the SAC (Matson and Stukenberg, 2011).

1.2 Spindle assembly checkpoint

Accurate genome transmission is a unique challenge facing eukaryotic cells during cell division. In the mitotic phase, the duplicated chromosomes should be segregated equally so that each daughter cell receives one copy of each chromosome. The daughter cells will deviate from the normal karyotype if errors occur at this point of the cell cycle. Consequently, inaccurate chromosome segregation could result in various diseases (Kops et al., 2005). This challenge is solved by sister chromatid cohesion, which consists of a multimeric protein structure that encloses the replicated sister chromatids (Nasmyth and Haering, 2009). The identity of sister chromatids is maintained by cohesion that holds the original and new chromatid together after DNA replication in S phase. Cohesion is maintained throughout the remainder of the S phase, G2 and into the early M phase (Lara-Gonzalez et al., 2012). During mitosis, the chromosomes align on the mitotic spindles at the equator of the cell. The mitotic spindles originate from two microtubule-organizing centres (centrosomes) that are positioned at opposing sides of the cell (Musacchio, 2015). The sister chromatids are separated when the cohesion ring is opened at the start of the anaphase (Watanabe, 2005). Spindle

microtubules pull them to the opposite poles of the cell (Nezi and Musacchio, 2009).

Sister chromatid cohesion is preserved until all chromosomes are aligned successfully on the mitotic spindle to ensure accurate chromosome segregation. The spindle assembly checkpoint (SAC), also known as mitotic checkpoint, monitors correct kinetochore-microtubule attachments (Musacchio and Salmon, 2007) (see Figure 1-1). The SAC acts as a surveillance mechanism that inhibits the onset of anaphase until all chromosomes are properly attached to the mitotic spindle and under tension (Kops, 2007, Musacchio, 2015). Unattached kinetochores enhance mitotic checkpoint complex (MCC) assembly, which keeps the cells arrested in mitosis, thereby inhibiting an ubiquitin ligase complex called anaphase-promoting complex or cyclosome (APC/C) (Rieder et al., 1995).

APC/C requires activation by a cofactor called Cdc20 (Nilsson et al., 2008). Mad2 and Mad3 associate with Cdc20 to inhibit APC/C activation (Fang, 2002). Mitotic checkpoint complex comprises Mad2, Bub3, BubR1 and Cdc20 as identified by purification of the MCC from HeLa cells (Sudakin et al., 2001). Pre-assembly of the Cdc20–Mad2 complex is required for Mad3–Cdc20 interactions and both complexes cooperate to antagonize APC/C activation (Burton and Solomon, 2007, Nilsson et al., 2008). The APC/C is responsible for proteolytic degradation of two key substrates securin and cyclin B1, which are the downstream targets of the SAC (Pines, 2011). Following bipolar attachment of all sister chromatids to microtubules, the SAC is turned off and the cell progresses from metaphase to anaphase (Maldonado and Kapoor, 2011).

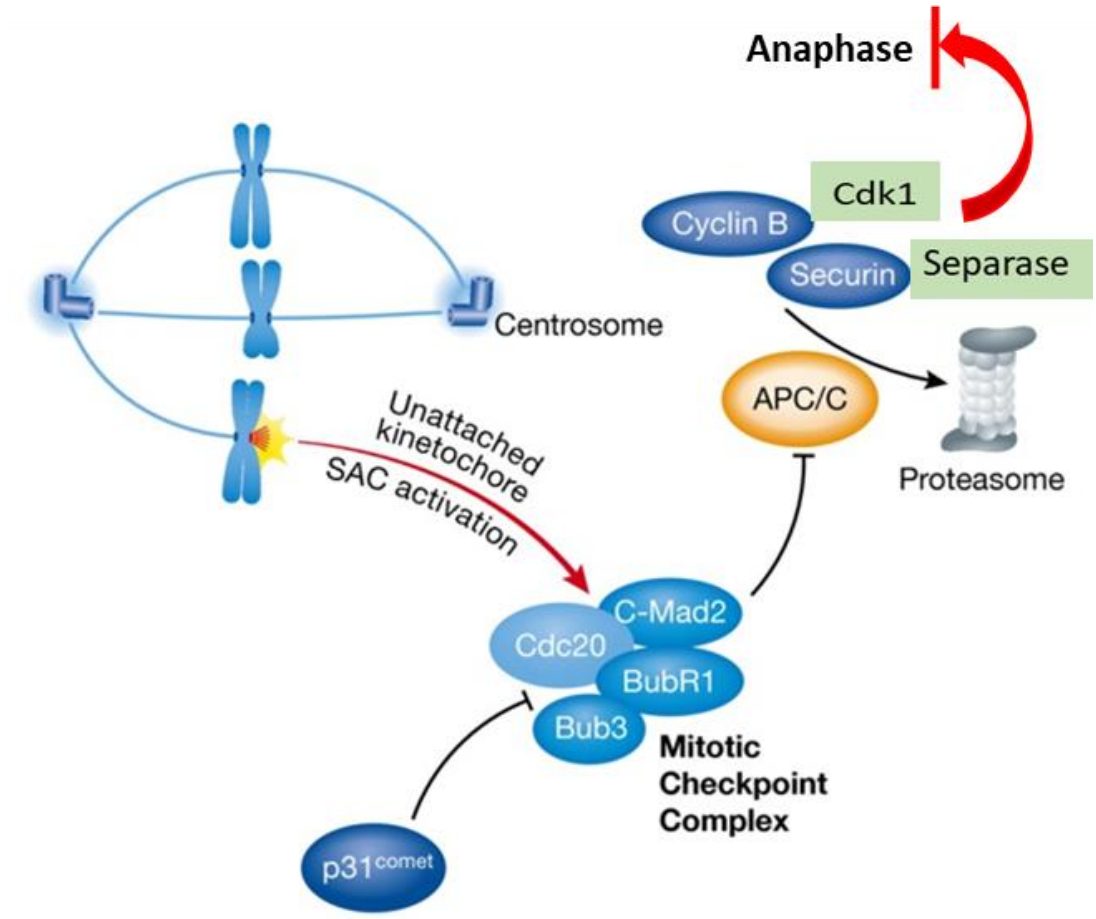

Figure 1-1: The mechanism of the SAC

Unattached kinetochores trigger the activation of the mitotic checkpoint complex (MCC). MCC consists of closed-Mad2 (active), Bub3, BubR1, and Cdc20; it blocks APC/C (E3 ubiquitin ligase complex) activity leading to inhibition of prometaphase to anaphase transition and the cells arrest in mitosis. When all sister chromatids are stably attached to spindle microtubules, MCC is turned off. Consequently, Cdc20 will be released to activate the APC/C. The activated APC/C causes proteolytic degradation of two key regulators of the cell cycle, securin and cyclin B1. Proteolytic degradation of securin allows the release of separase which consequently cleaves the Scc1 kleisin subunit of cohesin. Segregation of sister chromatids begins once the cohesion ring is opened (anaphase). Degradation of cyclin B1 inactivates Cdk1 and induces mitotic exit (Haschka et al., 2018).

Reversible phosphorylation of checkpoint proteins is a vital regulatory mechanism of the mitotic checkpoint. During (pro) metaphase, protein kinase Aurora B plays a key role in the regulation of mitotic checkpoint signalling (Saurin et al., 2011). Aurora B is responsible for recruitment of mitotic checkpoint component monopolar spindle (MPS) 1 kinase to unattached kinetochores

(Santaguida et al., 2011). MPS1 activity recruits other key checkpoint components such as the Mad1, Mad2, BUB3, and BUBR1 to form the mitotic checkpoint (sub) complexes (Santaguida et al., 2011, Saurin et al., 2011, Musacchio, 2015).

A Mad2 template model has been proposed that explains how mitotic checkpoint components (MCC) are recruited by unattached kinetochores (De Antoni et al., 2005). There are two native conformations of Mad2, an open conformation (O-Mad2) which converted to a closed conformation (C-Mad2) when it binds to one of its two binding partners Mad1 or Cdc-20 (Luo and Yu, 2008). The closed conformation is formed by moving two β-sheets toward the face of the protein and Mad-1 is trapped within this new conformation (De Antoni et al., 2005, Luo et al., 2004). When the cells enter M phase, the Mad1-C-Mad2 complex is recruited to kinetochores. Kinetochore-bound Mad1-C-Mad2 recruits Mad2 in the open conformation (Mapelli et al., 2007, De Antoni et al., 2005). Intriguingly, the Mad1-C-Mad2 template can catalyse the conversion of O-Mad2 to C-Mad2. C-Mad2 interacts with Cdc20 facilitating the formation of a C-Mad2-Cdc20 complex. This complex can associate with BUB3/BUBR1 to form a functional MCC, APC/C inhibitor (Han et al., 2013, Faesen et al., 2017) (Figure 1-2).

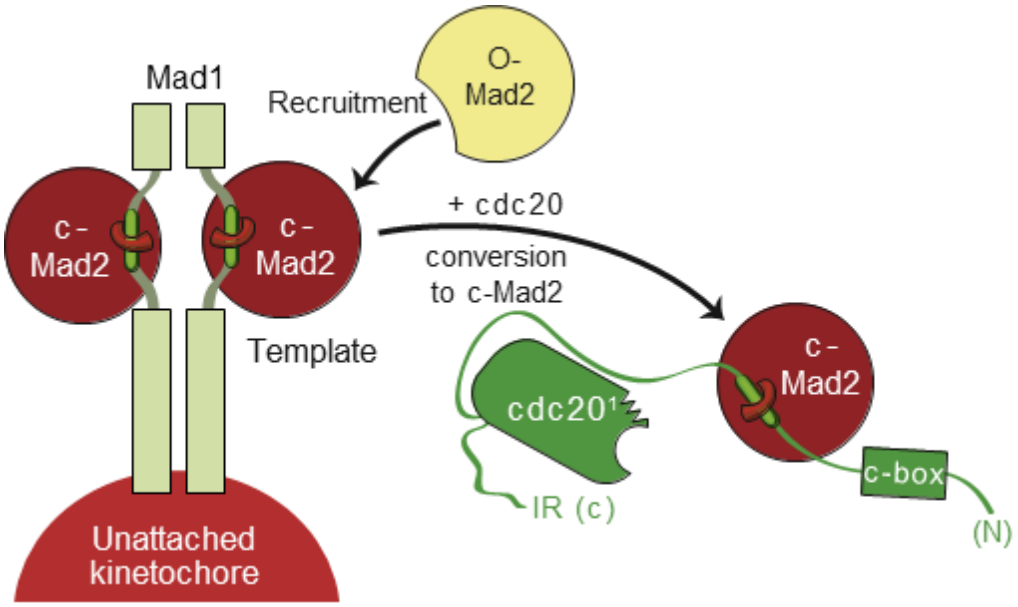

Figure 1-2: Schematic representation of the MAD2 template model.

At mitosis, kinetochore recruits Mad1: C-Mad2 complex. Mad1: C-Mad2 complex-bound kinetochore promotes the recruitment of O-Mad2. O-Mad2 binding to Mad1: C-Mad2 complex facilitates its conversion to a C-Mad2 (active). C-Mad2 interacts with Cdc20 facilitating the formation of a C-Mad2-Cdc20 complex. This complex associates with other components of the mitotic checkpoint to form a functional mitotic checkpoint complex (Faesen et al., 2017).

The formation of the C-Mad2-Cdc20 complex is the initial step in MCC assembly (De Antoni et al., 2005). A mitotic checkpoint signal downstream of kinetochores stimulates the C-Mad2-Cdc20 complex to recruit O-Mad2 forming additional C-Mad2-Cdc20 complexes in the cytosol (Musacchio and Salmon, 2007, Yu, 2006). Mad3/BubR1 contains a KEN box degron that acts as a pseudosubstrate for APC/C. Mad3 blocks the KEN-box-binding site of Cdc20 which then inhibits the APC/C from recognizing its substrates (Burton and Solomon, 2007).

Once all the chromosomes have successfully attached to microtubules, the mitotic checkpoint is turned off and the cell cycle can progress to anaphase (Musacchio, 2015). The kinetochore's shape and composition undergo dramatic changes when attached to spindle microtubules (Howell et al., 2001). Thus, the majority of centromeric Aurora B will be separated from its outer kinetochore substrates. Microtubule binding to the KMN (Knl1, Mis12 and Ndc80) dissociates

MPS1 kinase from the kinetochore. (Lesage et al., 2011). The KMN network is a part of the kinetochore that links centromeric DNA to the plus ends of spindle microtubules (Cheeseman and Desai, 2008). This in turn inhibits the critical phosphorylation events which are required for the recruitment of MCC components to the kinetochore. The Mad1-C-Mad2 complex is then removed from the kinetochores by a mechanism known as stripping (Hiruma et al., 2015, Ji et al., 2015).

Mitotic checkpoint shutdown can be achieved by several mechanisms. $P31^{comet}$ (a negative regulator of the SAC) appears to play a major role in the disassembly of the MCC (Teichner et al., 2011). $P31^{comet}$ can bind to the dimerisation motif of C-Mad2 and blocks the formation of Mad2 homodimers (Mapelli et al., 2006, Chao et al., 2012). From the structure of the C-Mad2–$P31^{comet}$ complex, it can be seen that $P31^{comet}$ inhibits conformational activation of O-Mad2 by binding to the dimerisation motif of C-Mad2 (Yang et al., 2007), and the Mad1–C-Mad2 core is stripped away from the kinetochores (Lara-Gonzalez et al., 2012). In addition, protein phosphatases PP1 (Pinsky et al., 2009, Vanoosthuyse and Hardwick, 2009, Lesage et al., 2011) and PP2A (Espert et al., 2014) oppose Aurora B to efficiently terminate mitotic checkpoint activity.

Anti-mitotic drugs such as Taxol and Nocodazole interfere with microtubule dynamics and prevent the spindle microtubules from attaching to kinetochores in the correct configuration. This induces sustained activation of the mitotic checkpoint and keeps the cells arrested in mitosis (Yang et al., 2009). The cells either escape from mitotic arrest into a polyploid interphase, by a process termed mitotic slippage or mitotic checkpoint adaption, or undergo apoptosis (Brito and Rieder, 2006). By a mechanism as yet unidentified, the apoptotic machinery is activated in mitotically-arrested cells and ultimately lead to activation of the caspase cascade and apoptosis (Haschka et al., 2018).

1.3 Apoptosis (Programmed cell death)

Programmed cell death was first defined by Lockshin and Williams in the context of insect development (Lockshin and Williams, 1965). In 1972, Kerr and co-workers observed two morphologically different types of cell death in humans, apoptosis and necrosis. Apoptosis is a form of regulated cell death and involves blebbing of the plasma membrane, overall cell shrinkage, chromatin condensation, DNA fragmentation and formation of the apoptotic bodies (Kerr et al., 1972). Apoptosis is initiated in response to developmental signals or cellular stresses and is followed by rapid engulfment of the apoptotic bodies by nearby phagocytic cells to inhibit the release of intracellular components (Hengartner, 2000, Hotchkiss et al., 2009). Apoptosis is also called clean cell death since it inhibits the release of the inflammatory factors, whereas in necrosis, the cells swell, plasma membranes rupture, and inflammatory cellular contents are released. Cell death that occurs during inflammation or infection was also found to be regulated by gene products and thus called necroptosis (Wallach et al., 2016).

Apoptosis suppression plays a crucial role in the growth of malignant cells (White and McCubrey, 2001). Anti-apoptotic signals promote cell survival through a variety of mechanisms, facilitating sustained tumour growth. The inhibitors of apoptosis (IAPs) are a family of proteins that can inhibit specific caspases and thereby protect cells from indiscriminate induction of death (Deveraux et al., 1997, Roy et al., 1997). IAPs can suppress apoptosis and enhance tumor growth and subsequent metastasis (LaCasse et al., 1998, Rathore et al., 2017). There are six isoforms of mammalian IAPs; inhibitor of apoptosis-1 (c-IAP1), inhibitor of apoptosis-2 (c-IAP2), neuronal apoptosis inhibitory protein (NAIP), survivin, X-linked inhibitor of apoptosis (XIAP), and BIR repeat-containing ubiquitin-conjugating enzyme (BRUCE) (Verhagen et al., 2001). Several studies reported that overexpression of exogenous IAPs in mammalian cells protects them from the induction of apoptosis (Listen et al., 1996, Ambrosini et al., 1997, Li et al.,

1998). A number of tumor suppressor genes, for example ATM, NBS1, BRCA1, BRCA2, Rb and p53, are also involved in cancer development. Mutation of one or more of these genes could compromise their function and leads to tumorigenesis (Dasika et al., 1999, Kaelin Jr, 1999, Drexler, 1998, Sionov and Haupt, 1999). Increased expression of anti-apoptotic Bcl-2 proteins is found in many cancer types, and it facilitates sustained tumour growth. The upregulation of anti-apoptotic Bcl-2 proteins can occur through different mechanisms, including chromosomal translocation, gene amplification and increased gene expression (Campbell and Tait, 2018).

Apoptosis plays a key role in embryonic development for successful organogenesis. In addition, it is also required to protect the healthy cells from damaged, infected, or mutated cells (Vaux and Korsmeyer, 1999, Meier and Finch, 2000). Studying the mechanism of apoptosis occupies an important field in biomedical research, since it is associated with many pathological conditions, including cancer, autoimmune, and neurodegenerative diseases (Wu et al., 2001, Green and Kroemer, 2004). There are two apoptotic pathways, the extrinsic pathway (death receptor) and the intrinsic (mitochondrial) pathway (Riedl and Salvesen, 2007) (see Figure 1-3).

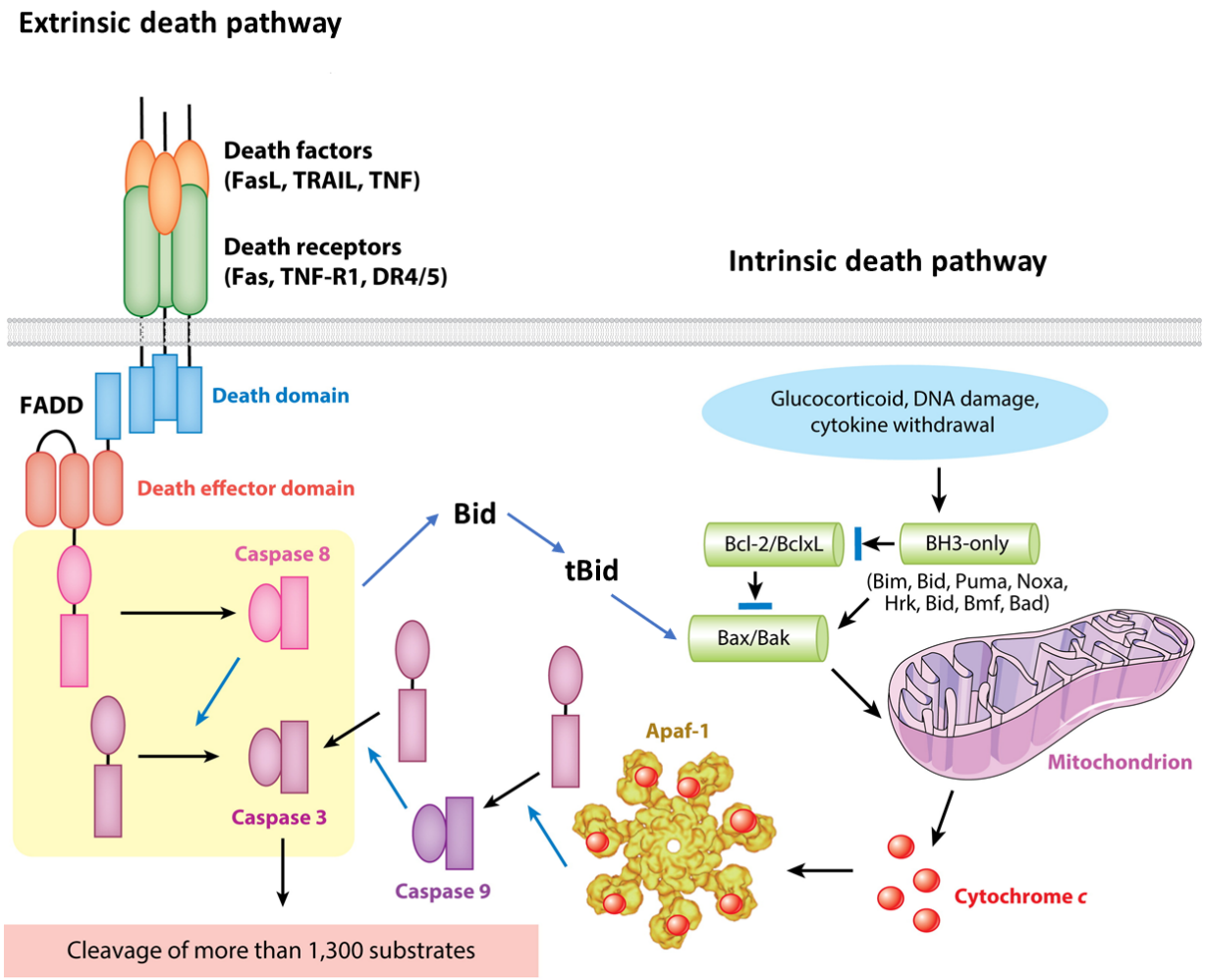

Figure 1-3: The extrinsic and the intrinsic pathways of apoptosis.

In the extrinsic pathway, plasma membrane receptors bind to death factors such as binding of the Fas to Fas ligand. Fas death domain recruits FADD (Fas-associated protein with death domain) and procaspase 8, and results in the formation of death inducing signalling complex (DISC) and activation of caspase 8. The cleavage form of the BH3 only protein Bid (tBid) connects the extrinsic to the intrinsic pathway of apoptosis. In the intrinsic pathway, the effector pro-apoptotic proteins Bak and Bax facilitate the release of cytochrome c from the intermembrane space of the mitochondria into the cytosol. Cytochrome c binds with the Apaf-1 and pro-caspase 9 which results in the formation of the apoptosome. This complex recruits monomeric procaspase 9 to form an active caspase-9. The activated caspase 8 and 9 then activate downstream caspases (caspase 3 and caspase7) inducing apoptosis (Nagata, 2018).

1.3.1 Extrinsic pathway of apoptosis

The extrinsic apoptotic pathway, also called the death receptor-mediated pathway, is initiated by binding of death receptors at the plasma membrane to death factors, such as the binding of Fas (also called APO-1 or CD95) to FasL (Li and Dewson, 2015). The cytoplasmic region of Fas, as well as those of TNF receptor 1 (TNF-R1), TRAIL-R1 (DR4), and TRAIL-R2 (DR5), contains the death domain. The death domain includes an approximately 80 amino acids, which is required for death signalling (O'Reilly et al., 2009, Krammer, 2000). The oligomerized Fas death domain recruits FADD (Fas-associated protein with death domain), procaspase 8 and a procaspase 8–like protein called Cellular FLICE-like inhibitory protein (c-FLIP) to form a complex (Nagata, 1997, Krammer, 2000, Walczak, 2013). This complex is called the DISC (death-inducing signalling complex) and it involves Fas, FADD, procaspase 8 and c-FLIP (Lavrik and Krammer, 2012).

Death factor–induced apoptotic signalling is divided into two pathways downstream of DISC. In pathway 1, DISC promotes the activation of caspase 8 which in turn activates caspase 3. In this pathway, for example in thymocytes, the release of cytochrome c is dispensable to mediate apoptosis (Nagata, 2018). In pathway 2, caspase 8 cleaves BH3-only protein Bid (BH3‑interacting domain death agonist). The truncated Bid (tBid) is capable of localizing to the MOM and activating the intrinsic pathway of apoptosis, for example in hepatocytes and fibroblasts (Strasser et al., 2009, Walczak, 2013). The active tBid links the death receptor-mediated apoptotic pathway to the intrinsic pathway of apoptosis (Kaufmann et al., 2007).

1.3.2 Intrinsic pathway of apoptosis

The intrinsic apoptotic pathway, also called the mitochondrial-dependent pathway, is triggered by different stimuli, including prolonged-mitotic arrest and DNA damage (Morales-Cano et al., 2013). The intrinsic pathway is regulated by Bcl-2 family members by controlling the permeability of the MOM. In response to cellular apoptotic stimuli, BH3-only pro-apoptotic members can be activated by transcriptional upregulation or proteolytic cleavage (Cartron et al., 2004, Letai et al., 2002). Anti-apoptotic members undergo posttranslational modification to antagonize their anti-apoptotic effects (Czabotar et al., 2014). Activator BH3-only proteins promote apoptosis by activating Bak and Bax in mitotically arrested cells (Kale et al., 2018). Ultimately Bak and Bax are activated, which facilitates their insertion into the MOM, and form oligomers to induce mitochondrial outer membrane permeabilization (Zamzami and Kroemer, 2001, Tait and Green, 2013). The key factor is cytochrome c. When it is released from the mitochondrial intermembrane space to the cytosol, it binds with apoptosis protease activating factor-1 (Apaf-1) to form a complex with procaspase-9 called the apoptosome (Wang et al., 2000). This complex recruit monomeric procaspase 9, which then undergoes autocatalytic cleavage to form an active caspase-9. Activated caspase 9 in turn processes and activates downstream caspases, caspase-3 and caspase-7. The executioner caspases 3 and 7 cleave multiple cellular proteins leading to DNA fragmentation, chromatin condensation and dismantling of the cell (Jost et al., 2009) (Figure 1-4 B).

Caspases are a family of cysteine-aspartic proteases that play an essential role in apoptosis. The 12 human caspases are synthesized as precursors. Specific cleavages at two positions generate an active enzyme by removing the pro-domain at the N terminus. An active enzyme contains two large and two small subunits (Crawford and Wells, 2011). These proteases have a motif consisting of histidine and cysteine residues at the active site (Crawford and Wells, 2011). At least five amino acid residues on the target proteins are identified by the active

site of proteases. Proteases cleave peptide bonds strictly after aspartate (Alnemri et al., 1996).

1.3.2.1 Bcl-2 family proteins

Intrinsic apoptosis pathway is tightly controlled by the members of the Bcl-2 (B cell lymphoma-2) family proteins (Czabotar et al., 2014, Moldoveanu et al., 2014). There are at least 15 members of this family in mammals (Adams and Cory, 1998). Each member of this family has a specific pro-apoptotic or anti-apoptotic role and the integrity of the MOM is regulated by the final result of the interaction between BCL-2 family proteins (Youle and Strasser, 2008). The Bcl-2 family can be divided into three functionally and structurally distinct classes. The first class is the pro-apoptotic pore-formers and it includes Bak (Bcl-2-associated killer), Bax (Bcl-2-associated X protein) and BOK (BCL-2 - related ovarian killer protein) (Gross et al., 1999). Bak and Bax play an essential role in apoptosis via their direct effects on the MOM permeability (Kvansakul et al., 2008).

The second class is the pro-apoptotic BH3-only proteins (sharing only the third Bcl-2 homology domain) such as Bim (BCL-2-interacting mediator of cell death; also known as BCL-2L11), Bid, Puma (p53 upregulated modulator of apoptosis; also known as BBC3), Noxa (also known as PMAIP1), and Bad (BCL‑2 antagonist of cell death) (Chen et al., 2005, Hinds et al., 2007). The BH3-only proteins can directly activate pro-apoptotic effector molecules or antagonize the anti-apoptotic Bcl-2 family proteins (Willis and Adams, 2005). The third class is the anti-apoptotic multidomain proteins such as Bcl-2 itself, Bcl-xL (B-cell lymphoma extra-large protein), Bcl-w (also known as BCL-2L2), A1 (also known as BFL1 in humans) and Mcl-1 (myeloid cell leukaemia sequence 1) (Kvansakul et al., 2008), containing all four BH domains Figure (1-4 A). Anti-apoptotic Bcl-2 members function as gatekeepers to inhibit apoptosis. Anti-apoptotic proteins can block the pro-apoptotic actions of Bax and Bak, or block the pro-apoptotic effects of BH3- only proteins (Yang et al., 2003, Adams and Cory, 2007).

Upregulation of anti-apoptotic Bcl-2 proteins can act as a barrier to apoptosis, even in the presence of high levels of BH3-only proteins (Campbell and Tait, 2018). Inhibitors of anti-apoptotic proteins can resensitize cells to BH3-only protein-upregulation and tip the balance in favour of apoptosis. The BH-3 mimetic drugs are small molecule inhibitors of anti-apoptotic proteins, occupying the hydrophobic groove on anti-apoptotic proteins (Vela and Marzo, 2015). ABT-737 was the first BH-3 mimetic drug, which was developed through NMR-based screening. ABT-737 mimics the BH-3 only protein Bad and interacts with Bcl-2, Bcl-xL and Bcl-w, displacing BH-3 only pro-apoptotic proteins to promote apoptosis (Oltersdorf et al., 2005). Clinical studies supported the use of Navitoclax (ABT-263) as a combination therapy in different solid tumours (Oakes et al., 2012, Chen et al., 2011). Navitoclax is a potent and orally bioavailable inhibitor of anti-apoptotic proteins Bcl-2, Bcl-xL and Bcl-w (Tse et al., 2008). Venetoclax (ABT-199) has been shown to have increased specificity for the anti-apoptotic protein Bcl-2 (Roberts et al., 2016) and has been used as a combination therapy in preclinical models of breast cancer (Vaillant et al., 2013). Encouraging effects of Venetoclax as a single agent have been seen in non-Hodgkin lymphomas, acute myeloid leukaemia and multiple myeloma a (Davids et al., 2017, Konopleva et al., 2016, Kumar et al., 2017).

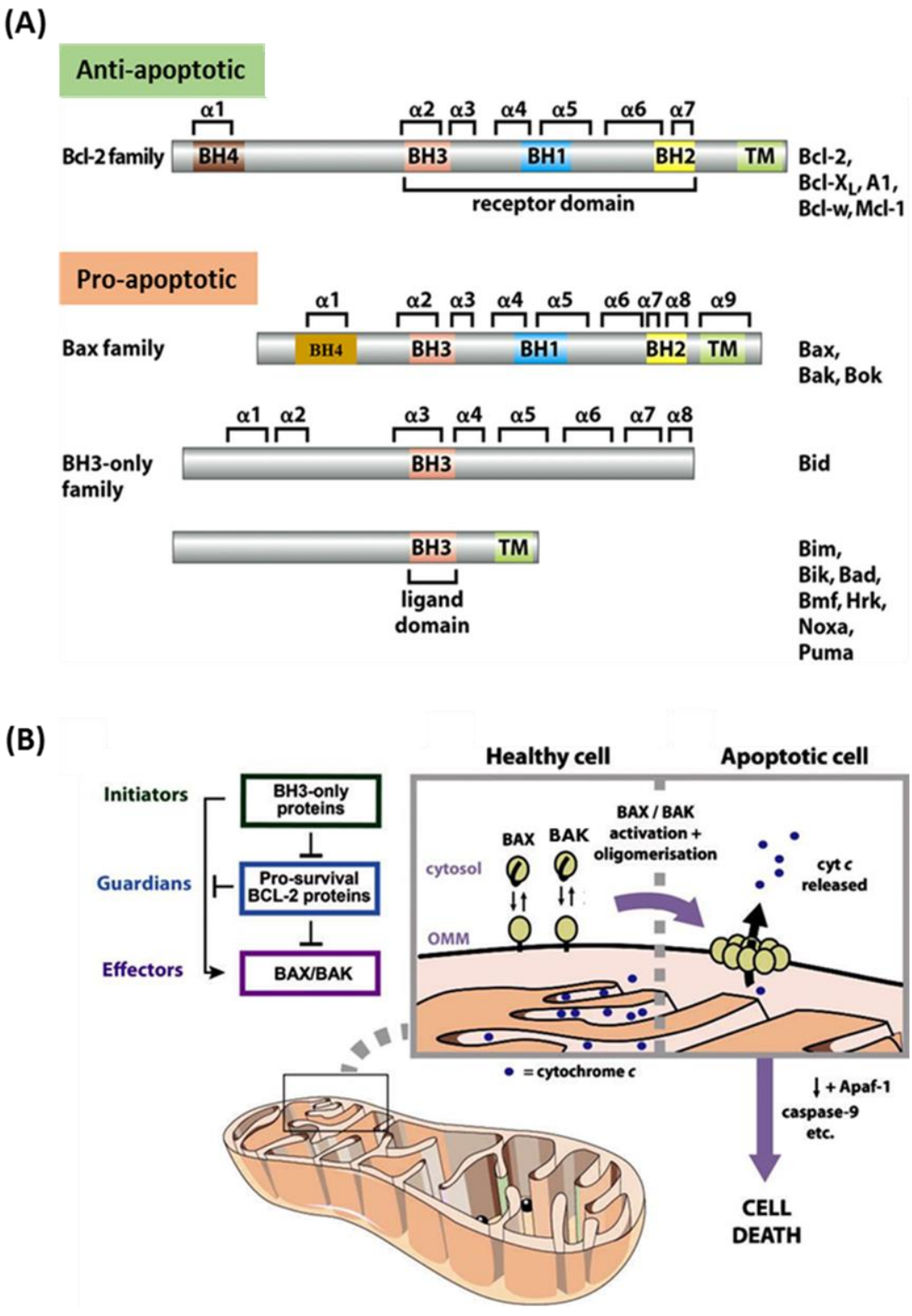

Figure 1-4: Schematic representation of Bcl-2 family proteins.

A) The Bcl-2 family is composed of prosurvival and two groups of pro-apoptotic proteins (pro-apoptotic effector and pro-apoptotic BH3 only proteins). This schematic representation illustrates the Bcl-2 homology domain (BH) and transmembrane-targeting domain (TMD). The TMD is present in pro-survival, effector and some BH3-only proteins such as BIM, BIK and HRK. The approximate position of the α-helices in the

BCL-2 core is marked at the top (Adams and Cory, 2018). The multidomain proteins (pro-apoptotic effector and anti-apoptotic members) share four Bcl-2 homology domains (BH1-4). The pro-apoptotic BH3-only proteins display only one BH3 domain. The BH3-only protein Bid (BH3-interacting domain death agonist) is the structural exception. Its fold resembles that of the multi-domain members (Chou et al., 1999, McDonnell et al., 1999). (B) Intrinsic apoptotic pathway is regulated by finely balanced interactions between Bcl-2 family members. In healthy cells, prosurvival Bcl-2 proteins function as guardians of mitochondrial integrity. In response to an apoptotic stimulus, BH3-only proteins can be up-regulated or activated. BH3-only proteins promote Bak and Bax activation. Activated Bak and Bax oligomerize in the MOM to form specific channels, leading to an irreversible step known as MOMP, which releases cytochrome c from the mitochondrial intermembrane space into the cytosol (Roy et al., 2014).

1.3.2.1.1 Bak and Bax oligomerization in Taxol-arrested cells

The key effector pro-apoptotic proteins Bak and Bax play a significant role in apoptosis (Wei et al., 2001). Under non-stressful conditions, Bax is a cytosolic inactive protein but associates with mitochondria upon cell death induction. However, Bak is predominantly located on the MOM (Wolter et al., 1997). Recent studies have indicated that both Bak and Bax are constantly shuttling between the cytosol and mitochondrial membrane. Shuttling of these proteins from the mitochondria to the cytosol is known as retrotranslocation and is possibly mediated by interaction with anti-apoptotic proteins (Edlich et al., 2011, Schellenberg et al., 2013, Todt et al., 2015). Because of the lower rate of retrotranslocation, Bak is mainly localized on the MOM (Todt et al., 2015).

In response to cytotoxic signals, Bax cannot be translocated from the mitochondria to the cytosol and ultimately it accumulates on the MOM (Todt et al., 2015, Edlich et al., 2011). Apoptotic stimuli cause both Bak and Bax change their conformation and insert into the MOM (Nechushtan et al., 2001, Zhou and Chang, 2008, Salvador-Gallego et al., 2016). The conformational changes include: exposure of the BH3 domain of both Bak and Bax (in the α2 helix), exposure of the N-terminus (in the α1 helix), and C-terminus (in the α9 helix) of Bax for membrane insertion (Wang et al., 1998, Roy et al., 2014). The BH3 domain of one

molecule interacts with the hydrophobic groove of another resulting in the formation of a symmetrical dimer. This dimer acts as a building block to form higher-order oligomers (Dewson et al., 2008, Dewson et al., 2012). These oligomers arrange into different structures such as arcs, lines or ring-like in the MOM and ultimately induce mitochondrial outer membrane permeabilization (MOMP) (Große et al., 2016, Salvador-Gallego et al., 2016).

The Bax oligomer is constructed of 6-8 molecules, while at least 18 molecules of Bak assemble to form an oligomer (Dewson et al., 2009, Er et al., 2006). Another study has reported that the size of the Bax oligomer comprises more than a hundred molecules (Zhou and Chang, 2008). Electron microscopy demonstrates that Bax movement to the MOM is the initial step in its activation, and the formation of Bak and Bax homo-oligomers in the MOM is the first pro-apoptotic structures (Nechushtan et al., 2001). The cells response to apoptotic stimuli is determined by the population of active Bak and active Bax that constitutively localize at the MOM (Schellenberg et al., 2013, Reichenbach et al., 2017).

1.3.2.1.2 Molecular biology of Bak and Bax

Bcl-2 family members including Bak/Bax are globular proteins composed of α-helices and characterized by the conserved Bcl-2 homology (BH1-4) domains. Both Bak and Bax are composed of 9α helices and display similar fold as other anti-apoptotic proteins Figure (1-5 A–B-C) (Suzuki et al., 2000, Wang et al., 2009). Several Bcl-2 family members contain a hydrophobic transmembrane (TM) domain at the C-terminus that allows them to localize to intracellular membranes. For example, the α9 helix of both Bak and Bax functions as a transmembrane domain allowing mitochondrial localization of both proteins (Popgeorgiev et al., 2018). In healthy cells, the TM domain of Bak is essential for its constitutive localization to the mitochondrial and endoplasmic reticulum membranes (Breckenridge et al., 2003). In Bax, this region is sequestered in its

hydrophobic groove clarifying why Bax is mainly cytosolic (Suzuki et al., 2000, Hsu et al., 1997).

The ratio of pro-apoptotic and anti-apoptotic Bcl-2 family members regulate the fine balance between cell survival and apoptosis (Roy et al., 2014). Activation of Bak and Bax can be fine-tuned by their binding to some BH3-only proteins (most notably Bim and Bid) (Letai et al., 2002, Kuwana et al., 2005). The BH3 domain of the BH3-only proteins can directly interact with the hydrophobic groove of Bak and Bax (Czabotar et al., 2013). The effector pro-apoptotic proteins share this critical site of interaction with anti-apoptotic proteins (Czabotar et al., 2013, Moldoveanu et al., 2013). BH3-only proteins sequester anti-apoptotic proteins by binding to their hydrophobic region (Czabotar et al., 2007). Interactions of key effector proteins with anti-apoptotic proteins also include the BH3 domain. Therefore, the BH3 domain / hydrophobic groove interaction is implicated when anti-apoptotic molecules inhibit apoptosis downstream by sequestering activated Bak and Bax and upstream by sequestering BH3-only proteins (Westphal et al., 2011).

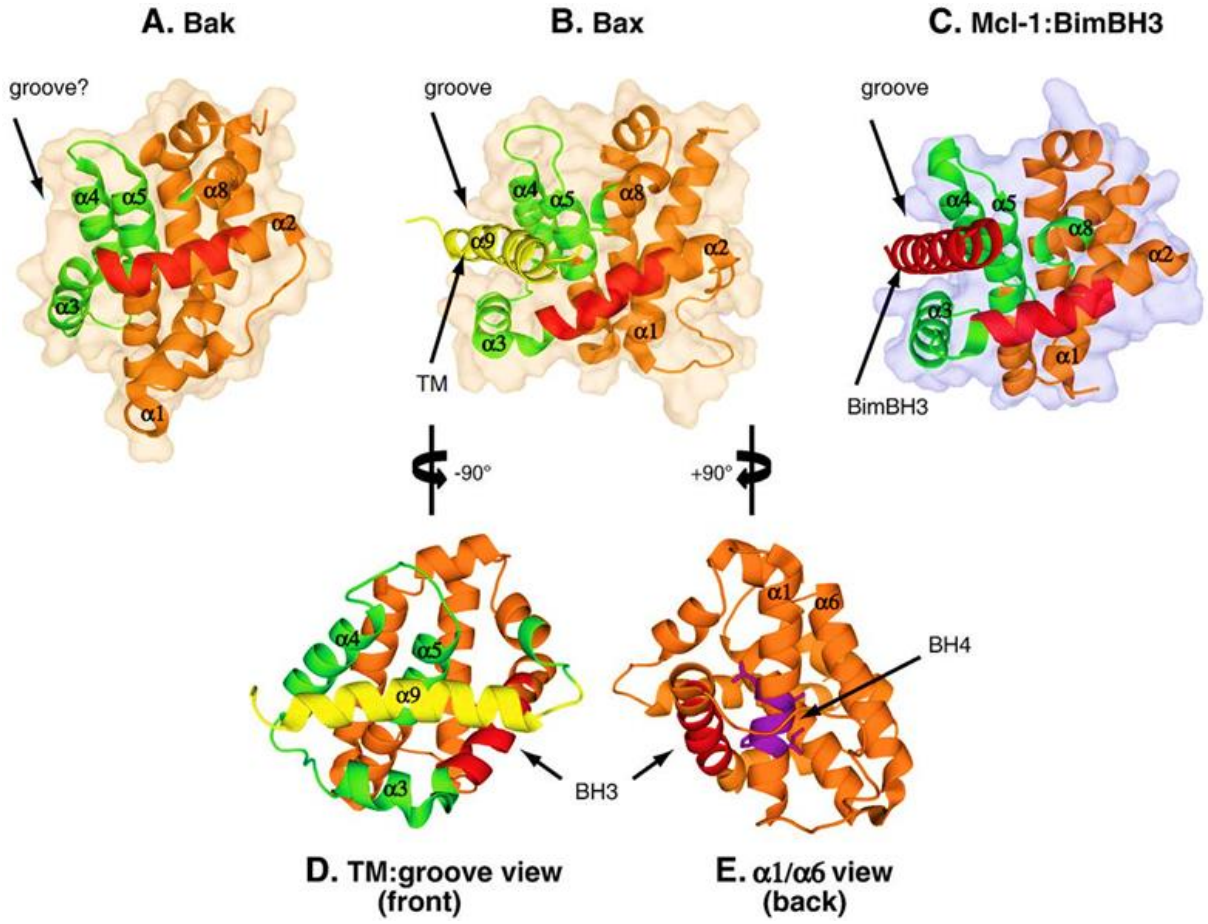

Figure 1-5: Structures of BCL-2 family members

Structures of Bak (A), Bax (B) and Mcl-1 (C). Both Bax family and anti-apoptotic proteins share four homology domains (BH1–BH4) as well as a similar overall fold. Mcl-1 is complexed with a Bim BH3 domain. Orange colour represents α-helices 1–8 except for those sections that include the hydrophobic groove (green colour) and BH3 domain (red colour). In Bax, the transmembra ne domain (TM) (in the α9 Helix) (yellow colour) at the C-terminus is sequestered along the hydrophobic groove, while Bim BH3 domain (red colour) is harboured by the Mcl-1 groove revealed that the BH3 domain of BH3-only protein Bim can bind to hydrophobic surface groove of Mcl-1. (D, E) Rotation of the Bax structure to view the interaction between transmembrane domain and hydrophobic groove as well as to display the α1/α6-helices on opposite sides of the molecule (Westphal et al., 2011).

1.3.2.1.3 Direct and indirect models of Bak/Bax activation

Bcl-2 family proteins set the apoptotic threshold and commit mitotically arrested cells to undergo mitotic death (Czabotar et al., 2014). In response to a cellular stress, an increase in BH3-only protein activity can trigger apoptosis (Kim et al., 2009). Two models have been proposed to clarify the mechanism of activation of Bak/Bax by BH3-only proteins (Westphal et al., 2011). In the direct model, some BH3‑only proteins can directly interact with Bak and Bax and trigger their activation (Letai et al., 2002, Cartron et al., 2004, Kuwana et al., 2005, Deng et al., 2007). Thus, these BH3-only proteins such as Bid, Bim and Puma are called activators (Kim et al., 2009, Letai et al., 2002). In this model, the other BH3-only proteins such as Bad and Noxa act as sensitizers, their binding to anti-apoptotic proteins frees up activator BH3-only proteins (Letai et al., 2002, Chipuk et al., 2010) (see Figure 1-6).

In the indirect model, BH3-only proteins indirectly activate Bak and Bax, the anti-apoptotic proteins that interacted with Bak or Bax are displaced by BH3-only proteins (Dewson and Kluck, 2009, Willis et al., 2007). The interaction of BH3-only proteins with anti-apoptotic proteins frees up the effector pro-apoptotic proteins Bak and Bax (Lauterwasser et al., 2019) (see Figure 1-6). Anti-apoptotic proteins such as Bcl-2 and Bcl-xL inhibit Bak/Bax homo-oligomerization and BH3-only proteins act to sequester anti-apoptotic proteins away from Bak/Bax (Andreu-Fernández et al., 2017). It is thought that characteristics of both direct and indirect models are important in the activation of the multidomain pro-apoptotic molecules and formation of their oligomers in the MOM (Leber et al., 2010).

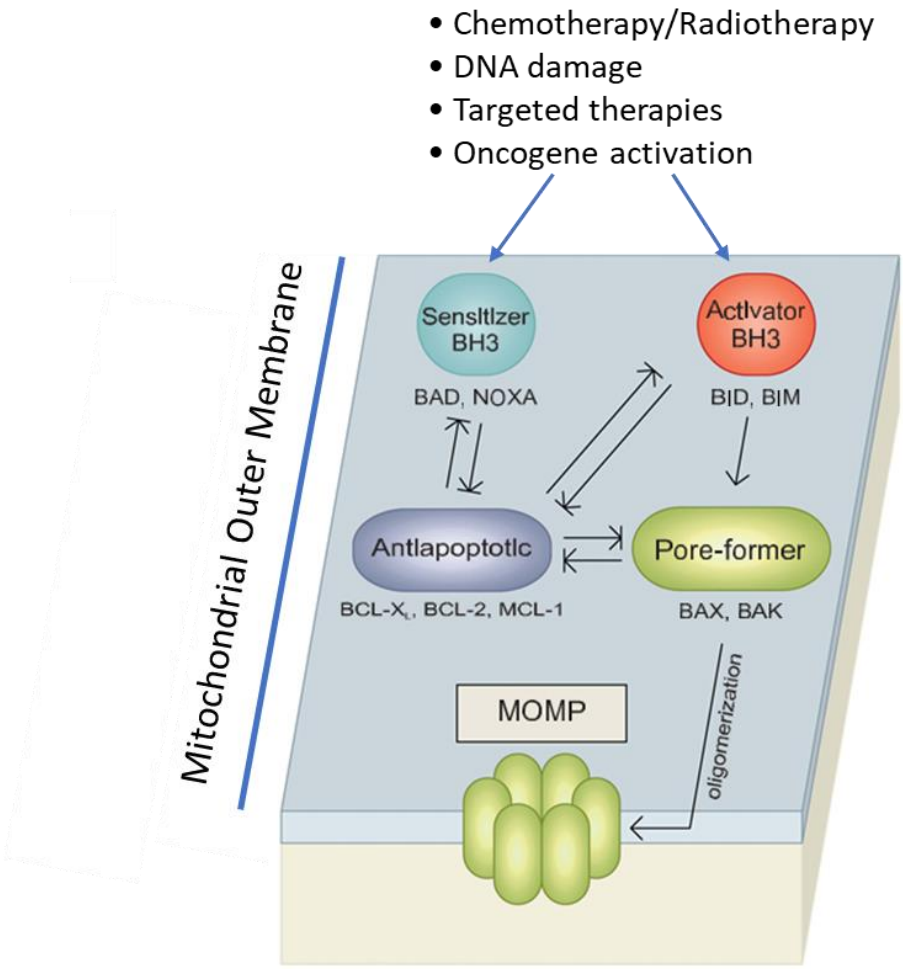

Figure 1-6: Direct and indirect models of Bax and Bak activation

In response to stress signalls, the pro-apoptotic BH3-only proteins can be upregulated by proleolytic cleavage or increased expression. In the direct model, BH3-only proteins directly bind to and activate Bax and Bak. In the indirect model, BH3-only proteins bind to and sequester the anti-apoptotic proteins to indirectly activate Bax and Bak. Once Bax and Bak are activated, they oligomerize to form specific channels or pores and induce MOMP which in turn allows the release of cytochrome c. Caspase cascade is activated by the release of cytochrome c and leads to cell death (Kale et al., 2018).

Pro-apoptotic effector proteins, Bak and Bax, are thought to accumulate at the mitochondrial outer membrane, oligomerize and form a complex with mitochondrial permeability–transition pore complex (PTPC) such as adenine nucleotide translocase 2 (ANT2) and voltage-dependent anion channel (VDAC) (Shimizu et al., 1999, Shimizu et al., 2000c, Galluzzi and Kroemer, 2007). The formation of this complex mediates mitochondrial outer membrane permeabilization (MOMP) (Zhou and Chang, 2008, Shimizu et al., 1999) (whether

this occurs due to the formation of Bak/Bax homo or hetero-oligomers or by interaction of Bak/Bax oligomers with mitochondrial PTPC components remains unclear). MOMP-mediated cytochrome c release is an irreversible step in the intrinsic pathway as the activation of the caspase cascade is difficult to interrupt (Roy et al., 2014).

In contrast to the previous model, another study reported that mouse embryonic fibroblast and isolated-mouse mitochondria deficient of all three VDAC isoforms exhibit identical cytochrome c release compared to the wild type. This result suggested that VDACs are dispensable for mitochondrial-mediated cell death (Baines et al., 2007). ANT-deficient mice are able to form mitochondrial PTPC (Kokoszka et al., 2004), inducing the argument about the roles of ANT in mitochondrial PTPC. Therefore, the impact of Bak/Bax-VDAC/ANT2 interaction and their role in mitochondrial-mediated apoptosis remains controversial.

1.4 Mitochondrial Permeability Transition Pore

Mitochondrial permeability transition (MPT) can be defined as an increased permeability of the mitochondrial inner membrane (MIM) in response to different stimuli such as oxidative stress, hypoxia, and cytotoxic drugs (Halestrap et al., 2004). MPT is initiated due to the formation of a large pore composed of a protein complex (Biasutto et al., 2016). The mitochondrial permeability transition pore (MPTP) is thought to form at contact sites between the inner and outer mitochondrial membranes (McCommis and Baines, 2012). MPTP is transiently opened under physiological condition to regulate Ca^{2+} homeostasis (Bernardi and von Stockum, 2012). Prolonged opening of the MPTP results in apoptotic cell death. MPTP opening causes permeabilization of both the mitochondrial inner and outer membranes and swelling of the mitochondria, which is followed by rupture of the mitochondrial outer membrane and release of apoptogenic factors into the cytosol (Bernardi et al., 2015). ANT2 and VDAC are the most abundant

protein in the inner and outer mitochondrial membranes respectively (Crompton et al., 1998, Zamzami and Kroemer, 2001). It is fairly well established that ANT2 and VDAC, in association with a matrix protein cyclophilin D, are candidates for MPTP components (Figure 1-7).

Recent genetic studies have identified new candidates of the MPTP. Based on this model, the MPTP is comprised of a variety of regulatory proteins in the mitochondrial inner membrane including ANT, PiC (phosphate carrier protein), F1F0 ATP synthase and Cyclophilin D as its regulator in the matrix of the mitochondria (Biasutto et al., 2016). These proteins function as direct pore-forming components of the MPTP (Kwong and Molkentin, 2015) (Figure 1-7). Leung and colleague suggested that mitochondrial PiC is a major component of the MPTP. PiC is localized in the MIM and plays a critical role in mitochondrial oxidative phosphorylation and energy production (Leung et al., 2008). PiC transports inorganic phosphate into the mitochondrial matrix that is required for ATP synthesis (Kolbe et al., 1984, Palmieri, 2004). The mitochondrial F1F0 ATP synthase is an inner membrane multi-subunit enzymatic complex that has been recently identified as a core component of the MPTP. F1F0 ATP synthase couples proton translocation across the MIM for ATP synthesis (Bonora et al., 2015). At the level of the MOM, the pro-apoptotic proteins Bak and Bax serve as part of a MPTP complex (Figure 1-7). In response to an apoptotic stimulus, Bak/Bax oligomerize in the MOM to mediate cytochrome c release and the subsequent steps in initiating apoptosis, thereby forming a larger pore with the MPTP componenets (Karch et al., 2013).

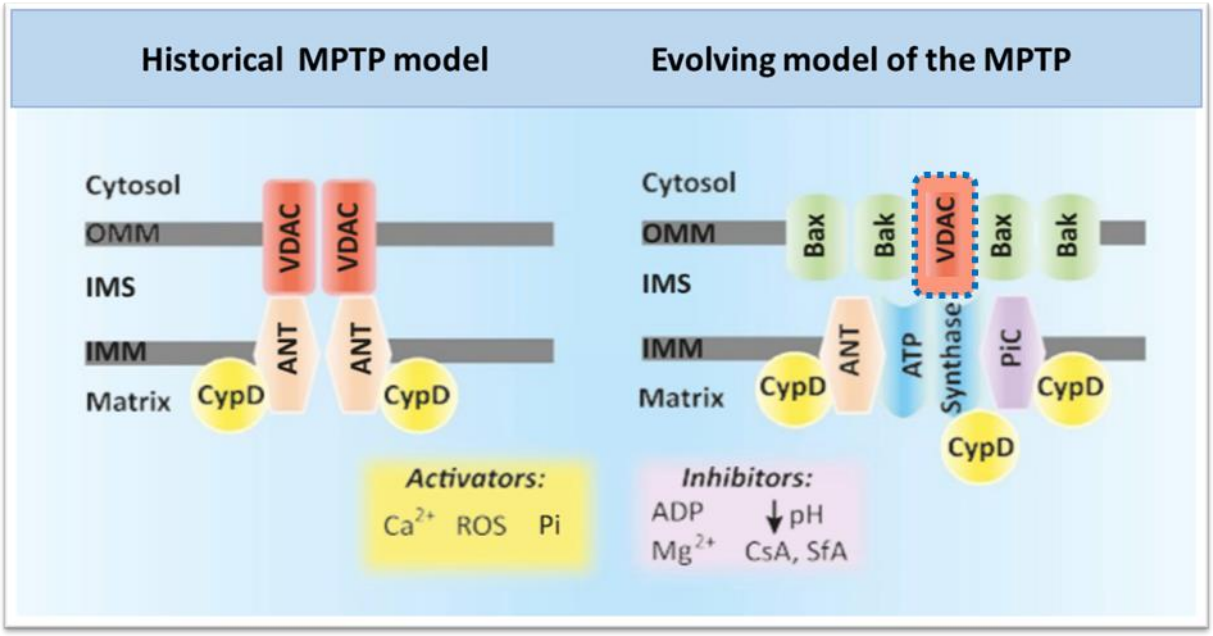

Figure 1-7: The Molecular Structure of the MPTP

The original model of the MPTP includes VDAC in the OMM (outer mitochondrial membrane), ANT in the IMM (inner mitochondrial membrane), and Cyclophilin D as the core constituents of the complex in the matrix. The genetic evaluation model of the MPTP has shown that ANT, PiC, and F1F0 ATP synthase as candidates for the inner membrane pore-forming unit. Cyclophilin D serves as a pore regulator of the MPTP. Whereas, the pro-apoptotic proteins Bak/Bax have been suggested as candidates in the OMM, thereby permitting mitochondrial swelling and rupture once the inner membrane complex opens (Kwong and Molkentin, 2015). It has been shown that VDAC is also participated in MPTP regulation during apoptosis (Liu et al., 2016).

1.4.1 Adenine Nucleotide Translocator

The adenine nucleotide translocator (ANT) is an integral protein located in the mitochondrial inner membrane (MIM) and involved in the regulation of the ATP/ADP ratios between the mitochondrial matrix and the intermembrane space (Brenner et al., 2011). The physiological function of ANT is to catalyse the substitution of ADP into the mitochondrial matrix in exchange for ATP across the inner mitochondrial membrane, as it is the most abundant protein in this membrane (Chevrollier et al., 2011). The crystal analysis of the bovine heart ANT showed that it consists of six transmembrane helices (Pebay-Peyroula et al., 2003). ANT plays a key role in cellular energy metabolism by transporting

mitochondrial ATP to the cytosol but the molecular mechanism of the ATP/ADP exchange is not completely understood (Baik and Lee, 2016).

There are four isoforms of human ANT (ANT1, ANT2, ANT3, and ANT4) (Brenner et al., 2011). ANT1 is the predominant isoform in non-dividing cells, heart and muscle cells (Doerner et al., 1997). In contrary, ANT2 is expressed at high levels in dividing cells, cells that are able to regenerate or proliferate such as liver cells, lymphoid and different cancers (Jang et al., 2008, Jang et al., 2016). ANT3 is expressed ubiquitously at lower levels independently of cell types. ANT4 is mainly localized in the testis and plays an essential role in spermatogenesis (Doerner et al., 1997, Brower et al., 2007). Thus, the expression of ANT isoforms is dependent on tissue types and proliferation status (Brenner et al., 2011).

Previous studies have been shown that both ANT1 and ANT3 act as pro-apoptotic factors (Zamora et al., 2004). ANT1 and ANT3 are components of the MPTP and their overexpression triggers caspase-3 and caspase-9 activation to induce mitochondrial-mediated cell death (Bauer et al., 1999, Zamora et al., 2004). In contrast, ANT2 and ANT4 display anti-apoptotic effects. In cancer cells, ANT2 has been found to exert an anti-apoptotic role by inhibiting mitochondrial membrane permeabilization (Jang et al., 2008). Thus, each isoform seems to have distinct apoptotic behaviour (Brenner et al., 2011).

Among ANT isoforms, ANT2 has been the protein of interest for many research groups as it is overexpressed in different kinds of cancer, including breast, ovary, stomach and lung cancers (Baik et al., 2016). Overexpression of ANT2 in different cancers may cooperate in cancer development (Jang et al., 2008, Baik et al., 2016). In particular, breast and ovarian cancer cells are characterized by upregulation of ANT2 expression. While, ANT1 and ANT3 are barely detected in these cancers. Therefore, ANT2 could be considered as a specific feature of breast and ovarian cancers (Jang et al., 2008). Recent studies demonstrate that ANT2 overexpression may induce resistance to cancer therapy in non–small cell lung

cancer. ANT2 depletion using ANT2 shRNA can effectively promote cell death and overcome tumour therapy resistance (Jang et al., 2008, Jang et al., 2016). Chevrollier and colleagues reported that ANT2 reversely imports ATP into the mitochondrial matrix. However, the mechanisms by which ANT2 regulates cell growth and supports cancer development are incompletely understood (Watanabe et al., 2017).

As a part of the MPTP complex, ANT2 is involved in mitochondrial membrane permeability and mitochondrial-mediated cell death (Halestrap and Brenner, 2003). Bcl-2 family members can physically interact with ANT to form a link between the inner and outer mitochondrial membrane (Brenner et al., 2011). The interaction of ANT with the pro-apoptotic protein Bax can modulate mitochondrial membrane permeability by forming the lethal pores (Marzo et al., 1998). In contrast, the pro-survival protein Bcl-2 supports ANT by inhibiting the formation of the apoptotic pores (Brenner et al., 2000).

1.4.2 Voltage-Dependent Anion Channel

The voltage-dependent anion channel protein (VDAC), also known as mitochondrial porin, is one component of the mitochondrial permeability transition pore (MPTP) (Shore, 2009). The VDAC family consists of three isoforms (VDAC1, VDAC2, and VDAC3) (Rostovtseva et al., 2002). The sub-mitochondrial distribution of the three VDAC isoforms has been determined by STED microscopy. VDAC1 and VDAC2 are mainly localized within the same distinct domains in the MOM. In contrast, VDAC3 is consistently distributed over the surface of the mitochondrion (Neumann et al., 2010). VDAC functions as a mitochondrial gatekeeper and regulates ion and metabolite flux between the mitochondria and cytosol (McCommis and Baines, 2012). Indeed, the VDAC protein is a key player in mitochondrial-mediated apoptosis, as it has a potential role in mitochondrial outer membrane permeabilization (MOMP) (Galluzzi and

Kroemer, 2007). Inducing MOMP is the critical step during apoptosis, which ultimately enables the release of cytochrome c into the cytosol (Youle and Strasser, 2008). The inner and outer mitochondrial membrane is spanned by the MPTP at membrane contact sites (McCommis and Baines, 2012). As VDAC is a part of the MPTP, it is closely involved in the regulation of the inner membrane potential and ATP production (Shore, 2009).

VDAC1 is over-expressed in many cancers and primarily associates with anti-apoptotic proteins such as Bcl-2, Bcl-xL and hexokinase, suggesting a critical role of this protein in cancer cell survival (Abu-Hamad et al., 2009, Geula et al., 2012, Arbel et al., 2012). Zheng and colleagues suggested that Arsenic trioxide (As_2O_3)-induced cytochrome c release via the MPTP can be inhibited by over-expression of Bcl-2 or Bcl-xL. Furthermore, Bcl-2 overexpression blocks As_2O_3- induced VDAC1 homodimerization (Zheng et al., 2004). However, VDAC1 has also been reported to interact with pro-apoptotic proteins such as Bim, tBid and Bax (Sugiyama et al., 2002, Banerjee and Ghosh, 2004). These interactions can directly activate VDAC to contribute in MPTP opening and induce cytochrome c release. The VDAC-Bim interaction was identified by incubating isolated rat liver mitochondria with recombinant Bim (Sugiyama et al., 2002). The VDAC-tBid/Bax interaction was examined by incubating isolated rat brain mitochondria with recombinant Bax and tBid (Banerjee and Ghosh, 2004). Similarly, Shimizu and colleagues reported that recombinant Bak and Bax directly interct with and cause VDAC opening, whereas Bcl-xL closes VDAC by binding to it (Shimizu et al., 1999).

On the other hand, VDAC2 has been shown to interact with pro-apoptotic proteins Bak and Bax, indicating a possible role of this protein in mitochondrial-mediated apoptosis (Galluzzi and Kroemer, 2007, Yamagata et al., 2009, San Chin et al., 2018). VDAC2 is a minor VDAC isoform in the MOM that acts to sequester the activation of Bak in healthy cells (Cheng et al., 2003). However, Bak activation is promoted when pro-apoptotic BH3 only protein tBid displaces Bak from VDAC (Shore, 2009). The VDAC2-Bak interaction is required for tBid-induced apoptosis

by recruiting more Bak to the MOM. Assembly of newly synthesized Bak and the formation of Bak oligomers at the MOM facilitate cytochrome c release, which is the point of no return in mitochondrial-mediated apoptosis (Roy et al., 2009). Fuethermore, a recent study indicated that Bax interaction with VDAC2 is critical for Bax-mediated apoptosis in response to chemotherapeutic agents both *in vitro* and *in vivo*. This study suggested that VDAC2 plays an important role in the mitochondrial localization of Bax, in which Bax localization to the mitochondria was disrupted in MEFs with deleted VDAC2 (San Chin et al., 2018). Thus, VDAC2 seems to be critical for the localization of both Bak and Bax in the MOM and the formation of their complexes.

It has been argued that either VDAC opening or closure results in mitochondrial-mediated apoptosis (Rostovtseva et al., 2005). Three models have been proposed to explain the role of VDAC in MOMP and cell death (McCommis and Baines, 2012). Model 1: VDAC indirectly induces apoptosis via activation of the MPTP, as it is a component of MPTP and interacts physically with pro-apoptotic proteins such as Bak and Bax. The formation of Bak/Bax/VDAC complex causes MOMP, that results in the swelling and rupture of mitochondria (Shimizu et al., 2000a, Rostovtseva et al., 2002, Galluzzi and Kroemer, 2007). Model 2: Apoptosis is initiated as a result of VDAC homo-oligomerization or hetero-oligomerization with Bak/Bax. VDAC oligomers form a larger channel in the MOM that enables the release of cytochrome c (Ran et al., 2005, Gonçalves et al., 2007). Model 3: closure of the VDAC channels causes accumulation of mitochondrial metabolites and decreases the exchange of ADP/ATP between mitochondria and cytosol. As a consequence, mitochondrial swelling induces MOMP through either an undefined mechanism or complete rupture of the MOM (Rostovtseva et al., 2004) (Figure 1-8).

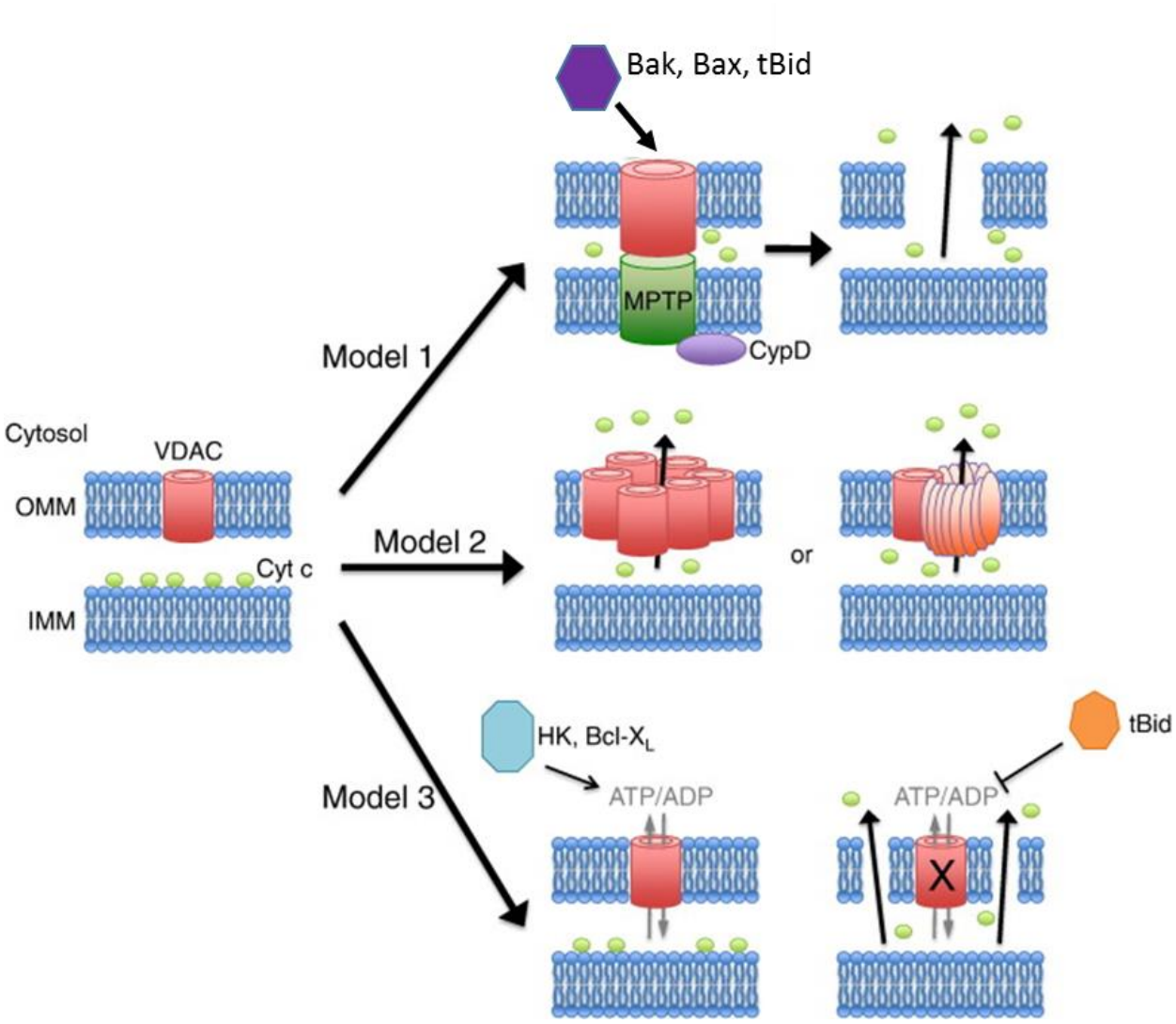

Figure 1-8: Proposed models for VDAC's role in the induction of apoptosis

In model 1: the VDAC is a component of the MPTP and it physically interacts with pro-apoptotic proteins Bak and Bax to form a larger complex. The formation of this complex causes mitochondrial outer membrane permeabilization (MOMP) and the release of cytochrome c from the mitochondrial intermembrane space to the cytosol. Model 2: in response to apoptotic stimuli, VDAC forms either homo-oligomerization or hetero-oligomerization channels with Bax/Bak to create a large pore capable of releasing cytochrome c. Model: 3 anti-apoptotic proteins such as Bcl-xL and hexokinase maintain VDAC to keep it in the normal physiological state, thereby maintaining mitochondrial outer membrane permeability. However, because of increasing the activity of pro-apoptotic proteins, VDAC channels have been shown to be closed. As a result, mitochondrial swelling and rupture causes the release of cytochrome c and cell death (McCommis and Baines, 2012).

1.5 Mammalian Cell Cycle

The cell cycle is an ordered series of biochemical events in which the cell contents, including DNA and other cellular components, are duplicated and segregated into two genetically identical daughter cells (Yu, 2002). The cell cycle is divided into two major phases: interphase and the mitotic phase. The interphase is subdivided into three phases Gap 1 (G1), S phase (DNA synthesis) and Gap 2 (G2). G1 and G2 are two growth phases. In G1, the cells grow and prepare for DNA synthesis. Whereas in G2, the cells continue to grow and prepare for DNA segregation. The two growth phases are separated by S phase by which the cells make an identical copy of their genetic materials (Sherr and Roberts, 1999).

Mitosis or M phase is the process by which one nucleus will turn into two nuclei, each with an identical genetic information. Mitosis is subdivided into five distinct phases: prophase, prometaphase, metaphase, anaphase and telophase (see Figure 1-9). The 1st phase of mitosis, prophase, involves the following events; DNA condenses into the condensed form, nuclear membrane starts to breakdown and two centrosomes migrate to opposite sides of the cell (Malumbres and Barbacid, 2009). In prometaphase, spindle microtubules extend from centrosomes toward each other and to near the kinetochores of the sister chromatids. Chromosomes start to line up in the middle of the cells and the spindle microtubules are attached to kinetochores at metaphase. In anaphase, microtubules start to pull on each of the sister chromatids to the opposite sides of the cell via disassembly of the spindle microtubules. The last phase of mitosis is called telophase and it involves: nuclear membrane begins to form around the DNA for each daughter cell and the cell membrane prepares for cytokinesis in preparation for cell splitting into two identical cells (Malumbres and Barbacid, 2009, Malumbres and Barbacid, 2005) (Figure 1-9). During cell division, the transition between the different cell cycle phases is regulated by the activation and inactivation of a family of serine/threonine kinases, the cyclin dependent kinases (Cdks), and their binding partners, the cyclins (Malumbres et al., 2009).

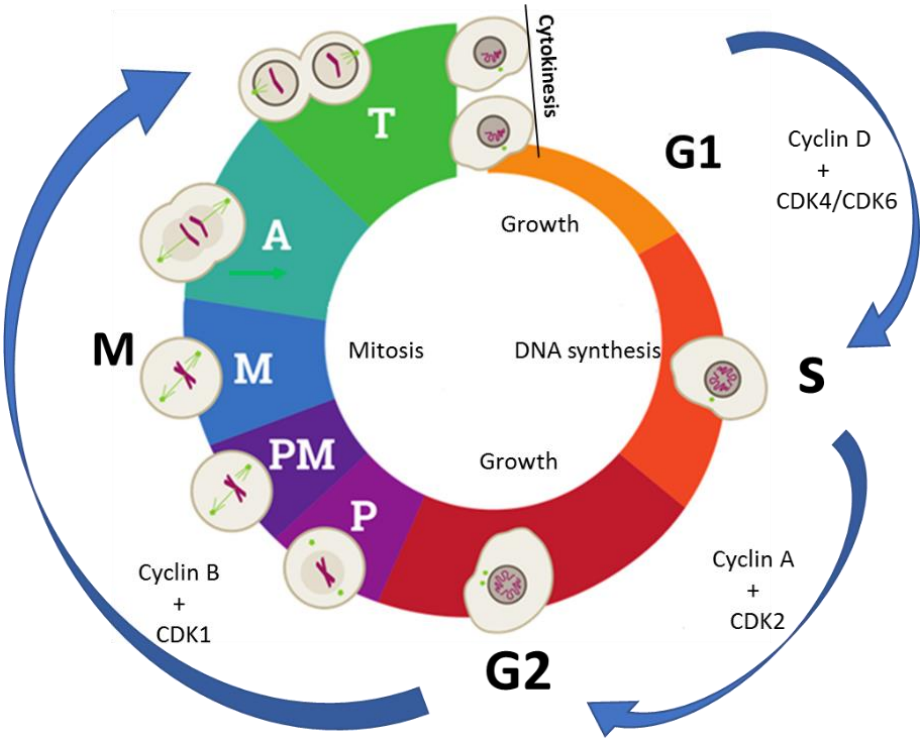

Figure 1-9: The regulation of the mammalian cell cycle.

The cell cycle is divided into interphase and mitosis (M). Interphase is subdivided into three distinct phases: Gap 1 (G1), DNA synthesis (S) and Gap 2 (G2). Interphase is monitored by three checkpoints during the cell cycle. Whereas, mitosis is tightly monitored by spindle assembly checkpoint. Growth factors activate Cdk4/6 and Cdk2 which allows the G1-to-S-phase transition. After DNA synthesis in S phase, the cells continue to grow and prepare for cell division in mitosis. During the 1st phase of mitosis, prophase, DNA condenses, nuclear membrane breaks down and two centrosomes migrate to opposite sides of the cells. Chromosomes line up in the middle of the cells and the spindle microtubules attach to kinetochores at metaphase. Sister chromatids separate and pull apart to the spindle poles at anaphase. In telophase, nuclear membrane begins to form around the DNA for each daughter cell and the cell prepares for cytokinesis to form two identical daughter cells (Malumbres and Barbacid, 2005) (Image taken and adapted from http://cellcycle.org.uk/).

1.5.1 Cyclin dependent kinases regulate mammalian cell cycle

Cyclin-dependent kinases (Cdks) are key regulators of the cell cycle in all eukaryotes. Unicellular organisms such as yeast requires a single Cdk, Cdc2, to regulate both G1-S phase and G2-M phase transitions (Nurse and Bissett, 1981). The ability of Cdks to drive transitions in the cell cycle depends on the association of these kinases with different cyclin partners. The kinase catalytic subunit/cyclin

complexes target distinct substrates (Lee and Nurse, 1987). In mammalian cells, the Cdk family includes more than 20 members (Choi and Anders, 2014). However, only a few Cdks have been identified that directly contribute to the cell division cycle (Hydbring et al., 2016).

Cdk1, Cdk2, Cdk4, and Cdk6 are involved in regulation of the cell cycle. Cdk4 and Cdk6 regulate the cell cycle during G1 phase and Cdk2 at the start of S phase (Tsai et al., 1991) (Meyerson et al., 1992). Cdk4/6 primarily bind cyclin D in response to growth factor stimulation and prepare the cell for S phase. Cdk2 binds cyclins E and A and contributes to the initiation of DNA synthesis and duplication of centrosomes (Wei et al., 2003, Lundberg and Weinberg, 1998). Cdk1 primarily binds cyclin B1 to initiate mitosis but also associates with cyclin A in mid S-phase (Hu et al., 2001, Merrick et al., 2011, Mitra et al., 2006). Cdk2 kinase activity is high in late S-G2 phase and may promote the activation of the Cdk1/cyclin B1 complex and entry in to mitosis. Overall, the Cdks (Cdk1, Cdk2, Cdk4 and Cdk6) play essential roles during interphase leading up to mitosis (Hu et al., 2001, Furuno et al., 1999).

Several studies have demonstrated the role of Cdks during the mammalian cell cycle. For example, transient transfection of dominant-negative mutants of Cdk4/6 were found to delay progression into S phase and expression of a dominant-negative mutant of Cdk2 blocks progression into either S phase or mitosis (van den Heuvel and Harlow, 1993, Hu et al., 2001). Furthermore, expression of a dominant-negative mutant of Cdk1 was found to block entry into mitosis (van den Heuvel and Harlow, 1993). Cdk1 kinase activity is low near to late S-G2 phase because of the inhibitory phosphorylation at its ATP-binding site and limited association with cyclin B1 (McGowan and Russell, 1993, McGowan and Russell, 1995). However, Cdk1 is the only essential Cdk during the cell cycle (Santamaría et al., 2007). Cdk1 kinase activity can perform all the events that are necessary to drive cell division in mouse embryos lacking all interphase Cdks (Cdk2, Cdk3, Cdk4 and Cdk6). Principally, a model has been proposed by Enders

in which Cdk4/6 initiate the mammalian cell cycle, Cdk2 initiates S phase, progression through S and G2 phases is dependent on Cdk2 and Cdk1 activity. Indeed, Cdk1 regulates both the entry into and the exit from mitosis (Enders, 2012).

1.5.2 Cyclin Dependent Kinase 1 regulates mitosis and apoptosis

The cell division cycle is controlled by Cyclin-dependent kinases (Cdks) via a highly ordered set of biochemical events (Hartwell and Weinert, 1989). Cdk1 kinase is one of the key mitotic kinases and it regulates the transition from G2 to M phase of the cell cycle (Nurse, 1990, Nigg, 2001). During mitosis, Cdk1/cyclin B1 complexes mediate phosphorylation of a variety of substrates to play an essential role in multiple processes, including chromosome condensation, nuclear envelope breakdown, centrosome separation, regulation of spindle microtubules, and the transition from metaphase to anaphase (Slangy et al., 1995, Kimura et al., 2001, Rudner and Murray, 2000). In addition to its localization in the cytoplasm, nuclear membrane and centrosome, a fraction of Cdk1/cyclin B1 complex is also localized into the matrix of mitochondria (Wang et al., 2014, Xie et al., 2018). Cdk1-mediated phosphorylation a group of mitochondrial proteins including complex I subunits enhances mitochondrial respiration and ATP generation to provide cells with sufficient energy for the G2/M transition (Wang et al., 2014).

Although Cdk1 is implicated in organising cell cycle progression, it has been found to play an important role in mitotic cell death (Sakurikar et al., 2012). Antimitotic drugs, such as Taxol, interfere with microtubule dynamics to prevent microtubule-kinetochore attachments (Dumontet and Jordan, 2010). This results in SAC-mediated prolonged mitotic arrest. Prolonged mitotic cell cycle arrest is achieved by inhibiting the inactivation of Cdk1 (Foley and Kapoor, 2013).

Sustained Cdk1 activation reduces the apoptotic threshold by phosphorylating anti-apoptotic proteins such as Bcl-2, Bcl-xL and Mcl-1 (Terrano et al., 2010).

The kinase most frequently involved in phosphorylating Bcl-2 at S70 is Cdk1 (Dai et al., 2013). Multiple alternative phospho-sites in Bcl-2 have been described such as phosphorylation at T69, S70, S87 targeted by JNK at G2/M (Yamamoto et al., 1999). Cdk1 also targets Bcl-xL on S62 (Terrano et al., 2010). Other kinases have been reported to target Bcl-xL on different phospho-sites, for example phosphorylation at S49, targeted by Polo-like kinase (PLK)3 (Wang et al., 2011) and phosphorylation on S62, targeted by JNK (Basu and Haldar, 2003). Numerous studies have suggested that Mcl-1 is the most critical survival factor within the Bcl-2 family. Like Bcl-2 and Bcl-xL, Mcl-1 is targeted on S64 and T92 by Cdk1 and it becomes highly phosphorylated during prolonged mitotic arrest. JNK, p38 and Casein Kinase II (CKII) also implicated in the phosphorylation of Mcl-1 (Wertz et al., 2011). Phosphorylation of Mcl-1 can influence protein stability and ultimately results in its degradation by APC/C E3-ligase (Harley et al., 2010, Haschka et al., 2015, Chu et al., 2012).

Cdk1-mediated phosphorylation of anti-apoptotic proteins (Bcl-2, Bcl-xL and Mcl-1) inhibits their anti-apoptotic effects. A change in the duration of Bcl-2 and Bcl-xL phosphorylation from transient during normal mitosis to sustained during Taxol-induced mitotic cell cycle arrest primes mitotically-arrested cells to undergo apoptosis (Scatena et al., 1998, Terrano et al., 2010, Sakurikar et al., 2012). Of note, Cdk1 inhibitor roscovitine can inhibit Cdk1-mediated phosphorylation of anti-apoptotic proteins (Han et al., 2014, Zhou et al., 2014). However, the molecular mechanism linking mitotic checkpoint activation to the initiation of cell death, in particular, how Cdk1 translocates from the cytoplasm to the MOM to phosphorylate anti-apoptotic proteins, has remained unknown.

1.6 Background to the project

Previous studies in our lab have shown that Taxol causes HeLa cells to arrest in mitosis and then undergo apoptosis via activation of the intrinsic pathway (Deacon et al., 2003). Preliminary studies have shown that depletion of the pro-apoptotic protein Bax by siRNA in HeLa cells treated with Taxol inhibits apoptosis by more than 80%. In addition, siRNA-mediated depletion of caspase-3 in HeLa cells also inhibited Taxol-induced apoptosis. Our lab has also shown that down-regulation of caspase-9 by siRNA in HeLa cells treated with Taxol induces a significant decrease in Taxol-induced apoptosis. Furthermore, cleaved caspase-3 was barely detected in caspase-9 siRNA-transfected cells in comparison to control-siRNA treated cells, suggesting that Taxol-induced apoptosis through activation of caspase-3 is dependent on activation of caspase-9.

1.7 Aim and objectives

Taxol, an anti-microtubule anti-cancer drug, interferes with the mitotic function of spindle microtubules and causes cell cycle arrest via activation of the spindle assembly checkpoint (SAC). Prolonged activation of the SAC keeps the cells arrested in mitosis by inhibiting the inactivation of Cdk1, followed by apoptotic cell death via activation of mitochondrial-dependent apoptosis. Although the molecular mechanism linking SAC activation to the induction of apoptosis has been the subject of intense research in the last few years, no clear mechanism has emerged. Moreover, the molecular mechanism of Taxol-induced apoptosis, particularly the organization of Bak and Bax in the MOM during mitotic cell death and their interaction(s) with other MOM/MIM proteins, remains incompletely understood.

In this study, my objectives were therefore to investigate:

1. Whether only Bax or both Bax and Bak are required for Taxol-induced mitotic cell death using siRNA approach.
2. Potential interaction between key pro-apoptotic proteins Bak and Bax using co-IP and immunofluorescence microscopy.
3. The putative interacting molecules (Bak and Bax-interacting proteins) that may mediate apoptosis in Taxol-arrested mitotic cells using mass spectrometry, co-IP assays and immunofluorescence microscopy.
4. The molecular link between activation of the SAC and the induction of apoptosis.

Chapter 2. Materials and methods

2.1 Materials

2.1.1 Chemicals and reagents

Table 2-1: List of chemicals and reagents used in this study

Reagent	Supplier
Agar	Gibco
Ammonium persulphate (APS)	Fisher
Aphidicolin	Sigma
Bovine serum albumin	Sigma
Cell Dissociation Medium (1X)	Sigma
3-[(3-cholamidopropyl) dimethylammonio]-1-propanesulfonate (CHAPS)	Fisher
Cover glass (Diameter 22mm)	Fisher
Digitonin	Santa Cruz Biotechnology
Dithiobis (succinimidyl propionate) (DSP)	ThermoScientific
Ethylene diamine tetra acetic acid (EDTA)	Fisher
Ethylene Glycol Tetra-acetic acid (EGTA)	Fisher
EZ-ECL Chemiluminescence detection kit	Geneflow
Foetal Bovine Serum (FBS)	Fisher

Reagent	Supplier
Formaldehyde solution	Sigma
FuGENE HD Transfection Reagent	Promega
Glycerol	Fisher
Glycine	Fisher
Hydroxyethyl piperazineethanesulfonic acid (HEPES)	Fisher
Hoechst 33342	Sigma
Hydrochloric acid	Fisher
Instant Blue (A Coomassie Based Staining Solution for Protein Gels)	Expedeon
Interferin siRNA Transfection Reagent	Polyplus
Magnesium Chloride	Fisher
Methanol	Fisher
Microscope slides	ThermoScientific
Mitotracker Red CMXRos (Chloromethyl-X-Rosamine)	Cell Signalling
Nitrocellulose Membrane	Santa Cruz Biotechnology, Inc
NP-40	MP Biomedicals

Reagent	Supplier
n-Propyl gallate	Sigma
Penicillin/ Streptomycin (stock 10,000 IU Penicillin and 10,000 µg/ml Streptomycin) (100X)	Fisher
Pierce Protein A/G Magnetic Beads	ThermoScientific
Poly-L-Lysine hydrobromide Mwt 150,000-300,000	Sigma
Polyoxyethylene (20) sorbitan monolaurate (Tween-20)	Calbiochem
Potassium Chloride	Fisher
Prestained Protein Ladder	ThermoScientific
Propidium iodide	Sigma
Protease inhibitors (Aprotinin, Leupeptin, Pepstatin)	Sigma
Phenylmethylsulfonyl Fluoride (PMSF)	Sigma
Protogel (30% w/v Arylamide/0.8% w/v Bisacrylamide)	Gene Flow
Qiagen Midi Plasmid Purification Kit	Qiagen
Sodium Chloride	Fisher
Sodium deoxycholate	Sigma

Reagent	Supplier
Sodium dodecyl sulfate (SDS)	Sigma
Sodium Fluoride	Fisons
Sodium Orthovanadate	Acros Organics
Sodium pyrophosphate	Acros Organics
Staurosporine	Sigma
Taxol	Sigma
Tetramethylethylenediamine (TEMED)	Fisher
Thymidine	Sigma Aldrich
Tris-base	Fisher
Triton X-100	Fisher
UltraCruz TM Autoradiography (X-Ray) Films	Insight Biotechnology
Vectorshield Mounting Medium	Vector Laboratories
Yeast Extract	Sigma
β-Glycerophosphate	Sigma
β-Mercaptoethanol	Acros Organics
[ϒ-^{32}P]-ATP 3000 Ci/mmol	PerkinElmer
ATP	Sigma
Histone H1	Millipore

2.1.2 Cell lines

Table 2-2: The following cell lines were used in this study

Cell line	Supplier
HeLa cells (a human epithelial cell line derived from cervical carcinoma)	Purchased from BioWhittaker
U2OS (Human Bone Osteosarcoma Epithelial cell line)	Provided by Andrew Fry (University of Leicester).
RPE1 (Retinal Pigment Epithelial Cell Line)	
(mesothelioma) Malignant pleural mesothelioma cell line MSTO-211H	
Melanoma (WM266C4; epithelial cells derived from human Skin metastasis)	Provided by Sally Prigent (University of Leicester).
RKO A19 (colorectal cancer cell lines), RKO A19 (BRAFV600E/−/−) cells carry a mutant BRAFV600E allele and have knockout of the WT allele.	Provided by Catrin Pritchard (University of Leicester).
RKO 143 (colorectal cancer cell lines)	
STK 5090 (lung cancer cell line)	
C2C12 (mouse myoblast cell line)	Provided by Sue Shackleton (University of Leicester).
HCT116 WT (colon carcinoma cell line)	Provided by Salvador Macip (University of Leicester).

Cell line	Supplier
HCT116 $Bax^{-/-}$ $Bak^{-/-}$ (colon carcinoma cell line)	provided by Richard Youle National Institute of Mental Health USA

2.1.3 Cell culture media

Table 2-3: List of cell culture media used in the study

Media	Supplier
Dulbecco's modified Eagle's medium	Sigma
Dulbecco's phosphate buffered saline, without Calcium chloride and magnesium chloride (DPBS)	
Dulbecco's modified Eagle's medium DMEM/F-12	Gibco by life technologies
Mc Coy's 5A medium	
Sodium Bicarbonate solution 7.5% w/v	
Enzyme free cell dissociation solution PBS based	Millipore

Table 2-4: Cell Culture Media Recipe per Cell Line

Cell Line	Media Recipe
HeLa Cells	Dulbecco's Modified Eagle's Medium (DMEM), 10 % v/v Foetal Bovine Serum (FBS), 1 % v/v Penicillin/Streptomycin (Pen/Strep).
U2OS cells	
Melanoma cells	
STK 5090	
RPE1 Cells	Dulbecco's Modified Eagle's Medium/ F-12 + L-Glutamine, + 15 mM HEPES, 10 % v/v Foetal Bovine Serum (FBS), 1 % v/v Penicillin/Streptomycin (Pen/Strep), 0.25 % v/v NaHCO3.
Mesothelioma	RPMI, 10 % v/v Foetal Bovine Serum (FBS), 1 % v/v Penicillin/Streptomycin (Pen/Strep).
RKO 143	Mc Coy's 5A, 10 % v/v Foetal Bovine Serum (FBS), 1 % v/v Penicillin/Streptomycin (Pen/Strep).
C2C12	Dulbecco's Modified Eagle's Medium/ F-12 + L-Glutamine, + 15 mM HEPES, 10 % v/v Foetal Bovine Serum (FBS), 1 % v/v Penicillin/Streptomycin (Pen/Strep)
RKO A19	Mc Coy's 5A, 10 % v/v Foetal Bovine Serum (FBS), 1 % v/v Penicillin/Streptomycin (Pen/Strep).
HCT116 WT	
HCT116 Bak/Bax DKO	

2.1.4 Buffers and solutions

Table 2-5: Protein extraction lysis buffers

Buffers	Composition
Radio-Immunoprecipitation Assay (RIPA) buffer	0.01 mol/L Tris-Hcl (PH 8.0), 0.15 mol/L NaCl, 0.1 % (w/v) SDS, 1 % (v/v) NP-40, 0.5 % (w/v) sodium deoxycholate, 50 mmol/L sodium fluoride, 30 mmol/L sodium pyrophosphate, 100 µM sodium Orthovanadate and protease inhibitors (1 mM PMSF, 10 µg/ml Leupeptin, 10 µg/ml Aprotinin, and 10 µg/ml Pepstatin)
Lysis buffer A	40 mM HEPES (PH 7.4), 0.15 M sodium chloride, 1 mM EGTA, 20 mM β-glycerophosphate, 1 mM sodium Orthovanadate, 50 mM sodium fluoride, 30 mM sodium pyrophosphate, 0.01 % (w/v) digitonin and protease inhibitors (1 mM PMSF, 10 µg/ml Leupeptin, 10 µg/ml Aprotinin, and 10 µg/ml Pepstatin)
Lysis buffer A with CHAPS	Buffer A containing 3 % (w/v) CHAPS
1 % (w/v) CHAPS lysis buffer for IP	20 mM Tris Hcl (pH 7.4), 135 mM sodium chloride, 1.5 mM magnesium chloride, 1 mM EGTA, 10 % (v/v) Glycerol, 1 % (w/v) CHAPS and protease inhibitors.
Lysis buffer B	10 mM Tris-Hcl (pH 7.4), 50 mM sodium chloride, 5 mM EDTA, 30 mM sodium pyrophosphate, 0.1 mM sodium Orthovanadate, 50 mM sodium fluoride, 1 % (v/v) NP-40, 0.1 % (w/v) BSA and protease inhibitors.

Buffers	Composition
Wash buffer (Tris-buffered saline (TBS-Tween) for IP	25 mM Tris, 150 mM sodium chloride, 0.05 % (v/v) Tween-20, (pH 7.5).
Cdk1 Lysis buffer	10 mM Hepes (pH7.4), 10 mM sodium chloride, 1 mM EDTA, 0.1 % (v/v) Triton X-100, 50 mM sodium fluoride, 80 mM β-glycerophosphate, 0.1 mM sodium Orthovanadate, and protease inhibitors
Cdk1 Assay wash buffer	25 mM Hepes (pH7.4), 150 mM sodium chloride and 0.1 % (v/v) Triton X-100
Cdk1 Assay buffer	50 mM Hepes (pH7.4), 1 mM DTT, 15 mM EGTA and 20 mM magnesium chloride, 4 mM ATP, 4 µCi of [ϒ-^{32}P]-ATP
Cdk1 Dilution buffer	20 mM MOPS/NaOH (pH 7.0), 1 mM EDTA, 5 % (v/v) glycerol, 0.01 % (v/v) Brji-35, 0.1 % (v/v) 2-mercaptoethanol.

Table 2-6: Composition of resolving (running) and stacking gel used for SDS-PAGE

Reagents	Resolving			Stacking
	7 %	10 %	12.5 %	3 %
Protogel	4.65	6.67 ml	8 ml	1.6 ml
Tris-Hcl pH 8.8	7.5 ml	7.5 ml	7.5 ml	____
Tris-Hcl pH 6.8	____	____	____	1.2 ml
SDS 10% (w/v)	100 µl	100 µl	100 µl	100 µl
APS 10% (w/v)	150 µl	150 µl	150 µl	75 µl
Temed	20 µl	20 µl	20 µl	12 µl
H_2O	7.58	5.6 ml	4.2 ml	7.6 ml

Table 2-7: Buffers used for Western Blotting

Buffer	Composition
1X SDS-PAGE Running Buffer	0.025M Tris-HCL, 0.192M Glycine, 1% (w/v) SDS.
SDS-PAGE transfer Buffer	25mM Tris-HCL, 192mM Glycine, 0.1% (w/v) SDS, 20% (v/v) Methanol.
1X Tris-Saline-Tween (TST)	0.01M Tris-HCL (pH 7.4), 0.15M NaCl, 0.1% (v/v) Tween-20
Blocking Buffer	5% (w/v) Bovine serum albumin or 5% (w/v) milk powder (Marvel) in TST buffer

Buffer	Composition
Stacking gel buffer	6.06 gm Tris-HCL (pH 8.8), 10 % (w/v) SDS 4 ml, H_2O to 100 ml.
Sample Buffer (5X)	60mM Tris-HCL (pH 6.8), 10 % (v/v) Glycerol, 2% (w/v) SDS, 0.01% (w/v) bromophenol blue, 5% (v/v) β-mercaptoethanol.
Sample Buffer (2X)	Glycerol 2ml, 10% (w/v) SDS 2 ml, 0.25mg bromophenol blue, 2.5 ml stacking gel buffer, 0.5 ml β-mercaptoethanol, H_2O to 10 ml.

Table 2-8: Buffer used for immunofluorescence

Buffer	Composition
Blocking buffer	1% (w/v) Bovine serum albumin in DPBS, 0.1% (v/v) Tween-20
Mounting medium	Glycerol 9 ml, 1M Tris-HCL (pH 8.0) 1 ml, n-propyl gallate 0.05 g. The n-propyl gallate was dissolved by stirring the solution for at least 10 h at RT (in a light-proof container). Mounting medium stored at 4 °C.

Table 2-9: Solution used for Fluorescence-Activated Cell Sorting (FACS)

Solution	Solution Composition
Stain solution	9.5 ml of 1X PBS, 0.5 ml of (10 µg/ml) RNase solution, and (200 µl) of 1 mg/ml PI solution.

2.1.5 Antibodies

Table 2-10: Primary antibodies used in this study

Antibody	Host species	Clonality	Dilution used	Application
Bak (N-20)	Goat	Polyclonal	1:500	Immunoprecipitation
Bak (D4E4)	Rabbit	Monoclonal	1:1000 1:100	Western Blotting Immunofluorescence
Bax (6A7)	Mouse	Monoclonal	1:500 1:100	Immunoprecipitation Immunofluorescence
Bax	Rabbit	Polyclonal	1:1000	Western Blotting
Caspase-3	Mouse	Monoclonal	1:1000	Western Blotting
Cleaved Caspase-3	Rabbit	Monoclonal	1:1000	Western Blotting
Caspase-9	Rabbit	Polyclonal	1:1000	Western Blotting
M30 CytoDEATH	Mouse	Monoclonal	1:10	Immunofluorescence
poly-(ADP-Ribose) polymerase (PARP)	Rabbit	Polyclonal	1:2000	Western Blotting
Bcl-2	Mouse	Monoclonal	1-1000	Western Blotting
Phospho-Bcl-2(Ser70)	Rabbit	Monoclonal	1-1000	Western Blotting

Antibody	Host species	Clonality	Dilution used	Application
Bcl-xL (610212)	Rabbit	Polyclonal	1-1000	Western Blotting
Bcl-xL (2762)	Rabbit	Polyclonal	1-1000	Western Blotting
Phospho-Bcl-xL (Ser62)	Rabbit	Polyclonal	1-1000	Western Blotting
Mcl-1	Rabbit	Polyclonal	1-1000	Western Blotting
Bim	Rabbit	Polyclonal	1-1000	Western Blotting
ANT2/SLC25A5 (E2B9D)	Rabbit	Monoclonal	1-1000 1-50	Western Blotting Immunofluorescence
VDAC	Rabbit	Polyclonal	1-1000 1-50	Western Blotting Immunofluorescence
Cyclin B1	Rabbit	Polyclonal	1-1000 1-50	Western Blotting Immunofluorescence
Cdc2 p34 (C-19)	Rabbit	Polyclonal	1-1000	Western Blotting
Cdc2 p34 (17)	Mouse	Monoclonal	1:500 1-50	Immunoprecipitation Immunofluorescence
Phospho-cdc2 (Tyr15)	Rabbit	Polyclonal	1-1000	Western Blotting
αPAK (N-20)	Rabbit	Polyclonal	1-1000	Western Blotting
α-tubulin	Mouse	Monoclonal	1-5000	Western Blotting

Table 2-11: Primary antibodies used in this study

Antibody	Catalogue Number	Supplier
Bak (N-20)	Sc-1035	Santa Cruz Biotechnology
Bak (D4E4)	12105	Cell Signalling
Bax (6A7)	Sc-23959	Santa Cruz Biotechnology
Bax	2772	Cell Signalling
Caspase-3	9668	Cell Signalling
Cleaved Caspase-3	9664	Cell Signalling
Caspase-9	9502	Cell Signalling
Anti-M30 CytoDEATH	2140322	Roche
Anti-poly-(ADP-Ribose) polymerase (PARP)	11835238001	Roche
Bcl-2	M 0887 Clone 124	Dako
Phospho-Bcl-2 (Ser70)	2827	Cell Signalling
Bcl-Xl	610212	BD Transduction Laboratories
Bcl-xL	2762	Cell Signalling
Phospho-Bcl-xL (Ser62)	GTX79124	Gene Tex
Mcl-1	sc-819	Santa Cruz Biotechnology
Bim	B7929	Sigma-Aldrich

Antibody	Catalogue Number	Supplier
ANT2/SLC25A5 (E2B9D)	14671	Cell Signalling
VDAC	4866	Cell Signalling
Cyclin B1	4138	Cell Signalling
Cdc2 p34 (C-19)	Sc-954	Santa Cruz Biotechnology
Cdc2p34(17)	Sc-54	Santa Cruz Biotechnology
Phospho-cdc2(Tyr15)	9111	Cell Signalling
αPAK (N-20)	Sc-882	Santa Cruz Biotechnology
α-tubulin	37981	SAB

Table 2-12: Secondary antibodies used in this study

Antibody	Dilution used	Application	Supplier
Alexa Fluor 488 Goat Anti-Mouse IgG	1:1000	Immunofluorescence	Life technologies
Alexa Fluor 488 Rabbit Anti-Goat IgG			
Alexa Fluor 594 Goat Anti-Rabbit IgG			
Alexa Fluor 594 Rabbit Anti-Mouse IgG			
Alexa Fluor 594 Rabbit Anti-Mouse IgG	1:1000	Immunofluorescence	Invitrogen

Antibody	Dilution used	Application	Supplier
Alexa Fluor 488 Goat Anti-Mouse IgG			
Alexa Fluor 647 Goat anti-Rabbit			
Alexa Fluor 555 Goat Anti-Rabbit	1:500	Immunofluorescence	Cell Signalling
Goat Anti-Rabbit IgG, HRP-linked antibody	1:1000	Western Blotting	
Goat Anti-mouse IgG, HRP-linked antibody	1-5000	Western Blotting	Bethyl
Rabbit IgG-heavy and light chain Antibody			

Table 2-13: GFP-Booster for Immunofluorescence of GFP-Fusion Proteins used in this study

GFP-Booster	Dilution used	Application	Supplier
GFP-Booster_ATTO488	1:100	Immunofluorescence	Chromotek
GFP-Booster_ATTO647			

2.2 Oligonucleotides

2.2.1 RNAi Oligonucleotides

The ON-TARGET plus set of four oligonucleotides for Human Bax, Bak and VDAC1 siRNA were purchased from Dharmacon (now Horizon Discovery). The sequences of the 4 sense strands for each siRNA were as follows:

Table 2-14: List of oligonucleotides used in this study

Name	Target sequence
Human Bax # 1	5’-GUGCCGGAACUGAUCAGAA-3’
Human Bax # 2	5’-ACAUGUUUUCUGACGGCAA-3’
Human Bax # 3	5’-CUGAGCAGAUCAUGAAGAC-3’
Human Bax # 4	5’-UGGGCUGGAUCCAAGACCA-3’
Human Bak1 # 1	5’-CGACAUCAACCGACGCUAU-3’
Human Bak1 # 2	5’-UAUGAGUACUUCACCAAGA-3’
Human Bak1 # 3	5’-GACGGCAGCUCGCCAUCAU-3’
Human Bak1 # 4	5’-AAUCAUGACUCCCAAGGGU-3’
Human VDAC1 # 1	5’-UAACACGCGCUUCGGAAUA-3’
Human VDAC1 # 2	5’-GAAACCAAGUACAGAUGGA-3’
Human VDAC1 # 3	5’-GAGUACGGCCUGACGUUUA-3’
Human VDAC1 # 4	5’-CCUGAUAGGUUUAGGAUAC-3’
Control siRNA	5’-UAGCGACUAAACACAUCAA-3’

Table 2-15: RNAi transfection reagents

Name	Supplier
RNAase-free eppendorf tubes	Ambion
RNAase-free pipette tips	
siRNA Control (scrambled siRNA sequence)	
siRNA transfection medium	Santa Cruz technologies
siRNA dilution buffer	
siRNA transfection reagent (INTERFERin)	Polyplus

Table 2-16: Recombinant Human Proteins used for Protein-protein Interaction Assay

Name	Catalog Number	Molecular Weight	Supplier
Cdk1 Protein (GST Tag at the N-terminus).	10739-H09B	60 kDa	Sino Biological Inc.,
Bax Protein	_____	21 kDa	Provided by Frank Edlich (University of Freiburg)
Bax Protein (GST Tag at the N-terminus).	H00000581-P01	46.86 kDa	Novus Biologicals
PAK alpha (GST Tag at the N-terminus).	_____	91 kDa	Purified as described in (Deacon et al., 2003)

2.3 Methods

2.3.1 Cell Culture

2.3.1.1 Culture and maintenance of human cell lines

HeLa and U2OS cells were cultured in Dulbecco's modified Eagle's medium (DMEM). RPE1 cells were cultured in DMEM F12. Cells were supplemented with 10% (v/v) heat inactivated foetal bovine serum (FBS) and 1% (v/v) Penicillin-Streptomycin solution (100 IU/ml and 100 µg/ml respectively) and maintained in a humidified incubator at 37 °C and 5% CO_2 atmosphere. Cells were passaged upon reaching 80-90% confluency. Cells were passaged by removing the medium, washing three times with 6 ml of DPBS, followed by addition of 2ml Cell Dissociation Medium and incubation of the cells for 15-20 minutes at 37 °C. After incubation, 8 ml complete medium was added to the plate and the cells were dissociated by gently pipetting the cell suspension. Subsequently, 2.5 ml of cell suspension was added to a new 10-cm culture plate containing 10 ml pre-warmed complete medium.

2.3.1.2 Storage of human cell lines

Cells were detached as described in section 2.3.1.1 and cell suspension was centrifuged at 1100 rpm for 5 min at RT. The supernatant was discarded, and 1.5 ml of Cell Freezing Medium was added to the cell pellet and the cells were resuspended gently by pipetting up and down. The cell suspension was then transferred to a sterile 2 ml cryovial and placed in an Isopropanol-filled cell freezing box for 2-3 days at - 80 °C, after which the cells were transferred to liquid nitrogen for long term storage.

2.3.1.3 Preparation of New Cell Stock from Liquid Nitrogen

A new stock of frozen cells was defrosted rapidly, and the cell suspension added to 10 ml of DMEM without FBS and Penicillin-Streptomycin. The cell suspension was centrifuged at 1100 rpm for 5 min. The supernatant was discarded, and the pellet was resuspended gently in 10 ml pre-warmed DMEM supplemented with 20 % (v/v) FBS and 1 % (v/v) Penicillin-Streptomycin in a sterile tissue culture plate. The plate was placed in the CO_2 incubator until the cells reached 80-90 % confluency.

2.3.1.4 Cell Synchronisation

HeLa cells were synchronised at the G1/S boundary by treatment of an asynchronous population with either Thymidine (2 mM) or Aphidicolin (5 µg/ml) for 24 hrs. Cells were released from the Thymidine or Aphidicolin block by washing four times with DPBS and incubating them in DMEM + Taxol (60 nM) to arrest cells in M-phase. Asynchronous cells were collected by washing cells three times with DPBS and incubation with 2 ml Cell Dissociation Medium for 20 minutes. Mitotic cells (Taxol-arrested cells) were harvested by mitotic shake-off (gentle shaking of the tissue culture plate to detach the mitotic cells).

2.3.1.5 Preparation of cell lysates from a synchronized cell population

HeLa cells were seeded overnight to reach 70- 80 % confluency the next day. The cells were blocked at the G1/S boundary with Thymidine (2 mM) for 24 hrs. After 24 hrs, the cells were washed four times with DPBS and released into pre-warmed complete DMEM and incubated in a CO_2 incubator at 37 °C. Following Thymidine release, cells were collected at different time points (0-17 hrs) and lysed in RIPA buffer to prepare total cell lysates. A parallel set of samples were collected for

FACS. The status of the anti-apoptotic proteins (Bcl-2 and Bcl-xL) and cyclin B1 during the normal cell cycle was examined by western blotting.

2.3.1.6 Cell treatment with Taxol and RO-3306

HeLa cells (70- 80% confluent) were blocked at G1/S phase with 2 mM Thymidine for 24 hrs. After 24 hrs, the cells were washed four times with DPBS and released into pre-warmed complete DMEM with Taxol (60 nM) and maintained in a CO_2 incubator at 37 °C for 12 hrs. After 12 hrs incubation with Taxol, the mitotically-arrested cells were incubated with Taxol + RO-3306 (1 or 5 µM) for varying times. Cell samples were collected at different time points and lysed in lysis buffer B to prepare total cell lysates. The effects of Taxol with or without RO-3306 on the anti-apoptotic proteins (Bcl-2 and Bcl-xL), PARP cleavage, cyclin B1 and Cdk1 were examined by western blotting.

2.3.1.7 PI staining for the cell cycle

Cells (asynchronous/ Thymidine or Taxol-arrested) were harvested and washed with DPBS and then fixed with 1 ml ice-cold (-20 °C) 70 % (v/v) ethanol and stored at -20 °C. Prior to analysis, the cells were centrifuged at 1100 rpm for 5 min at RT and resuspended in 1 ml stain solution (930 µl 1X PBS, 50 µl RNAase solution (10 mg/ml) and 20 µl Propidium iodide solution (1 mg/ml)). The cells were then incubated at RT in the dark for 1 to 6 hrs and analysed using the BD Accuri C6 Plus Flow Cytometer. Data was analysed using FlowJo (Version 10.0.6).

2.3.2 Molecular Biology Techniques

2.3.2.1 Plasmid DNA purification

Individual bacterial colonies were picked and grown in 10 ml of LB media with the appropriate antibiotic. The culture was incubated in a shaking incubator (225 rpm) for 16 hrs at 37°C. Following 16 hrs, 5 ml of the bacterial suspension was added to 250 ml of LB media supplemented with the appropriate antibiotic and incubated in a shaking incubator for a further 16 hrs. Following the second incubation, cells were harvested by centrifugation (3500 rpm) for 20 min at 4°C. The supernatant was discarded, and the pellet was used for DNA purification. Plasmid DNA purification of the EGFP vector (Invitrogen) and EGFP-Bax was performed using the QIAGEN Plasmid Midi Kit as outlined in the manufacture's protocol. A Nanodrop spectrophotometer (Nano Drop 2000, Thermo Scientific) was used to measure the plasmid DNA concentration.

2.3.2.2 Transient transfection (6-well Plate)

HeLa cells were cultured on sterile coverslips in 6 well plates, so that the cells reached 50-60% confluency on the day of the transfection. FuGENE HD transfection reagent (Promega) was used to transfect the cells as outlined in the manufacture's protocol. FuGENE HD (6 µl) was directly added to 93 µl of serum-free DMEM and mixed by gentle flicking. Plasmid DNA (0.5-1 µg) was added to the FuGENE HD/ serum-free DMEM mixture and mixed by gentle flicking. The mix was incubated for 20-30 min at RT. The medium in the 6 well plates was removed and replaced with 2 ml of fresh DMEM. The transfection mix was added dropwise to each well and the cells incubated for 36 hrs at 37 °C in a 5% CO_2 incubator.

2.3.2.3 siRNA Transfection (6 well plates)

siRNA was carried out using ON-TARGET plus Human siRNA-SMART pool (Dharmacon). INTERFERin® (Polyplus) was used as siRNA transfection reagent as described in the manufacture's protocol. The cells were 50-60 % confluent on the day of the transfection. The appropriate concentration of siRNA or control siRNA was added to 200 µl of the transfection medium and vortexed gently for 10 seconds. INTERFERin (8 µl) was added to siRNA/ transfection medium mixture and vortexed gently for 10 seconds. After 30 min incubation at RT, the transfection mix was added dropwise to a single well in 6-well plate containing 2ml complete DMEM. The transfected cells were incubated for 48 hrs at 37 °C in a 5% CO_2 incubator. One well of a 6-well plate was left untreated as an additional control. All steps were performed in a laminar flow cell culture hood using sterile techniques. After 48 hrs, the transfected cells were washed three times with DPBS and the cell lysates were prepared by adding 100 µl of RIPA buffer. Cell lysates were normalised using a Bradford assay and Western blot was used to confirm the siRNA-depletion of the targeted gene.

2.3.3 Microscopy

2.3.3.1 Glass coverslips Preparation

Glass coverslips (22 mm diameter) were rinsed three times in deionised water and incubated with 1 M HCL for 30 min. The coverslips were washed four times with deionised water and then rinsed in 100 % ethanol before they were air-dried at RT and autoclaved by heating in an oven for 30 min at 180 °C. The sterile coverslips were stored in sterile tissue culture plates until required.

2.3.3.2 Attaching Cells to Polylysine-coated Coverslips

Coverslips were immersed in Polylysine solution (1 mg/ml) in a six-well plate for 5-10 minutes. After removing the Polylysine solution, the coverslips were rinsed in deionised water and dried at RT in the same six-well plate. In the tissue culture hood, the cell suspension was added to the Polylysine-coated coverslips and incubated for 30 minutes in a CO_2 incubator to adhere cells before being fixed.

2.3.3.3 Immunofluorescence microscopy

Cells were grown on sterile glass coverslips in 6 well plates or attached to Polylysine-coated coverslips. Cells on the glass coverslips were fixed in ice-cold (-20 °C) methanol for 30 min at -20 °C. Alternatively, cells were fixed in 3.7 % (v/v) formaldehyde at RT for 20 min followed by permeabilization with 0.1 % (v/v) Triton X-100 for 10 min. Coverslips were then washed three times with DPBS prior to incubation with the blocking buffer. Nonspecific binding of antibody was blocked by incubating with 1% (w/v) bovine serum albumin (BSA) in PBS containing 0.1% (v/v) Tween-20 for 45-60 min at RT. Subsequently, the cells were incubated with appropriate primary antibodies for 1 hr at RT. The primary antibody was diluted in blocking buffer according to manufacturer's instruction. Coverslips were washed ×3 with DPBS. After washing, the cells were incubated with the appropriate secondary antibodies for 1 hr at RT in the dark. The secondary antibodies were also diluted in blocking buffer. After washing three times with DPBS, the DNA was stained by incubating the cells with Hoechst 33342 (1µg/ml in DPBS) for 2-5 min at RT. Coverslips were again washed three times with DPBS, mounted on glass slides with one drop of mounting medium (either n-propyl gallate or Vectorshield Mounting Medium), and sealed with clear nail varnish to prevent drying and observed under a fluorescence microscope.

Immunofluorescence images were acquired on a Nikon Eclipse (TE 300 semi-automatic, Tokyo, Japan) and captured by using Hamamatsu ORCA-R2 digital

camera (Photonics, Bridgewater, NJ). Alternatively, confocal images were acquired on a Leica Confocal SP5. Z stacks comprising 30-50 0.3µm sections were acquired and the images were analysed as maximum intensity projections using Image J software. Pearson's correlation coefficient was performed using the Pearson's correlation function in the SP5 software, and the mean values (±S.D.) were calculated from 10 images of 3 independent experiments.

2.3.4 Biochemical techniques

2.3.4.1 Preparation of cell lysates

Cell lysates of untreated or Staurosporine-treated cells were prepared by washing three times with DPBS followed by addition of 100 µl RIPA buffer. The cells were scraped, and the homogenates were transferred into pre-cooled eppendorf tubes. The cell lysates were vortexed for 10 seconds and kept on ice for 20 minutes. Subsequently, the cell lysates were clarified using an Eppendorf Centrifuge (5417R) at 14.000 rpm for 20 minutes at 4°C. The supernatant was transferred to a fresh pre-cooled eppendorf tube and stored at -80°C until required. For cells treated with Taxol, the mitotically-arrested cells were collected by mitotic shake–off and centrifuged at 1100 rpm for 5 minutes at RT. After centrifugation, the media was removed, and the pellet washed two times with DPBS, followed by lysis in 100 µl RIPA buffer. The cell lysates were prepared as described before and stored at -20 °C or -80 °C until required.

2.3.4.2 Preparation of cell lysates for examination of Bak and Bax oligomers

To examine oligomeric forms of Bak and Bax, the cells were treated with Taxol for 16-36 hrs. The mitotically-arrested cells were collected by shake-off and

centrifuged at 1100 rpm for 5 min at 4°C. Cell pellets were washed with DPBS and incubated with buffer A containing 0.01% (w/v) digitonin for 2 min at 4°C. The cross-linking agent DSP (1 mM final concentration) was added after cell permeabilization and quenched with 0.1 volume of (2 M) Tris-Hcl (pH 7.5). After centrifugation at 14000 rpm for 15 min, the membrane and organelle- bound proteins were released by incubating the pellets in buffer A containing 3% CHAPS for 45 min at 4 °C, and the supernatant was collected by centrifugation at 14000 rpm for 15 min at 4 °C. The samples were mixed with 5X SDS-PAGE sample buffer either with or without β-mercaptoethanol and heated at 70 °C for 5 min before loading onto SDS-PAGE gel and western blotting.

2.3.4.3 Protein assay

A protein assay kit (Bradford) was used to measure the protein concentration of the cell lysate. A standard curve was constructed by using bovine serum albumin (BSA) (Pierce, 2 mg/ml) according to the manufacturer's instructions. The absorbance of the samples was measured at 595 nm using a spectrophotometer (Norvaspec plus, Amersham Biosciences).

2.3.4.4 Sodium dodecyl Sulphate-Poly Acrylamide Gel Electrophoresis (SDS-PAGE)

Proteins were separated using SDS-PAGE (Bio-Rad Mini proteins 2). According to the reagents shown in Table 2.6, either 7 %, 10 % or 12.5 % SDS-polyacrylamide gels were prepared. A stacking gel (3 %) was prepared from the reagents shown in Table 2.6 and poured on the top of the polymerized running gel. Normalised cell lysates, containing 20-100 µg of protein, were mixed with 2X SDS-PAGE sample buffer in a 1: 1 ratio and heated at 95°C for 5 min. The protein samples

were centrifuged for 10 seconds and loaded on the gel. A molecular weight marker (5 µl), (Multicolour Broad Range Protein Ladder, ThermoScientific), was also loaded next to the samples. Gels were electrophoresed in running buffer at 120V for about one hour, till the running front reached the bottom of the gel. The gels were subsequently processed for Western Blotting.

2.3.4.5 Western Blotting

Following gel electrophoresis, the gel was soaked in transfer buffer for 10 min. Whatman chromatography paper 3 MM (6 pieces) and a nitrocellulose membrane (0.45 µM) were soaked in transfer buffer for 1 min. The gel was placed on a nitrocellulose membrane and sandwiched between 3 pieces of Whatman's paper on each side. Proteins were transferred by electroblotting at 60 mA/gel at RT for 1 hr using a Semi-Dry Transfer Unit (Amersham Biosciences). The blot was incubated in blocking buffer, dried milk powder or BSA (5% w/v) in Tris-Saline-Tween (TST), for 1 hr at RT to block nonspecific protein binding sites. The blot was then incubated with a primary antibody for 1 hr at RT or overnight at 4°C on a roller. After incubation, the blot was washed six times (10 minutes for each) with 1× TST to remove unbound antibody. The blot was then incubated with a secondary antibody conjugated with Horseradish Peroxidase (IgG-HRP) for 2 hrs at RT on a roller. Both the primary and secondary antibodies were diluted in blocking buffer. The blot was then washed six times with TST. The blot was incubated with EZ-ECL reagent (Chemiluminescence Detection Kit) for 5 minutes, enclosed in wrap, and immediately exposed to X-ray films (Santa Cruz Biotechnology) and developed in an automatic film processor (X-ray processor SRX-101A, Konica Minolta, UK).

The blots were scanned (CanoScan LiDE 90), and the images processed for clarity using Microsoft PowerPoint. ImageJ software was used to quantify the intensity of the bands. In brief, the background of the entire image was subtracted. The bands were then selected using the rectangle tool and the intensity profiles were

plotted by giving a number to each rectangle. The area under the peaks was measured using the magic wand tool and that represents a quantification of the intensity of the band. The intensity of the interested proteins was normalized to the intensity of the α-tubulin, and the mean values (±S.D.) were calculated from three independent experiments.

2.3.4.6 Immunoprecipitation and Co-immunoprecipitation (IP and co-IP)

Immunoprecipitation of proteins from cell lysates was performed using Pierce protein A/G magnetic beads. Untreated or Taxol-treated cells were lysed in lysis buffer B (to immunoprecipitate the active and inactive form of Bak and Bax) or 1 % CHAPS lysis buffer (to immunoprecipitate the active form of Bak and Bax). The magnetic beads (50 µL/sample) were collected with a magnetic stand and washed three times with ice-cold washing buffer. The cell lysate (1-1.5 mg) was precleared with 50µL (0.5mg) protein A/G magnetic beads according to the manufacture's protocol. The precleared cell lysate was incubated with 10 µL (2 µg) mouse monoclonal anti-active Bax (6A7) antibody or goat polyclonal anti-active Bak (N-20) antibody for 3-4 hrs at 4 °C on a rotator. The immunocomplexes (Bak and Bax IPs) were captured by adding prewashed magnetic beads (50µL) and incubated for an additional 3-4 hrs at 4 °C with mixing. The magnetic beads were then collected with the magnetic stand and washed three times with ice-cold washing buffer. The beads were re-suspended in 25 µL 2X SDS-PAGE sample buffer for 20 minutes at RT, to elute the immunoprecipitated proteins from the complex. The beads were sedimented with the magnetic stand and the supernatant collected, without heating, and analysed by Western blotting.

2.3.4.7 Preparation of samples for mass spectrometry

The immunoprecipitated Bak or Bax from untreated and Taxol-treated cells (60 nM for 24 hrs) were resolved on a 12.5% SDS-PAGE and the gel stained with colloidal coomassie instant blue stain overnight. The appropriate band was cut out from the gel and sent to the Protein and Nucleic Acid Chemistry Laboratory (PNACL), University of Leicester. The IPs were subjected to peptide mass fingerprint analysis (LTO-Orbitrap-Velos-ETD mass spectrometer) and the data were analysed using Scaffold software (Peptide threshold 95% and Protein Identification Probability 100%).

2.3.5 *In Vitro* Protein-Protein Interaction Assay

Bax-Cdk1 binding was carried out using a direct *in vitro* protein-protein interaction assay. Equimolar concentrations (50 µM) of human recombinant GST-Cdk1 and either wild type Bax or GST-Tag Bax were mixed and incubated in 1 % CHAPS lysis buffer for 2 hrs at 4 °C. GST-PAK alpha protein was used as a control. After incubation, Cdk1 was immunoprecipitated using a Cdk1-specific antibody Cdc2p34 (17) as described in section 2.3.4.6. The immunoprecipitated Cdk1 was washed three times in cold (4 °C) IP wash buffer and the beads resuspended in 30 µl 2X sample buffer. The IPs were resolved on a 12.5 % SDS-PAGE gel and western blotted for Cdk1, Bax and PAK-α using specific antibodies.

2.3.6 Histone H1 kinase assay

To assay Cdk1 kinase activity in Bax, Bak and Bax/Bak-depleted cells, an *in vitro* kinase assay was performed. Cdk1 was immunoprecipitated from either untreated or transfected (control siRNA, Bax siRNA, Bak siRNA or both Bax and Bak siRNA) HeLa cells using Cdk1-specific antibody Cdc2p34 (17). The transfected

cells were treated with Taxol (60 nM) for 12 hrs, and the cells collected by mitotic shake-off and lysed in Cdk1 Lysis buffer. As a control, a parallel set of Taxol-treated cells was incubated with RO-3306 (5 µM) for 4 hrs to inhibit Cdk1 activity.

The immunoprecipitated Cdk1 was washed three times in cold (4 °C) IP washing buffer and two times in cold (4 °C) Cdk1 assay buffer (Table 2.5, page 48). Following the final wash, the beads were resuspended in 20 µl of kinase assay mix. The kinase assay mix included 0.4 µl cold ATP (4 mM), 4 µCi of [ϒ-32P]-ATP, 2 µl of Histone H1 (20 mg/ml) and 17.2 µl of kinase assay buffer. The samples were incubated at 30 °C for 20 min and the reactions were stopped by adding 20 µl of 2X sample buffer. Each sample (20 µl) was run on a 12.5 % SDS-PAGE gel. The gel was stained with Instant Blue colloidal Coomassie and dried on a gel dryer (Bio-Rad). The dried gel was placed on X-Ray film and developed to visualise the phosphorylated histone H1.

2.3.7 Statistical analysis

GraphPad Prism 7.0. was used to analyse the data. The mean of at least three independent experiments and P values were calculated using one-way ANOVA, unless otherwise stated, $P<0.05$ was considered to be statistically significant. Correlation analysis was performed using Pearson's correlation coefficient with $P<0.05$ considered to be statistically significant.

Chapter 3. Taxol-induced apoptosis is dependent on both Bax and Bak

3.1 Introduction

Microtubule-targeting agents (MTAs), such as Taxol, interfere with the mitotic functions of microtubules and cause cell cycle arrest, which is then followed by cell death via activation of the mitochondrial-dependent pathway (Barbuti and Chen, 2015). Proteins of the Bcl-2 family tightly regulate mitochondrial-dependent apoptosis that causes mitochondrial outer membrane permeabilization (MOMP) (Roy et al., 2014). MOMP facilitates apoptogenic factors such as cytochrome c to be released from the mitochondrial intermembrane space into the cytoplasm, which triggers caspase activation and destruction of essential cellular components (Bratton and Salvesen, 2010).

The major pro-apoptotic proteins, Bax and Bak, commit mitotically arrested cells to undergo apoptosis by inducing MOMP (Westphal et al., 2011). It was reported that depletion of Bax was more effective than Bak in inhibiting Taxol-induced apoptosis in MDA-MB-231 cells (Bah et al., 2014). Another study reported that depletion of Bax does not have a major effect on Nocodazole-induced apoptosis in HeLa cells, whereas depletion of Bak significantly reduced mitotic cell death (Haschka et al., 2015). Although these pro-apoptotic proteins play an essential role in mitotic cell death upon receipt of an apoptotic stimulus, their specific contribution to Taxol-induced apoptosis remains unclear. In this chapter I asked whether only one of them or both are important to initiate mitotic cell death in response to Taxol.

3.2 Intracellular Bax and Bak were efficiently depleted using Bax and Bak siRNA

In order to examine the role of Bax and Bak in Taxol-induced mitotic death, Bax and Bak expression was depleted using siRNA. Protein expression levels of Bax and Bak were targeted individually using different concentrations of siRNA (25nM, 50nM and 100nM) to determine the effective siRNA concentrations that efficiently target Bax and Bak mRNA. HeLa cells extracts were prepared for untreated, control, and varying concentrations of Bax and Bak siRNA for Western blot analysis. As shown in Figure 3-1 the pro-apoptotic protein Bax was clearly detectable in control siRNA, untreated and 25 nM Bax siRNA-treated HeLa cells but was completely absent in 50 nM and 100 nM Bax siRNA treated cells. Likewise, Bak protein was clearly detectable in control siRNA and untreated HeLa cells. However, it was slightly detectable with 25 nM Bak siRNA but strongly depleted at 50 nM and 100 nM Bak siRNA treated cells (Figure 3-2). Immunoblot analysis revealed that Bax siRNA did not affect Bak expression and Bak siRNA did not affect Bax expression at the concentrations tested. These results suggest that intracellular Bax and Bak could be specifically and efficiently depleted by using siRNA.

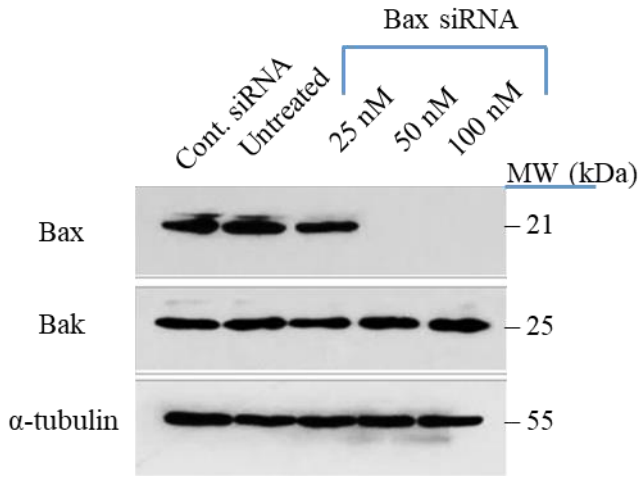

Figure 3-1: siRNA depletion of Bax

HeLa cells were either left untreated or transfected with either control (50 nM) or Bax siRNA (25-100nM) and incubated for 48 hrs. After 48 hrs, total cell extracts were prepared and subjected to immunoblot analysis with the indicated antibodies. α-tubulin was used as a loading control and the molecular weight markers are shown on the right. This result is representative of 2 independent experiments.

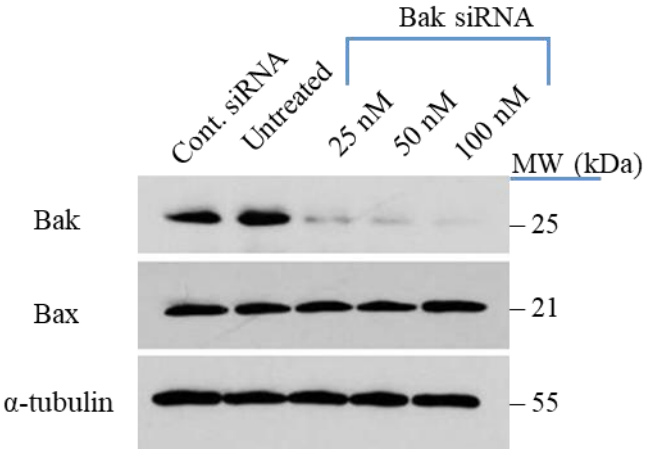

Figure 3-2: siRNA depletion of Bak

HeLa cells were either left untreated or transfected with either control (50 nM) or Bak siRNA (25-100nM) and incubated for 48 hrs. After 48 hrs, total cell extracts were prepared and subjected to immunoblot analysis with the indicated antibodies. α-tubulin was used as a loading control and the molecular weight markers are shown on the right. This result is representative of 2 independent experiments.

3.3 Depletion of Bax inhibits Taxol-induced apoptosis and re-expression of GFP-Bax can rescue Taxol-induced apoptosis in HeLa cells

I examined the effect of siRNA depletion of Bax on Taxol-induced apoptosis. To determine whether HeLa cells undergo apoptosis in response to Taxol treatment, the cells were either left untreated or transfected with either control or Bax siRNA; in one set of Bax siRNA-treated cells, Bax was re-expressed with GFP-Bax. The cells were then treated with Taxol for 24 hrs and collected by mitotic shake-off. Immunofluorescence analysis was performed using the CytoDEATH (M30) antibody, which recognizes caspase-cleaved cytokeratin 18 (Li et al., 2017). Mitotic death in response to Taxol treatment was reduced substantially in HeLa cells transfected with Bax siRNA in comparison to non-transfected or control siRNA-treated cells. My results indicated that depletion of Bax significantly reduced apoptosis from 83.3% in the control siRNA-treated cells to 22.3% in the Bax-depleted cells upon Taxol treatment (Figure 3-3 A and B). I next investigated whether re-expression of GFP-Bax could rescue mitotic death in the Bax-depleted HeLa cells. The cleavage of cytokeratin 18 was significantly increased upon re-expression with GFP-Bax and followed by Taxol treatment. The number of the apoptotic cells was increased from 22.3% in the Bax-depleted cells to 88% following re-expression of GFP-Bax, suggesting a key role for Bax in Taxol-induced apoptosis. This result also strongly suggested that in the absence of Bax, Bak was not sufficient to induce MOMP upon Taxol treatment (Figure 3-3 A and B).

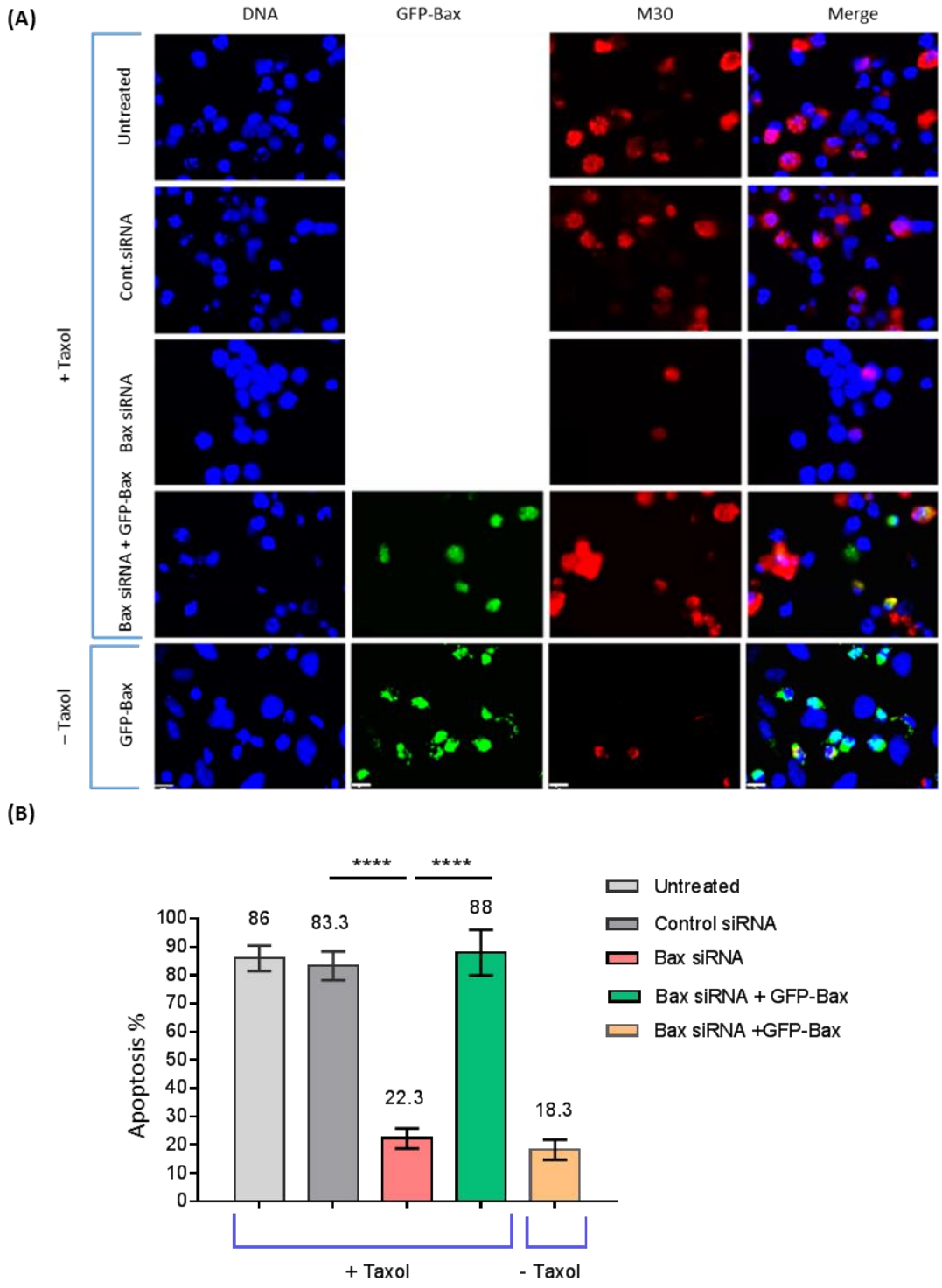

Figure 3-3: Depletion of Bax inhibits Taxol-induced apoptosis and re-expression of GFP-Bax can rescue apoptosis.

(A) Representative images of Taxol-induced apoptosis in HeLa cells after Bax depletion. HeLa cells were either left untreated or transfected with either control or Bax siRNA (50nM) and incubated for 48 hrs. After 48 hrs, one set of Bax siRNA-treated cells was re-expressed with GFP-Bax and incubated for further 24 hrs. The cells were then treated with Taxol (60nM) for 24 hrs. Mitotically arrested cells were collected by mitotic shake-off, fixed and stained with M30 antibody (red) and DNA was stained with Hoechst 33342

(blue), GFP-Bax (green). Results are representative of three independent experiments. **(B)** Quantitation of apoptosis for the experiment described in (A), 100 cells were counted in randomly selected fields and the mean values calculated from three independent experiment (±S.D.). P-values were calculated using one-way ANOVA (**** P value <0.0001).

3.4 Bak and Bax play a key role in Taxol-induced mitotic cell death

It has been reported that mitochondrial-mediated apoptosis requires the activation of either Bak or Bax to permeate the mitochondrial outer membrane (Bah et al., 2014, Haschka et al., 2015). I therefore examined whether only Bak or Bax or both proteins are required to induce apoptosis upon Taxol treatment. Either Bak, Bax or Bak/Bax siRNA (50nM) were used to deplete Bak and Bax mRNA in HeLa cells. Western blots were performed to verify the protein expression levels of both Bak and Bax (Figure 3-4). Untreated and transfected cells (control siRNA, Bax siRNA, Bak siRNA and both Bax/Bak siRNA) were treated with Taxol for 24 hrs and levels of apoptosis were analysed using M30 antibody. As shown in Figure 3-5 A and B, depletion of Bax caused a significant decrease in Taxol-induced apoptosis as judged by cytokeratin 18 cleavage (23.3% apoptosis) in comparison with the control siRNA-treated cells (71.3% apoptosis). Likewise, depletion of Bak also caused a marked decrease of Taxol-induced apoptosis (17%). Furthermore, depletion of both Bak and Bax resulted in inhibition of mitotic cell death to a larger extent than the depletion of either Bak or Bax alone. Cytokeratin 18 cleavage was significantly reduced in the Bak/Bax depleted cells (14.3% apoptosis) in comparison to control siRNA treated cells (71.3% apoptosis). These results suggested that depletion of Bax and Bak individually or in combination has an important role in reducing mitotic cell death induced by Taxol. Collectively, both Bak and Bax appear to play a critical role in the induction of mitotic cell death and suggests that both proteins are required for Taxol-induced apoptosis in HeLa cells.

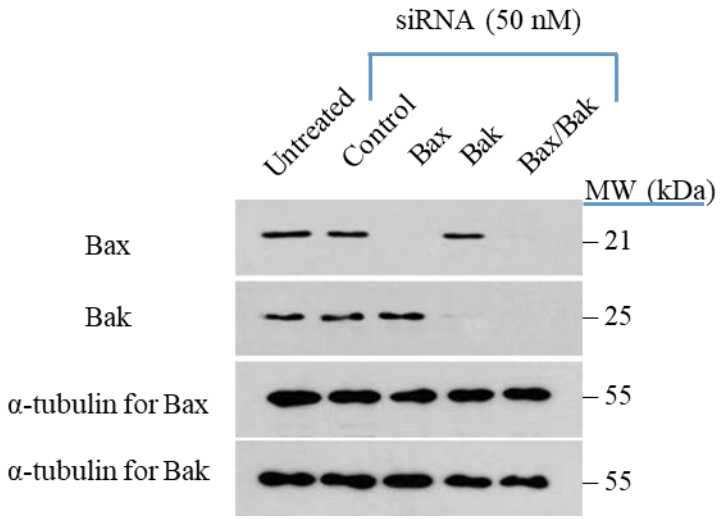

Figure 3-4: Depletion of either Bax, Bak, or both Bax and Bak expression

HeLa cells were either left untreated or transfected with control (50nM), Bax (50nM), Bak (50nM), or both Bak and Bax siRNA (50nM), and incubated for 48 hrs. After 48 hrs, cell extracts were prepared and subjected to Western blotting with the indicated antibodies. α-tubulin was used as a loading control and the molecular weight markers are shown on the right. This result is representative of 2 independent experiments.

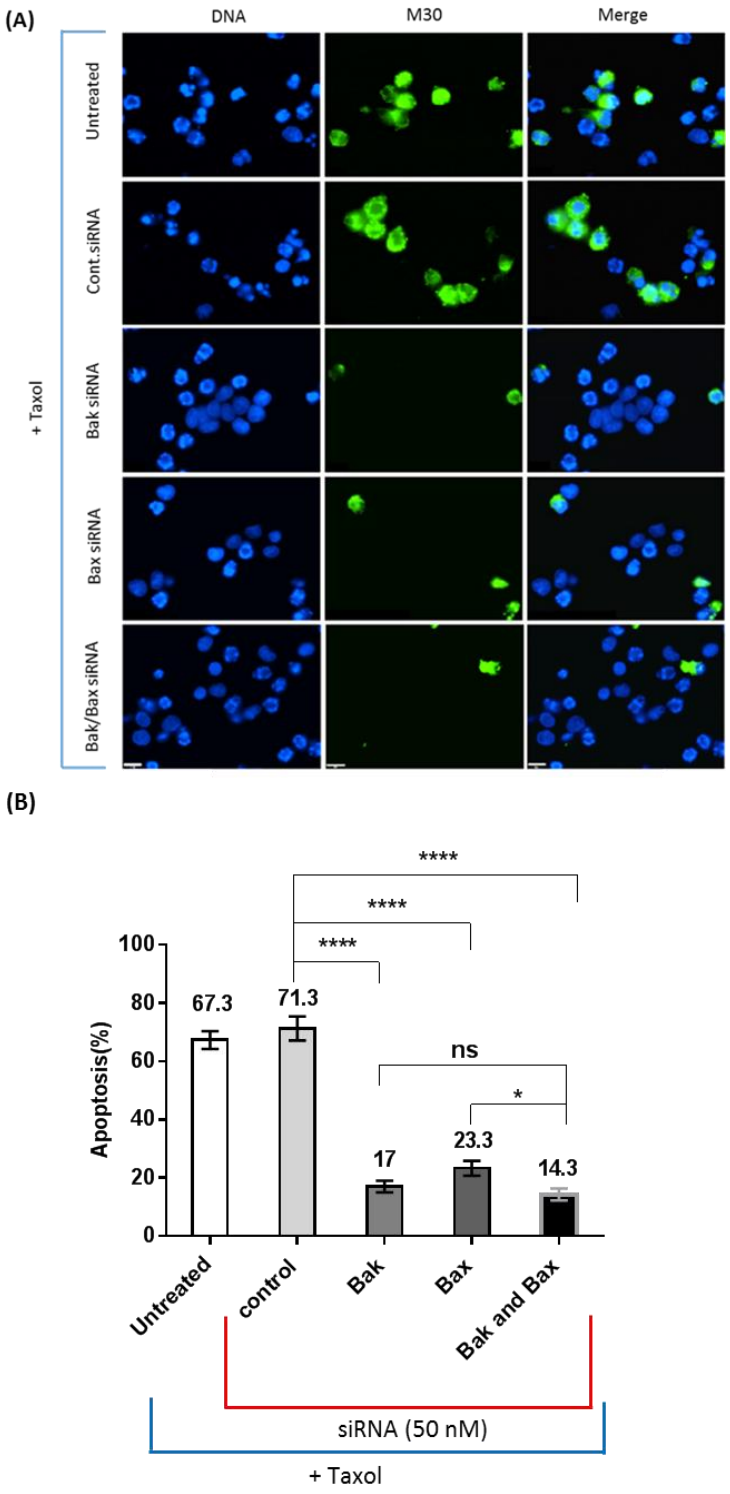

Figure 3-5: siRNA depletion of either Bak, Bax or both Bak and Bax inhibit Taxol-induced apoptosis.

(A) Representative images of Taxol-induced apoptosis in HeLa cells after Bak, Bax or both Bak/Bax depletion. HeLa cells were either left untreated or transfected with control, Bak, Bax or both Bak/Bax siRNA (50nM) and incubated for 48 hrs. After 48 hrs, the cells were treated with Taxol (60nM) for 24 hrs. Mitotically arrested cells were fixed and stained with M30 antibody (green colour) and DNA was stained with Hoechst 33342

(blue colour). Results are representative of three independent experiments. **(B)** Quantitation of apoptosis for the experiment described in (A), 100 cells were counted in randomly selected fields and the mean values calculated from three independent experiment (±S.D.). P-values were calculated using one-way ANOVA (* P value <0.05, **** P value <0.0001).

3.5 Bax and Bax expression in different cell lines

In order to further examine the role of Bax/Bak in Taxol-sensitivity in human cell lines, I determined the levels of both Bak and Bax in several human cancer cell lines, in addition to retinal pigment epithelium cells (RPE1) and mouse myoblast cells (C2C12). Bax and Bak levels were examined by Western blotting of total cell extracts prepared from non-transformed RPE-1, C2C12 and a number of cancer cell lines (HeLa, Melanoma, U2OS, Mesothelioma, RKO 143, STK 5090 and A19 RKO), previously described in section 2.1.2 page 44. My results shown that expression of Bax was significantly higher in lung cancer cell line (STK5090) and Melanoma compared to RPE1 cells (Figure 3-6 A and B). However, the expression of Bak was significantly higher in two colorectal cancer cell lines, RKO143 and A19RKO in comparison to RPE1 cells. Most strikingly, the lung cancer cell line STK5090 showed the lowest Bak expression, which is significantly lower in comparison to RPE1 cells (Figure 3-6 A and C). The low level of Bak in STK5090 cells promoted me to further investigate Taxol-induced apoptosis in this cell line.

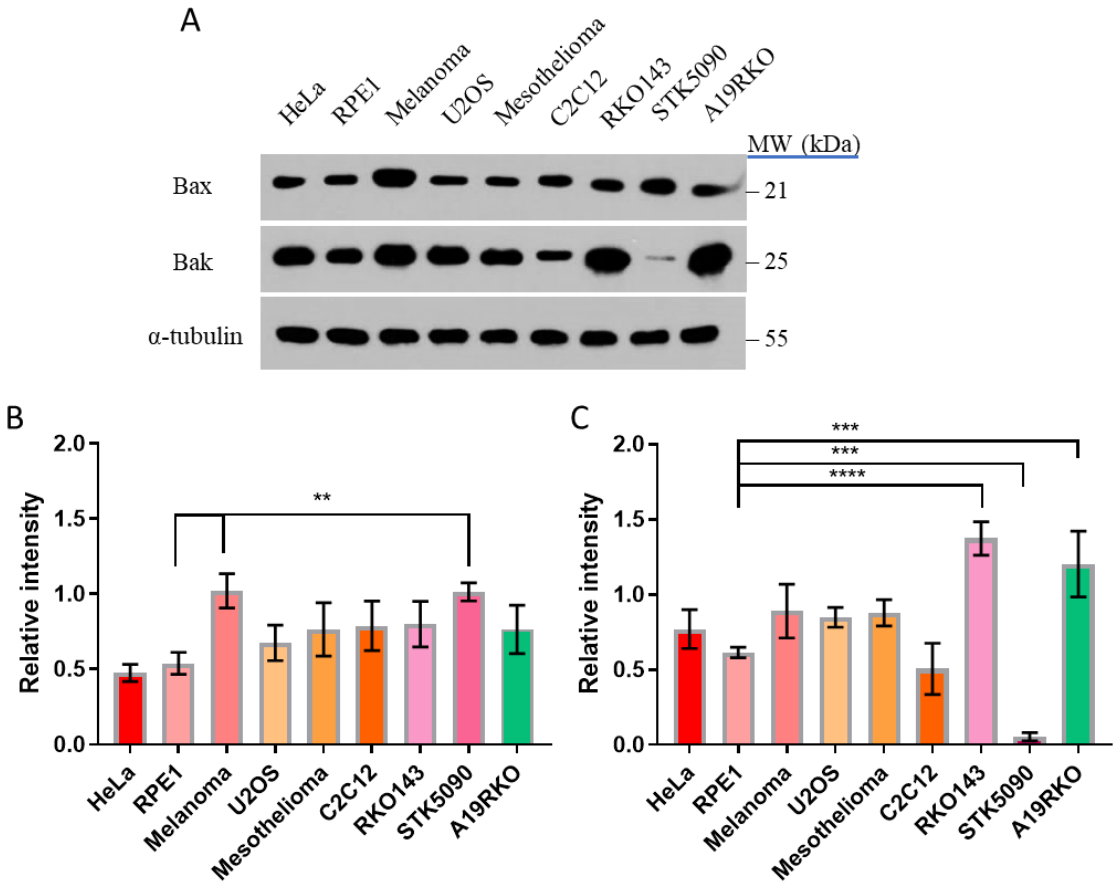

Figure 3-6: Protein expression of Bax and Bak in different cell lines.

(A) Exponentially growing HeLa, RPE1, Melanoma, U2OS, Mesothelioma, C2C12, RKO 143, STK 5090 and A19 RKO cells were lysed in RIPA buffer and the normalized cell extracts were subjected to immunoblotting for Bax and Bak. α-tubulin was used as a loading control and the molecular weight markers are shown on the right. This result is representative of 3 independent experiments. (B) and (C) Histograms represent the intensity of Bax and Bak expression in different cell lines normalized to α-tubulin from blots shown in A, respectively. Histograms represent the mean ± SD of three independent experiments. P-values were calculated using one-way ANOVA (** P value < 0.01), (*** P value < 0.001, **** P value <0.0001).

3.6 STK 5090 cells were resistant to Taxol treatment

We determined the levels of Bak protein in nine different cell lines. Among the cell lines we investigated, STK50590 showed the lowest Bak expression (Figure 3-6, page 79). In order to examine the role of Bak in Taxol-induced apoptosis in STK 5090 cell lines, synchronized population of STK 5090 cells were either left

untreated or treated with 1 µM Taxol for 24 hrs. As shown in Figure (3-7), STK 5090 cells were resistant to Taxol, suggesting that the level of Bak could determine Taxol sensitivity and supported the siRNA experiments, which indicated that both Bak and Bax may be required for Taxol-induced apoptosis in HeLa cells.

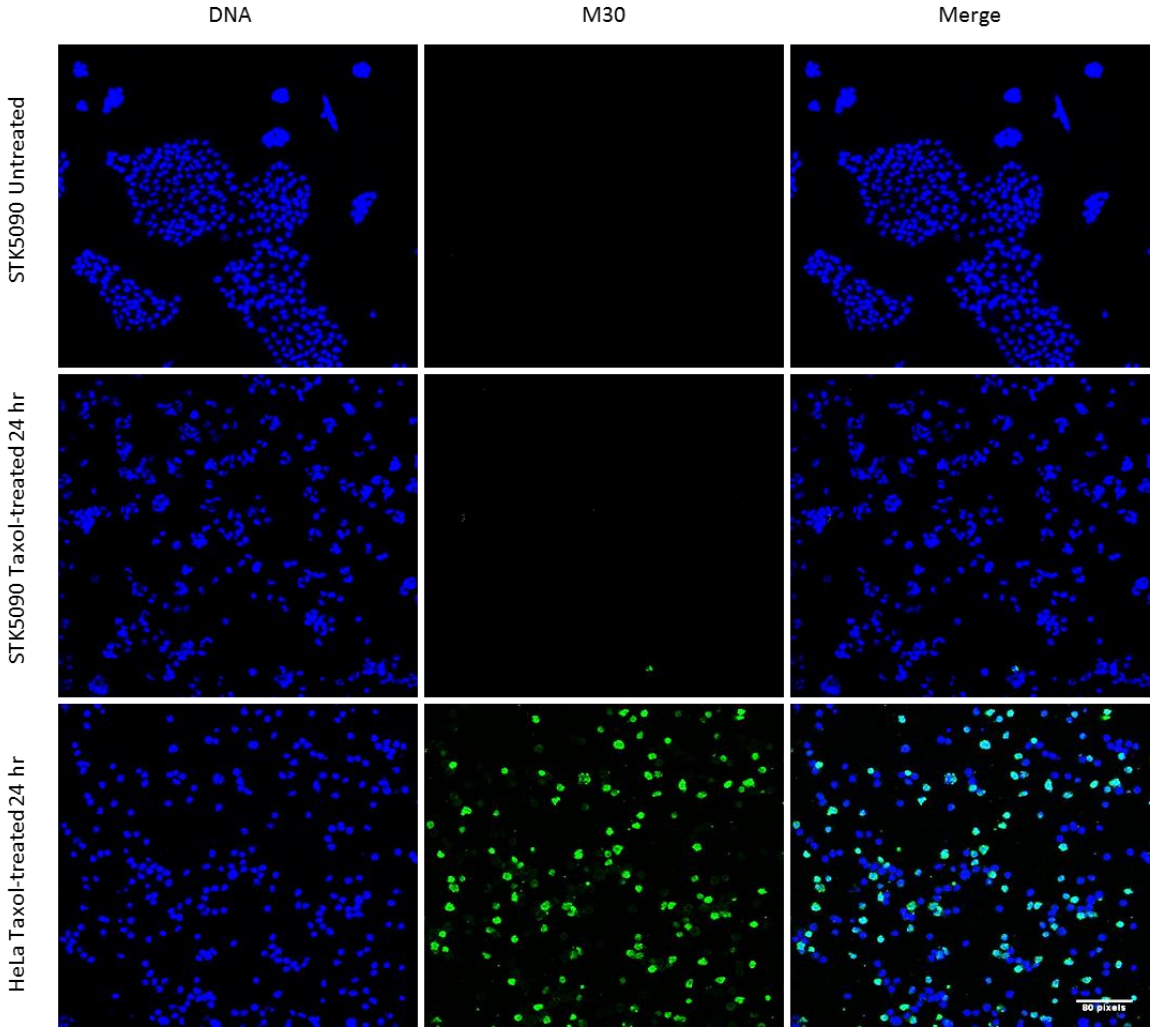

Figure 3-7: STK 5090 cells were resistant to Taxol-induced apoptosis.

STK 5090 cells were synchronized at the G1/S boundary by thymidine arrest for 24 hrs and released. The cells were either left untreated or treated with 1 µM Taxol for 24 hrs. One set of HeLa cells was treated with Taxol (60 nM) for 24 hrs as a control. Taxol-treated cells were collected by mitotic shake-off, fixed and stained with M30 antibody (green colour). DNA was stained with Hoechst 33342 (blue colour). Images are representatives from one out of two experiments yielding similar results.

3.7 Discussion

Taxol is one of the most common chemotherapeutic agents used against different types of blood or solid cancer. Taxol is a microtubule-stabilizer which suppresses dynamic instability of the microtubule, and causes mitotic arrest via activation of the mitotic checkpoint (Weaver, 2014). This in turn results in prolonged mitotic arrest and primes mitotically arrested cells to the intrinsic pathway of apoptosis (Jordan and Wilson, 2004). The transition between prolonged mitotic arrest and the induction of mitotic cell death involves the release of cytochrome c by changing the permeability of the mitochondrial outer membrane (Karch et al., 2013). The key effector pro-apoptotic proteins, Bak and Bax, commit mitotically arrested cells to apoptosis by modifying the permeability of the mitochondrial outer membrane and facilitating the release of cytochrome c (Adams and Cory, 2007). Although these pro-apoptotic proteins play a central role in mitotic cell death upon receipt of the apoptotic stimulus, the molecular mechanism of Taxol-induced mitotic arrest followed by mitotic death via activation of mitochondrial apoptotic pathway remains unclear.

Understanding the molecular pathways of mitotic cell death during sustained mitotic arrest and how these pro-apoptotic proteins trigger the intrinsic pathway of apoptosis is critical to improve the efficacy of antimitotic drugs. In this study, using RNAi, I have highlighted the prominent role of the multidomain Bax subfamily proteins, Bak and Bax, in initiating mitotic cell death during Taxol-induced apoptosis.

The mitochondrial apoptotic pathway is regulated by Bcl-2 family proteins (Adams and Cory, 2007). In particular, it has been shown that activated Bax assembles into a cluster, semi-ring or ring-like structure in the mitochondrial outer membrane during Actinomycin D-induced apoptosis in HeLa and U2OS cell lines (Große et al., 2016). I examined whether Bax is the major pro-apoptotic protein which was involved in the Taxol-mediated mitotic cell death. Cleavage of

cytokeratin 18 induced by Taxol treatment was significantly reduced in Bax depleted HeLa cells. My results showed that mitotic cell death was decreased to 22.3% in HeLa cells transfected with Bax siRNA in comparison to control siRNA (83% apoptosis). My data is consistent with the hypothesis that Bax has a critical role in triggering mitotic apoptosis (Bah et al., 2014, Upreti et al., 2006, Yamaguchi et al., 2004).

To further investigate the role of Bax in Taxol-mediated mitotic cell death, GFP-Bax was re-expressed in Bax-depleted HeLa cells. My data demonstrated that re-expression of GFP-Bax in Bax-depleted HeLa cells can rescue apoptosis and the mitotic cell death was significantly increased from 22.3 % to 88 %. These findings are in line with a recent study which clearly identifies the functional role of GFP-Bax in apoptotic mitochondria. After 7 hrs STS treatment, GFP-Bax organized into different shapes including arcs and complete rings when GFP-Bax was re-expressed in Bak/Bax DKO HCT116 cells. Similar shapes of GFP-Bax were observed in HeLa cells between 2 to 6 hrs of STS treatment (Salvador-Gallego et al., 2016). I thus speculated that mitotic cell death in Taxol-mediated mitotic arrest is Bax dependent.

The other key effector protein Bak has been shown to be involved in the initiation of mitotic cell death in response to multiple death stimuli (Wei et al., 2001). I performed RNAi depletion experiments in HeLa cells to investigate the hypothesis that Bak is also critical in inducing mitotic cell death upon Taxol treatment. Cleavage of cytokeratin 18 induced by Taxol treatment was significantly reduced by depletion of Bak expression. My results showed that mitotic cell death was reduced to 17 % in HeLa cells transfected with Bak siRNA in comparison to 71.3 % in control siRNA-treated cells. Consistent with a recent study conducted by Haschka and colleagues, my results indicated that depletion of Bak significantly reduces mitotic cell death in response to antimitotic drugs (Haschka et al., 2015). However, my data is in contrast with another study which demonstrated that depletion of Bax was more effective than Bak in inhibiting Taxol-induced

apoptosis (Bah et al., 2014). Of note, the latter study was carried out on different cell line, breast cancer cell line MDA-MB-231 and MCF-7.

My experiments with Bak/Bax double depletion further decreased the propensity of HeLa cells to undergo mitotic cell death. The apoptotic levels in Bak/Bax double depletion (14.3%) was slightly lower than Bax siRNA (23.3%) and Bak siRNA (17%), suggesting that co-depletion of Bak and Bax can further reduce mitotic cell death. Overall, most studies are consistent with the idea that the presence of Bak and Bax can induce more efficiently apoptosis (Bah et al., 2014, Haschka et al., 2015, Upreti et al., 2008a, Tait and Green, 2013, Campbell and Tait, 2018).

I further investigated the impact of Bak in the intrinsic pathway of apoptosis. Interestingly, the lung cancer cell line STK 5090 displayed the lowest levels of Bak expression among nine different cell lines. STK 5090 cells were resistant to Taxol treatment (1µM). One possibility is that Bak may play a key role in mitochondrial outer membrane permeabilization during Taxol treatment. The prosurvival proteins such as Bcl-xL can also prevent Bax-mediated apoptosis (Fletcher et al., 2008). In conclusion, my data shown that both Bak and Bax are required for initiating mitotic cell death on Taxol treatment. HeLa cells deficient in either Bak or Bax showed a significant decrease in the apoptotic levels indicating that both Bak and Bax are functionally important for Taxol-induced apoptosis in HeLa cells.

Chapter 4. Bak-Bax interaction is required for Taxol-induced apoptosis

4.1 Introduction

Although numerous studies have investigated the effect of Taxol in a number of human cancer cells, including HeLa cells, the molecular mechanism of Taxol-induced apoptosis, particularly the organization of Bak and Bax in the mitochondrial outer membrane (MOM) during apoptosis and their interactions with other MOM/MIM (mitochondrial inner membrane) proteins, remains unclear. In the present study, I examined if Taxol promotes the activation and oligomerization of Bak and Bax. The results indicate that Taxol induced activation and oligomerization of Bak and Bax. Both proteins were mainly monomeric in untreated cells, but oligomeric forms were observed in Taxol-arrested mitotic cells. Immunoprecipitation with anti-active Bak and anti-active Bax antibodies revealed that there was a time dependent increase in the amount of active Bak and active Bax following Taxol addition. Furthermore, reciprocal immunoprecipitation experiments demonstrated that Taxol induced an interaction between active Bax and Bak and between active Bak and Bax. The interaction between Bak and Bax correlated with the induction of apoptosis. Therefore, the formation of this complex seems to be the critical step in Taxol-induced mitotic cell death.

4.2 Taxol induces Bak and Bax Oligomerization

It has been reported that the active mitochondrial membrane-embedded Bak and Bax organize into symmetric dimers. Bak and Bax symmetric dimers work as building blocks to form larger complexes in the MOM (Bleicken et al., 2013, Czabotar et al., 2013, Subburaj et al., 2015). To determine whether Taxol treatment induces oligomerization of Bak and Bax, HeLa cells were treated with Taxol for 24-36 hrs. Digitonin was used for permeabilization and DSP [dithiobis (succinimidyl propionate)] was used as a cross-linking agent (Zeng et al., 2006). Both β-mercaptoethanol-reduced and non-reduced cell extracts were then separated on an SDS-PAGE gel and immunoblotted with either a Bax or a Bak antibody. As shown in Figure 4-1 and 4-2, in untreated samples, Bax and Bak migrated as monomers at 21 kDa and 25 kDa respectively. However, following Taxol treatment, a proportion of Bax migrated at 42 and 63 kDa and Bak migrated at 50 kDa, suggesting that Taxol-induced apoptosis involves activation and oligomerization of these proteins. The oligomeric forms were only detected in the absence of the reducing agent. Bak homodimers are formed via two disulfide bonds between cysteine residues (i.e., between 69C'/111C and 69C/111C') (Mandal et al., 2016). In contrast, the disulphide bonds in Bax homodimers are formed between cysteine residues in the BH3-groove region (56C'/94C and 56C/94C') (Dewson et al., 2012). The addition of β-mercaptoethanol caused elimination of the oligomeric forms of both Bak and Bax, suggesting that disulphide bonds are required for the formation and maintenance of the oligomers.

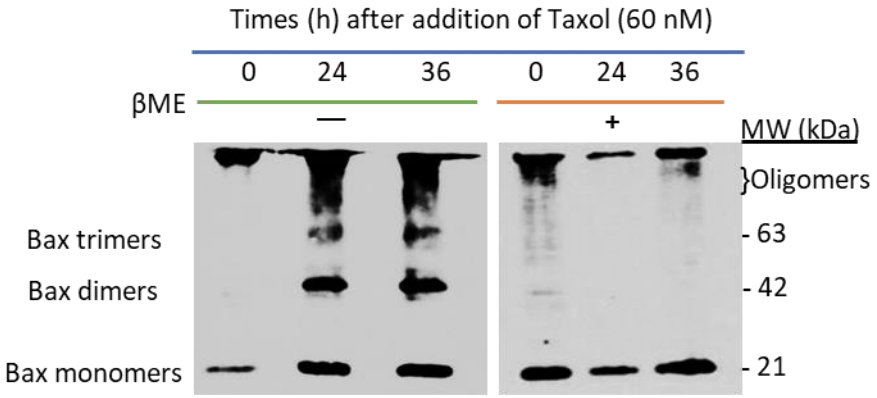

Figure 4-1: Bax oligomerization induced by Taxol.

HeLa cells were treated with Taxol (60 nM) for the indicated times and then permeabilized with 0.01% (w/v) digitonin for 2 minutes. Taxol-treated cells were lysed in a CHAPS buffer to release membrane- and organelle-bound proteins. The cell lysates were then incubated with 1 mM DSP for 10 minutes to cross-link proteins. The normalized cell extracts were subjected to immunoblotting for Bax in the absence or presence of the reducing agent (β-mercaptoethanol (βME)). The molecular weight markers are shown on the right. This result is representative of 2 independent experiments.

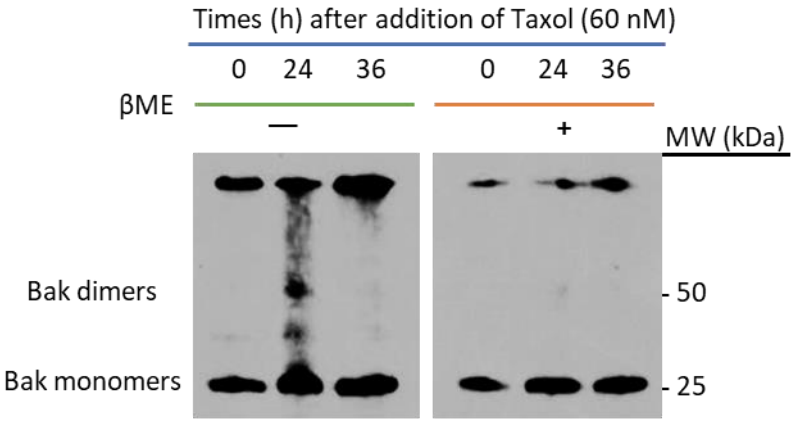

Figure 4-2: Bak oligomerization induced by Taxol.

HeLa cells were treated with Taxol (60 nM) for the indicated times and then permeabilized with 0.01% (w/v) digitonin for 2 minutes. Taxol-treated cells were lysed in a CHAPS buffer to release membrane- and organelle-bound proteins. The cell lysates were then incubated with 1 mM DSP for 10 minutes to cross-link proteins. The normalized cell extracts were subjected to immunoblotting for Bak in the absence or presence of the reducing agent (β-mercaptoethanol (βME)). The molecular weight markers are shown on the right. This result is representative of 2 independent experiments.

4.3 Bak and Bax Oligomerization occur independently of each other

To investigate the role of Bak in the reorganization and oligomerization of Bax and vice versa, either Bak or Bax was depleted using Bak or Bax siRNA, respectively. Untransfected and control siRNA samples were prepared as a positive control. Untransfected and siRNA-transfected cells were treated with Taxol for 24 hrs. As shown in Figure 4-3 and 4-4, oligomerization of Bak was detected in the absence of Bax and oligomerization of Bax was also detected in the absence of Bak. These results indicate that Bak and Bax oligomerize independently of each other in response to Taxol treatment. However, my previous results have shown that both Bak and Bax are necessary for Taxol-induced apoptosis.

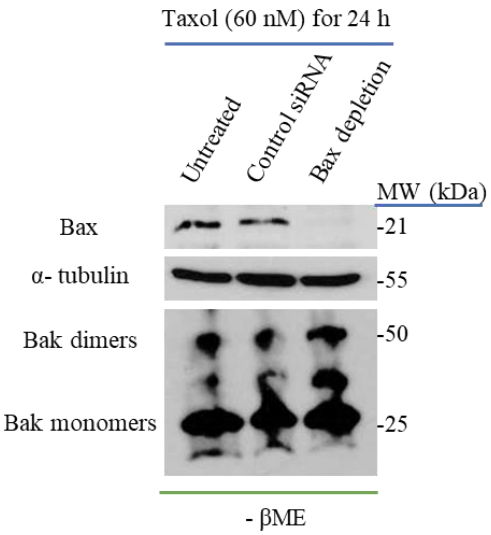

Figure 4-3: Oligomerization of Bak in Bax-depleted HeLa cells.

Hela cells were left untreated or transfected with either control siRNA (50 nM) or Bax siRNA (50 nM) for 48 hrs. After 48 hrs, the cells were treated with Taxol (60nM) for 24 hrs and permeabilized with 0.01% (w/v) digitonin. CHAPS lysis buffer was used to release membrane- and organelle-bound proteins and the cell lysates were incubated with 1 mM DSP. The samples were subjected to Immunoblotting for Bak in the absence of the reducing agent βME. α-tubulin was used as a loading control. The molecular weight markers are shown on the right. This result is representative of 2 independent experiments.

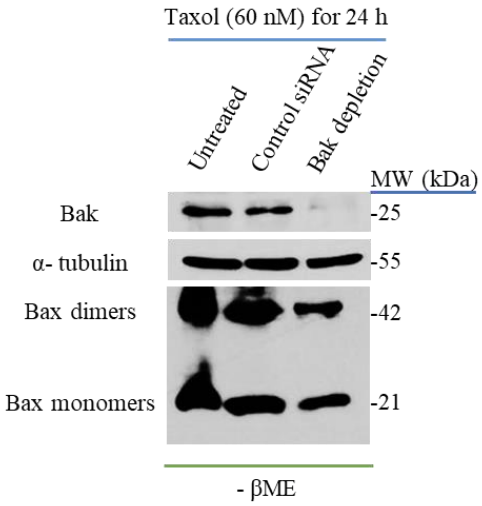

Figure 4-4: Oligomerization of Bax in Bak-depleted HeLa cells.

Hela cells were left untreated or transfected with either control siRNA (50 nM) or Bak siRNA (50 nM) for 48 hrs. After 48 hrs, the cells were treated with Taxol (60nM) for 24 hrs and permeabilized with 0.01% (w/v) digitonin. CHAPS lysis buffer was used to release membrane- and organelle-bound proteins and the cell lysates were incubated with 1 mM DSP. The samples were subjected to Immunoblotting for Bax in the absence of the reducing agent βME. α-tubulin was used as a loading control. The molecular weight markers are shown on the right. This result is representative of 2 independent experiments.

4.4 Taxol Induces Bak-Bax Interaction

Next, I tested the hypothesis that Taxol-induced apoptosis requires the formation of Bak and Bax hetero-oligomers by examining Bax/Bak interactions using co-immunoprecipitation (co-IP) assays. Under native conditions, co-IPs were carried out in untreated and Taxol-arrested HeLa cells using anti-Bak (N-20) goat polyclonal antibody and anti-Bax (6A7) mouse monoclonal antibody. The anti-Bak (N-20) antibody recognizes the conformationally active form of Bak and the anti-Bax (6A7) antibody recognizes the conformationally active form of Bax (Youle and Strasser, 2008). IPs were analysed by Western blotting using either anti-Bak or anti-Bax antibody. First, I immunoprecipitated the total Bax and Bak proteins using a non-CHAPS lysis buffer. As shown in Figure 4-5 and 4-6, the inactive and the active forms of Bax and Bak were immunoprecipitated in almost equal amounts from both the untreated and Taxol-treated cells respectively.

Interestingly, Bak was detected in the Taxol-arrested cells when the Bax IP was reblotted with anti-Bak antibody Figure (4-5). Similarly, Bax was also detected in Taxol-arrested cells when the Bak IP was reblotted with anti-Bax antibody Figure (4-6). These results suggest that Bak and Bax form a complex (directly or indirectly) in Taxol-treated cells. Immunoblotting verified the absence of Bak or Bax when the immunoprecipitations were performed in the absence of the antibodies or in the absence of the cell lysates.

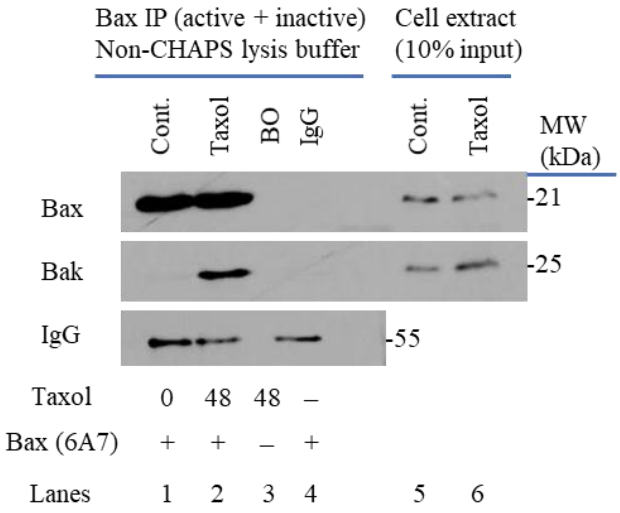

Figure 4-5: Bak co-immunoprecipitates with Bax (active and inactive).

Hela ells were either left untreated or treated with Taxol (60nM) for the indicated times and subjected to immunoprecipitation with anti-Bax (6A7) antibody (lanes 1-2) followed by immunoblotting for Bax or Bak. Lane 3 represents cell extracts plus magnetic beads only (BO) and lane 4 represents control IgG. The cell extracts of untreated (lanes 5) and Taxol-treated cells (lanes 6) were also immunoblotted as controls. The molecular weight markers are shown on the right. This is representative of 2 independent experiments.

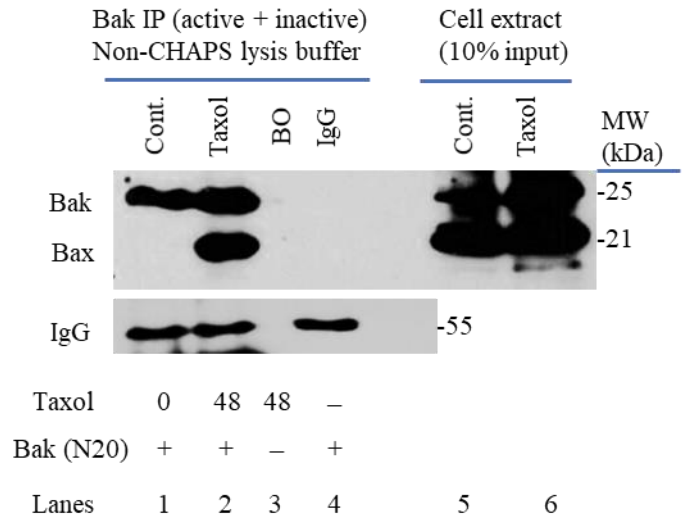

Figure 4-6: Bax co-immunoprecipitates with Bak (active and inactive).

HeLa cells were either left untreated or treated with Taxol (60nM) for the indicated times and subjected to immunoprecipitation with anti-Bak (N-20) antibody (lanes 1-2) followed by immunoblotting for Bak or Bax. Lane 3 represents cell extracts plus magnetic beads only (BO) and lane 4 represents control IgG. The cell extracts of untreated (lanes 5) and Taxol-treated cells (lanes 6) were also immunoblotted as controls. The molecular weight markers are shown on the right. This is representative of 2 independent experiments.

4.5 Interaction of active Bak and Bax in Taxol-arrested cells

Since Bak and Bax formed a complex only when they are activated, I then immunoprecipitated only active Bak or only active Bax using a CHAPS lysis buffer. Other non-ionic detergents such as Triton X-100 and NP-40 induce conformational changes and oligomerization of pro-apoptotic proteins Bak and Bax (Dewson, 2015). HeLa cells were either left untreated or treated with Taxol, and then Bax and Bak were immunoprecipitated from the cell lysates as described before (section 2.3.4.6, see page 67). My results indicated that the active forms of Bax and Bak were detected primarily in the Taxol-arrested cells, while, a small amount of Bak was detected in the untreated cells. Furthermore, Bak co-immunoprecipitated with active Bax in Taxol-arrested mitotic cells. Similarly, Bax also co-immunoprecipitated with active Bak in Taxol-arrested mitotic cells (Figures 4-7 and 4-8). These results suggested that Bak and Bax interaction is required or occurred during Taxol-induced mitotic cell death.

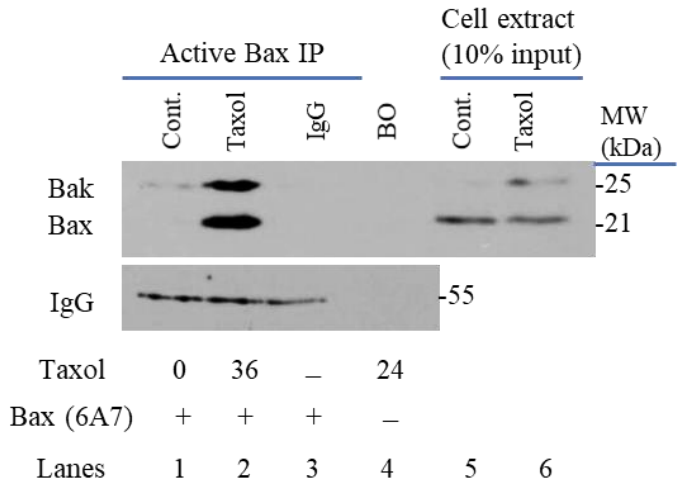

Figure 4-7: Bak co-immunoprecipitates with active Bax in Taxol-arrested cells only.

HeLa cells were either left untreated or treated with Taxol (60nM) for the indicated times and subjected to immunoprecipitation with anti-Bax (6A7) antibody (lanes 1-2) followed by immunoblotting for Bax or Bak. Lane 3 represents control IgG and lane 4 represents cell extracts plus magnetic beads only (BO). The cell extracts of untreated (lanes 5) and Taxol-treated cells (lanes 6) were also immunoblotted as controls. The molecular weight markers are shown on the right. This is representative of 2 independent experiments.

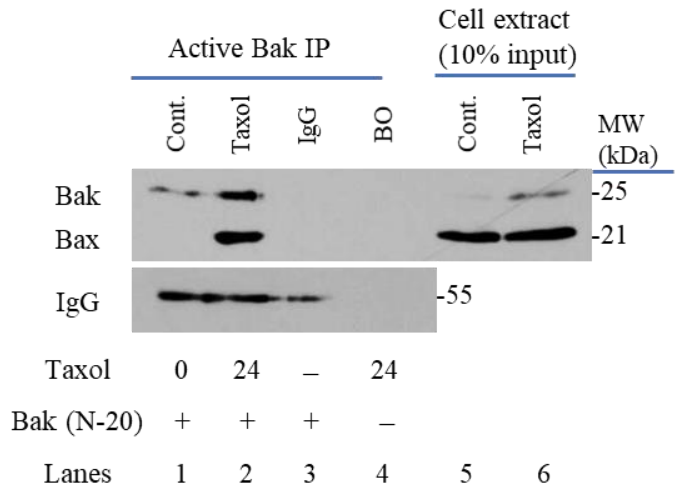

Figure 4-8: Bax co-immunoprecipitates with active Bak in Taxol-arrested cells only.

HeLa cells were either left untreated or treated with Taxol (60nM) for the indicated times and subjected to immunoprecipitation with anti-Bak (N-20) antibody (lanes 1-2) followed by immunoblotting for Bak or Bax. Lane 3 represents control IgG and lane 4 represents cell extracts plus magnetic beads only (BO). The cell extracts of untreated (lanes 5) and Taxol-treated cells (lanes 6) were also immunoblotted as controls. The molecular weight markers are shown on the right. This is representative of 2 independent experiments.

4.6 Time course analysis of active Bak and Bax interaction

To examine if there is any correlation between the active form of Bak and that of active Bax, time course IPs were carried out using anti-active Bak and Bax antibodies. Hela cells were synchronized with a thymidine block and then either left untreated or treated with Taxol for the indicated times. As expected, there was a time dependent increase in the amount of active Bax (Figure 4-9) and active Bak (Figure 4-10) that were immunoprecipitated following Taxol addition. Interestingly, the levels of Bak and Bax proteins associated with active Bax and active Bak respectively also increased between 12-36 hrs after Taxol addition. These results suggested that Bak and Bax form a complex which correlates with the induction of apoptosis Figures (4-9 and 4-10).

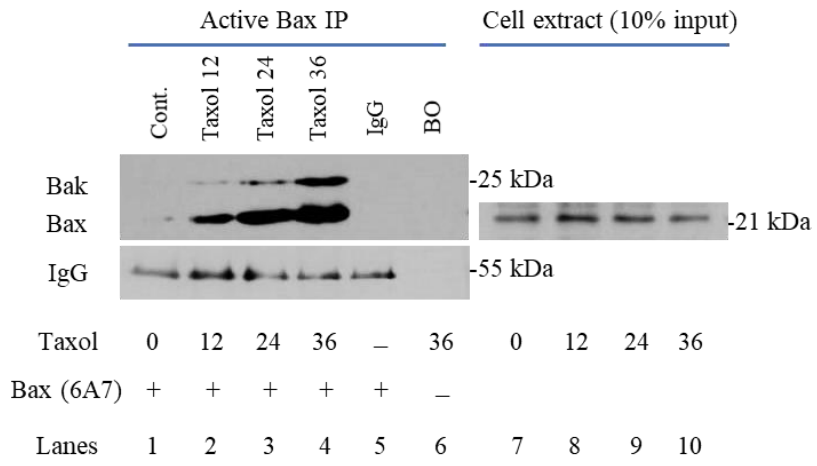

Figure 4-9: Time course of active Bax IP and its interaction with Bak following Taxol treatment.

Synchronized HeLa cells were either left untreated or treated with Taxol (60nM) for the indicated times and subjected to immunoprecipitation with anti-Bax (6A7) antibody (lanes 1-4) followed by immunoblotting for Bax and Bak. Lane 5 represents control IgG and lane 6 represents cell extracts plus magnetic beads only (BO). The cell extracts of untreated (lanes 7) and Taxol-treated cells (lane 8-10) were also immunoblotted as controls. The molecular weight markers are shown on the right. This is representative of 2 independent experiments.

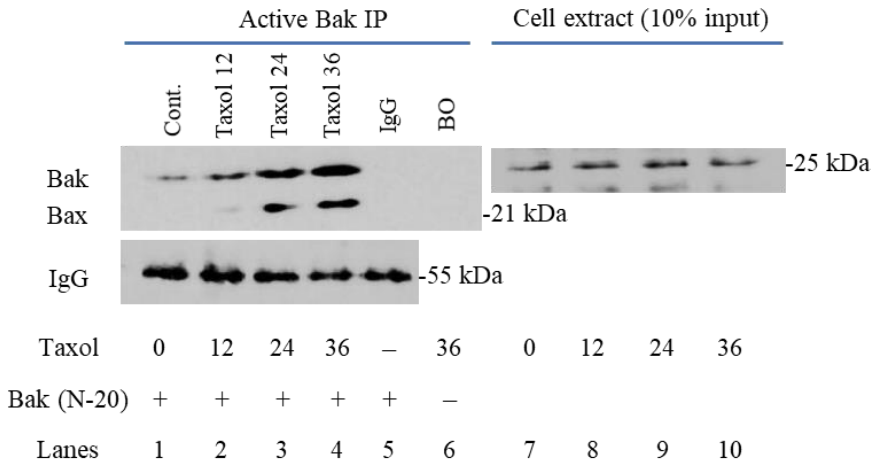

Figure 4-10: Time course of active Bak IP and its interaction with Bax following Taxol treatment.

Synchronized HeLa cells were either left untreated or treated with Taxol (60nM) for the indicated times and subjected to immunoprecipitation with anti-Bak (N-20) antibody (lanes 1-4) followed by immunoblotting for Bak and Bax. Lane 5 represents control IgG and lane 6 represents cell extracts plus magnetic beads only (BO). The cell extracts of untreated (lanes 7) and Taxol-treated cells (lane 8-10) were also immunoblotted as controls. The molecular weight markers are shown on the right. This is representative of 2 independent experiments.

4.7 Interaction of Bak and Bax in RPE1 cells

Next, we wanted to determine if the Bak and Bax interaction was specific for HeLa cells only or whether it also occurs in a normal diploid cell line. IP experiments were carried out in Retinal Pigment Epithelial Cell Line (RPE1 cells) using native conditions. RPE1 cells were synchronized with a thymidine block and then either left untreated or treated with Taxol for the indicated times and IPs were performed as described before. As shown in Figure 4-11 and 4-12, Taxol-induced interaction of active Bax with Bak and active Bak with Bax was identical in RPE1 cells to that found in HeLa cells. These findings indicated that Taxol-induced mitotic cell death is associated with the activation and interaction of both Bak and Bax, and this interaction occurs in a normal diploid cell line as well as in a cancer cell line. Furthermore, the propensity of these oligomers to co-IP may indicate a degree of affinity between Bak and Bax homo-oligomers or Bak and Bax may form hetero-oligomers.

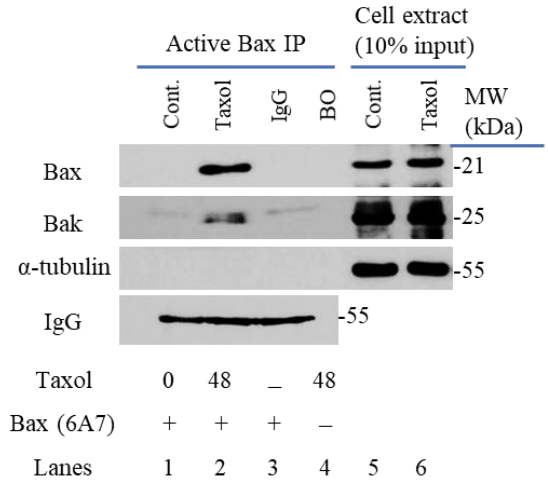

Figure 4-11: Bak co-immunoprecipitates only with active Bax IP in Taxol-arrested RPE1 cells.

RPE1 cells were synchronized by a thymidine block for 24 hrs and then either left untreated or treated with Taxol (1µM) for 48 hrs and subjected to immunoprecipitation with anti-Bax (6A7) antibody (lanes 1-2) followed by immunoblotting for Bax or Bak. Lane 3 represents control IgG and lane 4 represents cell extracts plus magnetic beads only (BO). The cell extracts of untreated (lanes 5) or Taxol-treated cells (lane-6) were also immunoblotted as controls. The molecular weight markers are shown on the right. This is representative of 2 independent experiments.

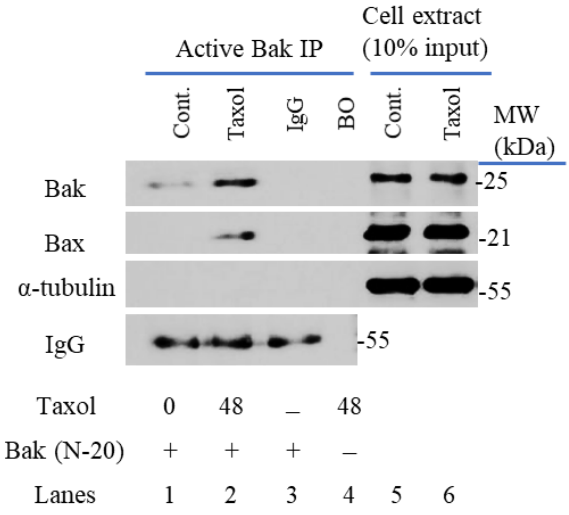

Figure 4-12: Bax co-immunoprecipitates only with active Bak IP in Taxol-arrested RPE1 cells.

RPE1 cells were synchronized by a thymidine block for 24 hrs and then either left untreated or treated with Taxol (1µM) for 48 hrs and subjected to immunoprecipitation with anti-Bak (N-20) antibody (lanes 1-2) followed by immunoblotting for Bak or Bax. Lane 3 represents control IgG and lane 4 represents cell extracts plus magnetic beads only (BO). The cell extracts of untreated (lanes 5) or Taxol-treated cells (lane-6) were also immunoblotted as controls. The molecular weight markers are shown on the right. This is representative of 2 independent experiments.

4.8 Bak and Bax co-localize in Taxol-arrested apoptotic cells

In healthy cells, Bak predominantly resides at the MOM, whereas Bax is a soluble monomer regularly shuttling between the cytosol and the MOM (Edlich et al., 2011). However, Bax re-translocation into the cytosol is reported to occur at a lower rate following prolonged-mitotic arrest (Todt et al., 2015). In an attempt to explain the mechanism of Bak/Bax-mediated mitochondrial apoptosis, confocal microscopy analysis was carried out to examine Bak and Bax localization in Taxol-arrested apoptotic cells.

Immunofluorescence analysis was performed in HeLa cells to determine the subcellular location of Bax and Bak and to monitor changes in intracellular localization following Taxol addition. HeLa cells were left untreated or treated with Taxol for the indicated times (0-24hrs) and co-stained with either an anti-Bax antibody and Mitotracker or an anti-Bak antibody and Mitotracker. In untreated cells or Taxol-treated cells that had not initiated apoptosis, Bax showed a diffuse distribution throughout the cell (Figure 4-13). However, Bax was located predominantly at the mitochondria at 24 hrs following Taxol addition (Figure 4-13). On the other hand, Bak co-localized with the mitochondria in healthy cells and it's associated with mitochondria in Taxol-treated cells Figure (4-14). Moreover, Bak-Bax co-localization was detected in Taxol-treated cells with fragmented nuclei, cells that were undergoing mitotic cell death Figure (4-15).

Furthermore, I analysed the co-localization of Bax or Bak with mitochondria using Pearson's correlation analysis (Neumann et al., 2010). As shown in Figure (4-13 C) Bax co-localization with Mitotracker was significantly increased at 24 hrs Taxol treatment in comparison to untreated and 16 hrs Taxol-arrested cells. In contrast, Bak co-localization with Mitotracker was similar at 16 and 24 hrs in comparison to untreated cells Figure (4-14 B). Immunofluorescence results revealed that Bak and Bax co-localized in Taxol-treated apoptotic cells. Identical results showing co-localization of Bax and Bak were obtained in U2OS cells (Figures 4-16, 4-17 and 4-

18). Co-localization of Bak and Bax, although not an indicator of direct binding, in apoptotic cells is consistent with my previous results that these proteins co-immunoprecipitate following Taxol treatment. This result is also consistent with my previous data showing that Bax or Bak depletion alone reduced apoptosis (see Figure 3-5 page 79). Overall, the results indicate that Bak-Bax association may be required for initiating mitotic cell death during Taxol treatment.

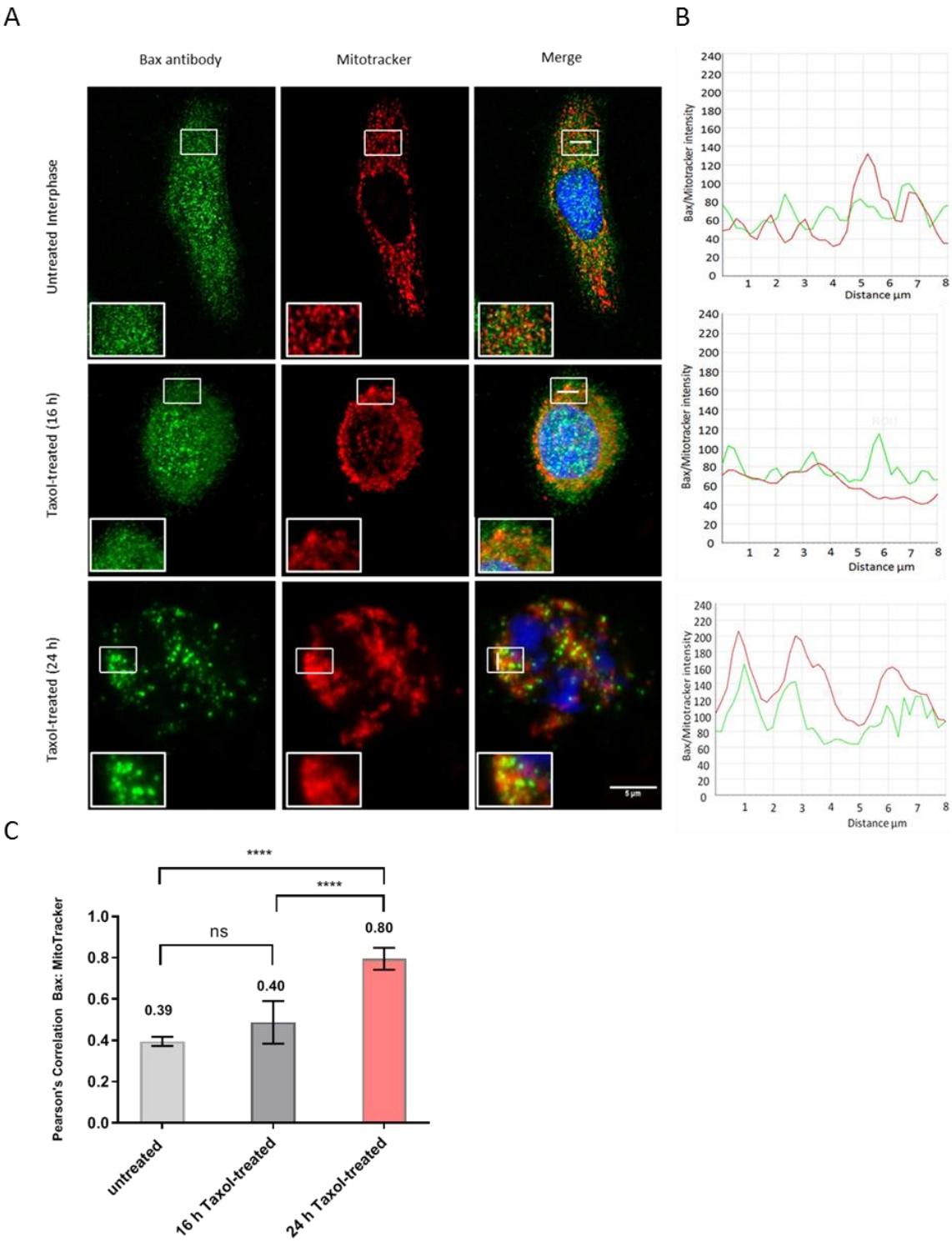

Figure 4-13: Localization of Bax in Taxol-treated cells.

A) HeLa cells were either left untreated or treated with Taxol for the indicated times and labelled with anti-Bax antibody (green). Mitochondria were labelled with Mitotracker (red). Merge panels include DNA (blue) stained with Hoechst 33258. Images are maximum intensity projections of z-stack data. Scale bar, 5 µm. B) The fluorescence intensity of Bax and Mitotracker was determined at the indicated lines in the images. C) Pearson's correlation coefficient between Bax and Mitotracker for cells shown in A.

Pearson's correlation coefficient was performed using Leica Confocal SP5 software. Histograms represent the mean ± SD of 10 images from 3 independent experiments, P-values were calculated using one-way ANOVA (ns = not significant, **** P value <0.0001).

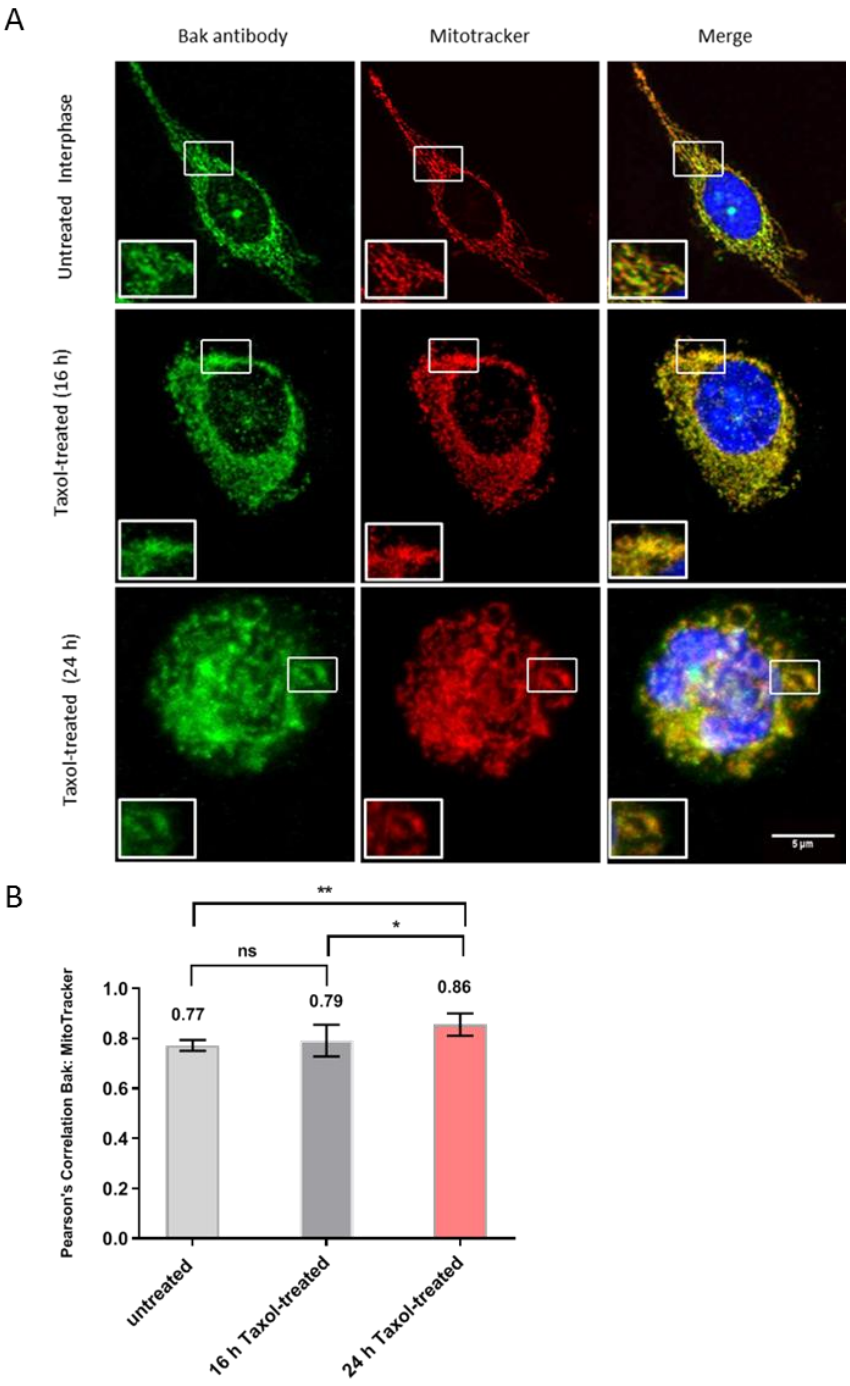

Figure 4-14: Localization of Bak in Taxol-treated cells.

A) HeLa cells either left untreated or treated with Taxol for the indicated times and labelled with anti-Bak antibody (green). Mitochondria were labelled with Mitotracker (red). Merge panels include DNA (blue) stained with Hoechst 33258. Images are

maximum intensity projections of z-stack data. Scale bar, 5 µm. B) Pearson's correlation coefficient between Bak and Mitotracker for cells shown in A. Pearson's correlation was performed using Leica Confocal SP5 software. Histograms represent the mean ± SD of 10 images from 3 independent experiments, P-values were calculated using one-way ANOVA (ns = not significant, * P value <0.05, *** P value <0.001).

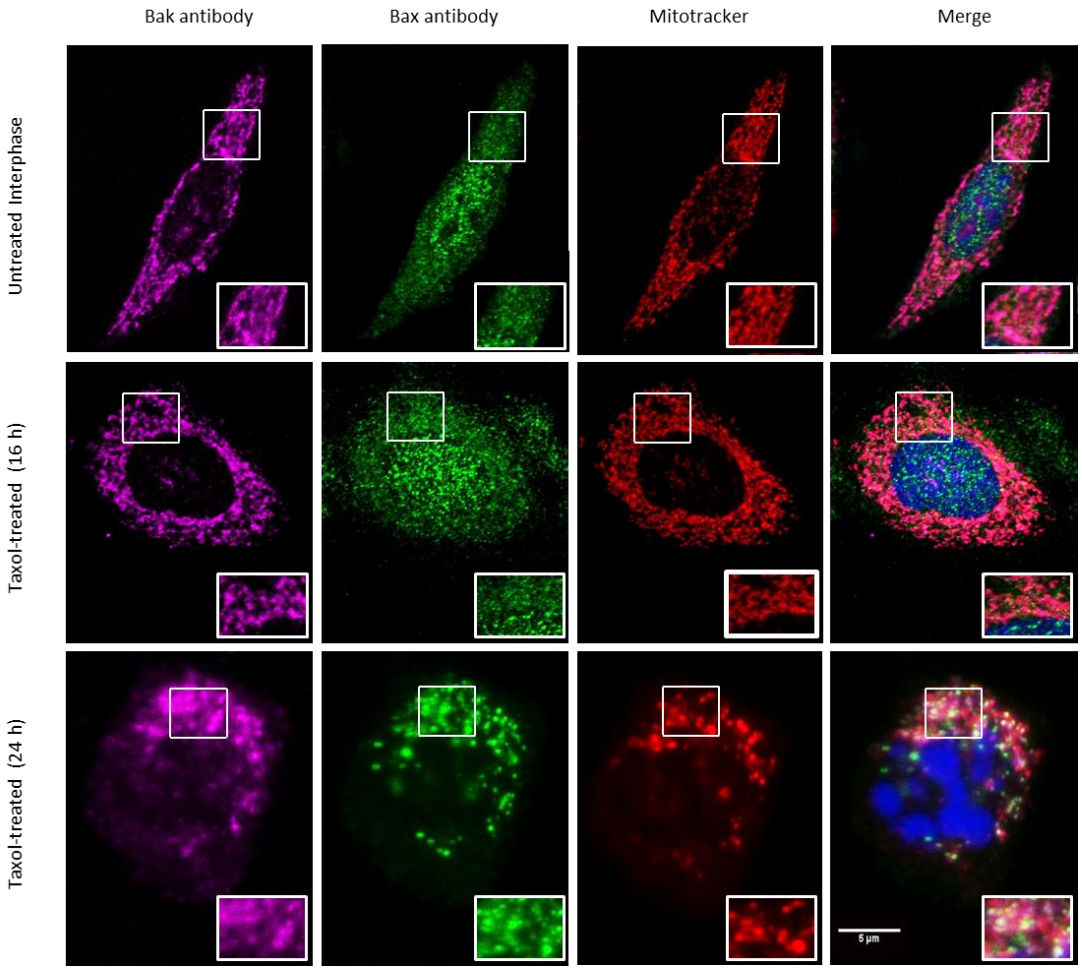

Figure 4-15: Co-localization of Bak and Bax in Taxol-treated cells.

HeLa cells were either left untreated or treated with Taxol for the indicated times and labelled with anti-Bak visualized with Alexa-flour 647 secondary antibody (magenta) and anti-Bax visualized with Alexa-flour 488 secondary antibody (green). Mitochondria were labelled with Mitotracker (red). Merge panels include DNA (blue) stained with Hoechst 33258. White = co-localization of Bak/Bax/Mitotracker. Results are representative of three independent experiments. Images are maximum intensity projections of z-stack data. Scale bar, 5 µm.

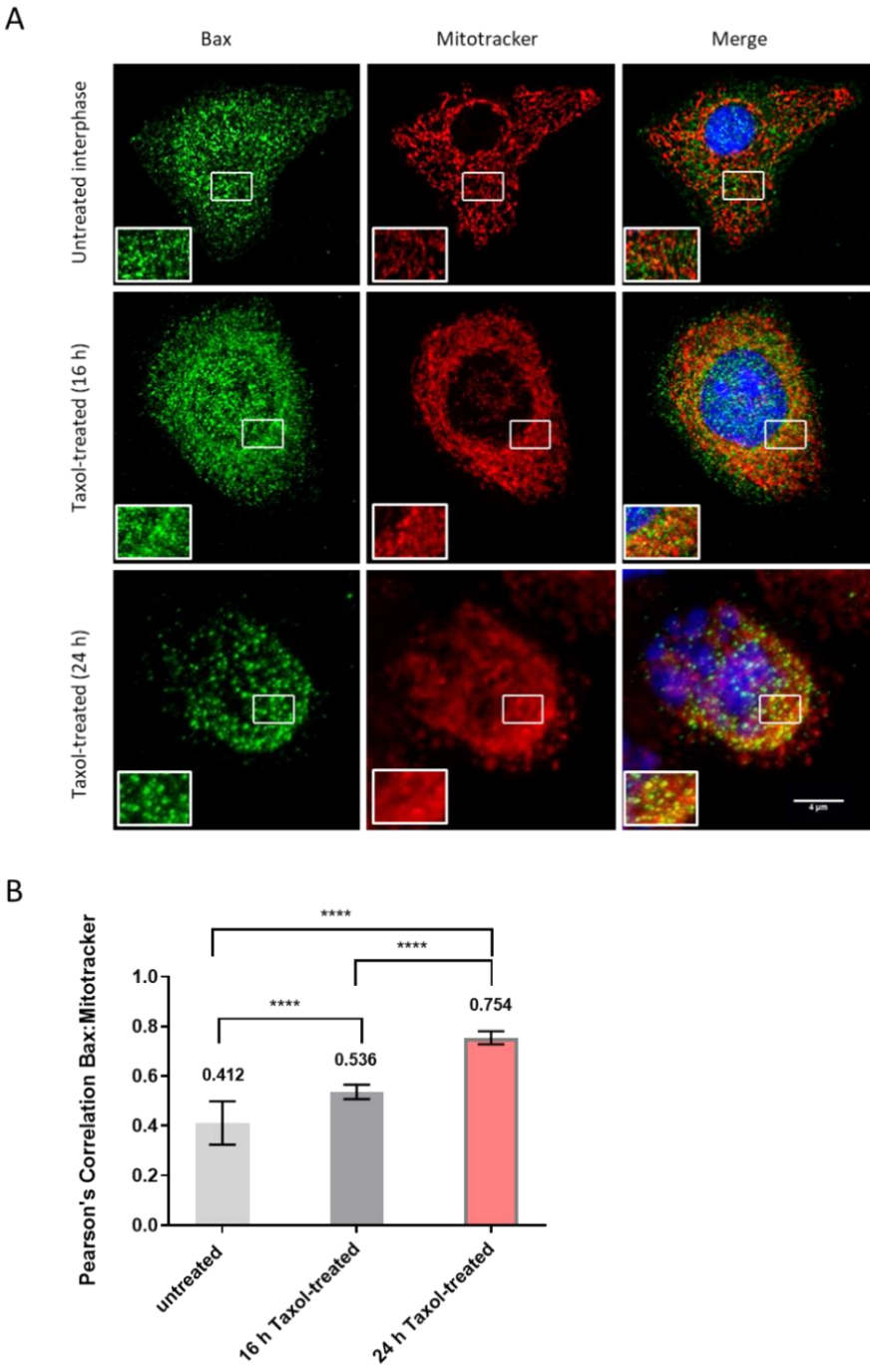

Figure 4-16: Localization of Bax in Taxol-treated U2OS cells.

A) U2OS cells were either left untreated or treated with Taxol for the indicated times and labelled with anti-Bax antibody (green). Mitochondria were labelled with Mitotracker (red). Merge panels include DNA (blue) stained with Hoechst 33258. Images are maximum intensity projections of z-stack data. Scale bar, 4 µm. B) Pearson's correlation coefficient between Bax and Mitotracker for cells shown in A. Pearson's correlation was performed using Leica Confocal SP5 software. Histograms represent the mean ± SD of 10 images from 3 independent experiments, P-values were calculated using one-way ANOVA (ns = not significant, **** P value <0.0001).

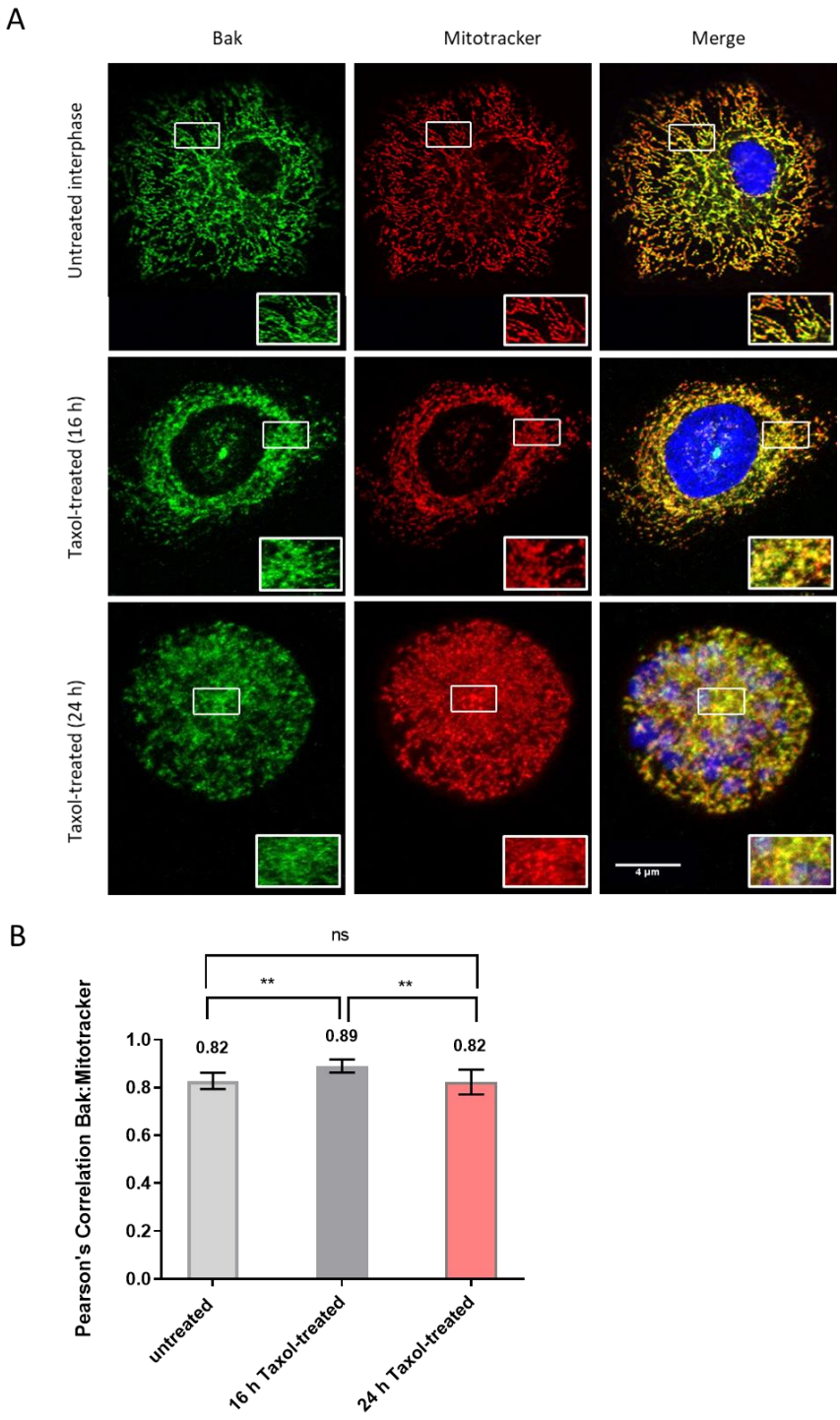

Figure 4-17: Localization of Bak in Taxol-treated U2OS cells.

A) U2OS cells were either left untreated or treated with Taxol for the indicated times and labelled with anti-Bak antibody (green). Mitochondria were labelled with Mitotracker (red). Merge panels include DNA (blue) stained with Hoechst 33258. Images are maximum intensity projections of z-stack data. Scale bar, 4 µm. B) Pearson's correlation coefficient between Bak and Mitotracker for cells shown in A. Pearson's correlation was performed using Leica Confocal SP5 software. Histograms represent the mean ± SD of 10 images from 3 independent experiments, P-values were calculated using one-way ANOVA (ns = not significant, ** P value <0.01).

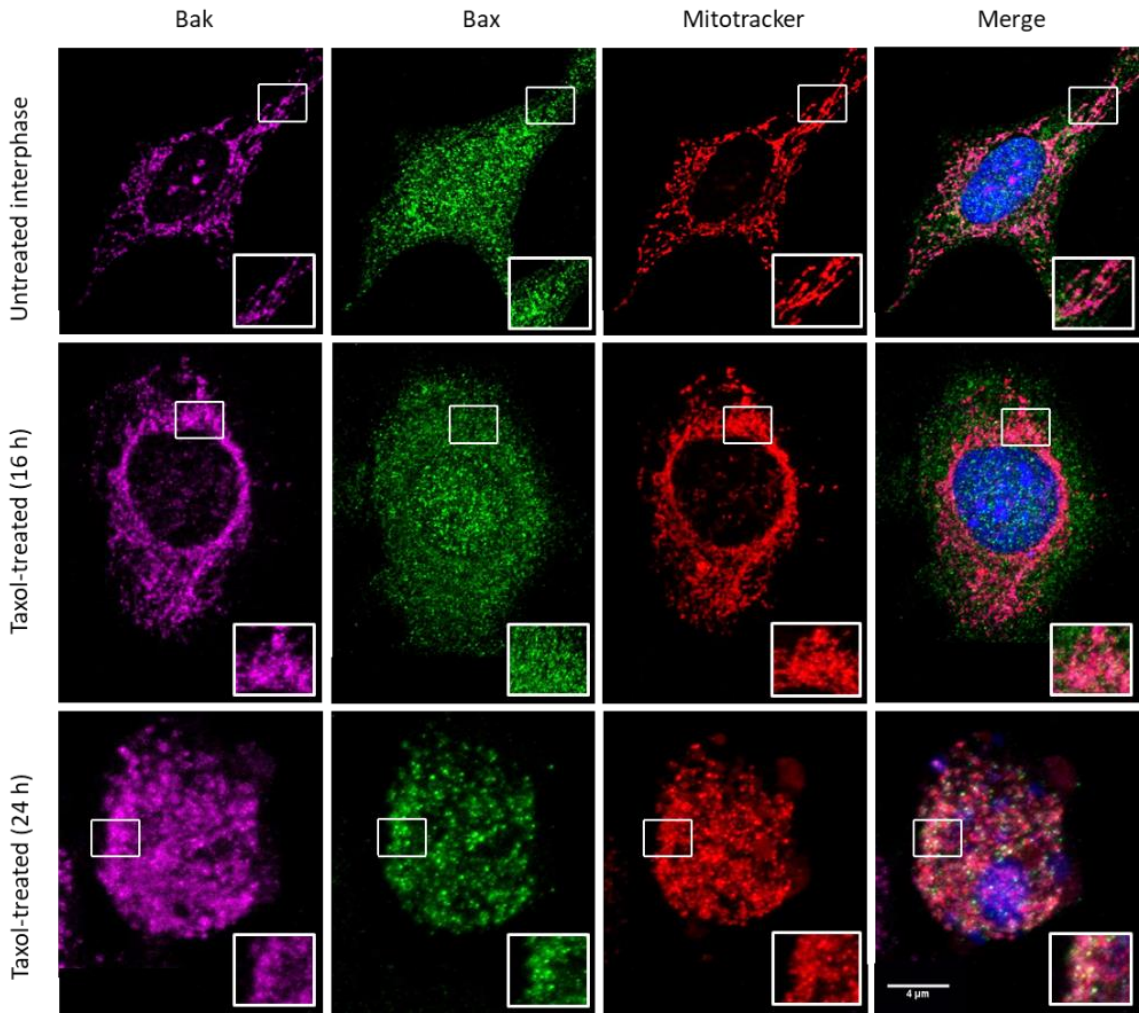

Figure 4-18: Co-localization of Bak and Bax in Taxol-treated U2OS cells.

U2OS cells were either untreated or treated with Taxol for the indicated times and labelled with anti-Bak visualized with Alexa-flour 647 secondary antibody (magenta) and anti-Bax visualized with Alexa-flour 488 secondary antibody (green). Mitochondria were labelled with Mitotracker (red). Merge panels include DNA (blue) stained with Hoechst 33258. White = co-localization of Bak/Bax/Mitotracker. Results are representative of three independent experiments. Images are maximum intensity projections of z-stack data. Scale bar, 4 µm.

Additionally, I also investigated whether GFP-Bax co-localizes to mitochondria in Taxol-arrested mitotic cells, because the intracellular localization of active Bax with the Bax antibody was not convincing. The region of Bax that is recognized by the Bax antibody could be masked when it interacts with other proteins in the

Taxol-arrested cells. To address this aspect, two cancer cell lines, HeLa and U2OS cells, were transfected with GFP-Bax. GFP-Bax transfected cells were either left untreated or treated with Taxol for varying times. Cells were stained with GFP-nanobody and then examined by confocal microscopy. In untreated cells, GFP-Bax showed a diffuse distribution throughout the cell in both cell lines. However, GFP-Bax co-localized with Mitotracker in Taxol-arrested cells at 16 and 24 hrs after Taxol addition Figures (4-19 and 4-20). These results are consistent with reports that Bax is translocated from the cytosol to the mitochondria in response to an apoptotic stimulus (Große et al., 2016, Salvador-Gallego et al., 2016).

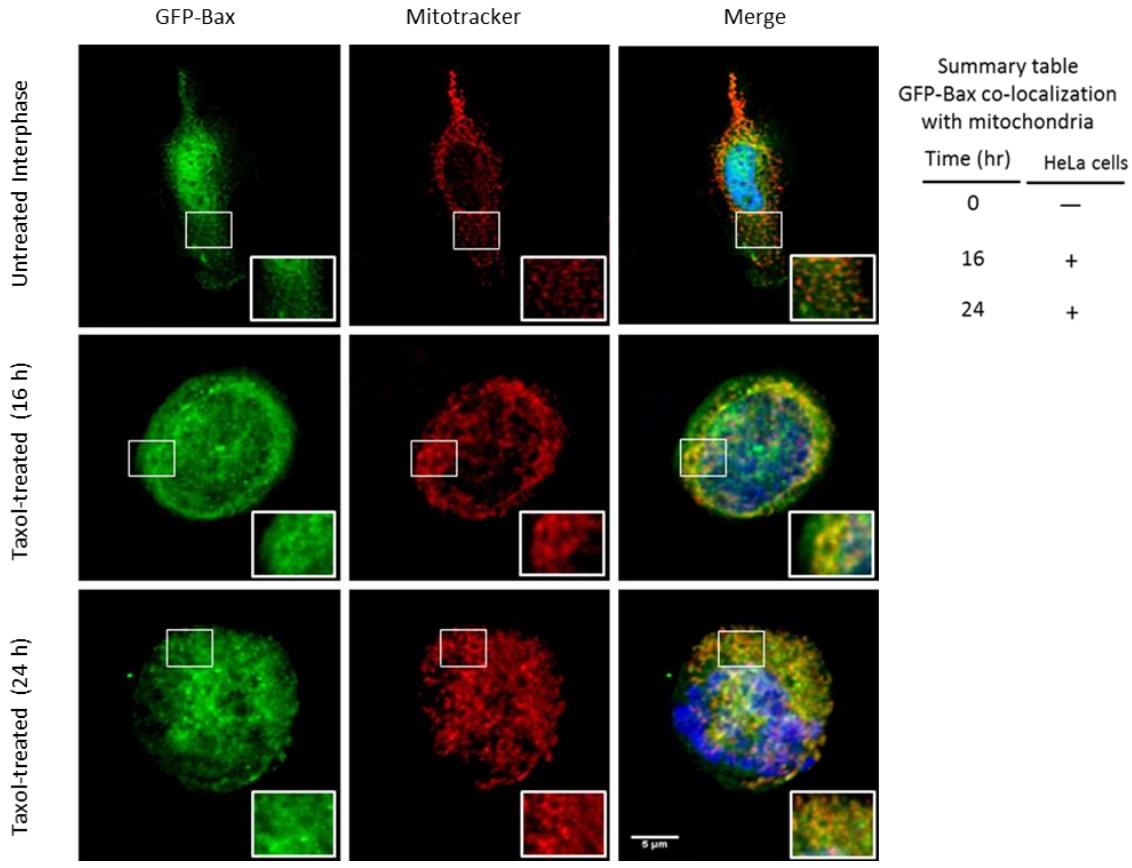

Figure 4-19: GFP-Bax co-localizes with mitochondria in Taxol-treated HeLa cells.

HeLa cell were cultivated on glass coverslips and then transfected with GFP-Bax (green) 1 µg for 36 hrs. GFP-Bax transfected cells were either left untreated or treated with Taxol (60nM) for the indicated times. Cells were fixed and permeabilized, stained with GFP-Nanobody and then examined by confocal microscopy. Mitochondria were labelled with Mitotracker (red). Merge panels include DNA (blue) stained with Hoechst 33258. Results

are representative of two independent experiments. Images are maximum intensity projections of z-stack data. Scale bar, 5 µm.

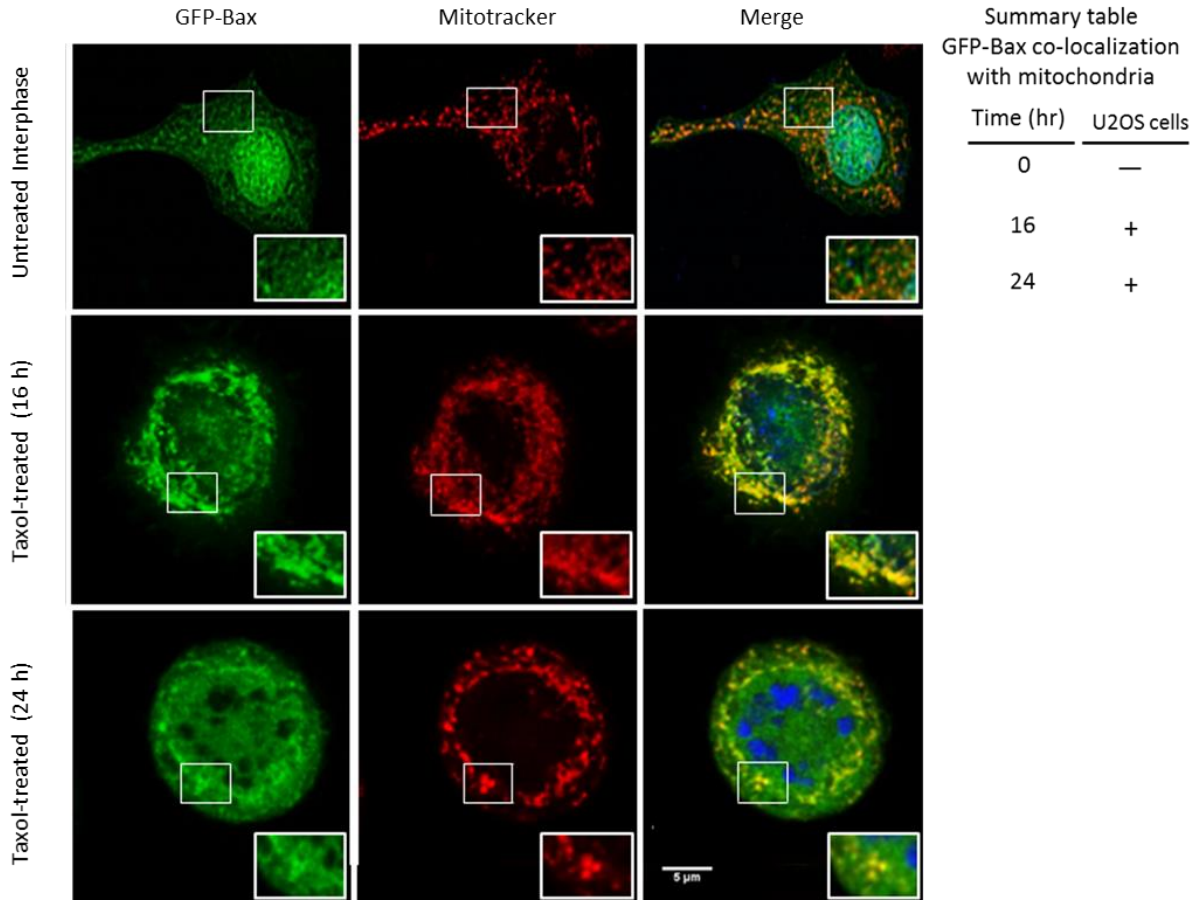

Figure 4-20: GFP-Bax co-localizes with mitochondria in Taxol-treated U2OS cells.

U2OS cell were cultivated on glass coverslips and then transfected with GFP-Bax (green) 1 µg for 36 hrs. GFP-Bax transfected cells were either left untreated or treated with Taxol (60nM) for the indicated times. Cells were fixed and permeabilized, stained with GFP-Nanobody and then examined by confocal microscopy. Mitochondria were labelled with Mitotracker (red). Merge panels include DNA (blue) stained with Hoechst 33258. Results are representative of two independent experiments. Images are maximum intensity projections of z-stack data. Scale bar, 5 µm.

4.9 Investigating signalling between SAC activation and apoptosis

This study was designed to investigate the signals that are generated following SAC activation which then trigger apoptosis. I looked at mitotic cell death in order to find the connection between activation of the mitotic checkpoint and the induction of apoptosis. To investigate the levels of apoptosis, synchronized population of HeLa cells were treated with Taxol for varying times. As shown in Figures (4-21 A and B), there was a time dependent increase in the number of cells staining positively for caspase-cleaved cytokeratin 18 (a substrate of caspase 3). After 6 and 12 hrs of Taxol treatment the levels of apoptosis were 3 and 9 % respectively. However, most of the cells underwent apoptosis between 24 and 36 hrs of Taxol treatment as indicated by cytokeratin 18 cleavage. Apoptosis was also confirmed by assessing the cleavage of poly (ADP-ribose) polymerase (PARP), pro-caspase-9, pro-caspase-3 and cleaved caspase-3 Figure (4-22A).

Next, I investigated whether the pro-apoptotic (Bak and Bax) or anti-apoptotic molecules (Bcl-2, Bcl-xL and Mcl-1) undergo alterations during Taxol-induced apoptosis. Cell extracts were prepared from the experiment described in Figure (4-21) and the expression of pro and anti-apoptotic proteins was determined by immunoblotting. As expected, both Bcl-2 and Bcl-xL underwent a transient mobility shift at 6 and 12 hrs of Taxol treatment. In contrast, Mcl-1 underwent degradation at 6 hrs treatment as expected and its levels were reduced by 24 and 36 hrs. The levels of the Bak or Bax protein were not affected by Taxol treatment. The possibility that Bak or Bax undergo small changes in mobility cannot be excluded as this experiment was unable to resolve the proteins adequately (Figure 4-22 B). Therefore, this result indicated that the phosphorylation of Bcl-2 and Bcl-xL and the degradation of Mcl-1 may provide the link between activation of the mitotic checkpoint and the initiation of apoptosis.

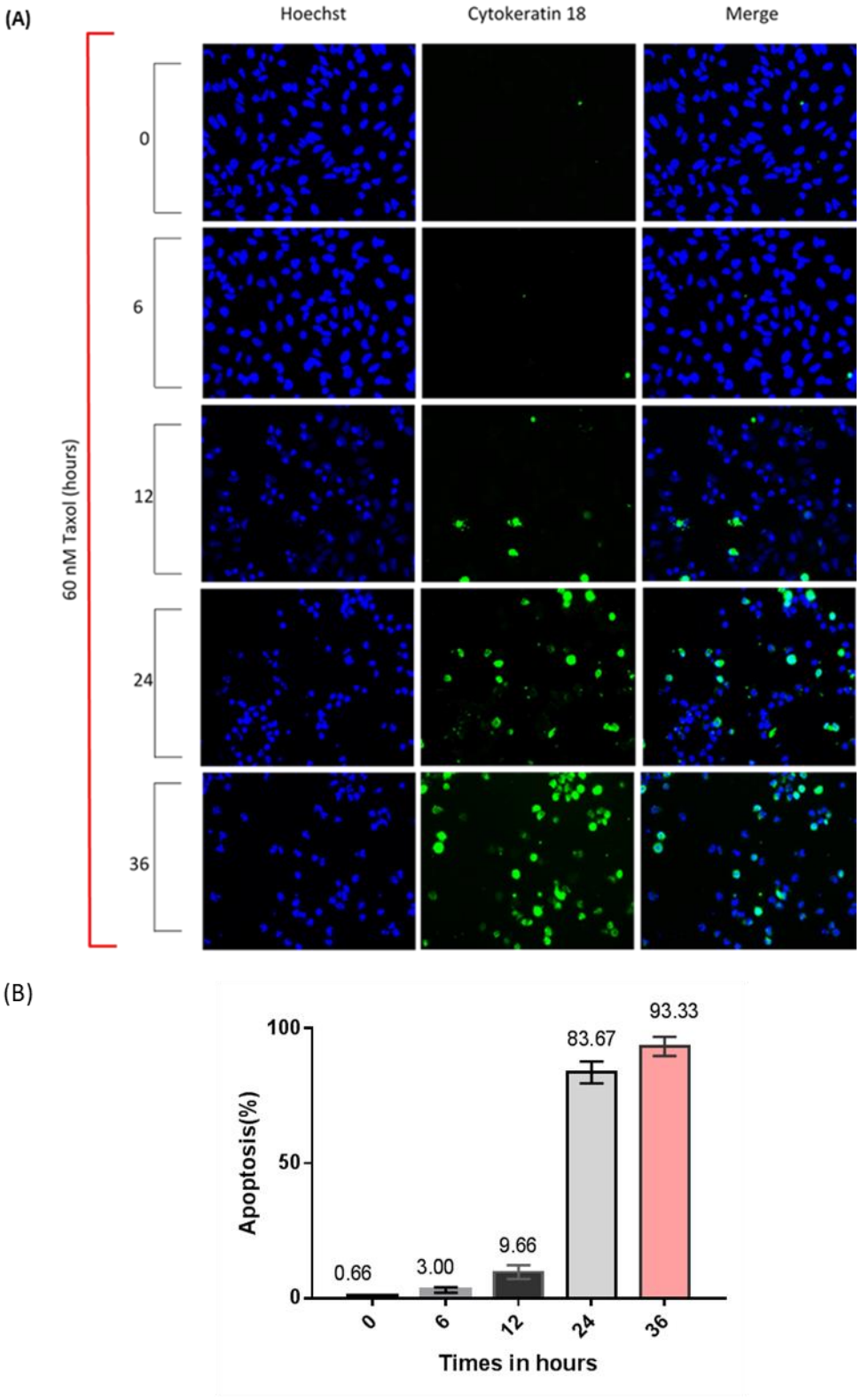

Figure 4-21: Time course of Taxol-induced apoptosis in synchronized HeLa cells.

(A) Representative images of Taxol-induced apoptosis. HeLa cells were synchronized at the G1/S boundary by thymidine block for 24 hrs, washed and released. The cells either left untreated or treated with Taxol (60 nM) for the indicated times. The cells were fixed and stained with CytoDEATH (M30) primary antibody and Alexa-Fluor 488 secondary

antibody (green). DNA was stained with Hoechst 33342 (blue). This result is representative of three independent experiments. (B) Quantitation of apoptosis for the experiment described in A. At least 100 cells were counted in randomly selected fields and the number of the apoptotic cells were quantitated. Histograms represent the mean ± SD of three independent experiments.

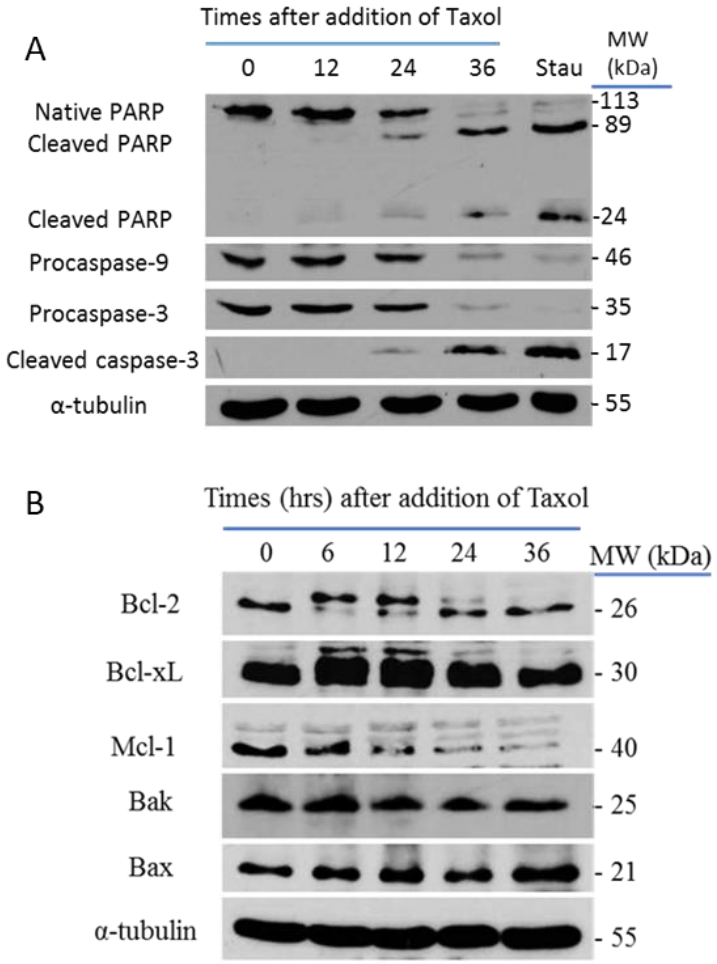

Figure 4-22: Taxol-induced PARP, caspase-9 and caspase-3 cleavage and alterations in anti-apoptotic proteins.

(A) Taxol-induced cleavage of PARP, caspase-9 and caspase-3. The cells were either left untreated or treated with Taxol (60 nM) for the indicated times and the cell lysates were prepared for Immunoblotting with PARP, pro-caspase-9, pro-caspase-3 and cleaved caspase-3. Stau= Staurosporine-treated cells. α-tubulin was used as a loading control and the molecular weight markers are shown on the right. This result is representative of 2 independent experiments. (B) HeLa cells were synchronized at the G1/S boundary by thymidine block for 24 hrs, washed and released. The cells either left untreated or treated with Taxol (60 nM) for the indicated times. Cell lysates were immunoblotted with antibodies for Bcl-2, Bcl-xL, Mcl-1, Bak and Bax. α-tubulin was used as a loading control and the molecular weight markers are shown on the right. This result is representative of 2 independent experiments.

4.10 Investigation of the Bax/Bak/ANT2/VDAC complex

In order to identify putative signalling molecules that may mediate apoptosis in Taxol-arrested mitotic cells, I looked at Bak and Bax-interacting proteins using mass spectrometry (MS). HeLa cells were treated with Taxol (60 nM) for 24 hrs and the cells were lysed in 1% CHAPS lysis buffer (Dewson, 2015). Active Bax and active Bak were immunoprecipitated from Taxol-arrested mitotic cells and subjected to peptide mass fingerprint analysis by MS. As a control, a parallel set of Bax and Bak IPs from untreated cells was subjected to MS analysis. My results indicated that after eliminating non-specific binding of proteins, 36 proteins were bound specifically to Bax in the Taxol-arrested cells. Interestingly, Bak, ANT2 and Cdk1 were detected in the Bax IP. Similarly, this investigation identified several Bak interacting partners (43 proteins) including Bax, ANT2, VDAC1, VDAC2 and VDAC3 (see Table 7-1, Appendix). Furthermore, several mitochondrial membrane proteins, from both outer and inner mitochondrial membranes, were also observed to be specifically bound to Bak and Bax in Taxol-arrested cells including ATP synthase subunit alpha, ATP synthase subunit beta, phosphate carrier protein and Peptidyl-prolyl cis-trans isomerase. The MS data indicates that Bak and Bax are inserted into the MOM to form a complex with a number of mitochondrial membrane proteins such as VDAC after Taxol addition. Moreover, this complex may be expanded to the MIM to include the inner membrane components of the MPTP such as ANT2, ATP synthase and phosphate carrier protein.

4.11 ANT2 co-immunoprecipitates with Bax and Bak in Taxol-arrested cells

To confirm the results of the MS analysis, I immunoprecipitated Bax or Bak and performed WB with specific antibodies to determine whether some of the proteins that were found to interact with Bax and Bak would also co-

immunoprecipitate. Bax and Bak were immunoprecipitated from untreated and Taxol-arrested HeLa cells and the IP's western blotted with specific antibodies. The results demonstrated that ANT2 specifically interacts with both Bax and Bak in Taxol-treated HeLa cells, but no interaction was observed in the untreated cells (see Figures 4-23 and 4-27 respectively).

ANT2 is a part of the mitochondrial permeability transition pore complex (MPTP) (Kwong and Molkentin, 2015) and its interaction with pro-apoptotic proteins such as Bak and Bax may modulate mitochondrial membrane permeability and cause the release of cytochrome c. These results suggest that ANT2 may be involved in the formation of the mitochondrial-apoptotic pores by forming a larger complex with Bak and Bax oligomers.

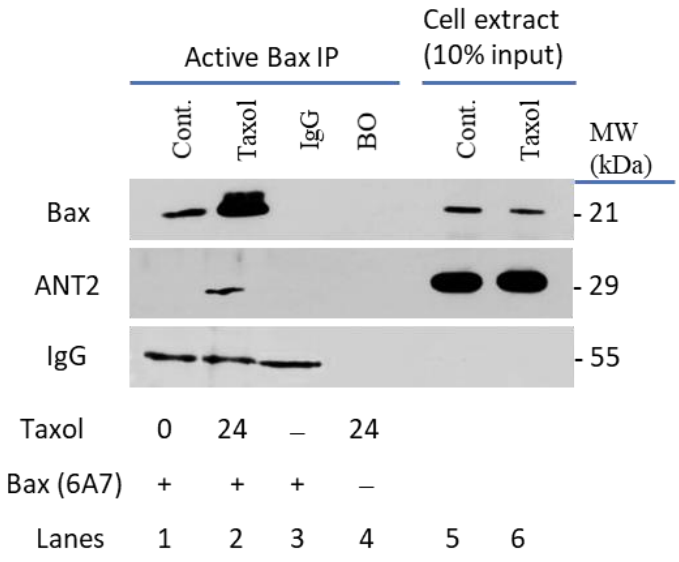

Figure 4-23: Interaction of Bax with ANT2 induced by Taxol treatment.

HeLa cells were either left untreated or treated with Taxol (60nM) for the indicated times and subjected to immunoprecipitation with anti-Bax (6A7) antibody (lanes 1-2) followed by immunoblotting for Bax and ANT2. Lane 3 represents control IgG and lane 4 represents cell extracts plus magnetic beads only (BO). The cell extracts of untreated (lanes 5) or Taxol-treated cells (lane-6) were also immunoblotted as controls. The molecular weight markers are shown on the right. This is representative of 2 independent experiments.

In the light of these results, I then determined whether Bax and ANT2 co-localized following Taxol treatment. HeLa cells were left untreated or treated with Taxol and co-stained with anti-Bax and anti-ANT2 antibodies. Our results (Figure 4-25) indicated that there is no co-localization between Bax and ANT2 in untreated cells. However, in Taxol-treated cells, the co-localization of Bax and ANT2 was clearly detected. This data supports my previous result showing the co-immunoprecipitation of these two proteins in Taxol-arrested mitotic cells (see Figure 4-23).

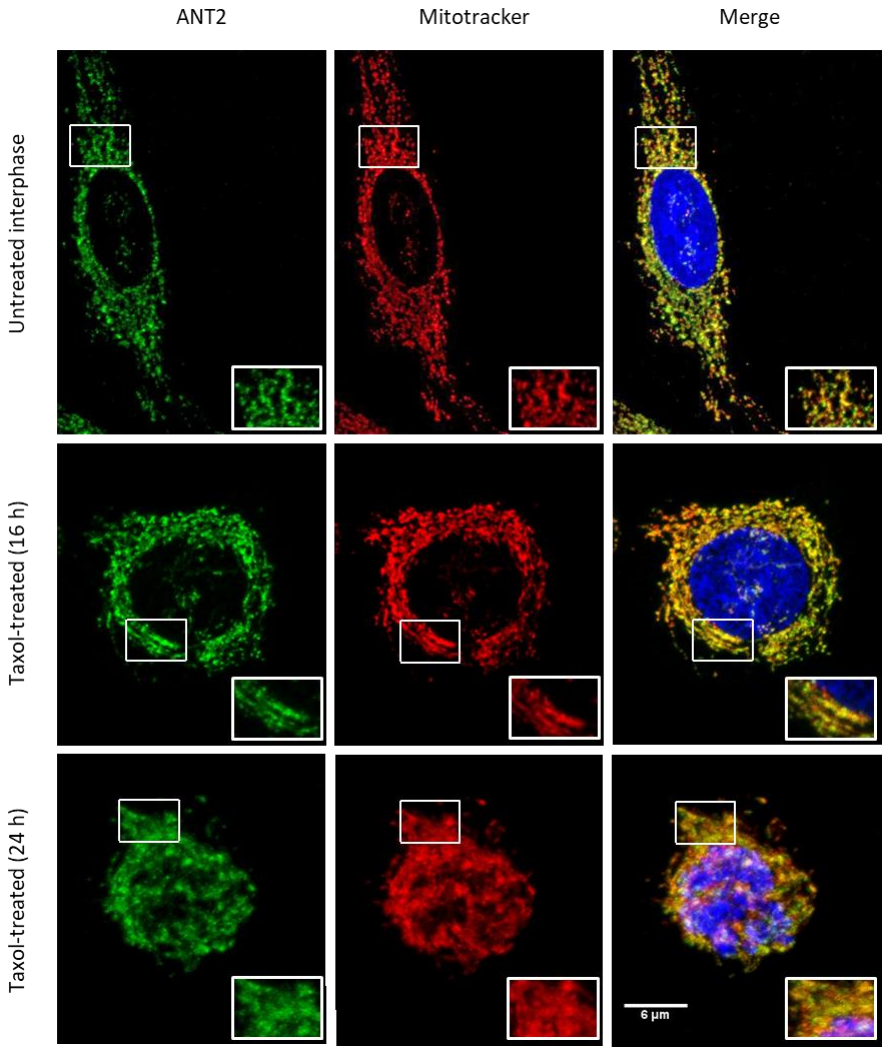

Figure 4-24: Localization of ANT2 in untreated Taxol-treated HeLa cells.

HeLa cells were either left untreated or treated with Taxol for the indicated times and labelled with anti-ANT2 antibody visualized with Alexa-flour 488 secondary antibody (green). Mitochondria were labelled with Mitotracker (red). Merge panels include DNA

(blue) stained with Hoechst 33258. Results are representative of two independent experiment. Images are maximum intensity projections of z-stack data. Scale bar, 6 µm.

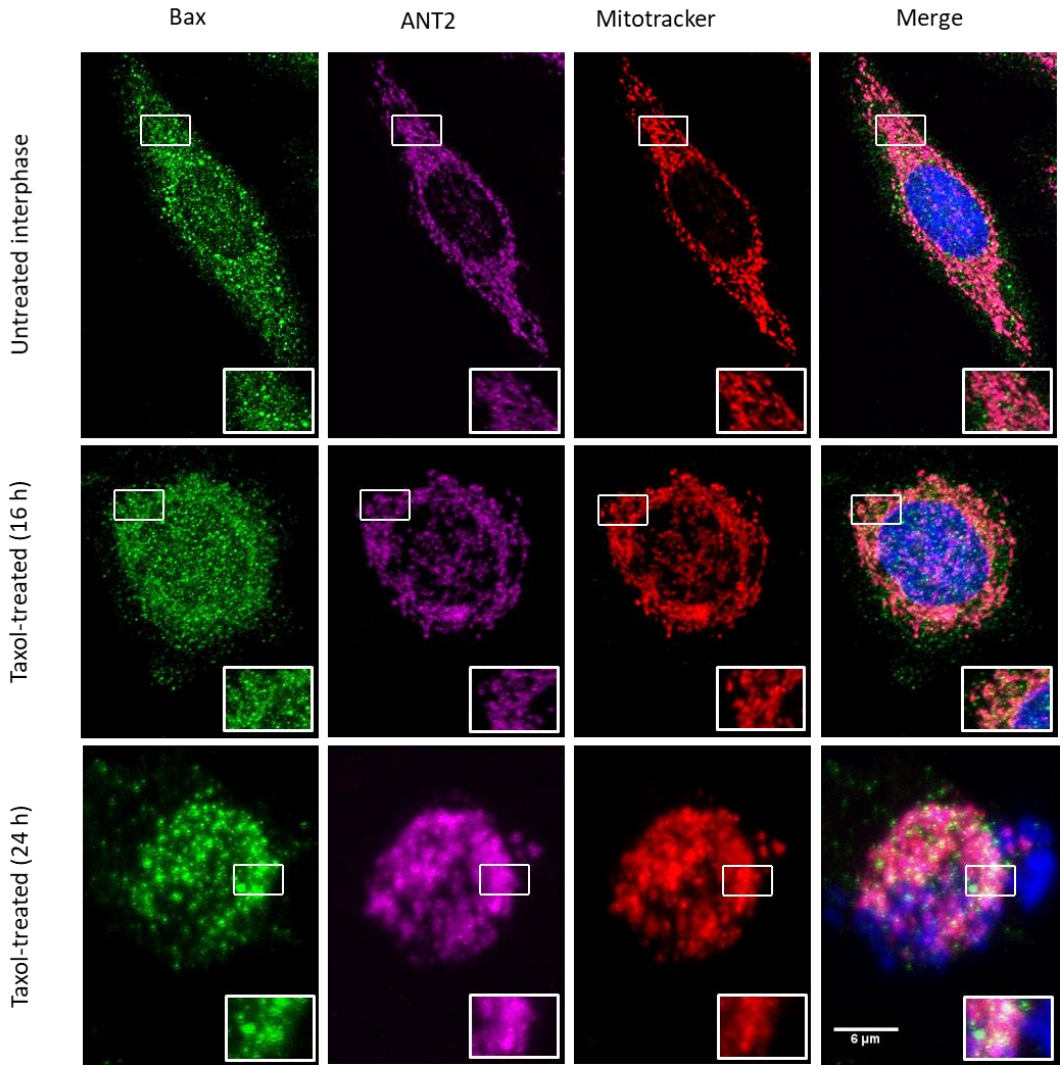

Figure 4-25: Co-localization of Bax-ANT2 in Taxol-treated HeLa cells.

HeLa cells were either left untreated or treated with Taxol for the indicated times and labelled with anti-Bax visualized with Alexa-flour 488 secondary antibody (green) and anti-ANT2 visualized with Alexa-flour 647 secondary antibody (magenta). Mitochondria was labelled with Mitotracker (red). Merge panels include DNA (blue) stained with Hoechst 33258. White = co-localization of Bax/ANT2/Mitotracker. Results are representative of two independent experiments. Images are maximum intensity projections of z-stack data. Scale bar, 6 µm.

4.12 VDAC interacts with Bak but not Bax in Taxol-arrested cells

To decipher the role of VDAC in Taxol-induced apoptosis and to determine if VDAC is a binding partner of the pro-apoptotic proteins Bak and Bax, co-IPs were carried out using HeLa cells extracts from untreated or Taxol-treated cells. As shown in Figure (4-26) anti-Bak antibody pulled down VDAC in Taxol-treated cells but not in untreated cells. In contrast, anti-Bax antibody did not co-immunoprecipitate VDAC (not shown). My results indicated that Bak forms a complex with VDAC and ANT2 in Taxol-arrested cells. Bak formation a complex with VDAC in Taxol-arrested cells but not in untreated cells indicated that Bak is inserted into MOM after Taxol addition. However, there is no interaction between VDAC and Bax even in Taxol-treated cells. This result is consistent with MS data that Bak IP had identified VDAC as a co-immunoprecipitating protein in Taxol-arrested cells (see Table 7-1, Appendix).

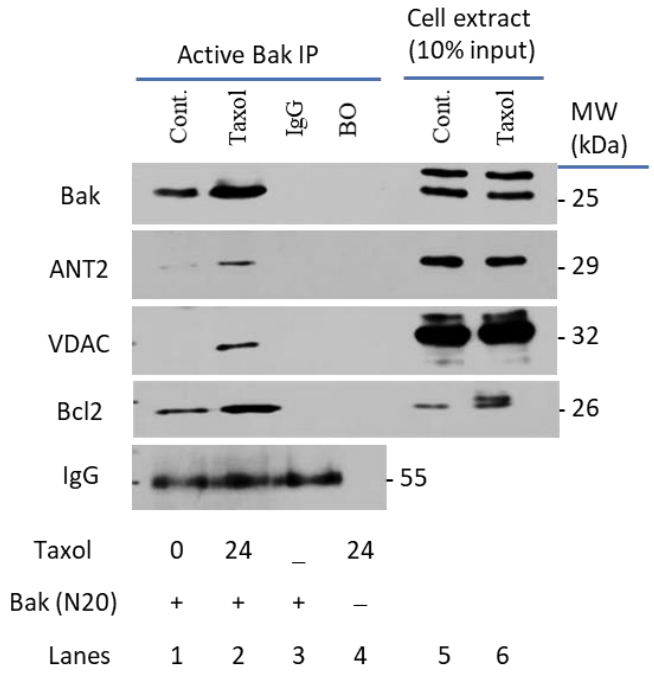

Figure 4-26: Interaction of Bak with ANT2, VDAC and Bcl-2 in Taxol-arrested cells.

HeLa cells were either left untreated or treated with Taxol (60nM) for the indicated times and subjected to immunoprecipitation with anti-Bak (N20) antibody (lanes 1-2) followed by immunoblotting for Bak, ANT2, VDAC and Bcl-2. Lane 3 represents control IgG and lane 4 represents cell extracts plus magnetic beads only (BO). The cell extracts

of untreated (lanes 5) or Taxol-treated cells (lane-6) were also immunoblotted as controls. The molecular weight markers are shown on the right. This is representative of 2 independent experiments.

4.13 Bcl-2 interacts with Bak in untreated and Taxol-treated cells

The anti-apoptotic protein Bcl-2 is known to protect the cells from apoptosis by forming a complex with pro-apoptotic protein Bak or Bax (Dai et al., 2009). Therefore, I wanted to determine whether Bcl-2 interacts with Bak in untreated and Taxol-arrested HeLa cells. My results indicated that a low level of Bcl-2 was complexed with Bak in untreated cells but the level of Bcl-2 was increased in Taxol-arrested mitotic cells as anti-Bak antibody pulled down more Bak in Taxol-treated cells compared to untreated cells (Figure 4-26). Furthermore, immunoblot analysis of the cell extracts with Bcl-2 showed a clear mobility shift in the Taxol-treated cells suggesting Bcl-2 phosphorylation following Taxol treatment (see Figure 4-26). However, co-immunoprecipitated Bcl-2 does not show any mobility shift indicating that Bcl-2 only interacted with Bak in the unphosphorylated form and not when phosphorylated.

4.14 The interaction between Bax and ANT2 is dependent on Bak

I determined if the interaction of the pro-apoptotic protein Bax with ANT2 was dependent on the presence of Bak. Anti-active Bax antibody was used to immunoprecipitate active Bax in Bak-depleted HeLa cells after 24 hrs Taxol treatment. My earlier results had indicated that Bax physically interacts with ANT2 only in Taxol-treated HeLa cells (Figure 4-23 page 111). Interestingly, in Bak-depleted cells (see Figure 4-27), a significant amount of active Bax was immunoprecipitated but it failed to co-immunoprecipitate ANT2 (Figure 4-27 lane 1). This result suggested that Bax does not directly interact with ANT2 and that Bak is required for this interaction. I concluded that Bak may be required for

targeting Bax to the outer mitochondrial membrane and inducing apoptosis. Therefore, there was a low level of apoptosis in the absence of either Bak or Bax. This is confirmed by my previous experiment (see Figure 3-5 page 79).

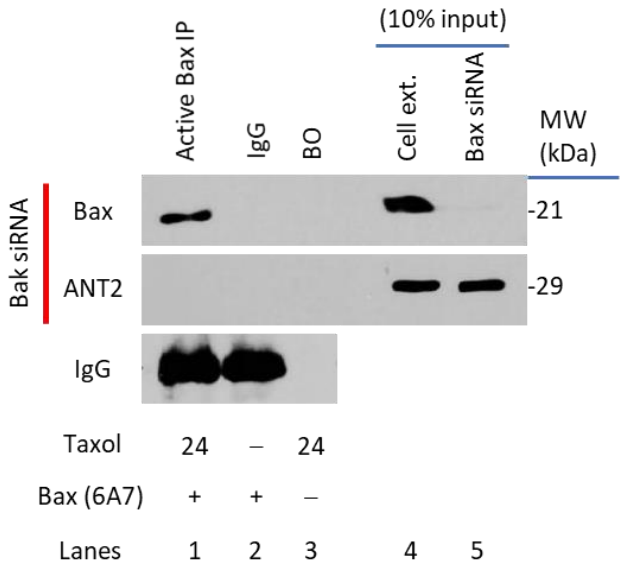

Figure 4-27: ANT2 interaction with Bax after Taxol addition requires Bak.

HeLa cells were transfected with Bak siRNA (50nM) for 48 hrs and treated with Taxol (60nM) for 24 hrs and subjected to immunoprecipitation with anti-Bax (6A7) antibody (lanes 1) followed by immunoblotting for Bax and ANT2. Lane 2 represents control IgG and lane 3 represents cell extracts plus magnetic beads only (BO). The cell extracts of Taxol-treated cells (lanes 4) or Bax-depleted extracts (lane 5) were also immuoblotted as controls. The molecular weight markers are shown on the right. This result is representative of 2 independent experiments.

4.15 The interaction of Bak with ANT2 and VDAC is independent of Bax

To evaluate the possible requirement of Bax for the formation of Bak-ANT2-VDAC complex during prolonged mitotic arrest, HeLa cells were transfected with Bax siRNA for 48 hrs, followed by 24 hrs Taxol treatment. Anti-active Bak (N-20) antibody was used to immunoprecipitate active Bak in the Bax-depleted cells. As shown in Figure (4-28), active Bak was efficiently immunoprecipitated and co-immunoprecipitated both ANT2 and VDAC from Taxol-arrested apoptotic cells. This result demonstrated that depletion of Bax does not affect the interaction of

Bak with either ANT2 or VDAC. Although Bak is activated and forms a complex with ANT2 and VDAC in the absence of Bax, there was no apoptosis (see Figure 3-5 page 79). The results of my previous experiments (see pages 77-79) demonstrated that cells deficient in either Bak or Bax showed resistance to Taxol-induced mitotic death, precluding the possibility that Bak or Bax can substitute for each other in Taxol-induced cell death. Therefore, my data suggested that the interaction of Bak with Bax, ANT2 and VDAC and that of Bax with Bak and ANT2 are occurred during Taxol-induced apoptosis.

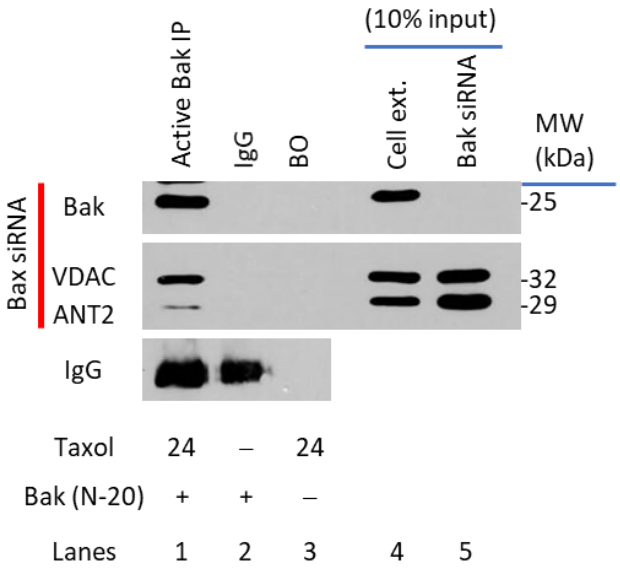

Figure 4-28: The interaction of Bak with ANT2 and VDAC in Bax-depleted cells.

HeLa cells were transfected with Bax siRNA (50nM) for 48 hrs and treated with Taxol (60nM) for 24 hrs and subjected to immunoprecipitation with anti-Bak (N-20) antibody (lanes 1) followed by immunoblotting for Bak, ANT2 and VDAC. Lane 2 represents control IgG and lane 3 represents cell extracts plus magnetic beads only (BO). The cell extracts of Taxol-treated cells (lanes 4) or Bak-depleted extracts (lane 5) were also immunoblotted as controls. The molecular weight markers are shown on the right. This result is representative of 2 independent experiments.

4.16 VDAC depletion

My MS data had shown that all VDAC isoforms (VDAC1, VDAC2 and VDAC3) were co-immunoprecipitated with Bak in Taxol-treated cells. As well as, a number of mitochondrial membrane proteins, from both inner and outer mitochondrial membrane, were identified in the Bak IP such as ATP synthase subunit alpha, ATP synthase subunit beta, heat shock protein (mitochondrial) and Peptidyl-prolyl cis-trans isomerase (see Table 7-1, Appendix). Furthermore, my co-IP experiments indicated that VDAC is found in a complex with Bak following Taxol treatment. VDAC1 is the most abundant protein in the MOM of any tissue (Yamamoto et al., 2006). VDAC1 is thought to be over-expressed in many cancers, suggesting that the protein may play an essential role in cancer cell survival (Arbel et al., 2012). Therefore, I wanted to examine the role of VDAC1 in Taxol-induced apoptosis and to investigate if VDAC1 is a component of the apoptosis machinery in mitotically-arrested cells. The VDAC1 protein was depleted using different concentrations of siRNA to identify the effective siRNA concentration that efficiently targets VDAC1 mRNA. HeLa cells extracts were prepared form untreated, control siRNA, and VDAC1 siRNA for Western blot analysis. As shown in Figure 4-29 A, VDAC1 was clearly detectable in untreated and control siRNA, but was strongly depleted to the same level with 25-300 nM siRNA.

Next, I wanted to investigate whether double VDAC1 depletion has more effect on depleting VDAC1 levels in comparison to a single depletion. VDAC1 was targeted using VDAC1 siRNA for 24 hrs followed by further transfection for 48 hrs. As shown in Figure 4-29 B, there was no difference between a single and a double depletion as the intensity of the bands were similar. My conclusion was that VDAC1 was efficiently depleted using 25 nM VDAC1 siRNA for 48 hrs.

In order to examine the role of VDAC1 in Taxol-induced apoptosis, a preliminary study was carried out using HeLa cells transfected with VDAC1 siRNA. VDAC1-depleted cells were either left untreated or treated with Taxol for 24 hrs and

apoptosis was analysed using the M30 antibody. A parallel set of exponentially growing HeLa cells was treated with Taxol as a control. The results of the preliminary study show that VDAC1 depletion alone caused 35% apoptosis. The percentage of apoptosis was increased to 68 % in VDAC-depleted cells treated with Taxol which is slightly higher in comparison with Taxol treatment only which resulted in 62 % of the cells undergoing apoptosis (Figures 4-30 and 4-31). My results indicated that VDAC1 depletion caused an increase in apoptosis, suggesting that VDAC1 has anti-apoptotic effects. Therefore, the results suggested that VDAC1 is largely dispensable for Taxol-induced apoptosis and further studies are needed to define the role of VDAC2 and VDAC3 in Taxol-induced apoptosis.

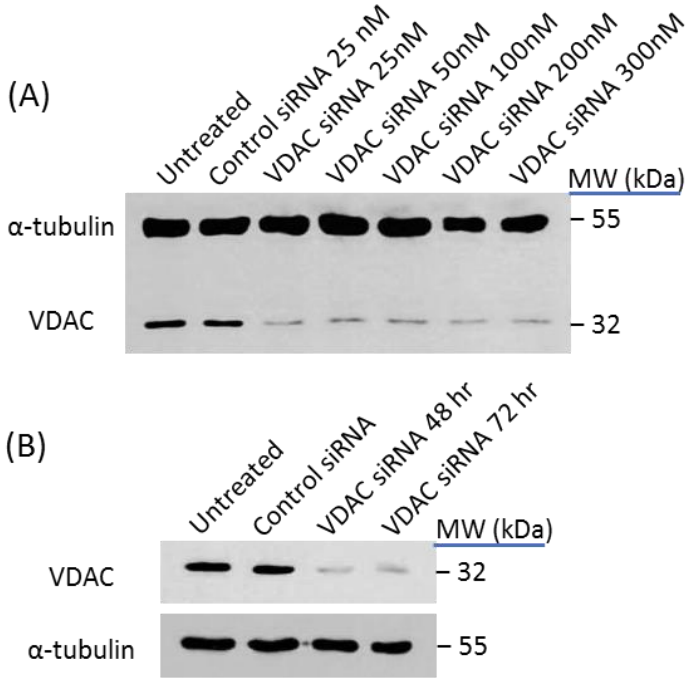

Figure 4-29: Depletion of VDAC expression using different concentrations of VDAC siRNA

(A) HeLa cells were either left untreated or transfected with control siRNA (25 nM) or VDAC1 siRNA (25-300 nM) and incubated for 48 hrs. Western blots were performed to verify the protein expression level of VDAC and α-tubulin was used as a loading control and the molecular weight markers are shown on the right. This result is representative of 2 independent experiments. (B) Single and double depletion of VDAC expression using

25 nM VDAC1 siRNA for 48 or 72 hrs respectively. After incubation with VDAC1 siRNA for 24 hrs, the transfected cells were also transfected with VDAC1 siRNA and incubated for a further 48 hrs. This result is representative of 2 independent experiments.

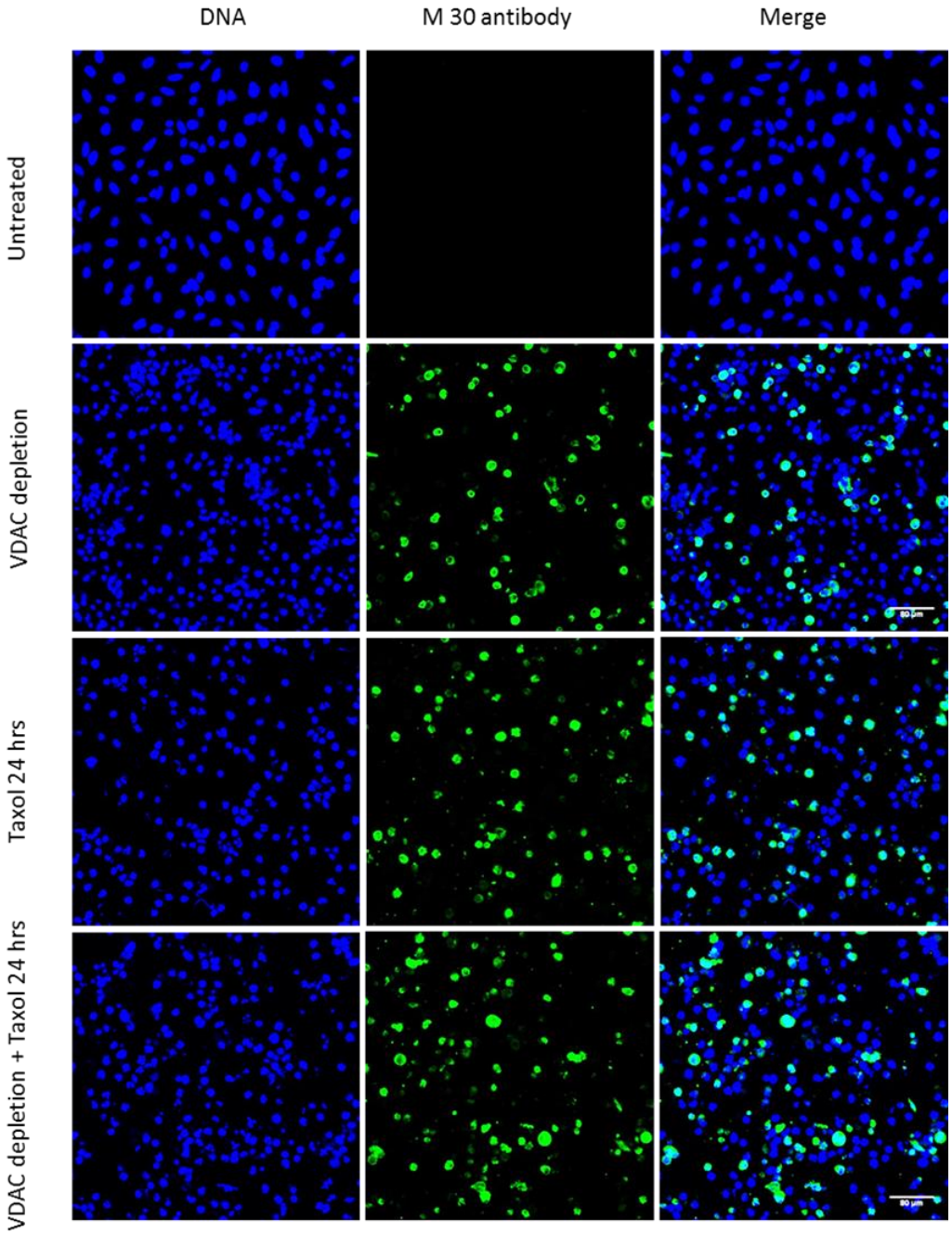

Figure 4-30: VDAC depletion induces activation of the mitochondrial pathway of apoptosis.

Hela cells were either left untreated or transfected with VDAC1 siRNA for 48 hrs. The VDAC1-siRNA cells were either left untreated or treated with Taxol (60 nM) for 24 hrs. The cells were fixed and stained with CytoDEATH (M30) primary antibody and Alexa-Fluor 488 secondary antibody (green). DNA was stained with Hoechst 33342 (blue). This result is representative of three independent experiments. Scale bar, 80 µm.

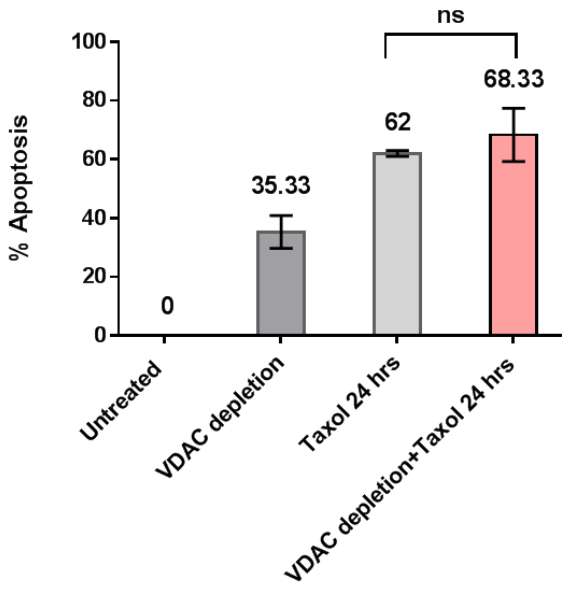

Figure 4-31: Quantitation of apoptosis in VDAC-depleted cells treated with Taxol

Hela cells were either left untreated or transfected with VDAC1 siRNA for 48 hrs. The VDAC1-siRNA treated cells were either left untreated or treated with Taxol (60 nM) for 24 hrs. The cells were fixed and stained with CytoDEATH (M30) primary antibody and Alexa-Fluor 488 secondary antibody. At least 100 cells were counted in randomly selected fields and the number of the apoptotic cells was quantitated. Histograms represent the mean ± SD of three independent experiments. P-values were calculated using one-way ANOVA (ns = not significant compared to 24 hrs Taxol treatment).

4.17 ANT2 and VDAC expression in different cell lines

The expression levels of ANT2 and VDAC were investigated in several human cancer cell lines, in addition to retinal pigment epithelium cells (RPE1) and mouse myoblast cells (C2C12). ANT2 and VDAC levels were examined by Western blotting of total cell extracts prepared from non-transformed RPE-1, C2C12 and a number of cancer cell lines (HeLa, Melanoma, U2OS, Mesothelioma, RKO 143, STK 5090 and A19 RKO). Quantitation of ANT2 expression indicated that there was no statistically significant difference in ANT2 expression between RPE1 cells and different cancer cell lines (Figure 4-32 A and B). While, the expression of VDAC in RPE1 cells is significantly lower compared to cancer cell lines U2OS and

Mesothelioma. However, the expression of VDAC in RPE1 cells is significantly higher compared to Melanoma (Figure 4-32 A and C). It would be interesting for future study to examine whether these cells, with low or high levels of ANT2 or VDAC, are more or less sensitive to Taxol or other anti-cancer drugs.

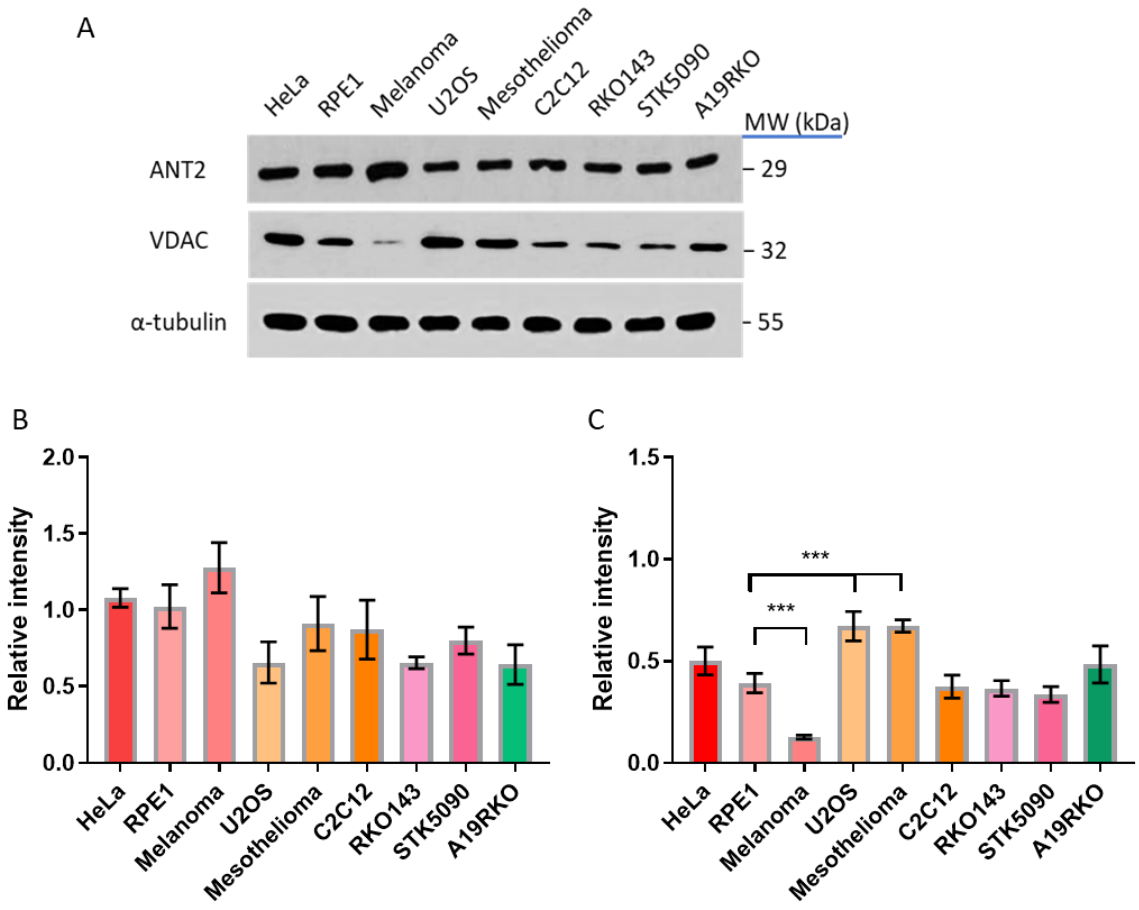

Figure 4-32: Protein expression of ANT2 and VDAC in different cell lines.

(A) Exponentially growing cells were lysed in RIPA buffer and the normalized cell extracts were subjected to immunoblotting for ANT2 and VDAC. α-tubulin was used as a loading control and the molecular weight markers are shown on the right. This result is representative of 3 independent experiments. (B) and (C) Histograms represent the intensity of ANT2 and VDAC expression in different cell lines normalized to α-tubulin from blots shown in A, respectively. Histograms represent the mean ± SD of three independent experiments. P-values were calculated using one-way ANOVA (*** P value < 0.001).

4.18 Discussion

Microtubule interfering agents (MIAs) such as Taxol exert their effects through the mitochondrial-dependent apoptosis (Morales-Cano et al., 2013). MIAs cause changes in mitochondrial outer membrane permeability and enable the release of cytochrome c and other apoptogenic factors (Adams and Cory, 2007). Following apoptotic stimuli, Bax is translocated from the cytosol to the MOM, where both Bak and Bax undergo major conformational changes. (Wolter et al., 1997, Lovell et al., 2008). The key regulators of apoptosis, Bax and Bak, begin to form specific pores or channels that permeate the MOM (Desagher and Martinou, 2000). Permeabilization of the MOM releases apoptogenic factors into the cytosol (García-Sáez et al., 2004, Annis et al., 2005). Although Bak and Bax are key regulators of mitochondrial-mediated apoptosis, the molecular mechanism of Bak/Bax arrangement in the MOM during cell death and their interaction(s) with other MOM/MIM proteins and how they induce release of cytochrome c remains unclear.

Several studies have shown Bak and Bax activation in response to a variety of apoptotic stimuli that induce mitotic arrest (Yamaguchi et al., 2004, Yamaguchi et al., 2002, Upreti et al., 2006, Upreti et al., 2008a, Miller et al., 2013). I examined Bak and Bax conformational change by using conformation-specific antibodies for Bak (N-20) and Bax (6A7). My results indicated that both Bak and Bax underwent conformational changes during Taxol treatment. Both Bak and Bax were mainly monomeric in untreated cells and oligomers were observed at 24 to 36 hrs of Taxol treatment. Consistent with our observation, it has been shown that vinblastine (a microtubule depolymerizing drug) induces Bak and Bax oligomerization in KB-3 human carcinoma cell line (Upreti et al., 2006, Upreti et al., 2008a). Additionally, my data indicates that Bax depletion had no effect on Bak oligomerization and vice versa suggesting that Bak and Bax can oligomerize independently in response to Taxol treatment. However, my previous data had shown that both Bak and Bax are required for Taxol-induced apoptosis in HeLa

cells. Addition of the reducing agent (β-mercaptoethanol) caused elimination of the Bak and Bax oligomers, indicating a requirement for disulphide bonds in their formation or maintenance of these oligomers (Gavathiotis et al., 2010).

The interaction between Bak and Bax homo-oligomers is required for ATP depletion-induced apoptosis in rat proximal tubule cells (Mikhailov et al., 2003). In another report, Bak/Bax interaction was observed in TNF-α-induced apoptosis in HeLa cells (Sundararajan et al., 2001). The interaction between Bak and Bax homo-oligomers has also been detected in Vinblastine-induced apoptosis in KB-3 cells (Upreti et al., 2008a). To the best of my knowledge, my study was the first to show the time dependent increase in the amount of active Bak and active Bax in Taxol-arrested mitotic cells. Using anti-active Bak and anti-active Bax antibodies, the time course IPs have shown the presence of increasing amounts of active Bax and active Bak between 12-36 hrs after Taxol addition. Immunoprecipitation of active Bax indicated the presence of Bak, and the reciprocal experiment showed that active Bak also co-immunoprecipitated Bax. Intriguingly, the levels of Bak and Bax that co-immunoprecipitated also increased following Taxol addition. These results indicated that Bax physically interacts with Bak either directly or indirectly in Taxol-arrested mitotic cells. The interaction of these two multidomain pro-apoptotic proteins correlates with the induction of apoptosis.

At the mitochondrial outer membrane, Bax and Bak oligomers are thought to oligomerize and/or interact with the Mitochondrial Permeability Transition Pore (MPTP) components such as VDAC and ANT to increase the permeability of the mitochondrial outer membrane which then leads to cytochrome c release and apoptosis (Shimizu et al., 1999, Galluzzi and Kroemer, 2007, Belzacq et al., 2003). ANT is an integral protein located in the inner mitochondrial membrane and is involved in the regulation of the ATP/ADP ratio between the mitochondria and the cytosol (Halestrap and Brenner, 2003). The physiological function of ANT is to catalyse the exchange of mitochondrial ATP with cytosolic ADP (Chevrollier et al.,

2011). The anti-apoptotic protein Bcl-2 is located in both the inner and outer mitochondrial membrane. In the inner mitochondrial membrane Bcl-2 interacts with ANT to enhance the translocase activity and maintain the ATP/ADP exchange at the mitochondrial membranes (Gotow et al., 2000, Belzacq et al., 2003). However, in response to the chemotherapeutic agent etoposide, Bax interacts with ANT to inhibit the translocase activity in human colon adenocarcinoma cell line HT29 (Belzacq et al., 2003). Bax interaction with ANT within the MPTP modulates mitochondrial membrane permeabilization and mediates apoptosis (Marzo et al., 1998).

In previous studies, ANT2 was reported to interact with Bax only in response to apoptotic stimulus (Belzacq et al., 2003, Brenner et al., 2000). However, my study indicated that ANT2 was co-immunoprecipitated with both Bak and Bax in Taxol-arrested mitotic cells but not in untreated cells suggesting that Bak and Bax can form a complex with MPTP components during Taxol treatment. Furthermore, in Bak-depleted cells, Bax did not interact with ANT2 indicating that Bax-ANT2 interaction is Bak dependant. Ma and colleagues reported that Bax requires Bak and VDAC2 for insertion of its hydrophobic C-terminus into the MOM (Ma et al., 2014). Consistent with this study, my results indicated that, in Bak-depleted cells, Bax is unable to form a complex with ANT2 even in the presence of VDAC.

Furthermore, my immunofluorescence analysis with antibodies against Bax and ANT2 demonstrated that Bax co-localized with ANT2 following Taxol addition. ANT2 is the major constituent of the MPTP complex and it's thought to be involved in mitochondrial-mediated apoptosis (Ito et al., 2010). My results support the hypothesis that Bak and Bax interaction with ANT2 in mitotically-arrested cells may reduce ANT2-mediated ATP/ADP exchange across the inner mitochondrial membrane, and disrupt the mitochondrial transmembrane potential, resulting in apoptosis and inhibition of tumour growth (Marzo et al., 1998, Belzacq et al., 2003, Chevrollier et al., 2011).

It has been reported that ANT2 depletion is associated with an increase in mitochondrial membrane permeability (Luciakova et al., 2003). siRNA-mediated depletion of ANT2 in human breast cancer cells (MDA-MB-231) decreased the intracellular ATP levels and inhibited cell growth, which ultimately induces apoptotic cell death (Jang et al., 2008, Jang et al., 2016). Therefore, ANT2 could be considered as anti-apoptotic protein such as Bcl-2 and Bcl-xL, that inhibits the nonspecific permeabilization of the mitochondrial membrane and cytochrome c release (Jang et al., 2008).

VDAC is one component of the MPTP (Rostovtseva et al., 2002). VDAC is a multi-functional mitochondrial protein, and it plays an important role in the regulation of metabolic and energetic functions of the mitochondria (McCommis and Baines, 2012). It also participates in mitochondrial-mediated apoptosis via interaction with Bcl-2 family members (Galluzzi and Kroemer, 2007). Both anti- and pro-apoptotic proteins, such as Bcl-2, Bcl-xL, Bim and Bax, were reported to interact with VDAC to regulate mitochondrial-mediated apoptosis (Shimizu et al., 2000b, Sugiyama et al., 2002, Malia and Wagner, 2007, Tajeddine et al., 2008, Arbel and Shoshan-Barmatz, 2010).

My MS data of the Bak IP had identified all VDAC isoforms (VDAC 1-3) as a co-immunoprecipitating protein in Taxol-arrested cells but not in the untreated cells. The MS data was confirmed by co-IP experiments, which indicated that Bak can form a complex with VDAC in Taxol-arrested cells. This result is consistent with a recent study which suggested that the middle domain of VDAC2 (sequence 123–179) is required for insertion of Bak to the MOM and tBid-mediated apoptosis (Naghdi et al., 2015). On the other hand, Bax insertion into MOM depends on the presence of VDAC 2 and Bak (the hetero-oligomerization partner of Bax) (Ma et al., 2014). These results suggested that Bak/Bax interaction with VDAC and ANT2 may activate the MPTP complex and induce cytochrome c release. The other possibility is that the formation of Bak-Bax-VDAC and ANT2 complex which may create a larger pore to initiate cytochrome c release. However, in contrast to the

previous reports, Baines and colleagues reported that cytochrome c release from mouse embryonic fibroblast and isolated-mouse mitochondria deficient of all VDAC isoforms was identical to the wild type (Baines et al., 2007). Another study revealed that isolated mitochondria lacking ANT are able to form MPTP, resulting in the release of the cytochrome c (Kokoszka et al., 2004). These studies suggested that VDAC and ANT are not essential components of the MPTP complex. Therefore, the roles of VDAC and ANT in mitochondrial-mediated apoptosis remain unclear.

Next, I examined the role of VDAC1 in Taxol-induced apoptosis. The dramatic increase of apoptosis in VDAC1-depleted cells can be explained by the important role of VDAC1 in maintaining the integrity of the MOM. The percentage of apoptosis was slightly higher in VDAC1-depleted cells treated with Taxol (68% apoptosis) in comparison with Taxol treatment only (62% apoptosis). A possible explanation is that some residual VDAC which has not been depleted may inhibit Taxol-induced apoptosis.

Several studies have shown the importance of VDAC1 in cell energy and cell proliferation. Depletion of VDAC1 by a single siRNA inhibits cell proliferation and cancer cell growth, it also decreases ATP levels (Koren et al., 2010, Arif et al., 2014, Arif et al., 2017). Another study suggested that VDAC1 interaction with hexokinase and Bcl-2 induces protection against apoptosis by inhibiting cytochrome c release Upon apoptotic signalling (Abu-Hamad et al., 2009). In contrast to my results, siRNA-mediated depletion of VDAC1 causes a reduction in endostatin-induced apoptosis in HMECs (Human Mammary Epithelial Cells) and overexpression of VDAC1 causes endostatin-induced MPT pore opening (Yuan et al., 2008). Similarly, siRNA depletion of VDAC1 inhibits cisplatin-induced apoptosis in A549 NSCLC (Non-small-cell lung carcinoma) (Tajeddine et al., 2008). These incompatible results could be explained by cell line specificity or using different apoptotic stimulus. However, further studies are needed to determine the role of VDAC in MOM permeabilization and cell death.

Dai and colleagues reported that Bcl-2 phosphorylation by Cdk1 enhances its binding to Bak in Taxol-treated K562 cells (human blood-chronic myelogenous leukaemia) (Dai et al., 2013). The phosphorylation of Bcl-2 and its interaction with Bak may support the anti-apoptotic function of Bcl-2 (Deng et al., 2000, Deng et al., 2004, Dai et al., 2013). However, other studies have demonstrated that phosphorylation of Bcl-2 antagonizes the protective effect of Bcl-2 (Haldar et al., 1995, Blagosklonny et al., 1997, Terrano et al., 2010). In particular, Bcl-2 S70A substitution blocked Bcl-2 post-translational modification and protected cells better than endogenous Bcl-2 (Yamamoto et al., 1999). These incompatible results could be explained by context-dependent effects or cell line specificity. However, my data supported a model in which Cdk1-induced Bcl-2 phosphorylation may inhibit its interaction with Bak and antagonize its anti-apoptotic function. I have shown that unphosphorylated Bcl-2 interacts with Bak but not the phosphorylated form. The Bak IP had identified unphosphorylated Bcl-2 as a co-immunoprecipitating protein in both untreated and Taxol-arrested mitotic cells. Furthermore, phosphorylated Bcl-2 was detected in the cell extract of Taxol-arrested cells but not in the co-immunoprecipitated Bcl-2 suggesting that Bcl-2 only interacted with Bak in the unphosphorylated form but not when phosphorylated (see Figure 4-27 page 113).

Based on my data, I propose a model for Taxol-induced apoptosis. My data indicated that Taxol-induced mitochondrion protein release, activation of the caspase cascade, and mitotic death is mediated by the activation of the pro-apoptotic proteins Bak and Bax. Activated Bax is translocated from the cytosol to the MOM where both Bak and Bax oligomerize to form specific pores or channels. My results indicated that Bak-Bax interaction is occurred during Taxol-induced apoptosis. Furthermore, Bak and Bax oligomers form a larger complex with MPTP components such as VDAC and ANT2. The formation of the apoptotic pore complex modulates the permeability of the MOM. MOM permeabilization induces the release of cytochrome c which results in the activation of the

caspases. Therefore, the formation of the apoptotic pores from Bak and Bax homo or hetero-oligomers, which induces MOMP, is the irreversible step in the mitochondrial pathway of apoptosis.

Chapter 5. Identification of the link between SAC and apoptosis

5.1 Introduction

Although the molecular link between cell cycle arrest and apoptosis has been the subject of intense research, no clear mechanism has been found so far. Previous studies have shown that extensive phosphorylation of the anti-apoptotic proteins Bcl-2, Bcl-xL and Mcl-1 by Cdk1 inactivates their anti-apoptotic activity and primes mitotically-arrested cells to undergo apoptosis (Geng et al., 2011, Sakurikar et al., 2012). Moreover, studies by Terrano and colleagues suggested that a change in the duration of Cdk1-mediated phosphorylation of Bcl-2 and Bcl-xL from transient during normal mitosis to sustained during mitotic arrest links the activation of the SAC to the initiation of apoptosis (Terrano et al., 2010). However, it is not known how Cdk1 moves from the cytoplasm to the mitochondria to phosphorylate certain Bcl-2 family members.

Recent data demonstrate that shuttling of the pro-apoptotic effector proteins, Bak and Bax, from the cytoplasm to the MOM is accelerated upon extended mitotic arrest (Todt et al., 2015, Salvador-Gallego et al., 2016, Große et al., 2016). Furthermore, Cdk1 is also reported to be translocated to the mitochondria in Vinblastine-arrested mitotic cells (Terrano et al., 2010). Upon prolonged SAC activation, Cdk1-mediated phosphorylation of Bcl-2, Bcl-xL and Mcl-1 inhibits their anti-apoptotic effects (Terrano et al., 2010, Geng et al., 2011, Sakurikar et al., 2012, Bah et al., 2014, Chu et al., 2012). In this chapter I examined the function of Cdk1, the master regulation of the cell cycle, in mitochondrial-mediated apoptosis.

5.2 Cdk1 co-immunoprecipitates with Bak and Bax in both untreated and Taxol-treated HeLa cells

My earlier mass spectrometry (MS) data of Bax IP (see Table 7-1, Appendix) had identified Cdk1 as a co-immunoprecipitating protein. To confirm the results of the MS analysis, co-immunoprecipitations were carried out to determine whether Cdk1 co-immunoprecipitates with Bax and Bak. Bax and Bak were immunoprecipitated from untreated and Taxol-treated HeLa cells using anti-Bax (6A7) and anti-Bak (N20) antibodies, respectively. Bax and Bak IPs were analysed by immunoblotting with Bax, Bak and Cdk1 antibodies. The results (Figures 5-1 and 5-2) demonstrated that a small amount of Cdk1 is complexed with both Bax and Bak in untreated cells but the amount of Cdk1 is increased in the Taxol-arrested cells.

It has been reported that Cdk1-mediated phosphorylation of anti-apoptotic proteins Bcl-2/ Bcl-xL decreases their anti-apoptotic effects (Terrano et al., 2010), which ultimately enables Bak and Bax to form oligomers at the mitochondrial outer membrane and disrupt the transmembrane potential (Große et al., 2016). These results suggest that a subpopulation of Cdk1 is initially associated with pro-apoptotic proteins Bax and Bak in normal interphase cells and the levels of Cdk1 associated with Bax and Bak is increased during Taxol-induced mitotic cell cycle arrest. This result suggested the hypothesis that Bax and Bak-associated Cdk1 is translocated from the cytoplasm to the MOM to phosphorylate Bcl-2 and Bcl-xL upon Taxol treatment.

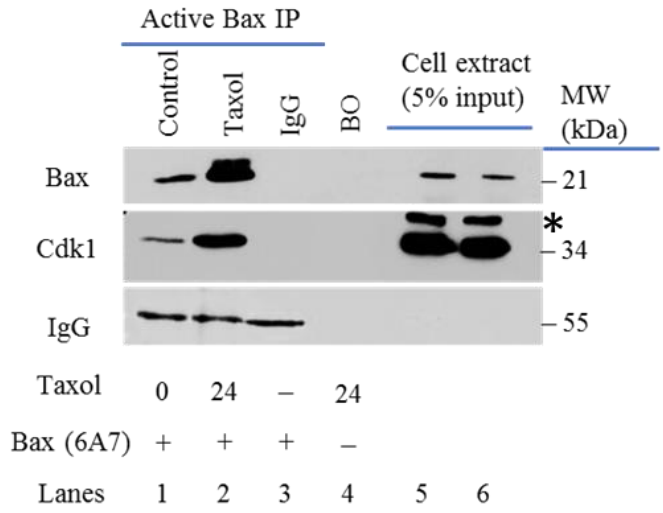

Figure 5-1: Cdk1 co-immunoprecipitates with Bax from both untreated and Taxol-arrested HeLa cells.

HeLa cells were either left untreated or treated with Taxol (60nM) for 24 hrs and subjected to immunoprecipitation with anti-Bax (6A7) antibody (lanes 1-2) followed by immunoblotting for Bax and Cdk1. Lane 3 represents Bax (6A7) antibody with magnetic beads and lane 4 represents cell extract with magnetic beads. Lane 5: cell extract from untreated. Lane 6: Taxol-treated cell extract. Molecular weight markers (kDa) are shown on the right. * indicates a non-specific protein detected by the Cdk1 antibody. This result is representative of 2 independent experiments.

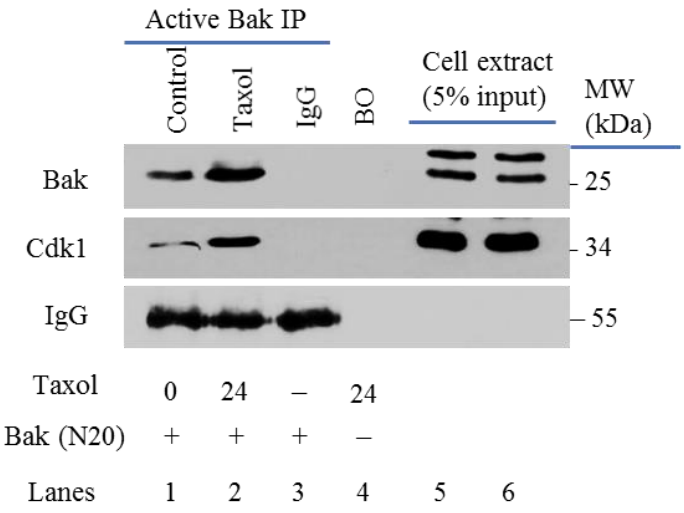

Figure 5-2: Cdk1 co-immunoprecipitates with Bak from both untreated and Taxol-arrested HeLa cells.

HeLa cells were either left untreated or treated with Taxol (60nM) for 24 hrs and subjected to immunoprecipitation with anti-Bak (N-20) antibody (lanes 1-2) followed by immunoblotting for Bak and Cdk1. Lane 3 represents Bak (N-20) antibody with magnetic beads and lane 4 represents cell extract with magnetic beads. Lane 5: cell extract from untreated. Lane 6: Taxol-treated cell extract. Molecular weight markers (kDa) are shown on the right. This result is representative of 2 independent experiments.

5.3 Cdk1 co-immunoprecipitates with Bak and Bax in U2OS and RPE1 cell lines

In order to investigate whether the Cdk1 interaction with Bak/Bax was specific for HeLa cells or whether it is a general phenomenon, I immunoprecipitated Bak and Bax from another cancer cell line (U2OS) and also from a normal diploid cell line (RPE1). The Cdk1 interaction with Bak/Bax was identified in both U2OS and RPE1 cells using native conditions. Immunoprecipitations were carried out using Bax-specific antibody (6A7) and Bak-specific antibody (N-20). Bax IPs were immunoblotted with Bax and Cdk1 antibodies, and Bak IPs were immunoblotted with Bak and Cdk1 antibodies. My data indicated that Cdk1 was specifically co-immunoprecipitated with both Bax and Bak in untreated and Taxol-arrested U2OS cells (Figures 5-3 and 5-4). Similarly, Bax was also associated with Cdk1 in Nocodazole-arrested U2OS cells (Figure 5-5). Identical results were also obtained with RPE1 cells (Figures 5-6 and 5-7). Therefore, I was able to co-IP a Cdk1 with Bak and Bax in different cell lines and in response to either Taxol (a microtubule stabilizing agent) or Nocodazole (a microtubule destabilizing agent) suggesting that this interaction is not drug specific and may be widely used by the cells to activate the intrinsic apoptotic pathway.

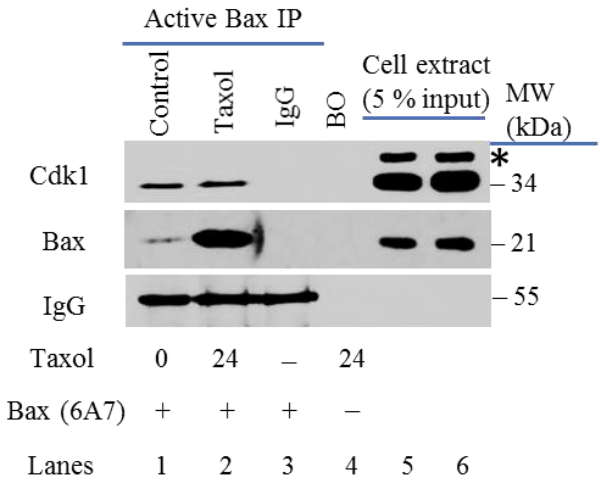

Figure 5-3: Cdk1 co-immunoprecipitates with Bax from both untreated and Taxol-arrested U2OS cells.

U2OS cells were either left untreated or treated with Taxol (1µM) for 24 hrs and subjected to immunoprecipitation with anti-Bax (6A7) antibody (lanes 1-2) followed by immunoblotting for Bax and Cdk1. Lane 3 represents Bax (6A7) antibody with magnetic beads and lane 4 represents cell extract with magnetic beads. Lane 5: cell extract from untreated. Lane 6: Taxol-treated cell extract. Molecular weight markers (kDa) are shown on the right. * indicates a non-specific protein detected by the Cdk1 antibody. This result is representative of 2 independent experiments.

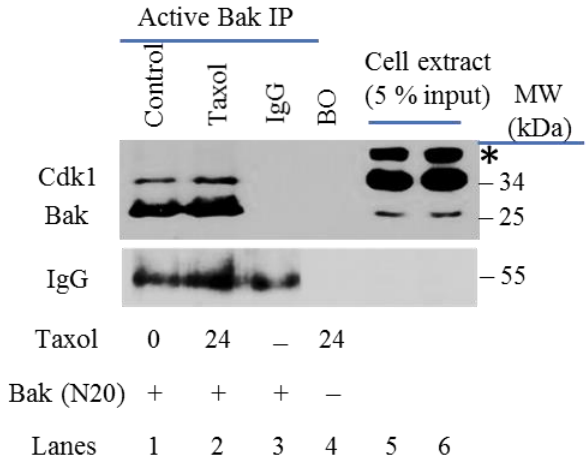

Figure 5-4: Cdk1 co-immunoprecipitates with Bak from both untreated and Taxol-arrested U2OS cells.

U2OS cells were either left untreated or treated with Taxol (1µM) for 24 hrs and subjected to immunoprecipitation with anti-Bak (N-20) antibody (lanes 1-2) followed by immunoblotting for Bak and Cdk1. Lane 3 represents Bak (N-20) antibody with magnetic beads and lane 4 represents cell extract with magnetic beads. Lane 5: cell extract from untreated. Lane 6: Taxol-treated cell extract. Molecular weight markers (kDa) are shown on the right. * indicates a non-specific protein detected by the Cdk1 antibody. This result is representative of 2 independent experiments.

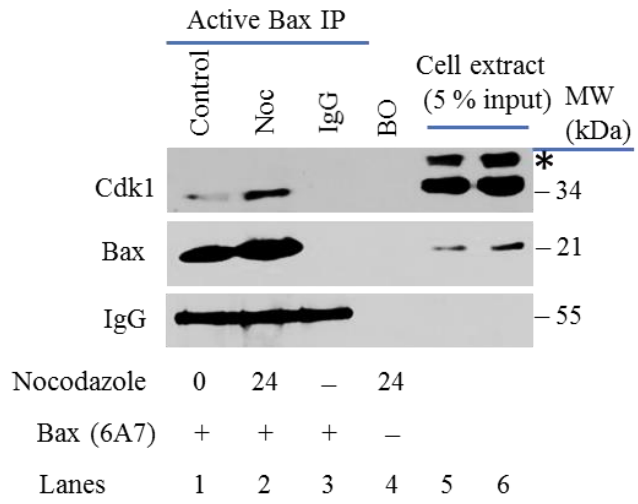

Figure 5-5: Cdk1 co-immunoprecipitates with Bax from both untreated and Nocodazole-arrested U2OS cells.

U2OS cells were either left untreated or treated with Nocodazole (5µM) for 24 hrs and subjected to immunoprecipitation with anti-Bax (6A7) antibody (lanes 1-2) followed by immunoblotting for Bax and Cdk1. Lane 3 represents Bax (6A7) antibody with magnetic beads and lane 4 represents cell extract with magnetic beads. Lane 5: cell extract from untreated. Lane 6: Taxol-treated cell extract. Molecular weight markers (kDa) are shown on the right. * indicates a non-specific protein detected by the Cdk1 antibody. This result is representative of 2 independent experiments.

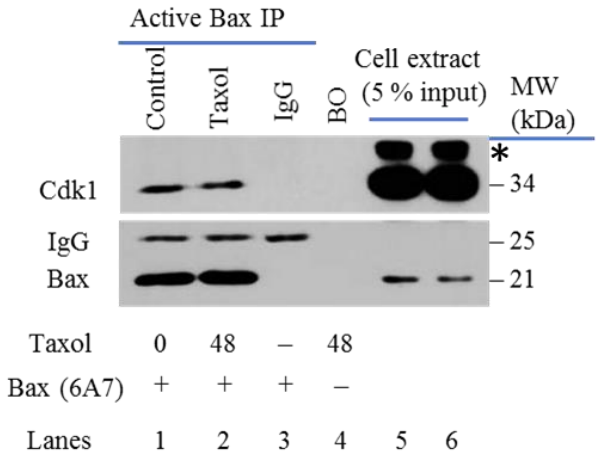

Figure 5-6: Cdk1 co-immunoprecipitates with Bax from both untreated and Taxol-arrested RPE1 cells.

RPE1 cells were either left untreated or treated with Taxol (1µM) for 48 hrs and subjected to immunoprecipitation with anti-Bax (6A7) antibody (lanes 1-2) followed by immunoblotting for Bax and Cdk1. Lane 3 represents Bax (6A7) antibody with magnetic beads and lane 4 represents cell extract with magnetic beads. Lane 5: cell extract from untreated. Lane 6: Taxol-treated cell extract. Molecular weight markers (kDa) are shown on the right. * indicates a non-specific protein detected by the Cdk1 antibody. This result is representative of 2 independent experiments.

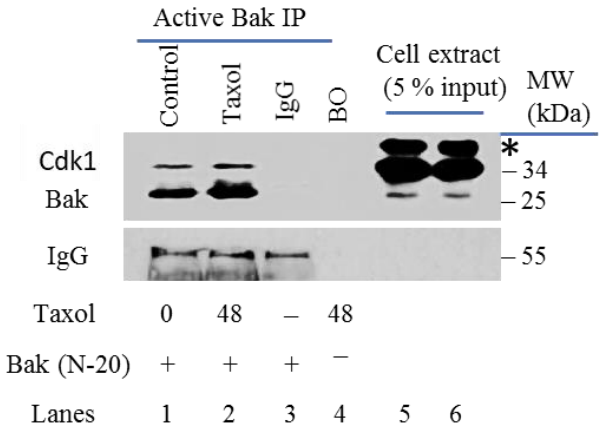

Figure 5-7: Cdk1 co-immunoprecipitates with Bak from both untreated and Taxol-arrested RPE1 cells.

RPE1 cells were either left untreated or treated with Taxol (1µM) for 48 hrs and subjected to immunoprecipitation with anti-Bak (N-20) antibody (lanes 1-2) followed by immunoblotting for Bak and Cdk1. Lane 3 represents Bak (N-20) antibody with magnetic beads and lane 4 represents cell extract with magnetic beads. Lane 5: cell extract from untreated. Lane 6: Taxol-treated cell extract. Molecular weight markers (kDa) are shown on the right. * indicates a non-specific protein detected by the Cdk1 antibody. This result is representative of 2 independent experiments.

5.4 Bak, Bax and cyclin B1 co-immunoprecipitate with Cdk1 in HeLa cells

To further confirm our co-IP results that Cdk1 is specifically associated with pro-apoptotic proteins Bak and Bax, I wanted to determine whether Bak and Bax would also co-immunoprecipitate with Cdk1. Immunoprecipitation of Cdk1 was performed using Cdk1-specific antibody Cdc2p34 (17) in untreated and Taxol-arrested HeLa cells. Cdk1-IPs were analysed by immunoblotting with cyclin B1 (the regulatory subunit of Cdk1), Bak, Bax and Cdk1 antibodies. Interestingly, complexes containing cyclin B1, Bak, and Bax were only detected in Taxol-arrested mitotic cells. Whereas, in exponentially growing HeLa cells, Cdk1 was only associated with Bak and Bax (Figure 5-8). These results indicate that Bak and Bax can form a complex with both active and inactive Cdk1. Cyclin B1 was co-immunoprecipitated with Cdk1 from Taxol-treated cells but not from untreated cells. My results indicate that pro-apoptotic proteins Bak and Bax can also co-IP with Cdk1, supporting the earlier results (see pages 130-135).

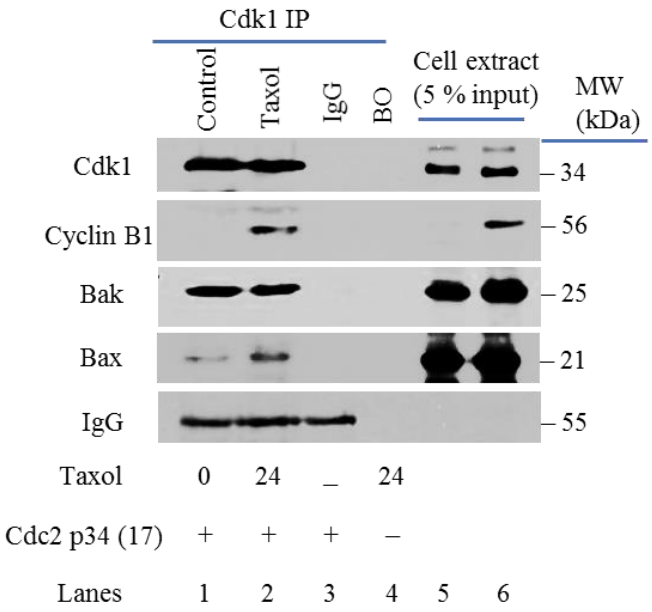

Figure 5-8: Bak, Bax and cyclinB1 co-immunoprecipitate with Cdk1 in HeLa cells.

HeLa cells were either left untreated or treated with Taxol (60nM) for the times indicated and subjected to immunoprecipitation with anti-Cdc2 p34 (17) antibody (lanes 1-2) followed by immunoblotting for cyclin B1, Bak, Bax and Cdk1. Lane 3 represents Cdc2 p34 (17) antibody with magnetic beads and lane 4 represents cell extract with magnetic beads. Lane 5: cell extract from untreated. Lane 6: Taxol-treated cell extract. Molecular weight markers (kDa) are shown on the right. This result is representative of 2 independent experiments.

5.5 Recombinant Cdk1 interacts with Bax *in vitro*

Although my MS and co-IP experiments strongly suggested that Bax and Cdk1 were present in a complex, it was important to determine if Bax and Cdk1 are able to interact directly or indirectly. First, I examined the purity of human, commercial recombinant proteins GST-Bax and GST-Cdk1, and GST-PAK-α (purified previously in our Lab) (Figure 5-9 A). Equimolar concentrations of GST-Bax (50 µM) and GST-Cdk1 (50 µM) were incubated in 1% CHAPS lysis buffer. An equimolar concentration of GST-PAK-α was incubated with GST-Cdk1 as a control. Subsequently, Cdk1 was then immunoprecipitated using a Cdk1-specific antibody Cdc2p34 (17) and the IPs were immunoblotted with Cdk1, Bax and PAK-α antibodies. My results indicated that Bax specifically interacts with Cdk1 *in vitro*. PAK-α was not detected in the Cdk1 IP (Figure 5-9 B). Similar results were also

obtained by incubating GST-Cdk1 with purified recombinant non-tagged wild type Bax protein (see Figure 5-10). These results indicate a direct interaction between the pro-apoptotic protein Bax and Cdk1 and support the results obtained by mass spectrometry and the co-IP experiments.

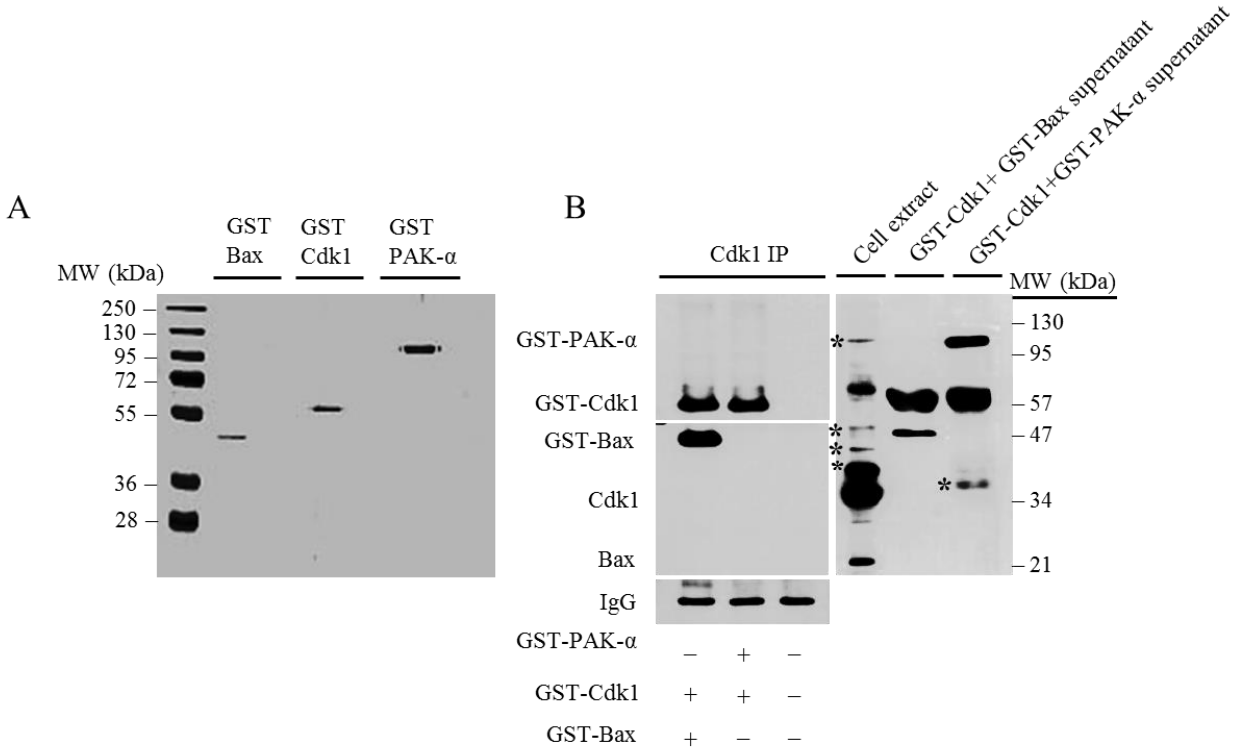

Figure 5-9: GST-Cdk1 specifically interacts with GST-Bax but not with GST-PAK-α *in vitro*.

(A) Coomassie-stained SDS-PAGE gel of purified, recombinant GST-Bax, GST-Cdk1 and GST-Pakα used in the study. Molecular weight markers (kDa) are indicated on the left. (B) Equimolar concentrations (50 µM) of GST-Tag Cdk1 and GST-Tag Bax were incubated in 1% CHAPS lysis buffer for 2 hrs at 4 °C. GST-Tag PAK alpha (50 µM) was also incubated with GST-Tag Cdk1 as a control. Cdk1 was then immunoprecipitated using Cdk1-specific antibody Cdc2p34 (17) and the IPs were analysed by immunoblotting for Cdk1, Bax and PAK-α antibodies. The post-IP supernatants (10 % of total volume) and cell lysate were run as positive controls. Molecular weight markers (kDa) are shown on the right. * indicates non-specific proteins. This result is representative of 2 independent experiments.

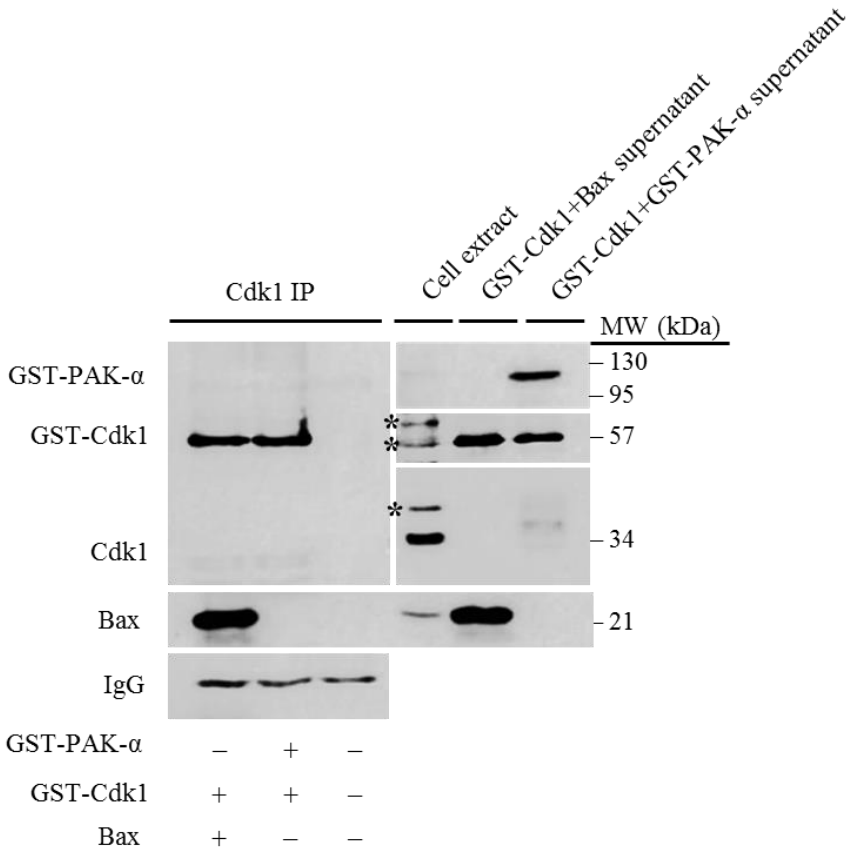

Figure 5-10: GST-Cdk1 specifically interacts with wild type Bax but not with GST-PAK-α *in vitro*.

Equimolar concentrations (50 µM) of GST-Tag Cdk1 and Bax (WT) were incubated in 1% CHAPS lysis buffer for 2 hrs at 4 °C. GST-Tag PAK alpha (50 µM) was incubated with GST-Tag Cdk1 under the same condition as a control. Cdk1 was then immunoprecipitated using Cdk1-specific antibody Cdc2p34 (17) and the IPs were analysed by immunoblotting for Cdk1, Bax and PAK-α antibodies. The post-IP supernatants (10 % of total volume) and cell lysate were run as positive controls. Molecular weight markers (kDa) are shown on the right. * indicates non-specific proteins. This result is representative of 2 independent experiments.

5.6 Depletion of Bax and Bak inhibits Cdk1-mediated Bcl-2/Bcl-xL phosphorylation during Taxol treatment

The anti-apoptotic Bcl-2 family members, such as Bcl-2 and Bcl-xL, have shown to be phosphorylated by Cdk1 kinase in response to microtubule interfering agents (Terrano et al., 2010). The anti-apoptotic function of Bcl-2 is reduced by Cdk1-mediated phosphorylation at serine 70 (Eichhorn et al., 2013). Cdk1-mediated

phosphorylation of Bcl-xL on serine 62 is reported to inhibit it's interaction with the pro-apoptotic protein Bax (Bah et al., 2014).

Next, I wanted to determine the physiological role of the interaction between Cdk1 and Bax, identified earlier (see pages 137-139). I examined the hypothesis that Bak and Bax were required for translocation of Cdk1 to the mitochondria to phosphorylate Bcl-2 and Bcl-xL in Taxol-arrested HeLa cells. HeLa cells were treated with siRNAs specific against human Bak and Bax and with control siRNA containing a scrambled sequence. After 48 hrs, the cell lysates were analysed by Western blotting to determine the level of Bak and Bax proteins. Both Bak and Bax proteins were detected in non-transfected and control siRNA cells. However, Bak and Bax proteins were efficiently depleted in the individual Bak and Bax siRNA-treated cells and in cells treated with both Bak/Bax siRNA (Figure 5-11).

Furthermore, the addition of Taxol induced phosphorylation of Bcl-2 and Bcl-xL in non-transfected and control siRNA cells, as indicated both by a mobility shift on SDS-PAGE and by immunoblotting with phospho-Bcl-2 and phospho-Bcl-xL antibodies (Figure 5-11). Importantly, depletion of Bax, Bak and both Bax and Bak completely inhibited Cdk1-mediated phosphorylation of Bcl-2 and Bcl-xL. Apart from a small level of Bcl-2 phosphorylation that was consistently observed in the Bak-depleted cells. One possible explanation for Bcl-2 phosphorylation in the absence of Bak is that Bax-mediated translocation of Cdk1 from the cytoplasm to the MOM may be primarily responsible for Bcl-2 phosphorylation. Cyclin B1 was expressed at low level in untreated cells but high level of cyclin B1 was maintained in Taxol-arrested mitotic cells indicating that Cdk1 is active during Taxol-induced cell cycle arrest. My data strongly suggest that both Bax and Bak may play a role in the translocation of Cdk1 from the cytoplasm to the outer mitochondrial membrane in Taxol-arrested mitotic cells.

During prolonged activation of the mitotic checkpoint, the phosphorylation of the anti-apoptotic proteins was sustained for several hours until apoptosis (Terrano

et al., 2010). These results suggest that translocation of Cdk1 to the MOM to phosphorylate Bcl-2/Bcl-xL is both Bax and Bak dependent during Taxol-induced cell cycle arrest. Furthermore, sustained translocation of Cdk1 by pro-apoptotic proteins Bax and Bak to the MOM provides the molecular basis for the link between activation of the mitotic checkpoint and initiation of apoptosis.

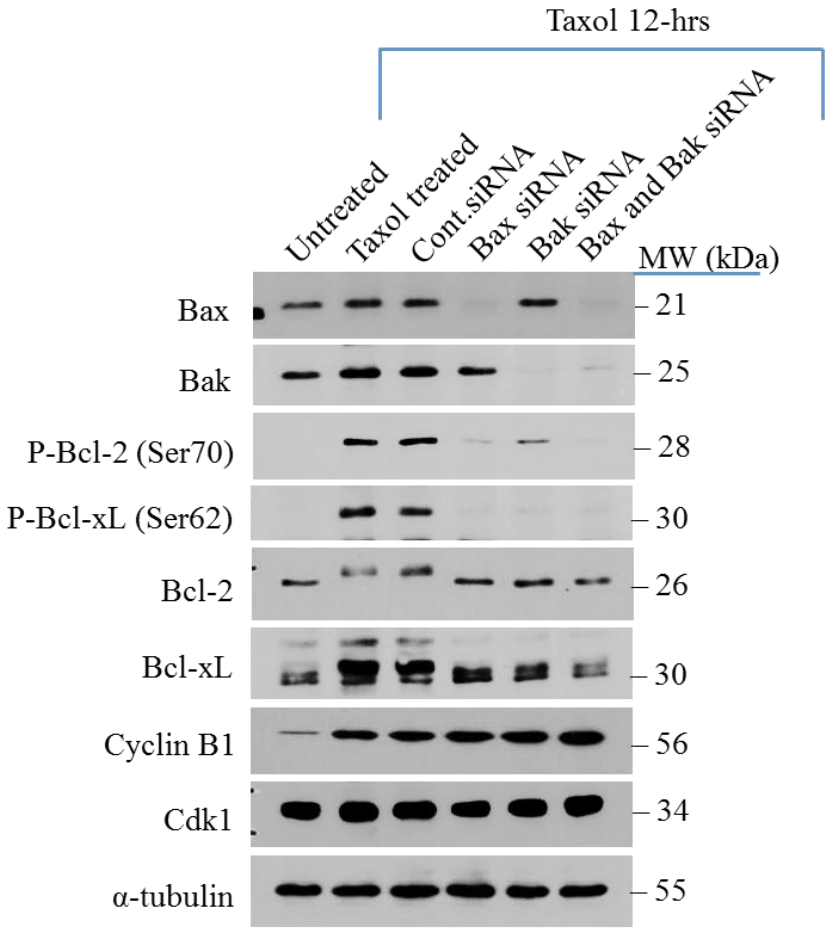

Figure 5-11: siRNA Depletion of Bax and Bak inhibits Cdk1-mediated phosphorylation of Bcl-2 and Bcl-xL in Taxol-arrested HeLa cells.

HeLa cells were either left untreated or transfected with control, Bax, Bak and both Bax and Bak siRNA (50nM) and incubated for 48 hrs. After the incubation period, the cells were treated with Taxol (60nM) for 12 hr. Cell lysates for untreated and 12-hr Taxol-treated cells were immunoblotted with antibodies for Bax, Bak, P-Bcl-2 (Ser70), P-Bcl-xL (Ser62), Bcl-2, Bcl-xL, cyclin B1 and Cdk1. α-tubulin was used as a loading control. Molecular weight markers (kDa) are shown on the right. This result is representative of 2 independent experiments.

5.6.1 Depletion of Bak and Bax does not affect Cdk1 kinase activation in Taxol-arrested mitotic cells

To investigate if Cdk1 was activated in the Bax/Bak-depleted HeLa cells in response to Taxol treatment, I performed an *in vitro* kinase assay using ^{32}p (ATP). Cdk1 was immunoprecipitated from either untreated or siRNA transfected cells (control siRNA, Bax siRNA, Bak siRNA and Bax/Bak siRNA) and Cdk1 activity was assessed using histone H1 as a substrate. In this assay I also wanted to confirm that the Cdk1 inhibitor RO-3306 (5 μM) inhibits Cdk1 kinase activity by pre-incubating Taxol-arrested mitotic cells with the inhibitor prior to the kinase assay.

As shown in Figure 5-12 A, control siRNA treated with Taxol showed a marked increase in histone H1 phosphorylation compared to untreated cells. The phosphorylation of histone H1 by Cdk1 in Bax siRNA, Bak siRNA and Bax/Bak siRNA treated with Taxol was similar to those seen in the control cells. Quantitation of the level of histone H1 phosphorylation indicated that there was no statistically significant difference in Cdk1 activity between control, Bax, Bak and Bax/Bak-siRNA treated cells (Figure 5-12 B). Furthermore, treatment of Taxol-arrested cells with the Cdk1-inhibitor (RO-3306) for 4 hrs caused a significant inhibition of the Cdk1 kinase activity (Figures 5-12 A and B).

To further confirm that siRNA depletion of Bak and Bax does not affect Cdk1 kinase activity in Taxol-arrested mitotic cells, cell cycle analysis was performed using flow cytometry. HeLa cells were either transfected with control or both Bax/Bak siRNA and then either left untreated or treated with Taxol for 12 hrs and analysed by flow cytometry. My results indicated that there was no statistically significant difference of the percentage of the cells in G2/M phase between control siRNA and Bax/Bak siRNA cells treated with Taxol for the same period of time (Table 5-1). Both the Cdk1 kinase assay and FACS analysis assay confirmed that Cdk1 is activated in the Bax/Bak-depleted HeLa cells in response to Taxol treatment.

From these results, I concluded that Cdk1 activation in Taxol-arrested cells is not affected by the absence of the pro-apoptotic proteins Bak and Bax and that cytoplasmic active Cdk1 is not sufficient to phosphorylate Bcl-2 and Bcl-xL. Therefore, the pro-apoptotic proteins Bak and Bax are required to facilitate the translocation of Cdk1 from the cytoplasm to the mitochondrial outer membrane in the Taxol-arrested mitotic cells.

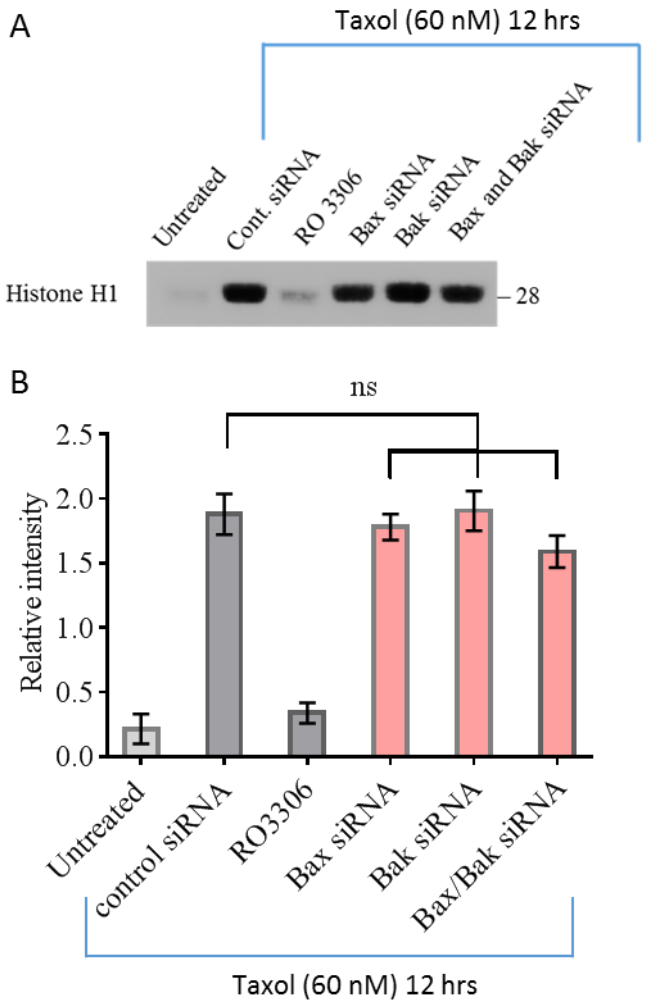

Figure 5-12: Cdk1 kinase assay in Bax and Bak-depleted cells.

A) HeLa cells were either left untreated or transfected with control siRNA (50 nM), Bax siRNA (50 nM), Bak siRNA (50 nM) and both Bax and Bak siRNA (50 nM) for 48 hrs. Cells then treated with Taxol (60 nM) for 12 hrs. Taxol-arrested mitotic cells were collected by mitotic shake-off and incubated with RO-3306 (5µM) for 4 hrs to inhibit Cdk1 kinase activity. The cells were then lysed in Cdk1 lysis buffer and Cdk1 was immunoprecipitated from the cell lysates using Cdk1-specific antibody Cdc2p34 (17). Histone H1 was used as substrate to assess Cdk1 kinase activity using an *in vitro* kinase assay. Samples were analysed by SDS-PAGE and the coomassie stained gels were dried for autoradiography. Molecular weight markers (kDa) are shown on the right. B) Histograms represent the

intensity of phosphorylated histone H1 normalized to α-tubulin from blots shown in A (the mean ± SD of three independent experiments). P-values were calculated using one-way ANOVA (ns = not significant compared to control siRNA).

Table 5-1: FACS analysis of untreated or Taxol treated HeLa cells transfected with control or Bax/Bak siRNA.

HeLa cells were either transfected with control (50nM) or both Bax and Bak siRNA (50nM) and incubated for 48 hrs. After the incubation period, the cells were either left untreated or treated with Taxol (60nM) for 12 hrs, and then fixed in Ethanol (70 % v/v) and stained with Propidium Iodide before FACS analysis. The mean values ± SD were calculated from 3 independent experiments.

Cell line	FACS Profile	G1	S	G2/M
		Mean ± SD	Mean ± SD	Mean ± SD
HeLa control siRNA untreated	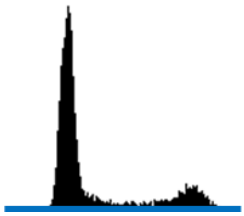	67.18±0.93	10.77±0.24	18.38±0.45
HeLa control siRNA Taxol-treated	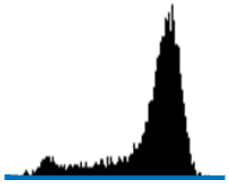	7.51±1.0	11.17±1.3	**74.86±2.49**
HeLa Bax/Bak siRNA untreated	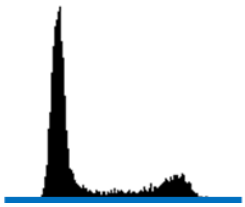	65.39±1.06	10.98±1.08	19.43±0.61
HeLa Bax/Bak siRNA Taxol-treated	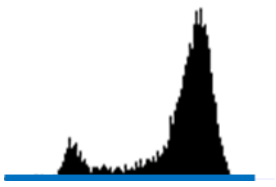	10.9± 3.72	12.53±2.62	**70.13±5.83**

5.7 Bcl-2 and Bcl-xL are not phosphorylated in Taxol-arrested Bax/Bak DKO HCT116 cells

Drawbacks of the siRNA technique are that it is transient, does not always produce complete depletion of the target, and is reported to produce off-target effects (Dorsett and Tuschl, 2004). Therefore, I examined Cdk1-mediated phosphorylation of Bcl-2 and Bcl-xL in HCT116 Bax/Bak DKO cells (Zhang et al., 2000, Wang and Youle, 2012) in response to Taxol treatment. Wild type HCT116 cells were used as controls. Both cell lines were either left untreated or treated with Taxol for 12 hrs and the total cell extracts were immunoblotted with Bax, Bak, P-Bcl-2, P-Bcl-xL, cyclin B1, Cdk1, and PARP antibodies. Western blotting confirmed the absence of Bak and Bax proteins in the HCT116 Bax/Bak DKO cells. Addition of Taxol induced Bcl-2 and Bcl-xL phosphorylation in HCT116 WT but not in HCT116 Bax/Bak DKO cells. Unexpectedly, a low level of Bcl-xL phosphorylation was detected in Taxol-arrested HCT116 Bax/Bak DKO cells. One possible explanation for Bcl-xL phosphorylation in HCT116 Bax/Bak DKO cells is that Bcl-xL is phosphorylated on Ser62 by a kinase other than Cdk1 (Figure 5-13 A).

I next wanted to determine if the low-level phosphorylation of Bcl-xL in HCT116 Bax/Bak DKO cells was sufficient for Taxol-induced apoptosis. Cell extracts of both HCT116 WT and HCT116 Bax/Bak DKO cells were prepared from untreated or 36 hrs Taxol-treated cells. PARP cleavage was clearly observed in HCT116 WT but not in HCT116 Bax/Bak DKO cells (see Figure 5-13 A), suggesting that phosphorylation of both Bcl-2 and Bcl-xL is required for Taxol-induced apoptosis. This result also confirmed the results obtained in the siRNA-depleted Bax/Bak cells (see Figure 5-11, page 141).

To determine if Cdk1 kinase is activated in the HCT116 Bax/Bak DKO cells during Taxol treatment, I performed an *in vitro* kinase assay using Cdk1 immunoprecipitated from either untreated or Taxol-arrested cells. As shown in Figure 5-13 A, histone H1 was phosphorylated efficiently by Cdk1 in HCT116 WT

treated with Taxol. A similar level of histone H1 phosphorylation was seen in HCT116 Bax/Bak DKO cells treated with Taxol for the same period of time. There was no statistically significant difference in the levels of histone H1 phosphorylation between HCT116 WT and HCT116 Bax/Bak DKO cells treated with Taxol for the same time (Figure 5-13 B). Unexpectedly, histone H1 kinase activity was also detected in untreated HCT116 Bax/Bak DKO cells, suggesting that a histone H1 kinase was co-immunoprecipitated with Cdk1 protein. However, Cdk1 was inactive in untreated HCT116 Bax/Bak DKO cells because cyclin B1 level was low compared to Taxol-arrested mitotic cells (see Figure 5-13 A). I confirmed that Cdk1 was inactive in the HCT116 Bax/Bak DKO cells as it was still phosphorylated on tyrosine 15 as assessed by a phospho-Cdk1 (Tyr 15) antibody. Furthermore, this unidentified histone H1 kinase was unable to phosphorylate Bcl-2 (Ser70) or Bcl-xL (Ser62) (Figure 5-13 A).

To further demonstrate that Cdk1 is activated in HCT116 Bax/Bak DKO cells in response to Taxol treatment, cell cycle analysis was performed in both HCT116 WT and HCT116 Bax/Bak DKO cells using flow cytometry. Both HCT116 WT and HCT116 Bax/Bak DKO cells were left untreated or treated with Taxol for 12 hrs and analysed by flow cytometry. My results indicated that there was no statistically significant difference in the percentage of the cells in G2/M phase between HCT116 WT and HCT116 Bax/Bak DKO cells treated with Taxol (Table 5-2). The flow cytometry data complemented the results of the histone H1 kinase assay and both confirmed that Cdk1 is activated in HCT116 Bax/Bak DKO cells treated with Taxol. These findings support our hypothesis that Bax and Bak are required for Cdk1 translocation to the MOM to phosphorylate Bcl-2 and Bcl-xL in Taxol-arrested mitotic cells.

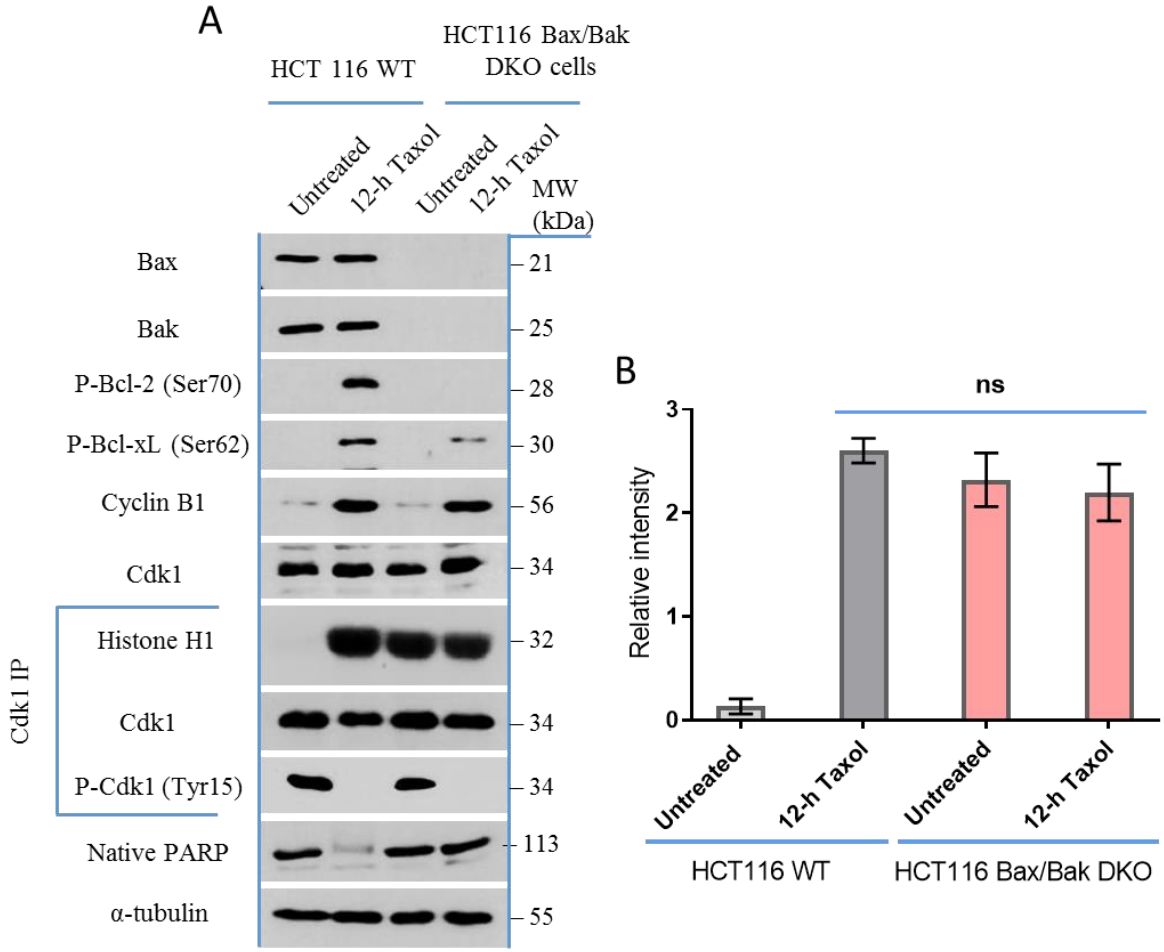

Figure 5-13: Taxol induces phosphorylation of Bcl-2 and Bcl-xL and PARP cleavage in HCT116 WT but not in HCT116 Bax/Bak DKO cells.

A) HCT116 WT and HCT116 Bax/Bak DKO cells were either left untreated or treated with Taxol (120 nM) for 12 hrs. Cell lysates for untreated and 12-hrs Taxol-treated cells were immunoblotted with antibodies for Bax, Bak, P-Bcl-2 (Ser70), P-Bcl-xL (Ser62), cyclin B1, Cdk1 and PARP. α-tubulin was used as a loading control. Molecular weight markers (kDa) are shown on the right. This result is representative of 2 independent experiments. For the histone H1 kinase assay, both HCT116 WT and HCT116 Bax/Bak DKO cells were either left untreated or treated with Taxol (120 nM) for 12 hrs. The cells were then lysed in Cdk1 lysis buffer and Cdk1 was immunoprecipitated from the cell lysates using Cdk1-specific antibody Cdc2p34 (17). Histone H1 was used as substrate to assess Cdk1 kinase activity using an *in vitro* kinase assay. Samples were analysed by SDS-PAGE and the coomassie stained gels were dried for autoradiography. B) Histograms represent the intensity of phosphorylated histone H1 normalized to α-tubulin from histone H1 blot shown in A (the mean ± SD of three independent experiments). P-values were calculated using one-way ANOVA (ns = not significant compared to HCT116 WT).

Table 5-2: FACS analysis of untreated or Taxol treated HCT116 WT and HCT116 Bax/Bak DKO cells.

HCT116 WT and HCT116 Bax/Bak DKO cells were either left untreated or treated with Taxol (120 nM) for 12 hrs, and then fixed in Ethanol (70 % v/v) and stained with Propidium Iodide before FACS analysis. The mean values ± SD were calculated from 3 independent experiments.

Cell line	FACS Profile	G1	S	G2/M
		Mean ± SD	Mean ± SD	Mean ± SD
HCT116 WT untreated	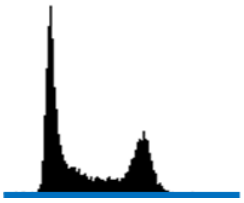	45 ± 0.82	19.2 ± 0.31	28.73± 1.42
HCT116 WT Taxol-treated		3.02 ± 0.45	5.39 ± 1.15	**87.4 ± 1.66**
HCT116 Bax/Bak DKO untreated	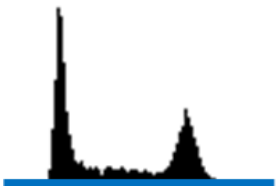	38.7 ± 1.56	22.5 ± 1.53	28.99± 1.42
HCT116 Bax/Bak DKO Taxol-treated		3.21 ± 0.41	3.7 ± 0.64	**86.16 ± 3.6**

5.8 Bcl-2 and Bcl-xL are transiently phosphorylated during G2/M phase of the cell cycle.

Cdk1 is a non-redundant cyclin-dependent kinase which plays an essential role in regulation of the mammalian cell cycle. It regulates the transition through late G2 and mitosis (Murray, 1994). Genetic studies have shown a critical role for Cdk1 in mitosis and it phosphorylates many substrates (Ubersax et al., 2003, Murray, 2004). To determine whether Bcl-2 and Bcl-xL were phosphorylated during the normal cell cycle and if their phosphorylation was related to Cdk1/cyclin B1 kinase activity, I performed a time course experiments using synchronized HeLa cells. The cells were synchronized by thymidine block and then released to proceed through the normal cell cycle. Cell extracts were prepared at various intervals after release from thymidine block and immunoblotted with cyclin B1, Bcl-2, P-Bcl-2, Bcl-xL and P-Bcl-xL. At the same time, samples were prepared for FACS analysis. After thymidine block, most of the cells were blocked at G1/S as assessed by FACS (Figure 5-14). Following release from the thymidine arrest, cyclin B1 levels increased at 6 hrs reaching maximum levels at 9-14 hrs after thymidine release (Figures 5-15 and 5-16). Cyclin B1 levels declined after 14 hrs indicating exit from mitosis. Immunoblot analysis of the cell extracts with Bcl-2 and Bcl-xL antibodies showed a clear mobility shift between 6-14 hrs following thymidine release, suggesting that phosphorylation of Bcl-2 and Bcl-xL is a normal mitotic event in HeLa cells. The phosphorylation of Bcl-2 and Bcl-xL during the normal cell cycle was confirmed by blotting the cell extracts with phospho-Bcl-2 (Ser70) and phospho-Bcl-xL (Ser62) antibodies (Figure 5-16). My data indicate that Cdk1 activity may be responsible for transient phosphorylation of Bcl-2/ Bcl-xL during normal mitosis.

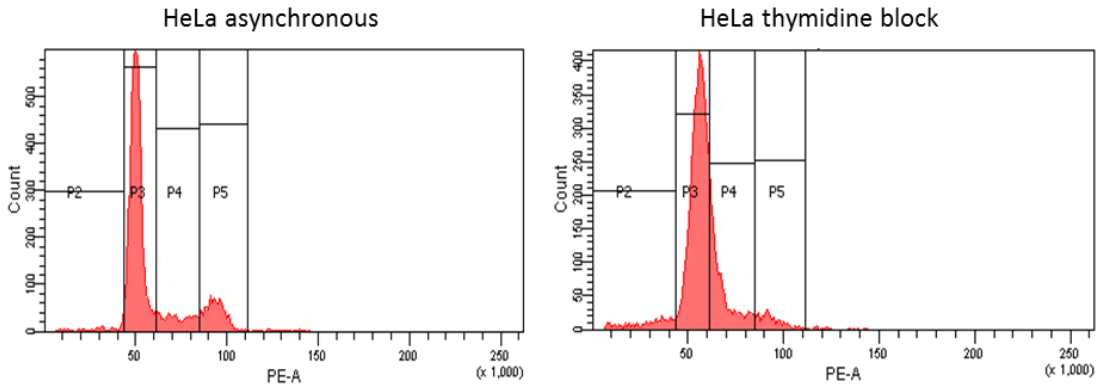

Figure 5-14: FACS profile of asynchronous and synchronous thymidine block (2 mM) Hela cells.

HeLa Cells were either left untreated or treated with thymidine (2 mM) for 24 hrs and then fixed in Ethanol (70 % v/v) and stained with Propidium Iodide before FACS analysis. This result is representative of 2 independent experiments.

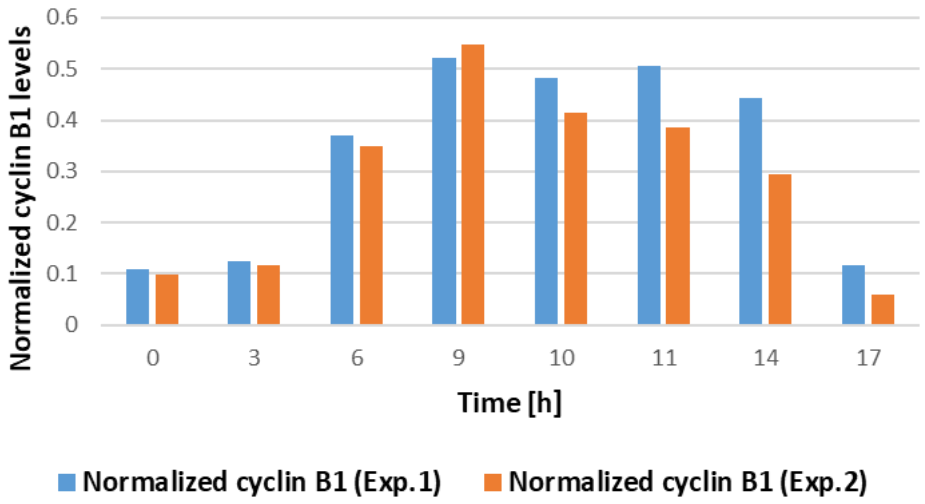

Figure 5-15: Cyclin B1 is highly expressed during G2/M phase of the cell cycle.

Hela cells were synchronized by a single thymidine block (2 mM) for 24 hrs, washed and released into fresh medium for the times indicated. The cells were lysed in RIPA buffer and the normalized cell extracts were subjected to immunoblotting for cyclin B1. Cyclin B1 correlation to α-tubulin was quantitated for every time course using Image J. This data indicates the results of 2 independent experiments.

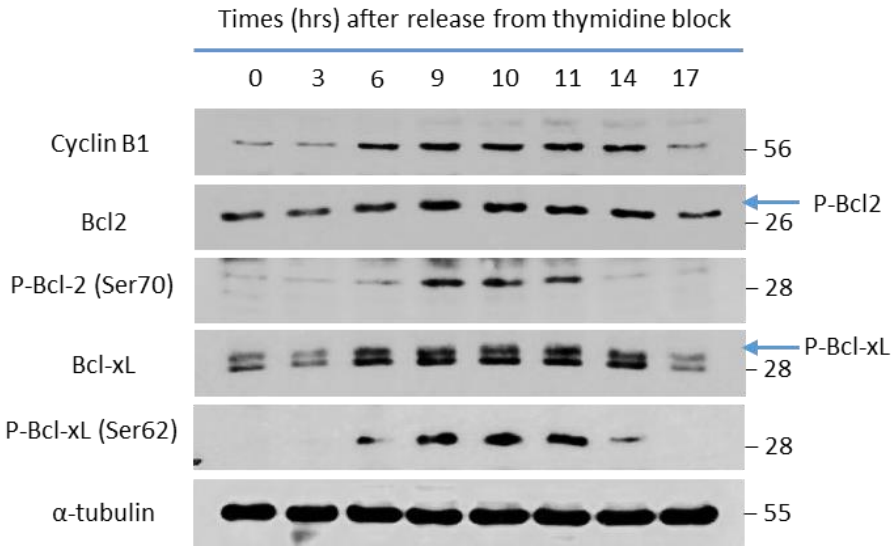

Figure 5-16: Bcl-2 and Bcl-xL are transiently phosphorylated during G2/M phase of the cell cycle.

Hela cells were synchronized by a thymidine block, washed and released into fresh medium for the times indicated. The cells were lysed in RIPA buffer and the normalized cell extracts were immunoblotted for cyclin B1, Bcl-2, P-Bcl-2 (Ser70), Bcl-xL, P-Bcl-xL (Ser62). α-tubulin was used as a loading control. Molecular weight markers (kDa) are shown on the right. This result is representative of 2 independent experiments.

5.9 RO-3306 inhibits Cdk1-mediated phosphorylation of Bcl-2 and Bcl-xL during Taxol treatment

To further examine the role of Cdk1 activity in mitochondrial-dependent apoptosis and to confirm that Cdk1 is responsible for Bcl-2 and Bcl-xL phosphorylation during Taxol-induced mitotic arrest, I examined Cdk1-mediated phosphorylation of Bcl-2 and Bcl-xL in the presence or absence of RO-3306. RO-3306 is a selective ATP-competitive inhibitor of Cdk1. It binds to the ATP pocket of Cdk1 to inhibit its activity (Vassilev et al., 2006).

Incubation of HeLa cells with RO-3306 blocks cell cycle progression to M phase (Vassilev et al., 2006). To avoid this problem, cells were synchronized by a thymidine block, released and then treated with Taxol for 12 hrs, and RO-3306 was added to Taxol-arrested mitotic cells. Addition of Taxol to a synchronized population of HeLa cells induced Bcl-2 and Bcl-xL phosphorylation at 12 and 16

hrs after Taxol addition (Figure 5-17). Both Bcl-2 and Bcl-xL showed a clear mobility shift at 12 and 16 hrs after Taxol addition. The phosphorylation of Bcl-2 and Bcl-xL was confirmed by immunoblotting with phospho-Bcl-2 (Ser70) and phospho-Bcl-xL (Ser 62) antibodies. The addition of RO-3306 (1µM) to the Taxol-arrested cells caused a slight reduction in Bcl-2 and Bcl-xL phosphorylation as assessed by the mobility shift but not with the phospho-antibodies. However, a higher concentration of RO-3306 (5µM) completely inhibited Bcl-2 and Bcl-xL phosphorylation as seen by the inhibition of the mobility shift and the absence of a band with the phospho-antibodies. This result indicates that Cdk1 activity is highly likely to be responsible for Bcl-2 and Bcl-xL phosphorylation during Taxol-induced mitotic arrest.

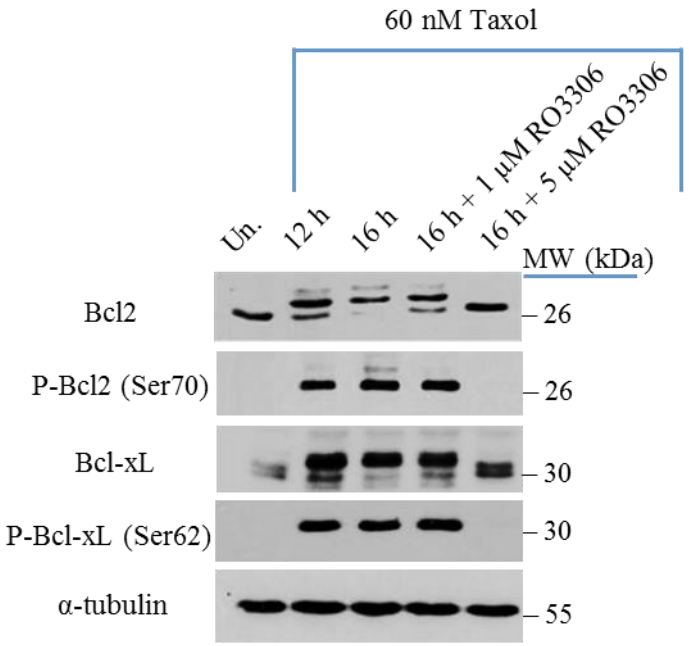

Figure 5-17: RO-3306 inhibits the phosphorylation of Bcl-2 and Bcl-xL in Taxol-arrested cells.

Hela cells were synchronized by a thymidine block for 24 hrs, and then either left untreated or treated with Taxol (60 nM) for 12 hrs. Taxol- arrested mitotic cells were collected by mitotic shake-off and either incubated with Taxol or Taxol + RO-3306 (1 and 5 µM) for the indicated times. Cell lysates were immunoblotted with antibodies to Bcl-2, P-Bcl-2 (Ser70), Bcl-xL, and P-Bcl-xL (Ser62). α-tubulin was used as a loading control. Molecular weight standards (kDa) are shown on the right. This result is representative of 2 independent experiments.

5.10 The Cdk1-inhibitor RO-3306 inhibits Taxol-induced apoptosis in HeLa cells

In order to further examine the role of Cdk1 in Taxol-induced mitotic cell death, I examined levels of apoptosis using cytokeratin 18 and PARP cleavage either in the presence or absence of RO-3306. Taxol-arrested HeLa cells were obtained by mitotic shake-off and either incubated with Taxol or Taxol plus RO-3306 (5 μM) for a further 12 or 24 hrs (total of 24 or 36 hrs). As shown in Figure (5-18 A and B), PARP cleavage was significantly reduced in Taxol-arrested cells incubated with 5 μM RO-3306 for 36 hrs when compared to Taxol treatment only. Moreover, the level of uncleaved PARP was significantly increased in Taxol-arrested cells incubated with 5 μM RO-3306 for 24 and 36 hrs in comparison to Taxol treatment only Figure (5-18 A and C).

The inhibition of Taxol-induced apoptosis by RO-3306 was further investigated by assessing cytokeratin 18 cleavage using the M30 antibody. In Taxol-arrested cells, there was a time dependent increase in the number of M30 antibody-stained cells. At 16 hrs Taxol treatment, 16% of the cells were stained for M30 antibody. Apoptosis was then increased to 75% and 92% at 24 and 36 hrs respectively. However, in the presence of the RO-3306 (5 μM), 6% of the cells were stained for M30 antibody at 16 hrs which then increased to 35% and 50 % at 24 and 36 hrs respectively. Cdk1 inhibitor RO-3306 significantly reduced the number of the apoptotic cells (see Figures 5-19 and 5-20). Taken together, our data suggest that chronic activation of Cdk1 may promote Taxol-induced apoptosis and supports the interpretation that sustained activation of Cdk1 has pro-apoptotic effects and identifies the link between SAC activation and the induction of apoptosis.

Furthermore, relatively high levels of cyclinB1 were detected at 12 and 16 hrs of Taxol addition, in which most of the cells were arrested in mitosis, in comparison to untreated cells. Cyclin B1 levels were similar in Taxol-arrested cells incubated with 1 μM RO-3306 when compared to Taxol-treated cells only. However, cyclin

B1 was degraded in Taxol-arrested cells incubated with 5 µM RO-3306 for the same times (see Figure 5-18 A). RO-3306 is a selective inhibitor of Cdk1 and it was efficiently inhibited Cdk1 activity at 5 µM (see Figure 5-12 A and B, page 145). By adding RO-3306 to Taxol-arrested mitotic cells, cyclin B1 was degraded and when cyclin B1 level drop below a critical threshold, the cells exit mitosis into a polyploid interphase (Haschka et al., 2018). Interestingly, by inhibiting Cdk1 activity with RO-3306, apoptosis was reduced to 35% after 24 hrs Taxol treatment. However, at the time of maximum Cdk1 activity, the number of the apoptotic cells was significantly increased to 75% at 24 hrs Taxol addition (see Figure 5-19). These results suggest that Taxol-induced apoptosis can be reduced by inhibition of Cdk1 activity, and that chronic activation of the Cdk1 and the subsequent phosphorylation of Bcl-2 and Bcl-xL is involved in Taxol-induced apoptosis.

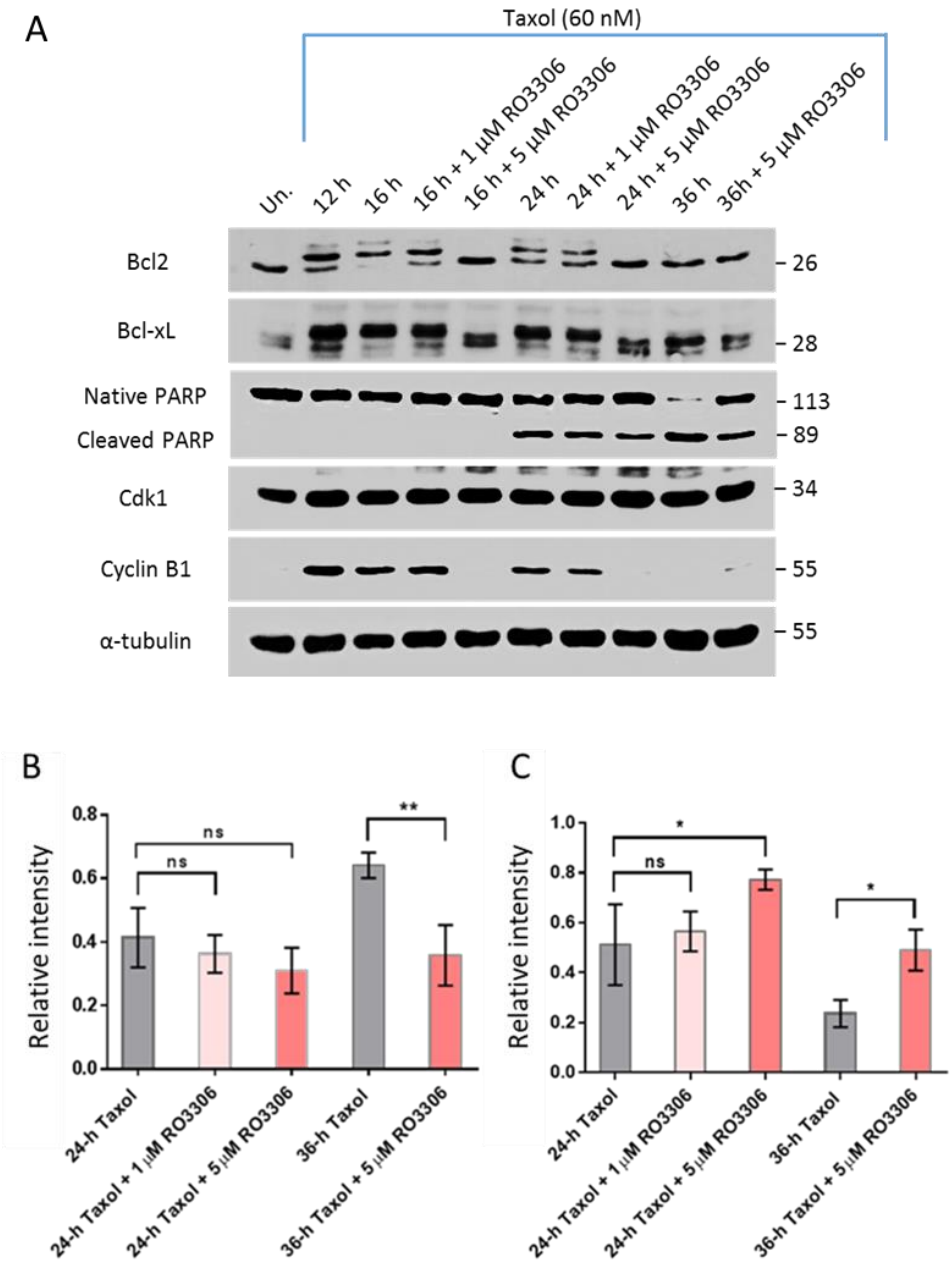

Figure 5-18: RO-3306 inhibits Bcl-2 and Bcl-xL phosphorylation-induced by Cdk1 and reduces PARP cleavage in Taxol-arrested cells.

A) Hela cells were synchronized by a thymidine block for 24 hrs, washed, and then either left untreated or treated with Taxol (60 nM) for 12 hrs. Taxol- arrested mitotic cells were collected by mitotic shake-off and either incubated with Taxol or Taxol + RO-3306 (1 and 5 µM) for the indicated times. Cell lysates were immunoblotted with antibodies for Bcl-2, Bcl-xL, PARP, Cdk1 and cyclin B1. α-tubulin was used as a loading control. Molecular weight standards (kDa) are shown on the right. This result is representative of 3 independent experiments. (B) and (C) Histograms represent the intensity of cleaved and uncleaved PARP, respectively, normalized to α-tubulin from blots shown in A (the mean ± SD of three independent experiments). P-values were calculated using one-way ANOVA (ns= not significant, P value * < 0.05, ** P value < 0.01).

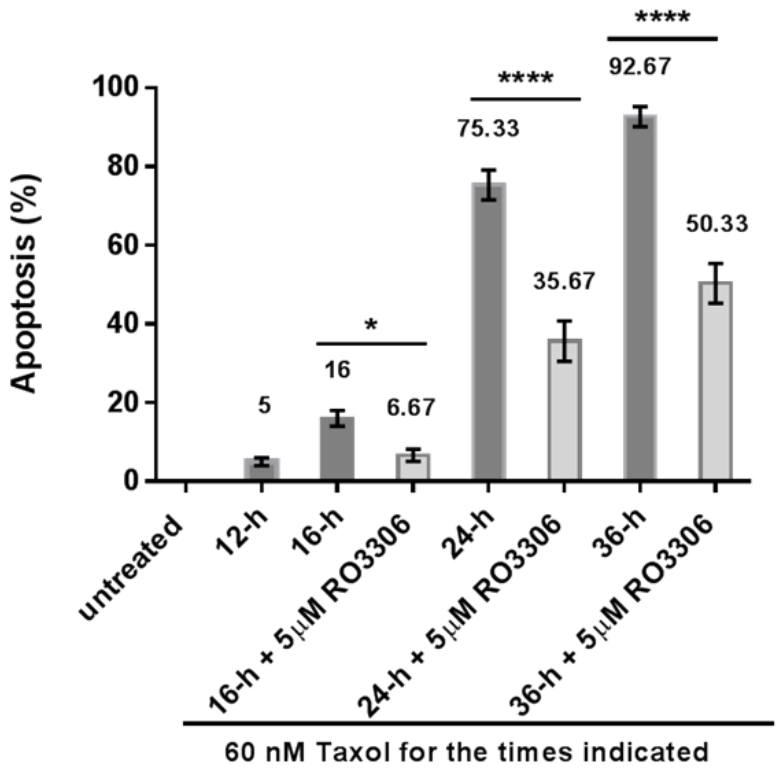

Figure 5-19: RO-3306 inhibits cytokeratin 18 cleavage in Taxol-arrested HeLa cells.

Hela cells were synchronized by a thymidine block for 24 hrs and then either left untreated or treated with Taxol (60 nM) for 12 hrs. Mitotically arrested cells were collected by mitotic shake-off and either incubated with Taxol or Taxol plus RO-3306 (5 μM) for the indicated times. The cells were fixed and stained with CytoDEATH (M30) primary antibody and Alexa-Fluor 488 secondary antibody. At least 100 cells were counted in randomly selected fields and the number of the apoptotic cells were quantitated. Histograms represent the mean ± SD of three independent experiments. P-values were calculated using one-way ANOVA (* P value < 0.05, P **** value < 0.0001).

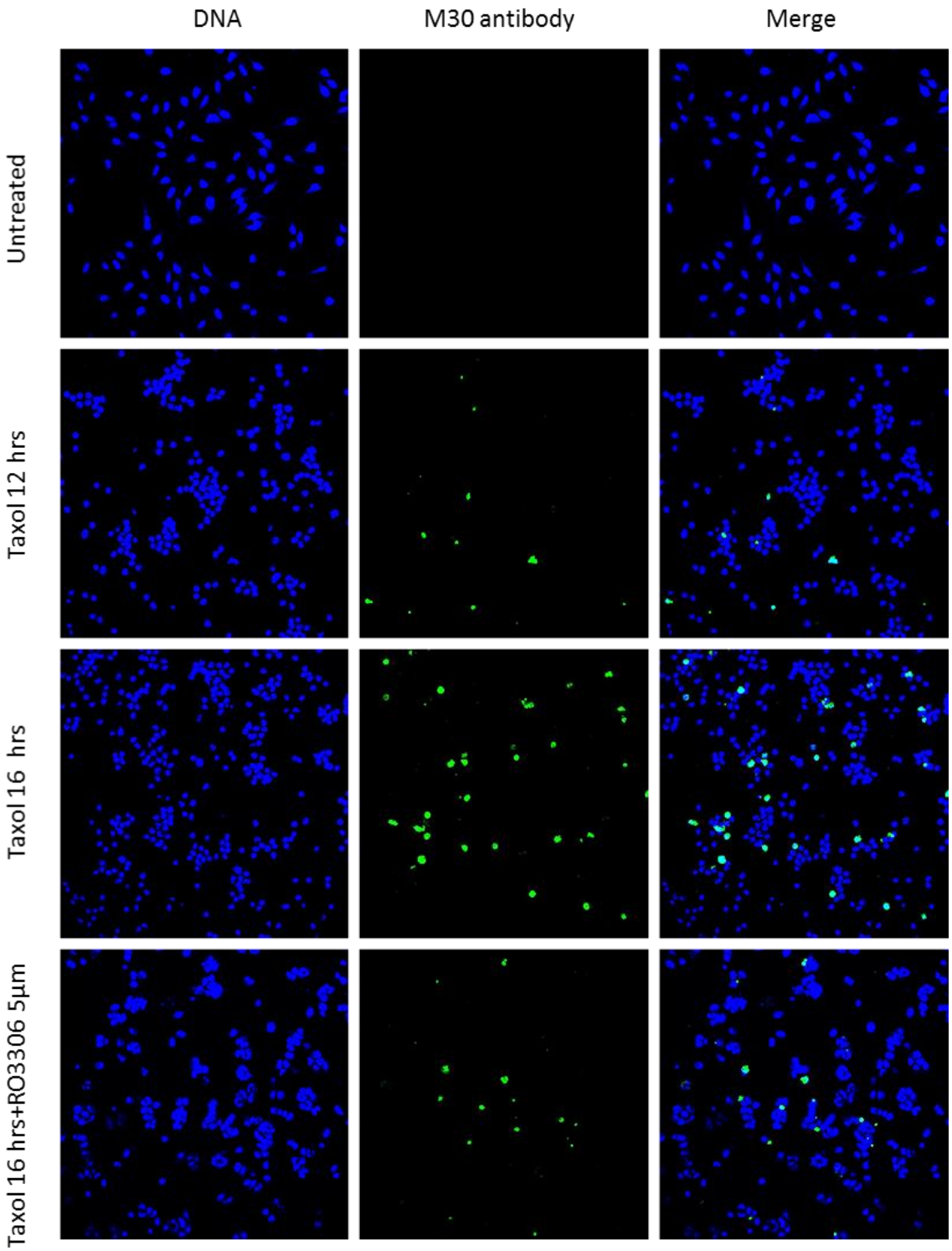

Followed by images of 24 and 36 hrs Taxol treatment

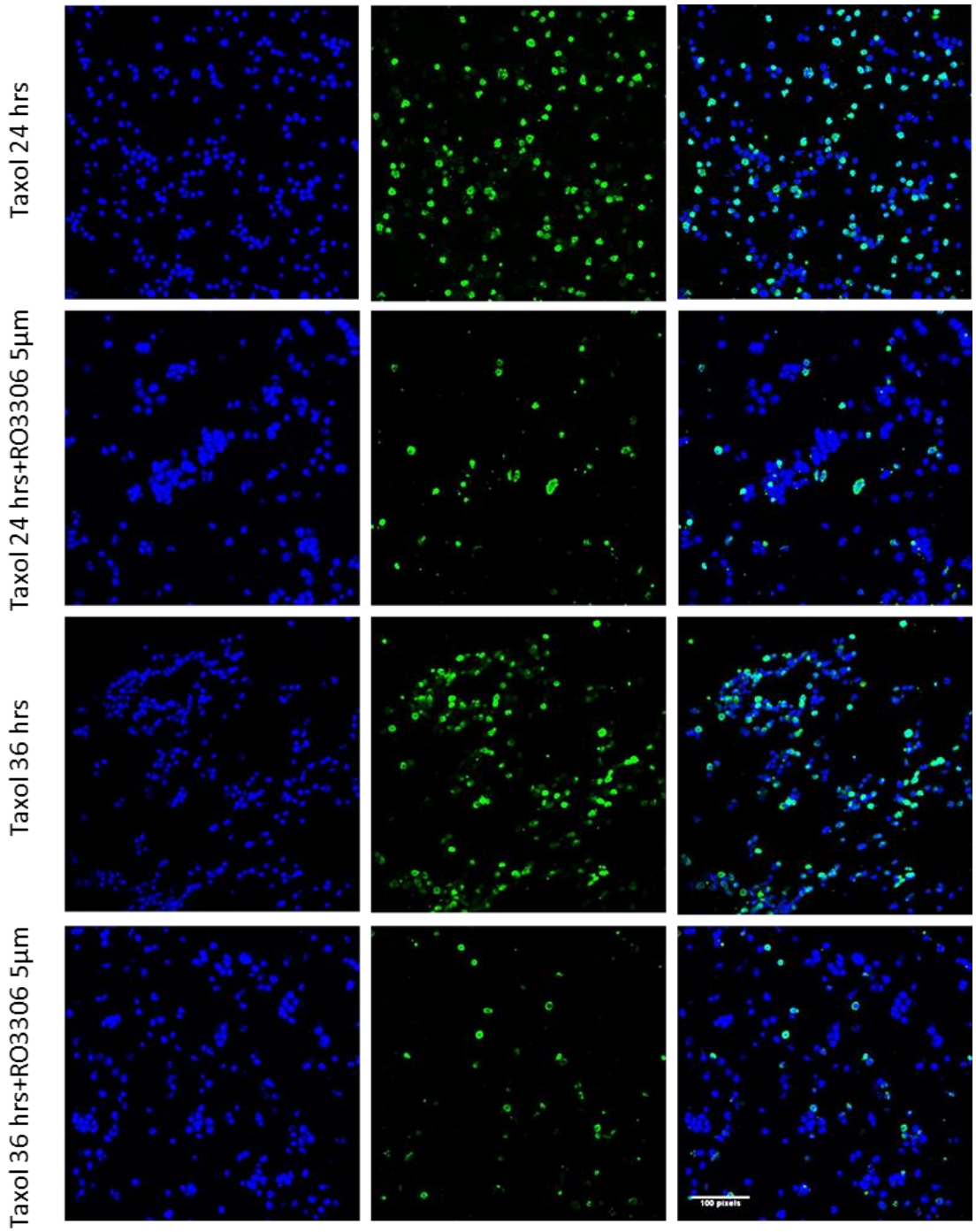

Figure 5-20: The Cdk1-inhibitor RO-3306 inhibits cytokeratin 18 cleavage in Taxol-arrested HeLa cells.

Representative fluorescence images of Taxol-induced apoptosis with or without RO-3306 in synchronized HeLa cells. Hela cells were synchronized by a thymidine block for 24 hrs, washed, and then either left untreated or incubated with Taxol (60 nM) for 12 hrs. Mitotically arrested cells were collected by mitotic shake-off and either incubated with Taxol or Taxol plus RO-3306 (5 µM) for the indicated times. The cells were fixed and stained with CytoDEATH (M30) primary antibody and Alexa-Fluor 488 secondary antibody (green). DNA was stained with Hoechst 33342 (blue). This result is representative of three independent experiments.

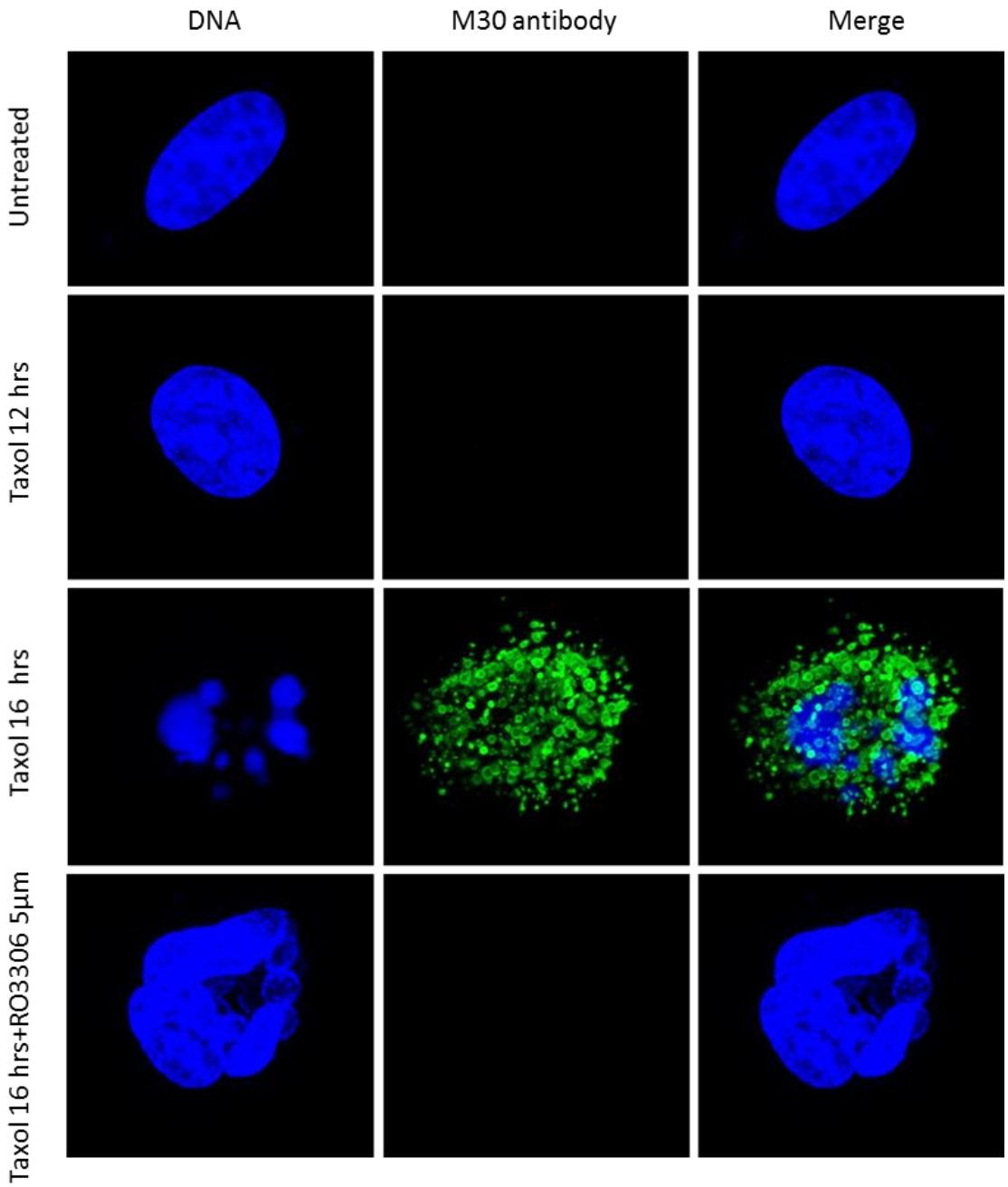

Followed by images of 24 and 36 hrs Taxol treatment

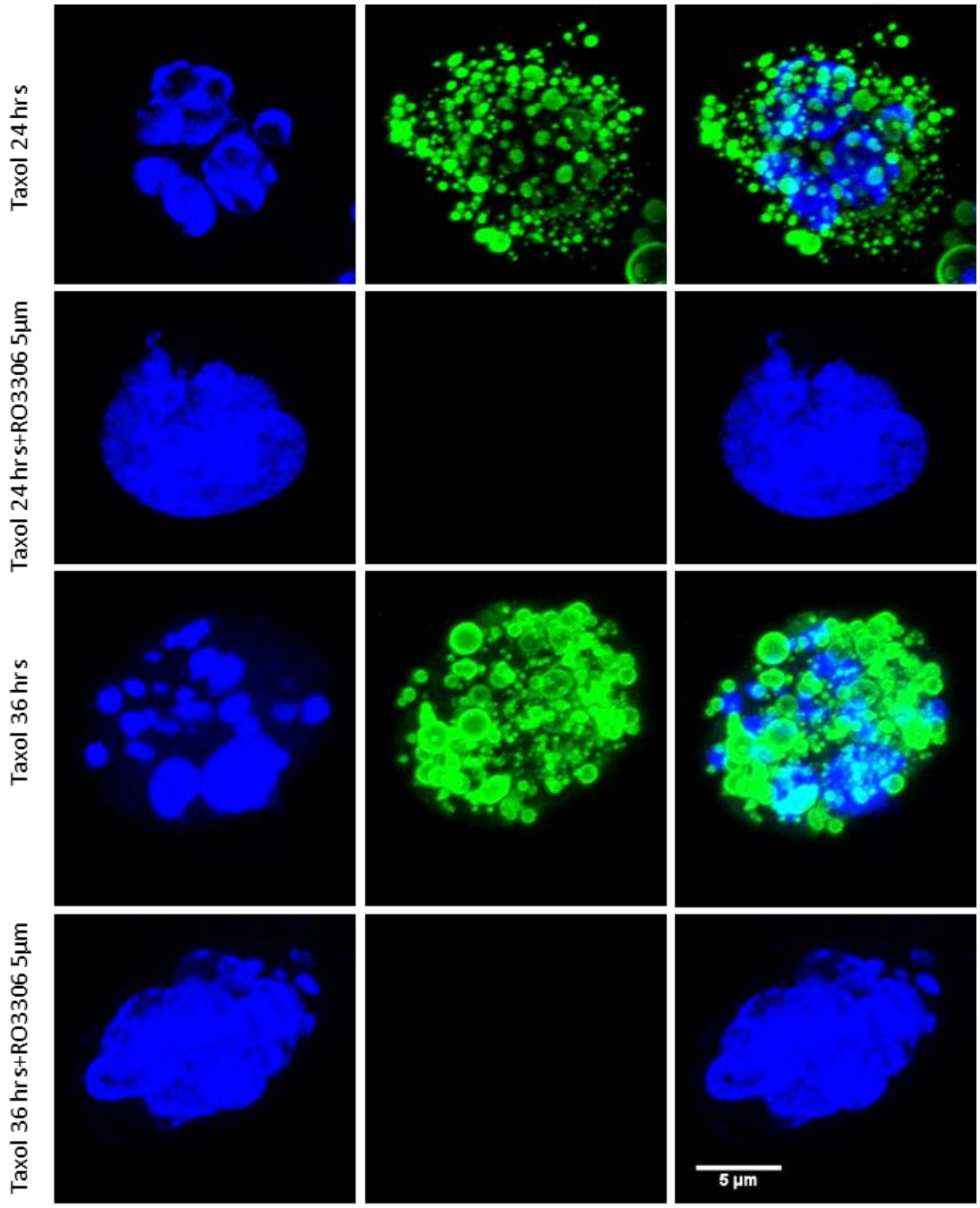

Figure 5-21: Representative images of Taxol-induced apoptosis with or without RO-3306.

Hela cells were synchronized by a thymidine block for 24 hrs and then either left untreated or treated with Taxol (60 nM) for 12 hrs. Mitotically arrested cells were collected by mitotic shake-off and either incubated with Taxol or Taxol plus RO-3306 (5 µM) for the indicated times. The cells were fixed and stained with CytoDEATH (M30) primary antibody and Alexa-Fluor 488 secondary antibody (green). DNA was stained with Hoechst 33342 (blue). This result is representative of three independent experiments.

5.11 Discussion

To date the molecular link between activation of the mitotic checkpoint and the initiation of apoptosis has not been clearly defined. Several studies have investigated post-translational modifications that control apoptosis during prolonged mitotic arrest. Phosphorylation of XIAP at S40 by Cdk1 inhibits the anti-apoptotic function of XIAP and reduces the threshold for the onset of apoptosis induced by a microtubule poison (Hou et al., 2016). Another study suggested that phosphorylation of caspase-9 at Thr125 by Cdk1 protects mitotically-arrested cells against apoptosis (Allan and Clarke, 2007). However, these mechanisms do not provide an explanation of the initiation of apoptosis because activation of caspases is downstream of Bak/Bax activation and MOM permeabilization. This study demonstrates a novel direct interaction between key proteins, the mitotic kinase Cdk1 with Bax, and provides a molecular explanation for the link between activation of the mitotic checkpoint and the initiation of apoptosis.

The microtubule stabilizing agent Taxol activates the mitotic checkpoint and blocks the proteasome-dependent degradation of two key proteins in mitosis, securin and cyclinB1 (Abal et al., 2003). This results in the chronic activation of Cdk1 and the cells arrest in mitosis. Prolonged-mitotic arrest is usually followed by mitotic cell death (Topham and Taylor, 2013). Chronic activation of Cdk1 causes phosphorylation of the anti-apoptotic proteins, Bcl-2 and Bcl-xL, and reduces the threshold for the onset of apoptosis (Terrano et al., 2010). It has generally been assumed that cytoplasmic active Cdk1 (generated at mitosis) would phosphorylate Bcl-2 and Bcl-xL. However, my data suggests that targeted delivery of Cdk1 via the translocation of Bax and Bak is necessary for the phosphorylation of the Bcl-2 and Bcl-xL and the initiation of Taxol-induced apoptosis.

The involvement of Cdk1 activity in the mitochondrial-mediated apoptosis has been reported in several studies (Terrano et al., 2010, Zhou et al., 2014).

Cdk1/cyclin B1 complexes have shown to localize to the MOM during Vinblastine-induced mitotic arrest (Terrano et al., 2010). Additionally, studies have reported that Cdk1-mediated phosphorylation of Bcl-2 and Bcl-xL switches mitotic arrest to apoptosis during treatment with microtubule interfering agents (Terrano et al., 2010, Chu et al., 2012, Sakurikar et al., 2012). However, how Cdk1 moves from the cytoplasm to the MOM remains elusive. Based on my results, we propose that the formation of an active Bax/Cdk1 complex is the signal that accumulates in mitotic cells, translocates to the MOM and is necessary for inactivation of the anti-apoptotic proteins Bcl-2 and Bcl-xL. My earlier MS data of the Bax IP had identified Cdk1 as a co-immunoprecipitating protein. My co-IP experiments have shown that a small amount of Cdk1 is specifically co-immunoprecipitated with Bak and with Bax in normal interphase cells, and the amount of Cdk1 is increased in the Taxol-arrested mitotic cells. This interaction was observed in three different cell lines HeLa, U2OS and RPE1, suggesting that Cdk1 interaction with Bak and with Bax is a general phenomenon.

Cdk1-Bax interaction was also seen in Nocodazole-arrested cells. Nocodazole is a microtubule interfering agent which exerts its effect by depolymerizing microtubules (Ren et al., 2005), whereas Taxol exerts its effect by stabilizing microtubules (Barbuti and Chen, 2015). Cdk1-Bax interaction in different cell lines and in both Taxol and Nocodazole-arrested cells suggests that Cdk1 interaction with Bax occurred in all cases and it is widely used by the cells to activate mitochondrial-mediated apoptosis. Furthermore, a direct Cdk1-Bax interaction was detected using human commercial recombinant proteins. An *in vitro* assay was complemented the results made by mass spectrometry and co-IP experiments. Although people have reported that both Cdk1 and cyclin B1 are translocated to mitochondria during Vinblastine-induced mitotic arrest (Terrano et al., 2010), the immunofluorescence images are not convincing. We have tried to examine that, but we have not found a clear localization. It may be that the

antibodies are not recognizing Cdk1, the binding site may be masked when Cdk1 is in a complex with Bak and with Bax.

Next, I wanted to determine the physiological role of the Cdk1 interaction with Bak and Bax in mitochondrial-dependent apoptosis. So, I examined whether Bak and Bax are required for Cdk1-mediated phosphorylation of Bcl-2 and Bcl-xL in Taxol-arrested HeLa cells. siRNA depletion of Bak and Bax inhibited Cdk1-induced phosphorylation of Bcl-2 and Bcl-xL, suggesting that Bak and Bax are required to target Cdk1 to the mitochondrion. Then I determined whether siRNA depletion of Bak, Bax or both Bak and Bax can affect Cdk1 kinase activity during Taxol treatment. We already shown that inhibition of Cdk1 activity with RO-3306 can inhibit phosphorylation of Bcl-2 and Bcl-xL. So, one criticism is that by depleting Bak and Bax, it causes inhibition of Cdk1 activity during Taxol treatment. In order to confirm that Cdk1 activity was not inhibited in Bak/Bax depleted cells, I performed an *in vitro* kinase assay using ^{32}p (ATP). My results have shown that in Bak, Bax and both Bak and Bax depleted HeLa cells, Cdk1 was activated but Bcl-2 and Bcl-xL were not phosphorylated.

Taxol induced Bcl-2 and Bcl-xL phosphorylation in HCT116 WT but not in HCT116 Bax/Bak DKO cells. Then I determined Cdk1 activity in HCT116 WT and HCT116 Bax/Bak DKO cells using an *in vitro* kinase assay. Histone H1 phosphorylation levels were similar in HCT116 WT and HCT116 Bax/Bak DKO cells treated with Taxol for the same time. An *in vitro* kinase assay suggested that Cdk1 is activated in both HCT116 WT and HCT116 Bax/Bak DKO in response to Taxol treatment. These results suggest that depletion Bak and Bax does not affect Cdk1 kinase activity, and the pro-apoptotic proteins Bak and Bax are required to target Cdk1 to the MOM to phosphorylate Bcl-2 and Bcl-xL. Therefore, Cdk1-mediated phosphorylation of Bcl-2 and Bcl-xL is Bak and Bax dependent during Taxol treatment. Although low level of Bcl-xL phosphorylation was observed in Taxol-arrested HCT116 Bax/Bak DKO cells. PARP cleavage was not detected in HCT116 Bax/Bak DKO cells upon Taxol treatment, suggesting that phosphorylation of both

Bcl-2 and Bcl-xL may be required for Taxol-induced apoptosis. Collectively, the data presented above demonstrate that Cdk1 interaction with Bak and with Bax appears to be particularly important for translocation of Cdk1 upon prolonged mitotic arrest.

Anti-apoptotic Bcl-2 proteins have been shown to undergo post-translational modifications or targeted for degradation by the proteasome, which ultimately reduces their anti-apoptotic functions (Barille-Nion et al., 2012). The anti-apoptotic protein Bcl-2 has been shown to be phosphorylated during prolonged-mitotic arrest. The phosphorylation sites include S70, S87, T69 (Yamamoto et al., 1999), and T56 (Han et al., 2014). However, Bcl-2 is mostly phosphorylated on S70 by Cdk1/ cyclin B1 (Dai et al., 2013, Ruvolo et al., 2001). Bcl-2 phosphorylation during prolonged-mitotic arrest can be inhibited by the Cdk1 inhibitor roscovitine (Han et al., 2014, Zhou et al., 2014), and it is rapidly de-phosphorylated by PP1 phosphatase during mitotic slippage (Brichese and Valette, 2002). Haschka and colleagues reported that exogenously overexpressed Bcl-2 also undergoes phosphorylation in mitotically arrested HeLa cells (Haschka et al., 2015). However, the precise role of Bcl-2 phosphorylation during SAC-induced mitotic arrest remains controversial. Several studies have shown that Bcl-2 phosphorylation blocks its anti-apoptotic function (Haschka et al., 2015, Yamamoto et al., 1999, Eichhorn et al., 2013). On the other hand, studies reported that Bcl-2 phosphorylation enhances its anti-apoptotic function (Deng et al., 2004, Zhou et al., 2014). My results support the hypothesis that Cdk1-mediated phosphorylation of Bcl-2 may inhibit its interaction with Bak and antagonize their anti-apoptotic function. My Bak IP had identified Bcl-2 as a co-immunoprecipitating protein in both untreated and Taxol-arrested HeLa cells. Furthermore, phosphorylated Bcl-2 was detected in the cell extract of Taxol-arrested cells but not in the co-immunoprecipitated Bcl-2 suggesting that Bcl-2 only interacted with Bak in unphosphorylated form but not when phosphorylated.

Cdk1/cyclin B1 is the most common kinase implicated in the phosphorylation of Bcl-xL (Terrano et al., 2010). Cdk1 targets Bcl-xL on S62 and it is the only mitotic phosphorylation site identified in Bcl-xL (Terrano et al., 2010). Cdk1-mediated phosphorylation of Bcl-xL on S62 inhibits the anti-apoptotic potential of Bcl-xL (Bah et al., 2014, Terrano et al., 2010). Other phosphorylation sites in Bcl-xL have been identified. For example, phosphorylation of S49 which is targeted by polo-like kinase 3 (PLK3). This post translational modification is detected in telophase (Wang et al., 2011). PLK3-induced Bcl-xL phosphorylation seems to be important for cell cycle fidelity. Overexpression of S49 mutants into diploid fibroblasts have negative effects on chromosomal stability (Baruah et al., 2016).

My data have shown that both Bcl-2 and Bcl-xL are subjected to phosphorylation during normal mitosis and in Taxol-arrested HeLa cells. Cdk1 transiently phosphorylates Bcl-2 (Ser 70) and Bcl-xL (Ser 62) during normal mitosis and to higher extent during Taxol-induced mitotic arrest. Furthermore, my results have shown that phosphorylation of these proteins occurs in a Cdk1-dependent manner and can be inhibited by a specific Cdk1 inhibitor (RO-3306 (5 µM)). Transient phosphorylation of Bcl-2 and Bcl-xL indicated that Cdk1 is active during normal mitosis. However, the cells exit mitosis when Cdk1 activity drops below the critical threshold (Terrano et al., 2010). It has been established that RO-3306 (5 µM) inhibits Cdk1 activity to induce G2/M-phase cell cycle arrest in acute myeloid leukaemia (AML) cells (Kojima et al., 2009). Another study reported that 9 µM RO-3306 can reversibly arrest cells at G2/M-phase and then cause exit from mitosis in colon cancer cell lines, HCT116 and SW480, and in HeLa cells (Vassilev et al., 2006). Taxol-arrested HeLa cells were incubated with different concentrations of RO-3306 (1, 5, and 10 µM data not shown). At 12 hrs Taxol treatment, Bcl-2 and Bcl-xL phosphorylation had almost reached a peak. My results indicated that 5 µM RO-3306 can efficiently inhibit Cdk1-mediated phosphorylation of Bcl-2 and Bcl-xL (see Figure 5-17 page 152). Histone H1 assay

also confirmed that Cdk1 kinase activity can be inhibited by 5 μM RO-3306 (see Figure 5-12, page 143).

It seems that chronic activation of Cdk1 has a pro-apoptotic effect during Taxol-induced mitotic arrest. Cdk1-mediated phosphorylation of Bcl-2 and Bcl-xL was clearly detected at 12, 16 and 24 hrs after Taxol addition. By 24 hrs Taxol treatment, 75% of the cells were in apoptosis. The level of apoptosis was increased to 92 % at 36 hrs after Taxol addition. While in the presence of the RO-3306 which inhibits Cdk1 activity and the subsequent phosphorylation of Bcl-2 and Bcl-xL, the number of the apoptotic cells was significantly reduced to 35% at 24 and 50% at 36 hrs. My results are consistent with other studies using different Cdk1 inhibitors (Chan et al., 2008, Shen et al., 1998, Yu et al., 1998). The Cdk1 inhibitor RO-3306 significantly reduced the number of the apoptotic cells, suggesting that chronic activation of Cdk1 is required for Taxol-induced apoptosis and provides a link between activation of the SAC and the induction of apoptosis.

Cdk1 kinase is involved in the regulation of the G2/M transition (Jackman and Pines, 1997). Incubation of HeLa cells with the Cdk1-specific inhibitor RO-3306 strongly blocks the cell cycle in the late G2 phase and prevents entry into mitosis (Vassilev et al., 2006). In this study, RO-3306 was added to Taxol-arrested mitotic cells, in which the majority of the cells were in mitosis. The cells were synchronized by a thymidine block, released and then treated with Taxol for 12 hrs. Mitotically-arrested cells were collected by mitotic shake-off and then incubated with Taxol and RO-3306 (5 μM) for 4 hrs. RO-3306 strongly inhibits Cdk1-mediated phosphorylation of Bcl-2 and Bcl-xL in Taxol-arrested mitotic cells suggesting that phosphorylation of the Bcl-2 and Bcl-xL is mediated via a Cdk1-dependent pathway. Furthermore, inhibition of Cdk1 activity was accompanied by degradation of cyclin B1 presumably by APC/C complex (Brito and Rieder, 2006). As cyclin B1 levels drop below a critical threshold, the cells exit mitosis into a polyploid interphase (Haschka et al., 2018, Vassilev et al., 2006, Kojima et al., 2009).

Phosphorylation of BCL-2 and Bcl-xL in mitotically-arrested cells results in a change of their relative binding affinities with Bak and Bax (Terrano et al., 2010, Upreti et al., 2008b). Subsequently, Bak and Bax oligomerize and form channels to change the permeability of the MOM (Todt et al., 2015, Salvador-Gallego et al., 2016). Studies in mammalian cell line have shown that inhibition or depletion of anti-apoptotic proteins can free Bax for activation and induce apoptosis (O'Neill et al., 2016). The pro-apoptotic effector proteins, Bax and Bak, have two functions in Taxol-induced apoptosis. The first function is to facilitate Cdk1 translocation from the cytoplasm to the MOM to phosphorylate certain Bcl-2 family proteins. Additionally, Bak and Bax can oligomerize at the MOM to form apoptotic channels and mediate cytochrome c release (Salvador-Gallego et al., 2016, Mandal et al., 2016).

In conclusion, my data have provided strong experimental evidence that Cdk1 specifically interacts with pro-apoptotic proteins Bak and Bax. In an in vitro assay, I show a direct interaction between recombinant Cdk1 and Bax. This novel direct interaction enables Cdk1 to localize to the MOM where anti-apoptotic proteins are predominantly located. Cdk1-mediated phosphorylation of Bcl-2 and Bcl-xL upon extended mitotic arrest has a pro-apoptotic effect. This interaction may be an important event that underlines the link between activation of the mitotic check point and induction of apoptosis.

Chapter 6. General discussion

Taxol belongs to the family of antimitotic drugs that interfere with microtubule dynamics and disrupt mitosis by preventing normal spindle assembly and chromosome segregation (Ren et al., 2018). As a result, the spindle assembly checkpoint (SAC) is activated, which blocks the proteasome-dependent degradation of securin and cyclinB1, leading to elevated levels of cyclin B1 and sustained activation of Cdk1 (Rieder and Maiato, 2004, Gascoigne and Taylor, 2009, Manchado et al., 2012). This is usually followed by an apoptotic cell death (Topham et al., 2015). Despite decades of clinical use, the mechanism of action of Taxol-induced cell death in patients is unclear (Komlodi-Pasztor et al., 2011, Mitchison, 2012). *In vivo* microscopy studies have investigated Taxanes effects on cultured cancer cells in compared to their corresponding xenografts in mice (Orth et al., 2011, Janssen et al., 2013). Orth and colleagues reported that Taxol induces fewer mitotic cells, more mitotic slippage and less apoptosis in tumours compared to cultured cells (Orth et al., 2011). In another study, Docetaxel-treated animals showed a wide scale mitotic arrest which then followed by apoptosis (Janssen et al., 2013).

It is well known that interfering with microtubule dynamics during mitosis causes chronic activation of the SAC (Weaver, 2014). However, there has been a lack of understanding of the molecular mechanisms linking SAC activation to the induction of apoptosis. This link needs to be identified in order to understand how Taxol and other antimitotic drugs ultimately provoke their lethal effects, which may be modulated for clinical advantage. My aim was therefore to identify the molecular machinery that is engaged to execute apoptotic cell death upon Taxol-induced mitotic arrest, with a focus identifying the cytoplasmic signal(s) that links SAC activation to the induction of apoptosis.

In this study, evidence is presented that cyclin-dependent kinase 1, a master regulator of mitosis, exists in a complex with two key pro-apoptotic mitochondrial pore-forming proteins Bak and Bax in healthy interphase cells. The formation of an active Bax/Cdk1/cyclin B1 complex is the signal that accumulates in mitotic cells, translocates to the mitochondrial outer membrane and is necessary for inactivation of the anti-apoptotic proteins Bcl-2 and Bcl-xL and the induction of apoptosis. The presence of MPTP proteins in the Bak and Bax IPs of Taxol-arrested mitotic cells indicates that activated Bak/Cdk1 and activated Bax/Cdk1 complexes translocate to the mitochondrial outer membrane during Taxol-induced mitotic arrest. Thus, my finding represents an important advance in our understanding of the mitotic cell death and its regulation. Second, I show that both Bak and Bax are required for Taxol-induced apoptosis in HeLa cells and depletion of either Bax or Bak reduced apoptosis. Thirdly, my results reveal that Bak specifically interacts with Bax in Taxol-arrested mitotic cells, and both Bak and Bax form a complex with MPTP components such as VDAC, ANT2, ATP synthase subunit alpha, ATP synthase subunit beta, phosphate carrier protein and Peptidyl-prolyl cis-trans isomerase during Taxol-induced mitotic arrest.

6.1 Taxol-induced apoptosis is dependent on both Bak and Bax

The intrinsic apoptotic pathway is controlled by the Bcl-2 family of proteins (Singh et al., 2019). The pro-death proteins of the Bcl-2 family, Bax and Bak, can commit mitotically arrested cells to undergo apoptosis by inducing MOMP. Previous studies with knockdown mice shown that Bak and Bax can functionally substitute each other in most of the stress-induced apoptotic pathways (Wei et al., 2001). Bah and colleagues reported that depletion of Bax was more effective than Bak in inhibiting Taxol-induced apoptosis (Bah et al., 2014). In contrast, another study revealed that depletion of Bak was more effective than Bax in reducing mitotic cell death following Nocodazole treatment (Haschka et al., 2015). Therefore, the

relative importance of Bak and Bax in SAC-mediated apoptosis has remained unclear.

I sought to examine whether Bak, Bax or both proteins are required to initiate Taxol-induced mitotic cell death. My results indicated that both Bak and Bax are required for Taxol-induced apoptosis in HeLa cells because siRNA-mediated depletion of either Bak or Bax individually caused a significant decrease in Taxol-induced apoptosis, suggesting that Taxol-induced apoptosis is dependent on both Bak and Bax. Depletion of Bak/Bax in combination resulted in inhibition of apoptosis to a similar extent compared to depletion of Bak or Bax alone. Consistent with my results, Kepp and colleagues have shown that both Bak and Bax are required for cisplatin-induced apoptosis in HeLa cells and both are functionally non-redundant (Kepp et al., 2007). Similarly, Rotolo and colleagues suggested that both Bax and Bak are necessary for radiation-induced endothelial cell death in the intestinal mucosa (Rotolo et al., 2008). Another study also reported a non-redundant function of Bax and Bak during viral infection (Cam et al., 2010). Altogether, my data is consistent with the previous studies which suggested that both Bak and Bax play a critical role in the induction of mitotic cell death.

6.2 Bak and Bax gradually oligomerise following Taxol addition

The pro-death proteins of the Bcl-2 family are key players of the intrinsic pathway of apoptosis (McArthur et al., 2018). In response to an apoptotic stimulus, Bak and Bax are incorporated into the mitochondrial outer membrane, oligomerize and form mitochondrion-permeabilizing pores to mediate cytochrome c release and ultimately lead to cell death. (Lopez and Tait, 2015, Cosentino and García-Sáez, 2017). Studying the molecular mechanism of the intrinsic pathway and how the pro-death proteins, Bax and Bak, permeabilize the mitochondrial outer

membrane during apoptosis has become a focus for research in recent years (Singh et al., 2019).

I therefore investigated the association between activated Bak and activated Bax in Taxol-arrested mitotic cells by using conformation-specific Bak and Bax antibodies. My data indicated that both Bak and Bax were gradually activated during the time course of Taxol-induced mitotic arrest. My data is the first to show, to the best of my knowledge, the time dependent accumulation of active Bak and active Bax during Taxol-induced mitotic arrest (the IPs of the active Bak and active Bax between 12-36 hrs after Taxol addition, see Figures 4-9 and 4-10, page 93). Consistent with my results, Riley and colleagues have shown using a high-resolution Airyscan microscope that Bax pores in the MOM gradually increased in size following ABT-737 treatment (Riley et al., 2018). Interestingly, my time-course experiments confirm that the levels of Bak and Bax that co-immunoprecipitated gradually increased following Taxol addition, indicating that there was an increase in the formation of Bak and Bax complexes (hetero-oligomers) following Taxol-induced mitotic arrest. The increase in the formation of Bak/Bax complexes correlated with the induction of apoptosis as shown by Figures (4-21 and 4-22, pages 106-107). It will be important in the future study to determine whether Bax is required for recruitment of Bak to the MOM and vice versa and to identify the structure of the Bak/Bax hetero-oligomers using a high-resolution imaging.

6.3 Bak and Bax oligomers form a complex with MPTP components

Several reports have shown that MPTP components VDAC, ANT2 and Cyclophilin D are overexpressed in various cancers, where they act as anti-apoptotic proteins (Simamura et al., 2008, Eliseev et al., 2009, Chevrollier et al., 2011). MPTP components interact with some anti-apoptotic proteins such as Bcl-2 to enhance their limiting effect against cytochrome c release from the intermembrane space

of the mitochondria (Gotow et al., 2000, Belzacq et al., 2003, Abu-Hamad et al., 2009, Eliseev et al., 2009, Arbel et al., 2012). My results reveal that active Bak forms a complex with VDAC in the mitochondrial outer membrane following Taxol addition. This complex is expanded to include the mitochondrial inner membrane as my Bak and Bax IPs had identified some inner membrane components of the MPTP such as, ANT2, ANT3, ATP synthase subunit alpha, ATP synthase subunit beta and phosphate carrier protein. Interestingly, my results also identified the presence of Peptidyl-prolyl cis-trans isomerase (Cyclophilin D) in the complex (see my model on page 177). These results indicate that the Bak/Bax oligomer spans the inner mitochondrial membrane and the outer mitochondrial membrane, thereby interacting with MPTP proteins present in both the outer and inner mitochondrial membranes.

Consistent with my results, recent studies have shown that Bak and Bax pores in the mitochondrial outer membrane gradually increased in size and expanded to the mitochondrial inner membrane, resulting in the release of the mitochondrial matrix proteins into the cytoplasm (Riley et al., 2018, McArthur et al., 2018). It is fairly well established that during apoptosis, Bak and Bax form oligomers in the mitochondrial outer membrane leading to cytochrome c release (Cosentino and García-Sáez, 2017). Bak and Bax interaction with VDAC, ANT2 and Cyclophilin D could be an additional mechanism of suppression of the anti-apoptotic effects of VDAC, ANT2 and Cyclophilin D. As such, further understanding of the molecular interactions between the pro-death proteins Bak/Bax with MPTP components that control the intrinsic pathway of apoptosis would pave the way to improve cancer treatment.

6.4 Cdk1 exists as two independent complexes with Bak and with Bax

In healthy cells, the anti-apoptotic proteins Bcl-2, Bcl-xL and Mcl-1 can directly interact with Bak or with Bax to neutralize their pro-apoptotic effects (Andreu-Fernández et al., 2017, Lee et al., 2016). This abates Bak and Bax pore-forming activity and prevents the nonspecific permeabilization of the MOM (Todt et al., 2013, Hockings et al., 2018, Kale et al., 2018). Taxol-induced SAC activation results in prolonged mitotic arrest, thereby inhibiting the inactivation of Cdk1 (Mollinedo and Gajate, 2003). Cdk1 has both pro and anti-apoptotic roles during mitotic arrest. Evidence has accumulated which suggests that sustained Cdk1 activity may be involved in the induction of apoptosis. For example, Cdk1-mediated Bad phosphorylation at S128 enhances its pro-apoptotic effect (Zhou et al., 2014). It has also been reported that Cdk1 phosphorylates Bim at S44 during prolong mitotic arrest to increase the sensitivity to Taxol-induced apoptosis (Mac Fhearraigh and Mc Gee, 2011).

Furthermore, it is well known that Bcl-2 and Bcl-xL are transiently and incompletely phosphorylated during normal mitosis and I have reproduced this result also during this investigation (Scatena et al., 1998, Furukawa et al., 2000, Terrano et al., 2010). Bcl-2 and Bcl-xL become highly phosphorylated upon prolonged mitotic arrest induced by microtubule poisons (Yamamoto et al., 1999, Basu and Haldar, 2003, Upreti et al., 2008b). Cdk1-mediated Bcl-2, Bcl-xL and Mcl-1 phosphorylation has a pro-apoptotic effect during prolonged mitotic arrest. Phosphorylation of Bcl-2 and Bcl-XL blocks their anti-apoptotic effect (Harley et al., 2010, Terrano et al., 2010, Sakurikar et al., 2012). In contrast, Cdk1-mediated phosphorylation of Mcl-1 results in its degradation and inactivation during Nocodazole-induced apoptosis (Zhou et al., 2014).

Downstream of Bak/Bax activation and the induction of MOM permeabilization, Cdk1 has also been shown to phosphorylate XIAP (X-linked inhibitor of apoptosis) and reduces the threshold for the onset of apoptosis in response to microtubule

poisons, thereby inhibiting the anti-apoptotic function of XIAP (Hou et al., 2016). A cytoprotective effect of Cdk1 has also been observed during mitosis. Cdk1 phosphorylates members of the caspase family, caspases-2, -8 and -9 has an anti-apoptotic effect and inhibits mitotic cell death during normal mitosis (Allan and Clarke, 2007, Andersen et al., 2009, Matthess et al., 2010).

However, there has been a lack of a clear understanding of how Cdk1 phosphorylates the anti-apoptotic proteins Bcl-2, Bcl-xL and Mcl-1. It was generally assumed that cytoplasmic activation of Cdk1 at mitosis was sufficient to phosphorylate Bcl-2, Bcl-xL and Mcl-1. During SAC-mediated apoptosis, the signal(s) that accumulate during prolonged mitotic arrest has remained unclear. I propose the hypothesis that Bax-mediated Cdk1 translocation from the cytoplasm to the MOM is the major driver of apoptotic cell death during chronic SAC activation.

My results show, for the first time, that the key mitotic kinase Cdk1 exists in a complex, with either Bak or Bax, in untreated interphase cells. Cdk1 specifically co-immunoprecipitated with Bak and with Bax in untreated and Taxol-arrested mitotic cells. This interaction was observed in three different cell lines (HeLa, U2OS and RPE1), indicating that Cdk1 interaction with Bak and with Bax is a general phenomenon and it is widely used by the cells to activate the intrinsic apoptotic pathway. In an *in vitro* assay, I demonstrated a direct interaction between recombinant Cdk1 and Bax. A direct interaction between the pro-apoptotic protein Bax and Cdk1 supported the results obtained by my mass spectrometry and co-IP experiments.

It has been reported that Cdk1 is uniformly activated in the cytoplasm at mitosis (Jackman et al., 2003, Lindqvist et al., 2007, Gavet and Pines, 2010). Upon Taxol-induced prolonged mitotic arrest, activated Cdk1 translocates with Bak and Bax from the cytoplasm to the MOM, as my Bak and Bax co-IP experiments had indentified some MPTP proteins such as VDAC, ANT2, ANT3, ATP synthase

subunit alpha, ATP synthase subunit beta and Cyclophilin D in Taxol-arrested mitotic cells but not in untreated cells. Bak and Bax mediated translocation of active Cdk1 to the MOM plays an important role in the apoptosis signalling pathway.

In support of my hypothesis, Lauterwasser and colleagues suggested that Bak and Bax translocate from the cytosol to the MOM and back into the cytosol by retrotranslocation (Lauterwasser et al., 2019). Retrotranslocation of Bak and Bax is reduced in the presence of microtubule poisons (Todt et al., 2015). As a result, Cdk1 in a complex with Bak and with Bax would accumulate on the MOM. Cdk1 is responsible for phosphorylation and inactivation of the anti-apoptotic proteins Bcl-2, Bcl-xL and Mcl-1 (Terrano et al., 2010, Chu et al., 2012). Consequently, Bak and Bax form oligomers in the MOM to induce MOMP and cytochrome c release (Cosentino and García-Sáez, 2017). Of note, my data showed clearly that cytoplasmic activation of Cdk1 in Bak/Bax deficient cells is not sufficient to phosphorylate Bcl-2 and Bcl-xL.

It is well known that RO-3306 (a reversible Cdk1 inhibitor) arrests cell cycle progression at the G2/M phase border, thereby inhibiting Cdk1 kinase activity (Bellail et al., 2014). In my study, RO-3306 was added to cells that had been synchronised and arrested with Taxol for 12 hrs, in which Bcl-2 and Bcl-xL phosphorylation had almost reached a peak. In line with several studies, my data indicated that inhibiting Cdk1 activity with RO-3306 during Taxol-induced mitotic arrest led to a reduction in Bcl-2 and Bcl-xL phosphorylation and reduced mitotic cell death (Yu et al., 1998, Shen et al., 1998, Chan et al., 2008). This result suggests that Cdk1 inhibitor, RO-3306, blocks Bcl-2 and Bcl-xL phosphorylation in mitotically arrested cells and that Cdk1-mediated phosphorylation of Bcl-2 and Bcl-xL is required for Taxol-induced apoptosis.

Next, I wanted to test the hypothesis that Cdk1 translocation to the MOM is dependent on Bak and Bax by examining the phosphorylation of Bcl-2 and Bcl-xL

in Bak and Bax-depleted HeLa cells. Intriguingly, siRNA-mediated depletion of Bax, Bak and both Bax and Bak completely inhibited Cdk1-mediated phosphorylation of Bcl-2 and Bcl-xL. To overcome the drawbacks of the siRNA technique, I sought to examine Cdk1-mediated phosphorylation of Bcl-2 and Bcl-xL in HCT116 Bax/Bak DKO cells in response to Taxol treatment. As expected, addition of Taxol induced Bcl-2 and Bcl-xL phosphorylation in HCT116 WT but not in HCT116 Bax/Bak DKO cells. These results suggest that translocation of the active Cdk1, and subsequent phosphorylation of anti-apoptotic proteins Bcl-2 and Bcl-xL upon Taxol-induced mitotic arrest, is dependent on the presence of Bak and Bax. Thus, Cdk1 interaction with Bak and with Bax provides the molecular basis for the link between SAC activation and the induction of apoptosis.

6.5 Bak and Bax have a dual function in Taxol-arrested mitotic cells

Based on my results, the key pro-apoptotic proteins Bak and Bax primarily have a dual role during Taxol-induced apoptosis. The translocation of active Cdk1 from the cytosol to the mitochondrial outer membrane on one hand and the formation of Bak/Bax oligomers in the mitochondrial outer membrane on the other (see Figure 6-1 page 178). Cdk1 specifically co-immunoprecipitated with Bak and with Bax in untreated and Taxol-arrested mitotic cells. In an in vitro assay, I demonstrated a direct interaction between recombinant Cdk1 and Bax. In functional assays, I show that the phosphorylation of the anti-apoptotic proteins Bcl-2 and Bcl-xL is dependent on the activated Cdk1/Bak and activated Cdk1/Bax complexes, suggesting that Bak and Bax may mediate the transfer of activated Cdk1 to the MOM. Cdk1 is directly involved in the phosphorylation and inactivation of anti-apoptotic proteins (Bcl-2, Bcl-xL and Mcl-1) during treatment with microtubule poisons (Terrano et al., 2010, Sakurikar et al., 2012). As a result, activated Bak and activated Bax oligomerize in the mitochondrial outer membrane to form apoptotic pores (Cosentino and García-Sáez, 2017).

Furthermore, activated Bak and activated Bax interact with MPTP components such as VDAC, ANT2, ATP synthase, phosphate carrier protein and Cyclophilin D to form a complex network of protein interactions, as my MS data of the Bak and Bax IPs had identified some outer and inner membrane components of the MPTP (VDAC, ANT2, ATP synthase, phosphate carrier protein and cyclophilin D). The MS data which indicated Bak interaction with VDAC and ANT2, and Bax interaction with ANT2, were confirmed by IP and Western blotting. Further studies are needed to determine whether active Bak and active Bax can interact with ATP synthase, phosphate carrier protein and cyclophilin D. The formation of this complex in Taxol-arrested cells may permeate mitochondrial outer membrane, leading to cytochrome c release, as illustrated in the model shown in Figure (6-1).

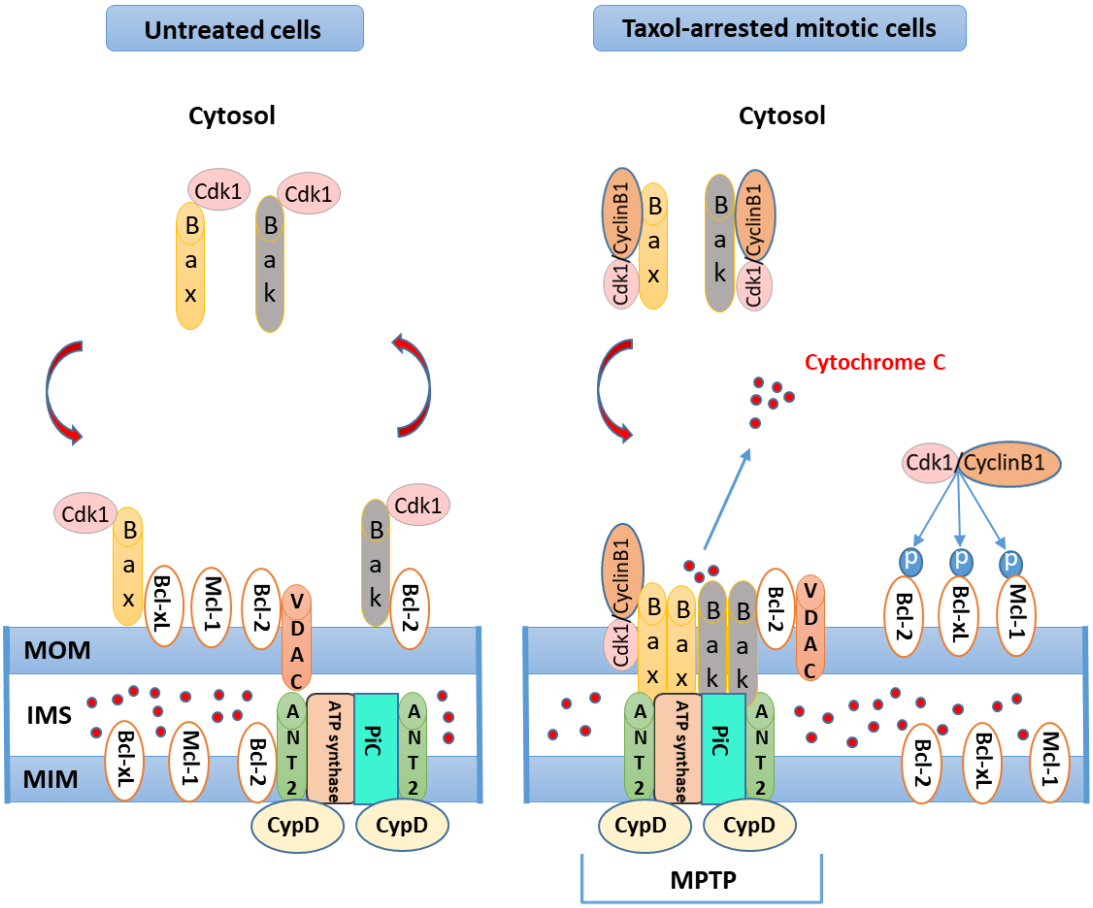

Figure 6-1: Proposed model for Taxol-induced apoptosis.

Based on my results, Cdk1 exists as two independent complexes with Bak and Bax in untreated healthy interphase cells. Bak and Bax are constantly shuttling between cytosol and mitochondrial outer membrane (Lauterwasser et al., 2019). Anti-apoptotic Bcl-2 family members Bcl-2, Bcl-xL and Mcl-1 localize at the MIM and MOM, and restrain the activity of pro-apoptotic members Bak and Bax at the MOM (Popgeorgiev et al., 2018). In response to Taxol treatment, the SAC is activated, leading to elevated levels of cyclin B1 and sustained activation of Cdk1 (Manchado et al., 2012). In addition, the retrotranslocation of Bak and Bax from the mitochondrial outer membrane to the cytosol is reduced (Todt et al., 2015). As a result, Cdk1/CyclinB1/Bak and Cdk1/CyclinB1/Bax complexes accumulate at the MOM, where Cdk1/cyclin B1 phosphorylates anti-apoptotic proteins Bcl-2, Bcl-xL and Mcl-1. Phosphorylation of Bcl-2, Bcl-xL and Mcl-1 antagonizes their anti-apoptotic effects. Subsequently, activated Bak and activated Bax form oligomers in the MOM, and interact with MPTP components such as VDAC, ANT2, ATP synthase, phosphate carrier protein and Cyclophilin D to form a larger complex. The formation of Bak and Bax homo or heterooligomers induces MOMP and cytochrome c release, and then triggers apoptosis.

6.6 Concluding remarks and future perspectives

In this study I have shown that Taxol-induced apoptosis is Bak and Bax dependent. I demonstrated that apoptosis could be rescued in Bax-depleted HeLa cells by re-expressing GFP-Bax. I also determined the expression levels of Bak and Bax in several human cancer cell lines. The lung cancer cell line STK50590 with the lowest Bak expression were resistant to Taxol-induced apoptosis. One possible explanation is that both Bak and Bax are required for Taxol-induced apoptosis. These findings highlighted the notion that both Bak and Bax are required for Taxol-induced apoptosis and excluded the possibility that Bak can substitute for Bax and vice versa. It would be interesting for a future study to examine whether the two colorectal cancer cell lines, RKO143 and A19RKO cells, with high Bak levels, are more sensitive to Taxol or other anti-cancer drugs.

I have demonstrated that the Taxol-induced apoptosis is highly likely the result of Bak and Bax oligomerization and interaction, and possibly their interactions with MPTP components such as VDAC and ANT2. I have also shown the subcellular location of both Bax and Bak. Confocal microscopy indicated that Bax is mainly cytosolic in untreated cells and, as expected, translocated to the mitochondria in the Taxol-arrested mitotic cells. However, Bak co-localised with mitochondria in both untreated and Taxol-treated cells. Moreover, Bak and Bax co-localized in Taxol-treated cells undergoing mitotic death. The co-localization of Bak and Bax supported the results of my co-IP experiments that Bak-Bax interaction is involved in Taxol-induced apoptosis. In a future study, it will be interesting to determine the structure of Bak and Bax oligomers in the MOM using a high-resolution microscope.

I also determined the putative interacting molecules that may mediate apoptosis in Taxol-arrested mitotic cells. Bak and Bax-interacting proteins were identified using mass spectrometry (MS). IPs of active Bax and active Bak from Taxol-arrested cells were subjected to peptide mass fingerprint analysis by MS. The

results indicated that Bak, ANT2 and Cdk1 were complexed specifically with Bax in Taxol-arrested cells. Similarly, Bax, ANT2, and all VDAC isoforms (VDAC1, 2 and 3) were bound specifically to Bak in Taxol-arrested cells. Furthermore, in Taxol-arrested mitotic cells, my proteomics analysis had identified some MIM proteins such as ANT3, ATP synthase subunit alpha, ATP synthase subunit beta and phosphate carrier protein as interacting proteins with active Bak and active Bax. This result suggests that Bak and Bax pores or channels are expanded from MOM to the MIM. In a future study, it will be interesting to use a high-resolution microscope and IP assays, and confirm the interaction between Bak and Bax oligomers with the MIM components of the MPTP such as ANT3, ATP synthase subunit alpha, ATP synthase subunit beta and phosphate carrier protein. It will be also important to explore whether the formation of this complex plays a critical role in Taxol-induced apoptosis and to determine whether Bak and Bax oligomers can directly interact with ANT3, ATP synthase and phosphate carrier protein.

Preliminary studies in our Lab indicated that VDAC1-depletion induced apoptosis by 35%, suggesting anti-apoptotic role of VDAC1. The percentage of apoptosis was slightly higher in VDAC1-depleted cells treated with Taxol (68% apoptosis) in comparison with Taxol treatment only (62% apoptosis). One possibility is that VDAC1 may act as anti-apoptotic protein collaborator and maintain the integrity of the mitochondrial outer membrane. However, further studies are needed to determine the role of VDAC2 and VDAC3 in Taxol-induced mitotic cell death. I also determined the expression levels of VDAC and ANT2 in several human cancer cell lines. It would be exciting for a future study to examine whether the two cancer cell lines, U2OS and Mesothelioma cell lines, with high VDAC levels, are more resistant to Taxol or other anti-cancer drugs. It would be also interesting to examine whether Melanoma cells, with low VDAC levels, are more sensitive to Taxol or other anti-mitotic agents.

The post-translational modification of anti-apoptotic proteins Bcl-2 and Bcl-xL was examined during normal mitosis and in Taxol-arrested mitotic cells. I have shown that both Bcl-2 and Bcl-xL undergo phosphorylation both during normal mitosis and in the Taxol-arrested mitotic cells. Furthermore, my data has shown that the phosphorylation of Bcl-2 and Bcl-xL is dependent on active Cdk1 as Bcl-2 and Bcl-xL phosphorylation was blocked by RO-3306, a specific inhibitor of Cdk1.

The present study is the first to identify the link between activation of the SAC and the induction of apoptosis. My data show for the first time a direct interaction between the key kinase of the cell cycle, Cdk1, and the two most important regulators of mitochondrial membrane permeability, Bak and Bax. This interaction provides molecular basis for the link between SAC activation and the initiation of the apoptosis. I show that Cdk1 exists as two independent complexes with Bak and with Bax in three different cell lines (HeLa, U2OS and RPE1), suggesting that it may be a general phenomenon. I have also demonstrated a novel direct interaction between the pro-apoptotic protein Bax and Cdk1 using purified recombinant proteins. In a future study, it will be interesting to use an *in vitro* assay and explore whether Cdk1 directly interacts with Bak.

Although Cdk1/cyclinB1 binds to Bax, it is not known if Cdk1 phosphorylates Bax. It will be interesting to use recombinant active Cdk1/cyclinB1 and purified Bax (provided by our collaborator Frank Adlich, University of Freiburg) and perform *an invitro* kinase assay to determine if Bax is phosphorylated by Cdk1/cyclinB1. If so, the phosphorylation sites can be identified by MS. The effects of Bax phosphorylation can be examined by making phosphomimetic and phosphonull mutants.

In functional assays, I have shown that the phosphorylation of the Bcl-2 and Bcl-xL is dependent on the activated Cdk1/Bak and activated Cdk1/Bax complexes. My results suggest that Bak and Bax may play a role in the translocation of Cdk1 from the cytoplasm to the mitochondrial outer membrane, where the anti-

apoptotic proteins Bcl-2 and Bcl-xL are predominantly located. It will be interesting to directly test Cdk1 translocation to the mitochondria in Taxol-arrested cells using GFP-Cdk1 and live cell imaging. My data indicated that Cdl1 interaction with Bak and with Bax is the cytoplasmic signal that may link SAC activation to the mitochondrial-mediated cell death. In future studies, it will be interesting to determine the specific domains that involved in Cdk1 interaction with Bak and with Bax.

Chapter 7. Appendix

Table 7-1: Bax and Bak interacting proteins

HeLa cells were treated with Taxol (60 nM) for 24 hrs and the cells were lysed in 1% CHAPS lysis buffer. Active Bax or Bak was immunoprecipitated suing anti-active Bax (6A7) antibody or anti-active Bak (N-20) antibody, respectively. The IPs were subjected to peptide mass fingerprint analysis by MS. 36 proteins were identified in the Bax IP and 43 proteins were identified in the Bak IP, after eliminating non-specific binding of proteins to the magnetic beads. Peptide threshold 95% and Protein Identification Probability 100%.

Protein	Bax IP		Bak IP	
	Score	Coverage (%)	Score	Coverage (%)
ADP/ATP translocase 2 OS=Homo sapiens	410	35	317	27
ADP/ATP translocase 3 OS=Homo sapiens	280	29	233	23
60 kDa heat shock protein, mitochondrial OS=Homo sapiens	426	23	256	12
14-3-3 protein zeta/delta OS=Homo sapiens	363	36	169	18
Apoptosis regulator BAX OS=Homo sapiens	776	55	459	35
Bcl-2 homologous antagonist/killer OS=Homo sapiens GN=BAK1	49	5.80	259	33
Peptidyl-prolyl cis-trans isomerase OS=Homo sapiens	370	37	139	30

Protein	Bax IP		Bak IP	
	Score	Coverage (%)	Score	Coverage (%)
ATP synthase subunit alpha, mitochondrial OS=Homo	169	26	386	22
ATP synthase subunit beta OS=Homo sapiens	196	13	210	23
L-lactate dehydrogenase A chain OS=Homo sapiens	236	26	98	16
Serpin H1 OS=Homo sapiens	250	15	310	36
Myosin regulatory light chain 12A OS=Homo sapiens	279	32	537	49
60S acidic ribosomal protein P0 OS=Homo sapiens	76	15	40	22
Cyclin-dependent kinase 1 OS=Homo sapiens	139	16		
Nucleophosmin OS=Homo sapiens	247	35		
Heterogeneous nuclear ribonucleoprotein M OS=Homo sapiens	345	18		
ATP-dependent RNA helicase DDX5 OS=Homo sapiens	146	9.90		
Triosephosphate isomerase OS=Homo sapiens	207	24		

Protein	Bax IP		Bak IP	
	Score	Coverage (%)	Score	Coverage (%)
Tropomyosin alpha-4 chain OS=Homo sapiens	117	14		
Clusterin OS=Homo sapiens	234	15		
Nucleoside diphosphate kinase OS=Homo sapiens	189	17		
Transgelin-2 OS=Homo sapiens	88	23		
Heterogeneous nuclear ribonucleoprotein K OS=Homo sapiens	74	10		
Protein disulfide-isomerase OS=Homo sapiens	160	17		
Receptor of-activated protein C kinase 1 OS=Homo sapiens	218	24		
Galectin-1 OS=Homo sapiens	66	19		
Reticulocalbin-1 OS=Homo sapiens	90	17		
DnaJ homolog subfamily A member 3, mitochondrial OS=Homo sapiens	70	11		
Drebrin OS=Homo sapiens	71	8.80		

Protein	Bax IP		Bak IP	
	Score	Coverage (%)	Score	Coverage (%)
Heterogeneous nuclear ribonucleoproteins C1/C2 OS=Homo sapiens	138	26		
10 kDa heat shock protein, mitochondrial OS=Homo sapiens	76	35		
Brain acid soluble protein 1 OS=Homo sapiens	52	28		
Plasminogen activator inhibitor 1 RNA-binding protein OS=Homo sapiens	87	9.30		
Heterogeneous nuclear ribonucleoprotein D0 OS=Homo sapiens	137	12		
Heterogeneous nuclear ribonucleoprotein A/B OS=Homo sapiens	110	11		
Filamin-A OS=Homo sapiens	867	15		
Tripartite motif-containing protein 47 OS=Homo sapiens			778	26
Probable ATP-dependent RNA helicase DDX41 OS=Homo sapiens			653	33

Protein	Bax IP		Bak IP	
	Score	Coverage (%)	Score	Coverage (%)
Erlin-2 OS=Homo sapiens			718	44
Erlin-1 OS=Homo sapiens			661	49
Voltage-dependent anion-selective channel protein 1 OS=Homo sapiens			545	34
Voltage-dependent anion-selective channel protein 2 OS=Homo sapiens			423	40
Phosphate carrier protein, mitochondrial OS=Homo sapiens			61	8.3
Stress-70 protein, mitochondrial OS=Homo sapiens			657	25
Mitochondrial carrier homolog 2			69	16
Transmembrane emp24 domain-containing protein 10 OS=Homo sapiens			150	22
Leucine-rich repeat-containing protein 59 OS=Homo sapiens			68	15
Surfeit locus protein 4 OS=Homo sapiens			199	15
Tropomyosin beta chain OS=Homo sapiens			237	17

Protein	Bax IP		Bak IP	
	Score	Coverage (%)	Score	Coverage (%)
Putative RNA-binding protein Luc7-like 2 OS=Homo sapiens			226	24
RNA-binding protein 39 OS=Homo sapiens			189	20
Lamin-B1 OS=Homo sapiens			139	14
Very-long-chain enoyl-CoA reductase OS=Homo sapiens			136	13
Sequestosome-1 OS=Homo sapiens			67	9.80
Calnexin OS=Homo sapiens			111	8.40
Transmembrane emp24 domain-containing protein 10 OS=Homo sapiens			150	22
4F2 cell-surface antigen heavy chain OS=Homo sapiens			60	6.50
Voltage-dependent anion-selective channel protein 3 OS=Homo sapiens			290	23
Surfeit locus protein 4 OS=Homo sapiens			199	15

Protein	Bax IP		Bak IP	
	Score	Coverage (%)	Score	Coverage (%)
Polypeptide N-acetylgalactosaminyltransferase 2 OS=Homo sapiens			69	5.10
Leucine-richrepeat-containing protein 59 OS=Homo sapiens			68	15
Dolichyl-diphosphooligosaccharide--protein glycosyltransferase 48 kDa subunit OS=Homo sapiens			101	6.40
Mitochondrial carrier homolog 2 OS=Homo sapiens			69	16
Bleomycin hydrolase OS=Homo sapiens			64	14
Serpin B3 OS=Homo sapiens			86	6.70
Desmocollin-1 OS=Homo sapiens			106	3.90

Chapter 8. Bibliography

ABAL, M., ANDREU, J. & BARASOAIN, I. 2003. Taxanes: microtubule and centrosome targets, and cell cycle dependent mechanisms of action. *Current cancer drug targets,* 3**,** 193-203.

ABU-HAMAD, S., ARBEL, N., CALO, D., ARZOINE, L., ISRAELSON, A., KEINAN, N., BEN-ROMANO, R., FRIEDMAN, O. & SHOSHAN-BARMATZ, V. 2009. The VDAC1 N-terminus is essential both for apoptosis and the protective effect of anti-apoptotic proteins. *Journal of cell science,* 122**,** 1906-1916.

ADAMS, J. & CORY, S. 2007. The Bcl-2 apoptotic switch in cancer development and therapy. *Oncogene,* 26**,** 1324-1337.

ADAMS, J. M. & CORY, S. 1998. The Bcl-2 protein family: arbiters of cell survival. *Science,* 281**,** 1322-1326.

ADAMS, J. M. & CORY, S. 2018. The BCL-2 arbiters of apoptosis and their growing role as cancer targets. *Cell death and differentiation,* 25**,** 27.

ALLAN, L. A. & CLARKE, P. R. 2007. Phosphorylation of caspase-9 by CDK1/cyclin B1 protects mitotic cells against apoptosis. *Molecular cell,* 26**,** 301-310.

ALNEMRI, E. S., LIVINGSTON, D. J., NICHOLSON, D. W., SALVESEN, G., THORNBERRY, N. A., WONG, W. W. & YUAN, J. 1996. Human ICE/CED-3 protease nomenclature. *Cell,* 87**,** 171.

AMBROSINI, G., ADIDA, C. & ALTIERI, D. C. 1997. A novel anti-apoptosis gene, survivin, expressed in cancer and lymphoma. *Nature medicine,* 3**,** 917.

ANDERSEN, J. L., JOHNSON, C. E., FREEL, C. D., PARRISH, A. B., DAY, J. L., BUCHAKJIAN, M. R., NUTT, L. K., THOMPSON, J. W., MOSELEY, M. A. & KORNBLUTH, S. 2009. Restraint of apoptosis during mitosis through interdomain phosphorylation of caspase-2. *The EMBO Journal,* 28**,** 3216-3227.

ANDREU-FERNÁNDEZ, V., SANCHO, M., GENOVÉS, A., LUCENDO, E., TODT, F., LAUTERWASSER, J., FUNK, K., JAHREIS, G., PÉREZ-PAYÁ, E. & MINGARRO, I. 2017.

Bax transmembrane domain interacts with prosurvival Bcl-2 proteins in biological membranes. *Proceedings of the National Academy of Sciences,* 114**,** 310-315.

ANNIS, M. G., SOUCIE, E. L., DLUGOSZ, P. J., CRUZ-AGUADO, J. A., PENN, L. Z., LEBER, B. & ANDREWS, D. W. 2005. Bax forms multispanning monomers that oligomerize to permeabilize membranes during apoptosis. *The EMBO journal,* 24**,** 2096-2103.

ARBEL, N., BEN-HAIL, D. & SHOSHAN-BARMATZ, V. 2012. Mediation of the antiapoptotic activity of Bcl-xL protein upon interaction with VDAC1 protein. *Journal of Biological Chemistry,* 287**,** 23152-23161.

ARBEL, N. & SHOSHAN-BARMATZ, V. 2010. Voltage-dependent anion channel 1-based peptides interact with Bcl-2 to prevent antiapoptotic activity. *Journal of Biological Chemistry,* 285**,** 6053-6062.

ARIF, T., KRELIN, Y., NAKDIMON, I., BENHARROCH, D., PAUL, A., DADON-KLEIN, D. & SHOSHAN-BARMATZ, V. 2017. VDAC1 is a molecular target in glioblastoma, with its depletion leading to reprogrammed metabolism and reversed oncogenic properties. *Neuro-oncology,* 19**,** 951-964.

ARIF, T., VASILKOVSKY, L., REFAELY, Y., KONSON, A. & SHOSHAN-BARMATZ, V. 2014. Silencing VDAC1 expression by siRNA inhibits cancer cell proliferation and tumor growth in vivo. *Molecular Therapy-Nucleic Acids,* 3.

BAH, N., MAILLET, L., RYAN, J., DUBREIL, S., GAUTIER, F., LETAI, A., JUIN, P. & BARILLÉ-NION, S. 2014. Bcl-xL controls a switch between cell death modes during mitotic arrest. *Cell death & disease,* 5**,** e1291.

BAIK, S. H. & LEE, J. 2016. Adenine nucleotide translocase 2: an emerging player in cancer.

BAIK, S. H., LEE, J., LEE, Y.-S., JANG, J.-Y. & KIM, C.-W. 2016. ANT2 shRNA downregulates miR-19a and miR-96 through the PI3K/Akt pathway and suppresses tumor growth in hepatocellular carcinoma cells. *Experimental & molecular medicine,* 48**,** e222.

BAINES, C. P., KAISER, R. A., SHEIKO, T., CRAIGEN, W. J. & MOLKENTIN, J. D. 2007. Voltage-dependent anion channels are dispensable for mitochondrial-dependent cell death. *Nature cell biology,* 9**,** 550.

BANERJEE, J. & GHOSH, S. 2004. Bax increases the pore size of rat brain mitochondrial voltage-dependent anion channel in the presence of tBid. *Biochemical and biophysical research communications,* 323**,** 310-314.

BARBUTI, A. M. & CHEN, Z.-S. 2015. Paclitaxel through the ages of anticancer therapy: exploring its role in chemoresistance and radiation therapy. *Cancers,* 7**,** 2360-2371.

BARILLE-NION, S., BAH, N., VEQUAUD, E. & JUIN, P. 2012. Regulation of cancer cell survival by BCL2 family members upon prolonged mitotic arrest: opportunities for anticancer therapy. *Anticancer research,* 32**,** 4225-4233.

BARNUM, K. J. & O'CONNELL, M. J. 2014. Cell cycle regulation by checkpoints. *Cell Cycle Control.* Springer.

BARUAH, P. S., BEAUCHEMIN, M., HÉBERT, J. & BERTRAND, R. 2016. Dynamic Bcl-xL (S49) and (S62) phosphorylation/dephosphorylation during mitosis prevents chromosome instability and aneuploidy in normal human diploid fibroblasts. *PloS one,* 11**,** e0159091.

BASU, A. & HALDAR, S. 2003. Identification of a novel Bcl-xL phosphorylation site regulating the sensitivity of taxol-or 2-methoxyestradiol-induced apoptosis. *FEBS letters,* 538**,** 41-47.

BATCHELOR, E., LOEWER, A., MOCK, C. & LAHAV, G. 2011. Stimulus-dependent dynamics of p53 in single cells. *Molecular systems biology,* 7**,** 488.

BAUER, M. K., SCHUBERT, A., ROCKS, O. & GRIMM, S. 1999. Adenine nucleotide translocase-1, a component of the permeability transition pore, can dominantly induce apoptosis. *The Journal of cell biology,* 147**,** 1493-1502.

BELLAIL, A. C., OLSON, J. J. & HAO, C. 2014. SUMO1 modification stabilizes CDK6 protein and drives the cell cycle and glioblastoma progression. *Nature communications,* 5**,** 4234.

BELZACQ, A.-S., VIEIRA, H. L., VERRIER, F., VANDECASTEELE, G., COHEN, I., PRÉVOST, M.-C., LARQUET, E., PARISELLI, F., PETIT, P. X. & KAHN, A. 2003. Bcl-2 and Bax modulate adenine nucleotide translocase activity. *Cancer research,* 63**,** 541-546.

BERNARDI, P., RASOLA, A., FORTE, M. & LIPPE, G. 2015. The mitochondrial permeability transition pore: channel formation by F-ATP synthase, integration in signal transduction, and role in pathophysiology. *Physiological reviews,* 95**,** 1111-1155.

BERNARDI, P. & VON STOCKUM, S. 2012. The permeability transition pore as a Ca2+ release channel: new answers to an old question. *Cell calcium,* 52**,** 22-27.

BIASUTTO, L., AZZOLINI, M., SZABO, I. & ZORATTI, M. 2016. The mitochondrial permeability transition pore in AD 2016: an update. *Biochimica et Biophysica Acta (BBA)-Molecular Cell Research,* 1863**,** 2515-2530.

BLAGOSKLONNY, M. V., GIANNAKAKOU, P., EL-DEIRY, W. S., KINGSTON, D. G., HIGGS, P. I., NECKERS, L. & FOJO, T. 1997. Raf-1/bcl-2 phosphorylation: a step from microtubule damage to cell death. *Cancer research,* 57**,** 130-135.

BLEICKEN, S., LANDETA, O., LANDAJUELA, A., BASAÑEZ, G. & GARCÍA-SÁEZ, A. J. 2013. Proapoptotic Bax and Bak form stable protein-permeable pores of tunable size. *Journal of Biological Chemistry***,** jbc. M113. 512087.

BONORA, M., WIECKOWSKI, M. R., CHINOPOULOS, C., KEPP, O., KROEMER, G., GALLUZZI, L. & PINTON, P. 2015. Molecular mechanisms of cell death: central implication of ATP synthase in mitochondrial permeability transition. *Oncogene,* 34**,** 1475.

BRATTON, S. B. & SALVESEN, G. S. 2010. Regulation of the Apaf-1–caspase-9 apoptosome. *J Cell Sci,* 123**,** 3209-3214.

BRECKENRIDGE, D. G., GERMAIN, M., MATHAI, J. P., NGUYEN, M. & SHORE, G. C. 2003. Regulation of apoptosis by endoplasmic reticulum pathways. *Oncogene,* 22**,** 8608.

BRENNER, C., CADIOU, H., VIEIRA, H. L., ZAMZAMI, N., MARZO, I., XIE, Z., LEBER, B., ANDREWS, D., DUCLOHIER, H. & REED, J. C. 2000. Bcl-2 and Bax regulate the channel activity of the mitochondrial adenine nucleotide translocator. *Oncogene,* 19**,** 329.

BRENNER, C., SUBRAMANIAM, K., PERTUISET, C. & PERVAIZ, S. 2011. Adenine nucleotide translocase family: four isoforms for apoptosis modulation in cancer. *Oncogene,* 30**,** 883.

BRICHESE, L. & VALETTE, A. 2002. PP1 phosphatase is involved in Bcl-2 dephosphorylation after prolonged mitotic arrest induced by paclitaxel. *Biochemical and biophysical research communications,* 294**,** 504-508.

BRITO, D. A. & RIEDER, C. L. 2006. Mitotic checkpoint slippage in humans occurs via cyclin B destruction in the presence of an active checkpoint. *Curr Biol,* 16**,** 1194-200.

BROWER, J. V., RODIC, N., SEKI, T., JORGENSEN, M., FLIESS, N., YACHNIS, A. T., MCCARREY, J. R., OH, S. P. & TERADA, N. 2007. Evolutionarily conserved mammalian adenine nucleotide translocase 4 is essential for spermatogenesis. *Journal of Biological Chemistry*.

BURTON, J. L. & SOLOMON, M. J. 2007. Mad3p, a pseudosubstrate inhibitor of APCCdc20 in the spindle assembly checkpoint. *Genes & development,* 21**,** 655-667.

CAM, M., HANDKE, W., PICARD-MAUREAU, M. & BRUNE, W. 2010. Cytomegaloviruses inhibit Bak-and Bax-mediated apoptosis with two separate viral proteins. *Cell death and differentiation,* 17**,** 655.

CAMPBELL, K. J. & TAIT, S. W. 2018. Targeting BCL-2 regulated apoptosis in cancer. *Open biology,* 8**,** 180002.

CANNON, L. A., KIMMELSTIEL, C. D., WHITE, A., HILL, R., GRADY, T. P., MYERS, P. R., UNDERWOOD, P. & DAWKINS, K. D. 2018. Clinical outcomes following implantation of the ION™ paclitaxel-eluting platinum chromium coronary stent in routine clinical practice: Results of the ION US post-approval study. *Catheterization and Cardiovascular Interventions*.

CARTRON, P.-F., GALLENNE, T., BOUGRAS, G., GAUTIER, F., MANERO, F., VUSIO, P., MEFLAH, K., VALLETTE, F. M. & JUIN, P. 2004. The first α helix of Bax plays a necessary role in its ligand-induced activation by the BH3-only proteins Bid and PUMA. *Molecular cell,* 16**,** 807-818.

CHAN, Y. W., MA, H. T., WONG, W., HO, C. C., ON, K. F. & POON, R. Y. 2008. CDK1 inhibitors antagonize the immediate apoptosis triggered by spindle disruption but promote apoptosis following the subsequent rereplication and abnormal mitosis. *Cell Cycle,* 7**,** 1449-1461.

CHAO, W. C., KULKARNI, K., ZHANG, Z., KONG, E. H. & BARFORD, D. 2012. Structure of the mitotic checkpoint complex. *Nature,* 484**,** 208-213.

CHEESEMAN, I. M. & DESAI, A. 2008. Molecular architecture of the kinetochore–microtubule interface. *Nature reviews Molecular cell biology,* 9**,** 33.

CHEN, J., JIN, S., ABRAHAM, V., HUANG, X., LIU, B., MITTEN, M. J., NIMMER, P., LIN, X., SMITH, M. & SHEN, Y. 2011. The Bcl-2/Bcl-XL/Bcl-w inhibitor, navitoclax, enhances the activity of chemotherapeutic agents in vitro and in vivo. *Molecular cancer therapeutics,* 10**,** 2340-2349.

CHEN, L., WILLIS, S. N., WEI, A., SMITH, B. J., FLETCHER, J. I., HINDS, M. G., COLMAN, P. M., DAY, C. L., ADAMS, J. M. & HUANG, D. C. 2005. Differential targeting of prosurvival Bcl-2 proteins by their BH3-only ligands allows complementary apoptotic function. *Molecular cell,* 17**,** 393-403.

CHENG, E. H.-Y., SHEIKO, T. V., FISHER, J. K., CRAIGEN, W. J. & KORSMEYER, S. J. 2003. VDAC2 inhibits BAK activation and mitochondrial apoptosis. *Science,* 301**,** 513-517.

CHEVROLLIER, A., LOISEAU, D., REYNIER, P. & STEPIEN, G. 2011. Adenine nucleotide translocase 2 is a key mitochondrial protein in cancer metabolism. *Biochimica et Biophysica Acta (BBA)-Bioenergetics,* 1807**,** 562-567.

CHIPUK, J. E., MOLDOVEANU, T., LLAMBI, F., PARSONS, M. J. & GREEN, D. R. 2010. The BCL-2 family reunion. *Molecular cell,* 37**,** 299-310.

CHOI, Y. & ANDERS, L. 2014. Signaling through cyclin D-dependent kinases. *Oncogene,* 33**,** 1890.

CHOU, J. J., LI, H., SALVESEN, G. S., YUAN, J. & WAGNER, G. 1999. Solution structure of BID, an intracellular amplifier of apoptotic signaling. *Cell,* 96**,** 615-624.

CHU, R., TERRANO, D. T. & CHAMBERS, T. C. 2012. Cdk1/cyclin B plays a key role in mitotic arrest-induced apoptosis by phosphorylation of Mcl-1, promoting its degradation and freeing Bak from sequestration. *Biochemical pharmacology,* 83**,** 199-206.

COSENTINO, K. & GARCÍA-SÁEZ, A. J. 2017. Bax and Bak pores: are we closing the circle? *Trends in cell biology,* 27**,** 266-275.

CRAWFORD, E. D. & WELLS, J. A. 2011. Caspase substrates and cellular remodeling. *Annual review of biochemistry,* 80**,** 1055-1087.

CROMPTON, M., VIRJI, S. & WARD, J. M. 1998. Cyclophilin-D binds strongly to complexes of the voltage-dependent anion channel and the adenine nucleotide translocase to form the permeability transition pore. *European Journal of Biochemistry,* 258**,** 729-735.

CZABOTAR, P. E., LEE, E. F., VAN DELFT, M. F., DAY, C. L., SMITH, B. J., HUANG, D. C., FAIRLIE, W. D., HINDS, M. G. & COLMAN, P. M. 2007. Structural insights into the degradation of Mcl-1 induced by BH3 domains. *Proceedings of the National Academy of Sciences,* 104**,** 6217-6222.

CZABOTAR, P. E., LESSENE, G., STRASSER, A. & ADAMS, J. M. 2014. Control of apoptosis by the BCL-2 protein family: implications for physiology and therapy. *Nature reviews Molecular cell biology,* 15**,** 49.

CZABOTAR, P. E., WESTPHAL, D., DEWSON, G., MA, S., HOCKINGS, C., FAIRLIE, W. D., LEE, E. F., YAO, S., ROBIN, A. Y. & SMITH, B. J. 2013. Bax crystal structures reveal how BH3 domains activate Bax and nucleate its oligomerization to induce apoptosis. *Cell,* 152**,** 519-531.

DAI, H., DING, H., MENG, X. W., LEE, S.-H., SCHNEIDER, P. A. & KAUFMANN, S. H. 2013. Contribution of Bcl-2 phosphorylation to Bak binding and drug resistance. *Cancer research***,** canres. 0940.2013.

DAI, H., MENG, X. W., LEE, S.-H., SCHNEIDER, P. A. & KAUFMANN, S. H. 2009. Context-dependent Bcl-2/Bak interactions regulate lymphoid cell apoptosis. *Journal of Biological Chemistry***,** jbc. M109. 004770.

DASIKA, G. K., LIN, S.-C. J., ZHAO, S., SUNG, P., TOMKINSON, A. & LEE, E. Y. P. 1999. DNA damage-induced cell cycle checkpoints and DNA strand break repair in development and tumorigenesis. *oncogene,* 18**,** 7883.

DAVIDS, M. S., ROBERTS, A. W., SEYMOUR, J. F., PAGEL, J. M., KAHL, B. S., WIERDA, W. G., PUVVADA, S., KIPPS, T. J., ANDERSON, M. A. & SALEM, A. H. 2017. Phase I first-in-human study of venetoclax in patients with relapsed or refractory non-Hodgkin lymphoma. *Journal of Clinical Oncology,* 35**,** 826.

DE ANTONI, A., PEARSON, C. G., CIMINI, D., CANMAN, J. C., SALA, V., NEZI, L., MAPELLI, M., SIRONI, L., FARETTA, M. & SALMON, E. D. 2005. The Mad1/Mad2 complex as a template for Mad2 activation in the spindle assembly checkpoint. *Current Biology,* 15**,** 214-225.

DEACON, K., MISTRY, P., CHERNOFF, J., BLANK, J. L. & PATEL, R. 2003. p38 Mitogen-activated protein kinase mediates cell death and p21-activated kinase mediates cell survival during chemotherapeutic drug-induced mitotic arrest. *Molecular biology of the cell,* 14**,** 2071-2087.

DENG, J., CARLSON, N., TAKEYAMA, K., DAL CIN, P., SHIPP, M. & LETAI, A. 2007. BH3 profiling identifies three distinct classes of apoptotic blocks to predict response to ABT-737 and conventional chemotherapeutic agents. *Cancer cell,* 12**,** 171-185.

DENG, X., GAO, F., FLAGG, T. & MAY, W. S. 2004. Mono-and multisite phosphorylation enhances Bcl2's antiapoptotic function and inhibition of cell cycle entry functions. *Proceedings of the National Academy of Sciences,* 101**,** 153-158.

DENG, X., RUVOLO, P., CARR, B. & MAY, W. S. 2000. Survival function of ERK1/2 as IL-3-activated, staurosporine-resistant Bcl2 kinases. *Proceedings of the National Academy of Sciences,* 97**,** 1578-1583.

DESAGHER, S. & MARTINOU, J.-C. 2000. Mitochondria as the central control point of apoptosis. *Trends in cell biology,* 10**,** 369-377.

DESAI, A. & MITCHISON, T. J. 1997. Microtubule polymerization dynamics. *Annual review of cell and developmental biology,* 13**,** 83-117.

DEVERAUX, Q. L., TAKAHASHI, R., SALVESEN, G. S. & REED, J. C. 1997. X-linked IAP is a direct inhibitor of cell-death proteases. *Nature,* 388**,** 300.

DEWSON, G. 2015. Investigating Bak/Bax activating conformation change by immunoprecipitation. *Cold Spring Harbor Protocols,* 2015**,** pdb. prot086454.

DEWSON, G. & KLUCK, R. M. 2009. Mechanisms by which Bak and Bax permeabilise mitochondria during apoptosis. *Journal of cell science,* 122**,** 2801-2808.

DEWSON, G., KRATINA, T., CZABOTAR, P., DAY, C. L., ADAMS, J. M. & KLUCK, R. M. 2009. Bak activation for apoptosis involves oligomerization of dimers via their α6 helices. *Molecular cell,* 36**,** 696-703.

DEWSON, G., KRATINA, T., SIM, H. W., PUTHALAKATH, H., ADAMS, J. M., COLMAN, P. M. & KLUCK, R. M. 2008. To trigger apoptosis, Bak exposes its BH3 domain and homodimerizes via BH3: groove interactions. *Molecular cell,* 30**,** 369-380.

DEWSON, G., MA, S., FREDERICK, P., HOCKINGS, C., TAN, I., KRATINA, T. & KLUCK, R. 2012. Bax dimerizes via a symmetric BH3: groove interface during apoptosis. *Cell death and differentiation,* 19**,** 661.

DOERNER, A., PAUSCHINGER, M., BADORFF, A., NOUTSIAS, M., GIESSEN, S., SCHULZE, K., BILGER, J., RAUCH, U. & SCHULTHEISS, H.-P. 1997. Tissue-specific transcription pattern of the adenine nucleotide translocase isoforms in humans. *FEBS letters,* 414**,** 258-262.

DORSETT, Y. & TUSCHL, T. 2004. siRNAs: applications in functional genomics and potential as therapeutics. *Nature reviews Drug discovery,* 3**,** 318.

DREXLER, H. 1998. Review of alterations of the cyclin-dependent kinase inhibitor INK4 family genes p15, p16, p18 and p19 in human leukemia–lymphoma cells. *Leukemia,* 12**,** 845.

DUMONTET, C. & JORDAN, M. A. 2010. Microtubule-binding agents: a dynamic field of cancer therapeutics. *Nat Rev Drug Discov,* 9**,** 790-803.

EDLICH, F., BANERJEE, S., SUZUKI, M., CLELAND, M. M., ARNOULT, D., WANG, C., NEUTZNER, A., TJANDRA, N. & YOULE, R. J. 2011. Bcl-xL retrotranslocates Bax from the mitochondria into the cytosol. *Cell,* 145**,** 104-116.

EICHHORN, J., SAKURIKAR, N., ALFORD, S., CHU, R. & CHAMBERS, T. 2013. Critical role of anti-apoptotic Bcl-2 protein phosphorylation in mitotic death. *Cell death & disease,* 4**,** e834.

ELIE-CAILLE, C., SEVERIN, F., HELENIUS, J., HOWARD, J., MULLER, D. J. & HYMAN, A. A. 2007. Straight GDP-tubulin protofilaments form in the presence of taxol. *Current Biology,* 17**,** 1765-1770.

ELISEEV, R. A., MALECKI, J., LESTER, T., ZHANG, Y., HUMPHREY, J. & GUNTER, T. E. 2009. Cyclophilin D interacts with Bcl2 and exerts an anti-apoptotic effect. *Journal of Biological Chemistry,* 284**,** 9692-9699.

ELLEDGE, S. J. 1996. Cell cycle checkpoints: preventing an identity crisis. *Science,* 274**,** 1664-1672.

ENDERS, G. H. 2012. Mammalian interphase cdks: dispensable master regulators of the cell cycle. *Genes & cancer,* 3**,** 614-618.

ER, E., OLIVER, L., CARTRON, P.-F., JUIN, P., MANON, S. & VALLETTE, F. M. 2006. Mitochondria as the target of the pro-apoptotic protein Bax. *Biochimica et Biophysica Acta (BBA)-Bioenergetics,* 1757**,** 1301-1311.

ESPERT, A., ULUOCAK, P., BASTOS, R. N., MANGAT, D., GRAAB, P. & GRUNEBERG, U. 2014. PP2A-B56 opposes Mps1 phosphorylation of Knl1 and thereby promotes spindle assembly checkpoint silencing. *J Cell Biol,* 206**,** 833-842.

FAESEN, A. C., THANASOULA, M., MAFFINI, S., BREIT, C., MÜLLER, F., VAN GERWEN, S., BANGE, T. & MUSACCHIO, A. 2017. Basis of catalytic assembly of the mitotic checkpoint complex. *Nature,* 542**,** 498.

FANG, G. 2002. Checkpoint protein BubR1 acts synergistically with Mad2 to inhibit anaphase-promoting complex. *Molecular biology of the cell,* 13**,** 755-766.

FLETCHER, J. I., MEUSBURGER, S., HAWKINS, C. J., RIGLAR, D. T., LEE, E. F., FAIRLIE, W. D., HUANG, D. C. & ADAMS, J. M. 2008. Apoptosis is triggered when prosurvival Bcl-2 proteins cannot restrain Bax. *Proceedings of the National Academy of Sciences,* 105**,** 18081-18087.

FOLEY, E. A. & KAPOOR, T. M. 2013. Microtubule attachment and spindle assembly checkpoint signalling at the kinetochore. *Nature reviews Molecular cell biology,* 14**,** 25-37.

FURUKAWA, Y., IWASE, S., KIKUCHI, J., TERUI, Y., NAKAMURA, M., YAMADA, H., KANO, Y. & MATSUDA, M. 2000. Phosphorylation of Bcl-2 protein by CDC2 kinase during G2/M phases and its role in cell cycle regulation. *Journal of Biological Chemistry*.

FURUNO, N., DEN ELZEN, N. & PINES, J. 1999. Human cyclin A is required for mitosis until mid prophase. *The Journal of cell biology,* 147**,** 295-306.

GALLUZZI, L. & KROEMER, G. 2007. Mitochondrial apoptosis without VDAC. *Nature cell biology,* 9**,** 487.

GARCÍA-SÁEZ, A. J., MINGARRO, I., PÉREZ-PAYÁ, E. & SALGADO, J. 2004. Membrane-insertion fragments of Bcl-xL, Bax, and Bid. *Biochemistry,* 43**,** 10930-10943.

GASCOIGNE, K. E. & TAYLOR, S. S. 2009. How do anti-mitotic drugs kill cancer cells? *Journal of cell science,* 122**,** 2579-2585.

GAVATHIOTIS, E., REYNA, D. E., DAVIS, M. L., BIRD, G. H. & WALENSKY, L. D. 2010. BH3-triggered structural reorganization drives the activation of proapoptotic BAX. *Molecular cell,* 40**,** 481-492.

GAVET, O. & PINES, J. 2010. Progressive activation of CyclinB1-Cdk1 coordinates entry to mitosis. *Developmental cell,* 18**,** 533-543.

GENG, F., TANG, L., LI, Y., YANG, L., CHOI, K.-S., KAZIM, A. L. & ZHANG, Y. 2011. Allyl isothiocyanate arrests cancer cells in mitosis, and mitotic arrest in turn leads to apoptosis via BCL-2 phosphorylation. *Journal of Biological Chemistry***,** jbc. M111. 278127.

GEULA, S., BEN-HAIL, D. & SHOSHAN-BARMATZ, V. 2012. Structure-based analysis of VDAC1: N-terminus location, translocation, channel gating and association with anti-apoptotic proteins. *Biochemical Journal,* 444**,** 475-485.

GONÇALVES, R. P., BUZHYNSKYY, N., PRIMA, V., STURGIS, J. N. & SCHEURING, S. 2007. Supramolecular assembly of VDAC in native mitochondrial outer membranes. *Journal of molecular biology,* 369**,** 413-418.

GOTOW, T., SHIBATA, M., KANAMORI, S., TOKUNO, O., OHSAWA, Y., SATO, N., ISAHARA, K., YAYOI, Y., WATANABE, T. & LETERRIER, J. 2000. Selective localization of Bcl-2 to the inner mitochondrial and smooth endoplasmic reticulum membranes in mammalian cells. *Cell death and differentiation,* 7**,** 666.

GREEN, D. R. & KROEMER, G. 2004. The pathophysiology of mitochondrial cell death. *science,* 305**,** 626-629.

GROSS, A., MCDONNELL, J. M. & KORSMEYER, S. J. 1999. BCL-2 family members and the mitochondria in apoptosis. *Genes & development,* 13**,** 1899-1911.

GROßE, L., WURM, C. A., BRÜSER, C., NEUMANN, D., JANS, D. C. & JAKOBS, S. 2016. Bax assembles into large ring-like structures remodeling the mitochondrial outer membrane in apoptosis. *The EMBO journal,* 35**,** 402-413.

HALDAR, S., JENA, N. & CROCE, C. M. 1995. Inactivation of Bcl-2 by phosphorylation. *Proceedings of the National Academy of Sciences,* 92**,** 4507-4511.

HALESTRAP, A. P. & BRENNER, C. 2003. The adenine nucleotide translocase: a central component of the mitochondrial permeability transition pore and key player in cell death. *Current medicinal chemistry,* 10**,** 1507-1525.

HALESTRAP, A. P., CLARKE, S. J. & JAVADOV, S. A. 2004. Mitochondrial permeability transition pore opening during myocardial reperfusion—a target for cardioprotection. *Cardiovascular research,* 61**,** 372-385.

HAN, C. R., LEE, J. Y. & KIM, Y. H. 2014. Prometaphase arrest-dependent phosphorylation of Bcl-2 and Bim reduces the association of Bcl-2 with Bak or Bim, provoking Bak activation and mitochondrial apoptosis in nocodazole-treated Jurkat T cells. *Apoptosis,* 19**,** 224-240.

HAN, J. S., HOLLAND, A. J., FACHINETTI, D., KULUKIAN, A., CETIN, B. & CLEVELAND, D. W. 2013. Catalytic assembly of the mitotic checkpoint inhibitor BubR1-Cdc20 by a Mad2-induced functional switch in Cdc20. *Molecular cell,* 51**,** 92-104.

HANAHAN, D. 2000. Robert Weinberg. *The Hallmarks of Cancer Review***,** 57-70.

HARLEY, M. E., ALLAN, L. A., SANDERSON, H. S. & CLARKE, P. R. 2010. Phosphorylation of Mcl-1 by CDK1–cyclin B1 initiates its Cdc20-dependent destruction during mitotic arrest. *The EMBO journal,* 29**,** 2407-2420.

HARTWELL, L. H. & WEINERT, T. A. 1989. Checkpoints: controls that ensure the order of cell cycle events. *Science,* 246**,** 629-634.

HASCHKA, M., KARBON, G., FAVA, L. L. & VILLUNGER, A. 2018. Perturbing mitosis for anti-cancer therapy: is cell death the only answer? *EMBO reports,* 19**,** e45440.

HASCHKA, M. D., SORATROI, C., KIRSCHNEK, S., HÄCKER, G., HILBE, R., GELEY, S., VILLUNGER, A. & FAVA, L. L. 2015. The NOXA-MCL1-BIM axis defines lifespan on extended mitotic arrest. *Nature communications,* 6.

HENGARTNER, M. O. 2000. The biochemistry of apoptosis. *Nature,* 407**,** 770-776.

HIDEHIKOSAWA, T. K., MUKAI, K., ZHANG, W. & SHIKU, H. 2000. Bax overexpression enhances cytochrome c release from mitochondria and sensitizes KATOIII gastric cancer cells to chemotherapeutic agent-induced apoptosis. *International journal of oncology,* 16**,** 745-749.

HINDS, M., SMITS, C., FREDERICKS-SHORT, R., RISK, J., BAILEY, M., HUANG, D. & DAY, C. 2007. Bim, Bad and Bmf: intrinsically unstructured BH3-only proteins that undergo a localized conformational change upon binding to prosurvival Bcl-2 targets. *Cell death and differentiation,* 14**,** 128.

HIRUMA, Y., SACRISTAN, C., PACHIS, S. T., ADAMOPOULOS, A., KUIJT, T., UBBINK, M., VON CASTELMUR, E., PERRAKIS, A. & KOPS, G. J. 2015. Competition between MPS1 and microtubules at kinetochores regulates spindle checkpoint signaling. *Science,* 348**,** 1264-1267.

HOCKINGS, C., ALSOP, A. E., FENNELL, S. C., LEE, E. F., FAIRLIE, W. D., DEWSON, G. & KLUCK, R. M. 2018. Mcl-1 and Bcl-x L sequestration of Bak confers differential resistance to BH3-only proteins. *Cell Death & Differentiation,* 25**,** 719.

HOLMES, F. A., WALTERS, R. S., THERIAULT, R. L., BUZDAR, A. U., FRYE, D. K., HORTOBAGYI, G. N., FORMAN, A. D., NEWTON, L. K. & RABER, M. N. 1991. Phase

II trial of taxol, an active drug in the treatment of metastatic breast cancer. *JNCI: Journal of the National Cancer Institute,* 83**,** 1797-1805.

HONORE, S., PASQUIER, E. & BRAGUER, D. 2005. Understanding microtubule dynamics for improved cancer therapy. *Cell Mol Life Sci,* 62**,** 3039-56.

HOTCHKISS, R. S., STRASSER, A., MCDUNN, J. E. & SWANSON, P. E. 2009. Cell death. *New England Journal of Medicine,* 361**,** 1570-1583.

HOU, Y., ALLAN, L. A. & CLARKE, P. R. 2016. Phosphorylation of XIAP by CDK1-cyclin B controls mitotic cell death. *J Cell Sci***,** jcs. 192310.

HOWELL, B., MCEWEN, B., CANMAN, J., HOFFMAN, D., FARRAR, E., RIEDER, C. & SALMON, E. D. 2001. Cytoplasmic dynein/dynactin drives kinetochore protein transport to the spindle poles and has a role in mitotic spindle checkpoint inactivation. *The Journal of cell biology,* 155**,** 1159-1172.

HSU, Y.-T., WOLTER, K. G. & YOULE, R. J. 1997. Cytosol-to-membrane redistribution of Bax and Bcl-XL during apoptosis. *Proceedings of the National Academy of Sciences,* 94**,** 3668-3672.

HU, B., MITRA, J., VAN DEN HEUVEL, S. & ENDERS, G. H. 2001. S and G2 phase roles for Cdk2 revealed by inducible expression of a dominant-negative mutant in human cells. *Molecular and Cellular Biology,* 21**,** 2755-2766.

HUANG, S., TANG, R. & RANDY, Y. P. 2016. BCL-W is a regulator of microtubule inhibitor-induced mitotic cell death. *Oncotarget,* 7**,** 38718.

HYDBRING, P., MALUMBRES, M. & SICINSKI, P. 2016. Non-canonical functions of cell cycle cyclins and cyclin-dependent kinases. *Nature reviews Molecular cell biology,* 17**,** 280.

ITO, S., TAN, L. J., ANDOH, D., NARITA, T., SEKI, M., HIRANO, Y., NARITA, K., KURAOKA, I., HIRAOKA, Y. & TANAKA, K. 2010. MMXD, a TFIIH-independent XPD-MMS19 protein complex involved in chromosome segregation. *Molecular cell,* 39**,** 632-640.

JACKMAN, M., LINDON, C., NIGG, E. A. & PINES, J. 2003. Active cyclin B1–Cdk1 first appears on centrosomes in prophase. *Nature cell biology,* 5**,** 143.

JACKMAN, M. & PINES, J. 1997. Cyclins and the G2/M transition. *Cancer surveys,* 29**,** 47-73.

JANG, J.-Y., CHOI, Y., JEON, Y.-K. & KIM, C.-W. 2008. Suppression of adenine nucleotide translocase-2 by vector-based siRNA in human breast cancer cells induces apoptosis and inhibits tumor growth in vitro and in vivo. *Breast Cancer Research,* 10**,** R11.

JANG, J.-Y., KIM, Y.-G., NAM, S. J., KEAM, B., KIM, T. M., JEON, Y. K. & KIM, C. W. 2016. Targeting adenine nucleotide translocase-2 (ANT2) to overcome resistance to epidermal growth factor receptor tyrosine kinase inhibitor in non-small cell lung cancer. *Molecular cancer therapeutics***,** molcanther. 0089.2015.

JANSSEN, A., BEERLING, E., MEDEMA, R. & VAN RHEENEN, J. 2013. Intravital FRET imaging of tumor cell viability and mitosis during chemotherapy. *PloS one,* 8**,** e64029.

JEONG, J.-Y., KIM, K.-S., MOON, J.-S., SONG, J.-A., CHOI, S.-H., KIM, K.-I., KIM, T.-H. & AN, H.-J. 2013. Targeted inhibition of phosphatidyl inositol-3-kinase p110β, but not p110α, enhances apoptosis and sensitivity to paclitaxel in chemoresistant ovarian cancers. *Apoptosis,* 18**,** 509-520.

JI, Z., GAO, H. & YU, H. 2015. Kinetochore attachment sensed by competitive Mps1 and microtubule binding to Ndc80C. *Science,* 348**,** 1260-1264.

JORDAN, M. A. & WILSON, L. 2004. Microtubules as a target for anticancer drugs. *Nature Reviews Cancer,* 4**,** 253-265.

JOST, P. J., GRABOW, S., GRAY, D., MCKENZIE, M. D., NACHBUR, U., HUANG, D. C., BOUILLET, P., THOMAS, H. E., BORNER, C. & SILKE, J. 2009. XIAP discriminates between type I and type II FAS-induced apoptosis. *Nature,* 460**,** 1035-1039.

KAELIN JR, W. G. 1999. The p53 gene family. *Oncogene,* 18**,** 7701.

KALE, J., OSTERLUND, E. J. & ANDREWS, D. W. 2018. BCL-2 family proteins: changing partners in the dance towards death. *Cell death and differentiation,* 25**,** 65.

KARCH, J., KWONG, J. Q., BURR, A. R., SARGENT, M. A., ELROD, J. W., PEIXOTO, P. M., MARTINEZ-CABALLERO, S., OSINSKA, H., CHENG, E. H. & ROBBINS, J. 2013. Bax

and Bak function as the outer membrane component of the mitochondrial permeability pore in regulating necrotic cell death in mice. *Elife,* 2**,** e00772.

KAUFMANN, T., TAI, L., EKERT, P. G., HUANG, D. C., NORRIS, F., LINDEMANN, R. K., JOHNSTONE, R. W., DIXIT, V. M. & STRASSER, A. 2007. The BH3-only protein bid is dispensable for DNA damage-and replicative stress-induced apoptosis or cell-cycle arrest. *Cell,* 129**,** 423-433.

KEPP, O., RAJALINGAM, K., KIMMIG, S. & RUDEL, T. 2007. Bak and Bax are non-redundant during infection-and DNA damage-induced apoptosis. *The EMBO journal,* 26**,** 825-834.

KERR, J. F., WYLLIE, A. H. & CURRIE, A. R. 1972. Apoptosis: a basic biological phenomenon with wideranging implications in tissue kinetics. *British journal of cancer,* 26**,** 239.

KIENITZ, A., VOGEL, C., MORALES, I., MÜLLER, R. & BASTIANS, H. 2005. Partial downregulation of MAD1 causes spindle checkpoint inactivation and aneuploidy, but does not confer resistance towards taxol. *Oncogene,* 24**,** 4301-4310.

KIM, H., TU, H.-C., REN, D., TAKEUCHI, O., JEFFERS, J. R., ZAMBETTI, G. P., HSIEH, J. J.-D. & CHENG, E. H.-Y. 2009. Stepwise activation of BAX and BAK by tBID, BIM, and PUMA initiates mitochondrial apoptosis. *Molecular cell,* 36**,** 487-499.

KIMURA, K., CUVIER, O. & HIRANO, T. 2001. Chromosome Condensation by a Human Condensin Complex inXenopus Egg Extracts. *Journal of Biological Chemistry,* 276**,** 5417-5420.

KOJIMA, K., SHIMANUKI, M., SHIKAMI, M., ANDREEFF, M. & NAKAKUMA, H. 2009. Cyclin-dependent kinase 1 inhibitor RO-3306 enhances p53-mediated Bax activation and mitochondrial apoptosis in AML. *Cancer science,* 100**,** 1128-1136.

KOKOSZKA, J. E., WAYMIRE, K. G., LEVY, S. E., SLIGH, J. E., CAI, J., JONES, D. P., MACGREGOR, G. R. & WALLACE, D. C. 2004. The ADP/ATP translocator is not essential for the mitochondrial permeability transition pore. *Nature,* 427**,** 461.

KOLBE, H., COSTELLO, D., WONG, A., LU, R. & WOHLRAB, H. 1984. Mitochondrial phosphate transport. Large scale isolation and characterization of the phosphate

transport protein from beef heart mitochondria. *Journal of Biological Chemistry,* 259**,** 9115-9120.

KOMLODI-PASZTOR, E., SACKETT, D., WILKERSON, J. & FOJO, T. 2011. Mitosis is not a key target of microtubule agents in patient tumors. *Nature reviews Clinical oncology,* 8**,** 244.

KONOPLEVA, M., POLLYEA, D. A., POTLURI, J., CHYLA, B., HOGDAL, L., BUSMAN, T., MCKEEGAN, E., SALEM, A. H., ZHU, M. & RICKER, J. L. 2016. Efficacy and biological correlates of response in a phase II study of venetoclax monotherapy in patients with acute myelogenous leukemia. *Cancer discovery,* 6**,** 1106-1117.

KOPS, G. 2007. The kinetochore and spindle checkpoint in mammals. *Frontiers in bioscience: a journal and virtual library,* 13**,** 3606-3620.

KOPS, G. J., WEAVER, B. A. & CLEVELAND, D. W. 2005. On the road to cancer: aneuploidy and the mitotic checkpoint. *Nature Reviews Cancer,* 5**,** 773-785.

KOREN, I., RAVIV, Z. & SHOSHAN-BARMATZ, V. 2010. Downregulation of voltage-dependent anion channel-1 expression by RNA interference prevents cancer cell growth in vivo. *Cancer biology & therapy,* 9**,** 1046-1052.

KRAMMER, P. H. 2000. CD95's deadly mission in the immune system. *Nature,* 407**,** 789.

KRUISWIJK, F., LABUSCHAGNE, C. F. & VOUSDEN, K. H. 2015. p53 in survival, death and metabolic health: a lifeguard with a licence to kill. *Nature reviews Molecular cell biology,* 16**,** 393.

KUMAR, S., KAUFMAN, J. L., GASPARETTO, C., MIKHAEL, J., VIJ, R., PEGOURIE, B., BENBOUBKER, L., FACON, T., AMIOT, M. & MOREAU, P. 2017. Efficacy of venetoclax as targeted therapy for relapsed/refractory t (11; 14) multiple myeloma. *Blood,* 130**,** 2401-2409.

KUTUK, O. & LETAI, A. 2010. Displacement of Bim by Bmf and Puma rather than increase in Bim level mediates paclitaxel-induced apoptosis in breast cancer cells. *Cell death and differentiation,* 17**,** 1624.

KUWANA, T., BOUCHIER-HAYES, L., CHIPUK, J. E., BONZON, C., SULLIVAN, B. A., GREEN, D. R. & NEWMEYER, D. D. 2005. BH3 domains of BH3-only proteins differentially

regulate Bax-mediated mitochondrial membrane permeabilization both directly and indirectly. *Molecular cell,* 17**,** 525-535.

KVANSAKUL, M., YANG, H., FAIRLIE, W., CZABOTAR, P., FISCHER, S., PERUGINI, M., HUANG, D. & COLMAN, P. 2008. Vaccinia virus anti-apoptotic F1L is a novel Bcl-2-like domain-swapped dimer that binds a highly selective subset of BH3-containing death ligands. *Cell death and differentiation,* 15**,** 1564.

KWONG, J. Q. & MOLKENTIN, J. D. 2015. Physiological and pathological roles of the mitochondrial permeability transition pore in the heart. *Cell metabolism,* 21**,** 206-214.

LACASSE, E. C., BAIRD, S., KORNELUK, R. G. & MACKENZIE, A. E. 1998. The inhibitors of apoptosis (IAPs) and their emerging role in cancer. *Oncogene,* 17**,** 3247.

LARA-GONZALEZ, P., WESTHORPE, F. G. & TAYLOR, S. S. 2012. The spindle assembly checkpoint. *Current Biology,* 22**,** R966-R980.

LAUTERWASSER, J., FIMM-TODT, F. & EDLICH, F. 2019. Assessment of Dynamic BCL-2 Protein Shuttling Between Outer Mitochondrial Membrane and Cytosol. *BCL-2 Family Proteins.* Springer.

LAVRIK, I. & KRAMMER, P. 2012. Regulation of CD95/Fas signaling at the DISC. *Cell death and differentiation,* 19**,** 36.

LEBER, B., LIN, J. & ANDREWS, D. 2010. Still embedded together binding to membranes regulates Bcl-2 protein interactions. *Oncogene,* 29**,** 5221-5230.

LEE, E. F., GRABOW, S., CHAPPAZ, S., DEWSON, G., HOCKINGS, C., KLUCK, R. M., DEBRINCAT, M. A., GRAY, D. H., WITKOWSKI, M. T. & EVANGELISTA, M. 2016. Physiological restraint of Bak by Bcl-xL is essential for cell survival. *Genes & development,* 30**,** 1240-1250.

LEE, M. G. & NURSE, P. 1987. Complementation used to clone a human homologue of the fission yeast cell cycle control gene cdc2. *Nature,* 327**,** 31.

LESAGE, B., QIAN, J. & BOLLEN, M. 2011. Spindle checkpoint silencing: PP1 tips the balance. *Current Biology,* 21**,** R898-R903.

LETAI, A., BASSIK, M. C., WALENSKY, L. D., SORCINELLI, M. D., WEILER, S. & KORSMEYER, S. J. 2002. Distinct BH3 domains either sensitize or activate mitochondrial apoptosis, serving as prototype cancer therapeutics. *Cancer cell,* 2**,** 183-192.

LEUNG, A. W., VARANYUWATANA, P. & HALESTRAP, A. P. 2008. The mitochondrial phosphate carrier interacts with cyclophilin D and may play a key role in the permeability transition. *Journal of Biological Chemistry,* 283**,** 26312-26323.

LI, F., AMBROSINI, G., CHU, E. Y., PLESCIA, J., TOGNIN, S., MARCHISIO, P. C. & ALTIERI, D. C. 1998. Control of apoptosis and mitotic spindle checkpoint by survivin. *Nature,* 396**,** 580.

LI, J., VERHAAR, A. P., PAN, Q., DE KNEGT, R. J. & PEPPELENBOSCH, M. P. 2017. Serum levels of caspase-cleaved cytokeratin 18 (CK18-Asp396) predict severity of liver disease in chronic hepatitis B. *Clinical and experimental gastroenterology,* 10**,** 203.

LI, M. X. & DEWSON, G. 2015. Mitochondria and apoptosis: emerging concepts. *F1000prime reports,* 7.

LI, R., MOUDGIL, T., ROSS, H. J. & HU, H.-M. 2005. Apoptosis of non-small-cell lung cancer cell lines after paclitaxel treatment involves the BH3-only proapoptotic protein Bim. *Cell Death & Differentiation,* 12**,** 292-303.

LINDQVIST, A., VAN ZON, W., ROSENTHAL, C. K. & WOLTHUIS, R. M. 2007. Cyclin B1–Cdk1 activation continues after centrosome separation to control mitotic progression. *PLoS biology,* 5**,** e123.

LISTEN, P., ROY, N., TAMAI, K., LEFEBVRE, C., BAIRD, S., CHERTON-HORVAT, G., FARAHANI, R., MCLEAN, M., MACKENZIE, A. & KORNELUK, R. G. 1996. Suppression of apoptosis in mammalian cells by NAIP and a related family of IAP genes. *Nature,* 379**,** 349.

LIU, G., WANG, Z.-K., WANG, Z.-Y., YANG, D.-B., LIU, Z.-P. & WANG, L. 2016. Mitochondrial permeability transition and its regulatory components are implicated in apoptosis of primary cultures of rat proximal tubular cells exposed to lead. *Archives of toxicology,* 90**,** 1193-1209.

LIU, Q.-Y. & STEIN, C. 1997. Taxol and estramustine-induced modulation of human prostate cancer cell apoptosis via alteration in bcl-xL and bak expression. *Clinical cancer research,* 3**,** 2039-2046.

LOCKSHIN, R. A. & WILLIAMS, C. M. 1965. Programmed cell death—I. Cytology of degeneration in the intersegmental muscles of the Pernyi silkmoth. *Journal of insect physiology,* 11**,** 123-133.

LOPEZ, J. & TAIT, S. 2015. Mitochondrial apoptosis: killing cancer using the enemy within. *British journal of cancer,* 112**,** 957.

LOVELL, J. F., BILLEN, L. P., BINDNER, S., SHAMAS-DIN, A., FRADIN, C., LEBER, B. & ANDREWS, D. W. 2008. Membrane binding by tBid initiates an ordered series of events culminating in membrane permeabilization by Bax. *Cell,* 135**,** 1074-1084.

LUCIAKOVA, K., BARATH, P., POLIAKOVA, D., PERSSON, A. & NELSON, B. D. 2003. Repression of the human ANT2 gene in growth-arrested human diploid cells: the role of nuclear factor 1 (NF-1). *Journal of biological chemistry*.

LUNDBERG, A. S. & WEINBERG, R. A. 1998. Functional inactivation of the retinoblastoma protein requires sequential modification by at least two distinct cyclin-cdk complexes. *Molecular and cellular biology,* 18**,** 753-761.

LUO, X., TANG, Z., XIA, G., WASSMANN, K., MATSUMOTO, T., RIZO, J. & YU, H. 2004. The Mad2 spindle checkpoint protein has two distinct natively folded states. *Nature structural & molecular biology,* 11**,** 338-345.

LUO, X. & YU, H. 2008. Protein metamorphosis: the two-state behavior of Mad2. *Structure,* 16**,** 1616-1625.

MA, S., NGUYEN, T., TAN, I., NINNIS, R., IYER, S., STROUD, D., MENARD, M., KLUCK, R., RYAN, M. & DEWSON, G. 2014. Bax targets mitochondria by distinct mechanisms before or during apoptotic cell death: a requirement for VDAC2 or Bak for efficient Bax apoptotic function. *Cell Death & Differentiation,* 21**,** 1925-1935.

MAC FHEARRAIGH, S. & MC GEE, M. M. 2011. Cyclin B1 interacts with the BH3-only protein Bim and mediates its phosphorylation by Cdk1 during mitosis. *Cell cycle,* 10**,** 3886-3896.

MALDONADO, M. & KAPOOR, T. M. 2011. Constitutive Mad1 targeting to kinetochores uncouples checkpoint signalling from chromosome biorientation. *Nature cell biology,* 13**,** 475-482.

MALIA, T. J. & WAGNER, G. 2007. NMR structural investigation of the mitochondrial outer membrane protein VDAC and its interaction with antiapoptotic Bcl-xL. *Biochemistry,* 46**,** 514-525.

MALUMBRES, M. & BARBACID, M. 2005. Mammalian cyclin-dependent kinases. *Trends in biochemical sciences,* 30**,** 630-641.

MALUMBRES, M. & BARBACID, M. 2009. Cell cycle, CDKs and cancer: a changing paradigm. *Nature reviews cancer,* 9**,** 153.

MALUMBRES, M., HARLOW, E., HUNT, T., HUNTER, T., LAHTI, J. M., MANNING, G., MORGAN, D. O., TSAI, L.-H. & WOLGEMUTH, D. J. 2009. Cyclin-dependent kinases: a family portrait. *Nature cell biology,* 11**,** 1275.

MANCHADO, E., GUILLAMOT, M. & MALUMBRES, M. 2012. Killing cells by targeting mitosis. *Cell death and differentiation,* 19**,** 369.

MANDAL, T., SHIN, S., ALUVILA, S., CHEN, H.-C., GRIEVE, C., CHOE, J.-Y., CHENG, E. H., HUSTEDT, E. J. & OH, K. J. 2016. Assembly of Bak homodimers into higher order homooligomers in the mitochondrial apoptotic pore. *Scientific reports,* 6**,** 30763.

MAPELLI, M., FILIPP, F. V., RANCATI, G., MASSIMILIANO, L., NEZI, L., STIER, G., HAGAN, R. S., CONFALONIERI, S., PIATTI, S. & SATTLER, M. 2006. Determinants of conformational dimerization of Mad2 and its inhibition by p31comet. *The EMBO journal,* 25**,** 1273-1284.

MAPELLI, M., MASSIMILIANO, L., SANTAGUIDA, S. & MUSACCHIO, A. 2007. The Mad2 conformational dimer: structure and implications for the spindle assembly checkpoint. *Cell,* 131**,** 730-743.

MARZO, I., BRENNER, C., ZAMZAMI, N., JÜRGENSMEIER, J. M., SUSIN, S. A., VIEIRA, H. L., PRÉVOST, M.-C., XIE, Z., MATSUYAMA, S. & REED, J. C. 1998. Bax and adenine nucleotide translocator cooperate in the mitochondrial control of apoptosis. *Science,* 281**,** 2027-2031.

MATSON, D. R. & STUKENBERG, P. T. 2011. Spindle poisons and cell fate: a tale of two pathways. *Molecular interventions,* 11**,** 141.

MATTHESS, Y., RAAB, M., SANHAJI, M., LAVRIK, I. N. & STREBHARDT, K. 2010. Cdk1/cyclin B1 controls Fas-mediated apoptosis by regulating caspase-8 activity. *Molecular and cellular biology,* 30**,** 5726-5740.

MCARTHUR, K., WHITEHEAD, L. W., HEDDLESTON, J. M., LI, L., PADMAN, B. S., OORSCHOT, V., GEOGHEGAN, N. D., CHAPPAZ, S., DAVIDSON, S. & SAN CHIN, H. 2018. BAK/BAX macropores facilitate mitochondrial herniation and mtDNA efflux during apoptosis. *Science,* 359**,** eaao6047.

MCCOMMIS, K. S. & BAINES, C. P. 2012. The role of VDAC in cell death: friend or foe? *Biochimica et Biophysica Acta (BBA)-Biomembranes,* 1818**,** 1444-1450.

MCDONNELL, J. M., FUSHMAN, D., MILLIMAN, C. L., KORSMEYER, S. J. & COWBURN, D. 1999. Solution structure of the proapoptotic molecule BID: a structural basis for apoptotic agonists and antagonists. *Cell,* 96**,** 625-634.

MCGOWAN, C. H. & RUSSELL, P. 1993. Human Wee1 kinase inhibits cell division by phosphorylating p34cdc2 exclusively on Tyr15. *The EMBO journal,* 12**,** 75-85.

MCGOWAN, C. H. & RUSSELL, P. 1995. Cell cycle regulation of human WEE1. *The EMBO journal,* 14**,** 2166-2175.

MCGROGAN, B. T., GILMARTIN, B., CARNEY, D. N. & MCCANN, A. 2008. Taxanes, microtubules and chemoresistant breast cancer. *Biochim Biophys Acta,* 1785**,** 96-132.

MCGUIRE, W. P., ROWINSKY, E. K., ROSENSHEIN, N. B., GRUMBINE, F. C., ETTINGER, D. S., ARMSTRONG, D. K. & DONEHOWER, R. C. 1989. Taxol: a unique antineoplastic agent with significant activity in advanced ovarian epithelial neoplasms. *Annals of internal medicine,* 111**,** 273-279.

MEIER, P. & FINCH, A. 2000. Evan. G. *Apoptosis in development. Nature,* 407**,** 796-801.

MERRICK, K. A., WOHLBOLD, L., ZHANG, C., ALLEN, J. J., HORIUCHI, D., HUSKEY, N. E., GOGA, A., SHOKAT, K. M. & FISHER, R. P. 2011. Switching Cdk2 on or off with

small molecules to reveal requirements in human cell proliferation. *Molecular cell,* 42**,** 624-636.

MEYERSON, M., ENDERS, G. H., WU, C.-L., SU, L.-K., GORKA, C., NELSON, C., HARLOW, E. & TSAI, L. 1992. A family of human cdc2-related protein kinases. *The EMBO journal,* 11**,** 2909-2917.

MICHALAK, E., VILLUNGER, A., ERLACHER, M. & STRASSER, A. 2005. Death squads enlisted by the tumour suppressor p53. *Biochemical and biophysical research communications,* 331**,** 786-798.

MIKHAILOV, V., MIKHAILOVA, M., DEGENHARDT, K., VENKATACHALAM, M. A., WHITE, E. & SAIKUMAR, P. 2003. Association of Bax and Bak Homo-oligomers in Mitochondria Bax REQUIREMENT FOR Bak REORGANIZATION AND CYTOCHROMEc RELEASE. *Journal of Biological Chemistry,* 278**,** 5367-5376.

MILLER, A. V., HICKS, M. A., NAKAJIMA, W., RICHARDSON, A. C., WINDLE, J. J. & HARADA, H. 2013. Paclitaxel-induced apoptosis is BAK-dependent, but BAX and BIM-independent in breast tumor. *PloS one,* 8**,** e60685.

MITCHISON, T., EVANS, L., SCHULZE, E. & KIRSCHNER, M. 1986. Sites of microtubule assembly and disassembly in the mitotic spindle. *Cell,* 45**,** 515-527.

MITCHISON, T. J. 2012. The proliferation rate paradox in antimitotic chemotherapy. *Molecular biology of the cell,* 23**,** 1-6.

MITRA, J., ENDERS, G. H., AZIZKHAN-CLIFFORD, J. & LENGEL, K. L. 2006. Dual regulation of the anaphase promoting complex in human cells by cyclin A-Cdk2 and cyclin A-Cdk1 complexes. *Cell Cycle,* 5**,** 662-667.

MOLDOVEANU, T., FOLLIS, A. V., KRIWACKI, R. W. & GREEN, D. R. 2014. Many players in BCL-2 family affairs. *Trends in biochemical sciences,* 39**,** 101-111.

MOLDOVEANU, T., GRACE, C. R., LLAMBI, F., NOURSE, A., FITZGERALD, P., GEHRING, K., KRIWACKI, R. W. & GREEN, D. R. 2013. BID-induced structural changes in BAK promote apoptosis. *Nature structural & molecular biology,* 20**,** 589-597.

MOLLINEDO, F. & GAJATE, C. 2003. Microtubules, microtubule-interfering agents and apoptosis. *Apoptosis,* 8**,** 413-450.

MORALES-CANO, D., CALVINO, E., RUBIO, V., HERRAEZ, A., SANCHO, P., TEJEDOR, M. C. & DIEZ, J. C. 2013. Apoptosis induced by paclitaxel via Bcl-2, Bax and caspases 3 and 9 activation in NB4 human leukaemia cells is not modulated by ERK inhibition. *Exp Toxicol Pathol,* 65**,** 1101-8.

MOUDI, M., GO, R., YIEN, C. Y. S. & NAZRE, M. 2013. Vinca alkaloids. *International journal of preventive medicine,* 4**,** 1231.

MURRAY, A. W. 1994. Cyclin-dependent kinases: regulators of the cell cycle and more. *Chemistry & biology,* 1**,** 191-195.

MURRAY, A. W. 2004. Recycling the cell cycle: cyclins revisited. *Cell,* 116**,** 221-234.

MUSACCHIO, A. 2015. The molecular biology of spindle assembly checkpoint signaling dynamics. *Current biology,* 25**,** R1002-R1018.

MUSACCHIO, A. & SALMON, E. D. 2007. The spindle-assembly checkpoint in space and time. *Nature reviews Molecular cell biology,* 8**,** 379-393.

NAGATA, S. 1997. Apoptosis by death factor. *cell,* 88**,** 355-365.

NAGATA, S. 2018. Apoptosis and clearance of apoptotic cells. *Annual review of immunology,* 36**,** 489-517.

NAGHDI, S., VÁRNAI, P. & HAJNÓCZKY, G. 2015. Motifs of VDAC2 required for mitochondrial Bak import and tBid-induced apoptosis. *Proceedings of the National Academy of Sciences,* 112**,** E5590-E5599.

NASMYTH, K. & HAERING, C. H. 2009. Cohesin: its roles and mechanisms. *Annual review of genetics,* 43**,** 525-558.

NECHUSHTAN, A., SMITH, C. L., LAMENSDORF, I., YOON, S.-H. & YOULE, R. J. 2001. Bax and Bak coalesce into novel mitochondria-associated clusters during apoptosis. *The Journal of cell biology,* 153**,** 1265-1276.

NEUMANN, D., BÜCKERS, J., KASTRUP, L., HELL, S. W. & JAKOBS, S. 2010. Two-color STED microscopy reveals different degrees of colocalization between hexokinase-I and the three human VDAC isoforms. *PMC biophysics,* 3**,** 4.

NEZI, L. & MUSACCHIO, A. 2009. Sister chromatid tension and the spindle assembly checkpoint. *Current opinion in cell biology,* 21**,** 785-795.

NIGG, E. A. 2001. Cell division: mitotic kinases as regulators of cell division and its checkpoints. *Nature reviews Molecular cell biology,* 2**,** 21.

NILSSON, J., YEKEZARE, M., MINSHULL, J. & PINES, J. 2008. The APC/C maintains the spindle assembly checkpoint by targeting Cdc20 for destruction. *Nature cell biology,* 10**,** 1411-1420.

NOGALES, E., WHITTAKER, M., MILLIGAN, R. A. & DOWNING, K. H. 1999. High-resolution model of the microtubule. *Cell,* 96**,** 79-88.

NOGALES, E., WOLF, S. G. & DOWNING, K. H. 1998. Correction: Structure of the αβ tubulin dimer by electron crystallography. *Nature,* 393**,** 191.

NURSE, P. 1990. Universal control mechanism regulating onset of M-phase. *Nature,* 344**,** 503.

NURSE, P. & BISSETT, Y. 1981. Gene required in G1 for commitment to cell cycle and in G2 for control of mitosis in fission yeast. *Nature,* 292**,** 558.

O'NEILL, K. L., HUANG, K., ZHANG, J., CHEN, Y. & LUO, X. 2016. Inactivation of prosurvival Bcl-2 proteins activates Bax/Bak through the outer mitochondrial membrane. *Genes & development*.

O'REILLY, L. A., TAI, L., LEE, L., KRUSE, E. A., GRABOW, S., FAIRLIE, W. D., HAYNES, N. M., TARLINTON, D. M., ZHANG, J.-G. & BELZ, G. T. 2009. Membrane-bound Fas ligand only is essential for Fas-induced apoptosis. *Nature,* 461**,** 659.

OAKES, S. R., VAILLANT, F., LIM, E., LEE, L., BRESLIN, K., FELEPPA, F., DEB, S., RITCHIE, M. E., TAKANO, E. & WARD, T. 2012. Sensitization of BCL-2–expressing breast tumors to chemotherapy by the BH3 mimetic ABT-737. *Proceedings of the National Academy of Sciences,* 109**,** 2766-2771.

OLTERSDORF, T., ELMORE, S. W., SHOEMAKER, A. R., ARMSTRONG, R. C., AUGERI, D. J., BELLI, B. A., BRUNCKO, M., DECKWERTH, T. L., DINGES, J. & HAJDUK, P. J. 2005. An inhibitor of Bcl-2 family proteins induces regression of solid tumours. *Nature,* 435**,** 677.

ORTH, J. D., KOHLER, R. H., FOIJER, F., SORGER, P. K., WEISSLEDER, R. & MITCHISON, T. J. 2011. Analysis of mitosis and antimitotic drug responses in tumors by in vivo microscopy and single-cell pharmacodynamics. *Cancer research,* 71**,** 4608-4616.

ORTH, J. D., LOEWER, A., LAHAV, G. & MITCHISON, T. J. 2012. Prolonged mitotic arrest triggers partial activation of apoptosis, resulting in DNA damage and p53 induction. *Molecular biology of the cell,* 23**,** 567-576.

PALMIERI, F. 2004. The mitochondrial transporter family (SLC25): physiological and pathological implications. *Pflügers Archiv,* 447**,** 689-709.

PANDA, D., MILLER, H. P. & WILSON, L. 2002. Determination of the size and chemical nature of the stabilizing “cap” at microtubule ends using modulators of polymerization dynamics. *Biochemistry,* 41**,** 1609-1617.

PASQUIER, E. & KAVALLARIS, M. 2008. Microtubules: a dynamic target in cancer therapy. *IUBMB life,* 60**,** 165-170.

PEBAY-PEYROULA, E., DAHOUT-GONZALEZ, C., KAHN, R., TRÉZÉGUET, V., LAUQUIN, G. J.-M. & BRANDOLIN, G. 2003. Structure of mitochondrial ADP/ATP carrier in complex with carboxyatractyloside. *Nature,* 426**,** 39.

PINES, J. 2011. Cubism and the cell cycle: the many faces of the APC/C. *Nature reviews Molecular cell biology,* 12**,** 427-438.

PINSKY, B. A., NELSON, C. R. & BIGGINS, S. 2009. Protein phosphatase 1 regulates exit from the spindle checkpoint in budding yeast. *Current Biology,* 19**,** 1182-1187.

POPGEORGIEV, N., JABBOUR, L. & GILLET, G. 2018. Subcellular Localization and Dynamics of the Bcl-2 Family of Proteins. *Frontiers in Cell and Developmental Biology,* 6**,** 13.

RAN, Z., ISRAELSON, A., GARTY, E. S., AZOULAY-ZOHAR, H. & SHOSHAN-BARMATZ, V. 2005. Oligomeric states of the voltage-dependent anion channel and cytochrome c release from mitochondria. *Biochemical Journal,* 386**,** 73-83.

RATHORE, R., MCCALLUM, J. E., VARGHESE, E., FLOREA, A.-M. & BÜSSELBERG, D. 2017. Overcoming chemotherapy drug resistance by targeting inhibitors of apoptosis proteins (IAPs). *Apoptosis,* 22**,** 898-919.

REICHENBACH, F., WIEDENMANN, C., SCHALK, E., BECKER, D., FUNK, K., SCHOLZ-KREISEL, P., TODT, F., WOLLESCHAK, D., DOHNER, K. & MARQUARDT, J. U. 2017. Mitochondrial BAX determines the predisposition to apoptosis in human AML. *Clinical Cancer Research***,** clincanres. 1941.2016.

REN, X., ZHAO, B., CHANG, H., XIAO, M., WU, Y. & LIU, Y. 2018. Paclitaxel suppresses proliferation and induces apoptosis through regulation of ROS and the AKT/MAPK signaling pathway in canine mammary gland tumor cells. *Molecular medicine reports,* 17**,** 8289-8299.

REN, Y., LIU, W., JIANG, H., JIANG, Q. & FENG, J. 2005. Selective vulnerability of dopaminergic neurons to microtubule depolymerization. *Journal of Biological Chemistry*.

RIEDER, C. L., COLE, R. W., KHODJAKOV, A. & SLUDER, G. 1995. The checkpoint delaying anaphase in response to chromosome monoorientation is mediated by an inhibitory signal produced by unattached kinetochores. *The Journal of cell biology,* 130**,** 941-948.

RIEDER, C. L. & MAIATO, H. 2004. Stuck in division or passing through: what happens when cells cannot satisfy the spindle assembly checkpoint. *Developmental cell,* 7**,** 637-651.

RIEDL, S. J. & SALVESEN, G. S. 2007. The apoptosome: signalling platform of cell death. *Nature reviews Molecular cell biology,* 8**,** 405.

RILEY, J. S., QUARATO, G., CLOIX, C., LOPEZ, J., O'PREY, J., PEARSON, M., CHAPMAN, J., SESAKI, H., CARLIN, L. M. & PASSOS, J. F. 2018. Mitochondrial inner membrane permeabilisation enables mtDNA release during apoptosis. *The EMBO journal,* 37**,** e99238.

ROBERTS, A. W., DAVIDS, M. S., PAGEL, J. M., KAHL, B. S., PUVVADA, S. D., GERECITANO, J. F., KIPPS, T. J., ANDERSON, M. A., BROWN, J. R. & GRESSICK, L. 2016. Targeting BCL2 with venetoclax in relapsed chronic lymphocytic leukemia. *New England Journal of Medicine,* 374**,** 311-322.

ROSTOVTSEVA, T. K., ANTONSSON, B., SUZUKI, M., YOULE, R. J., COLOMBINI, M. & BEZRUKOV, S. M. 2004. Bid, but not Bax, regulates VDAC channels. *Journal of Biological Chemistry,* 279**,** 13575-13583.

ROSTOVTSEVA, T. K., KOMAROV, A., BEZRUKOV, S. M. & COLOMBINI, M. 2002. Dynamics of nucleotides in VDAC channels: structure-specific noise generation. *Biophysical journal,* 82**,** 193-205.

ROSTOVTSEVA, T. K., TAN, W. & COLOMBINI, M. 2005. On the role of VDAC in apoptosis: fact and fiction. *Journal of bioenergetics and biomembranes,* 37**,** 129-142.

ROTH, W., WAGENKNECHT, B., GRIMMEL, C., DICHGANS, J. & WELLER, M. 1998. Taxol-mediated augmentation of CD95 ligand-induced apoptosis of human malignant glioma cells: association with bcl-2 phosphorylation but neither activation of p53 nor G2/M cell cycle arrest. *British journal of cancer,* 77**,** 404.

ROTOLO, J. A., MAJ, J. G., FELDMAN, R., REN, D., HAIMOVITZ-FRIEDMAN, A., CORDON-CARDO, C., CHENG, E. H.-Y., KOLESNICK, R. & FUKS, Z. 2008. Bax and Bak do not exhibit functional redundancy in mediating radiation-induced endothelial apoptosis in the intestinal mucosa. *International Journal of Radiation Oncology* Biology* Physics,* 70**,** 804-815.

ROY, M., VOM, A., CZABOTAR, P. & LESSENE, G. 2014. Cell death and the mitochondria: therapeutic targeting of the BCL-2 family-driven pathway. *British journal of pharmacology,* 171**,** 1973-1987.

ROY, N., DEVERAUX, Q. L., TAKAHASHI, R., SALVESEN, G. S. & REED, J. C. 1997. The c-IAP-1 and c-IAP-2 proteins are direct inhibitors of specific caspases. *The EMBO journal,* 16**,** 6914-6925.

ROY, S. S., EHRLICH, A. M., CRAIGEN, W. J. & HAJNÓCZKY, G. 2009. VDAC2 is required for truncated BID-induced mitochondrial apoptosis by recruiting BAK to the mitochondria. *EMBO reports,* 10**,** 1341-1347.

RUDNER, A. D. & MURRAY, A. W. 2000. Phosphorylation by Cdc28 activates the Cdc20-dependent activity of the anaphase-promoting complex. *The Journal of cell biology,* 149**,** 1377-1390.

RUVOLO, P., DENG, X. & MAY, W. 2001. Phosphorylation of Bcl2 and regulation of apoptosis. *Leukemia,* 15**,** 515.

SAKURIKAR, N., EICHHORN, J. M. & CHAMBERS, T. C. 2012. Cyclin dependent kinase-1 (Cdk1)/cyclin B1 dictates cell fate after mitotic arrest via phospho-regulation of anti-apoptotic Bcl-2 proteins. *Journal of Biological Chemistry***,** jbc. M112. 391854.

SALVADOR-GALLEGO, R., MUND, M., COSENTINO, K., SCHNEIDER, J., UNSAY, J., SCHRAERMEYER, U., ENGELHARDT, J., RIES, J. & GARCÍA-SÁEZ, A. J. 2016. Bax assembly into rings and arcs in apoptotic mitochondria is linked to membrane pores. *The EMBO journal,* 35**,** 389-401.

SAN CHIN, H., VAN DELFT, M. F., NINNIS, R. L., MARK, L. X., TAN, I. K., RELJIC, B., SCICLUNA, K., DAGLEY, L. F., SANDOW, J. J. & KELLY, G. L. 2018. BAX requires VDAC2 to mediate apoptosis and to limit tumor development. *bioRxiv***,** 266668.

SANDLER, A., GRAY, R., PERRY, M. C., BRAHMER, J., SCHILLER, J. H., DOWLATI, A., LILENBAUM, R. & JOHNSON, D. H. 2006. Paclitaxel–carboplatin alone or with bevacizumab for non–small-cell lung cancer. *New England Journal of Medicine,* 355**,** 2542-2550.

SANTAGUIDA, S., VERNIERI, C., VILLA, F., CILIBERTO, A. & MUSACCHIO, A. 2011. Evidence that Aurora B is implicated in spindle checkpoint signalling independently of error correction. *The EMBO journal,* 30**,** 1508-1519.

SANTAMARÍA, D., BARRIÈRE, C., CERQUEIRA, A., HUNT, S., TARDY, C., NEWTON, K., CÁCERES, J. F., DUBUS, P., MALUMBRES, M. & BARBACID, M. 2007. Cdk1 is sufficient to drive the mammalian cell cycle. *Nature,* 448**,** 811.

SAURIN, A. T., VAN DER WAAL, M. S., MEDEMA, R. H., LENS, S. M. & KOPS, G. J. 2011. Aurora B potentiates Mps1 activation to ensure rapid checkpoint establishment at the onset of mitosis. *Nature communications,* 2**,** 316.

SCATENA, C. D., STEWART, Z. A., MAYS, D., TANG, L. J., KEEFER, C. J., LEACH, S. D. & PIETENPOL, J. A. 1998. Mitotic phosphorylation of Bcl-2 during normal cell cycle progression and Taxol-induced growth arrest. *Journal of Biological Chemistry,* 273**,** 30777-30784.

SCHELLENBERG, B., WANG, P., KEEBLE, J. A., RODRIGUEZ-ENRIQUEZ, R., WALKER, S., OWENS, T. W., FOSTER, F., TANIANIS-HUGHES, J., BRENNAN, K. & STREULI, C. H. 2013. Bax exists in a dynamic equilibrium between the cytosol and mitochondria to control apoptotic priming. *Molecular cell,* 49**,** 959-971.

SCHIFF, P. & HORWITZ, S. B. 1980. Taxol stabilizes microtubules in mouse fibroblast cells. *Proceedings of the National Academy of Sciences,* 77**,** 1561-1565.

SHEN, S. C., HUANG, T. S., JEE, S. H. & KUO, M. L. 1998. Taxol-induced p34cdc2 kinase activation and apoptosis inhibited by 12-O-tetradecanoylphorbol-13-acetate in human breast MCF-7 carcinoma cells. *Cell growth & differentiation: the molecular biology journal of the American Association for Cancer Research,* 9**,** 23-29.

SHERR, C. J. & ROBERTS, J. M. 1999. CDK inhibitors: positive and negative regulators of G1-phase progression. *Genes & development,* 13**,** 1501-1512.

SHIMIZU, S., IDE, T., YANAGIDA, T. & TSUJIMOTO, Y. 2000a. Electrophysiological study of a novel large pore formed by Bax and the voltage-dependent anion channel that is permeable to cytochrome c. *Journal of Biological Chemistry,* 275**,** 12321-12325.

SHIMIZU, S., KONISHI, A., KODAMA, T. & TSUJIMOTO, Y. 2000b. BH4 domain of antiapoptotic Bcl-2 family members closes voltage-dependent anion channel and inhibits apoptotic mitochondrial changes and cell death. *Proceedings of the National Academy of Sciences,* 97**,** 3100-3105.

SHIMIZU, S., NARITA, M. & TSUJIMOTO, Y. 1999. Bcl-2 family proteins regulate the release of apoptogenic cytochrome c by the mitochondrial channel VDAC. *Nature,* 399**,** 483.

SHIMIZU, S., SHINOHARA, Y. & TSUJIMOTO, Y. 2000c. Bax and Bcl-x L independently regulate apoptotic changes of yeast mitochondria that require VDAC but not adenine nucleotide translocator. *Oncogene,* 19**,** 4309.

SHORE, G. C. 2009. Apoptosis: it's BAK to VDAC. *EMBO reports,* 10**,** 1311-1313.

SIMAMURA, E., SHIMADA, H., HATTA, T. & HIRAI, K.-I. 2008. Mitochondrial voltage-dependent anion channels (VDACs) as novel pharmacological targets for anti-cancer agents. *Journal of bioenergetics and biomembranes,* 40**,** 213-217.

SINGH, P., RATHINASAMY, K., MOHAN, R. & PANDA, D. 2008. Microtubule assembly dynamics: an attractive target for anticancer drugs. *IUBMB Life,* 60**,** 368-75.

SINGH, R., LETAI, A. & SAROSIEK, K. 2019. Regulation of apoptosis in health and disease: the balancing act of BCL-2 family proteins. *Nature Reviews Molecular Cell Biology***,** 1.

SIONOV, R. V. & HAUPT, Y. 1999. The cellular response to p53: the decision between life and death. *Oncogene,* 18**,** 6145.

SLANGY, A., LANE, H. A., D'HÉRIN, P., HARPER, M., KRESS, M. & NIGGT, E. A. 1995. Phosphorylation by p34cdc2 regulates spindle association of human Eg5, a kinesin-related motor essential for bipolar spindle formation in vivo. *Cell,* 83**,** 1159-1169.

SLOSS, O., TOPHAM, C., DIEZ, M. & TAYLOR, S. 2016. Mcl-1 dynamics influence mitotic slippage and death in mitosis. *Oncotarget,* 7**,** 5176.

SNYDER, J. P., NETTLES, J. H., CORNETT, B., DOWNING, K. H. & NOGALES, E. 2001. The binding conformation of Taxol in β-tubulin: a model based on electron crystallographic density. *Proceedings of the National Academy of Sciences,* 98**,** 5312-5316.

STRASSER, A., JOST, P. J. & NAGATA, S. 2009. The many roles of FAS receptor signaling in the immune system. *Immunity,* 30**,** 180-192.

SUBBURAJ, Y., COSENTINO, K., AXMANN, M., PEDRUEZA-VILLALMANZO, E., HERMANN, E., BLEICKEN, S., SPATZ, J. & GARCÍA-SÁEZ, A. J. 2015. Bax monomers form dimer units in the membrane that further self-assemble into multiple oligomeric species. *Nature communications,* 6**,** 8042.

SUDAKIN, V., CHAN, G. K. & YEN, T. J. 2001. Checkpoint inhibition of the APC/C in HeLa cells is mediated by a complex of BUBR1, BUB3, CDC20, and MAD2. *The Journal of cell biology,* 154**,** 925-936.

SUGIYAMA, T., SHIMIZU, S., MATSUOKA, Y., YONEDA, Y. & TSUJIMOTO, Y. 2002. Activation of mitochondrial voltage-dependent anion channel by apro-apoptotic BH3-only protein Bim. *Oncogene,* 21**,** 4944.

SUNDARARAJAN, R., CUCONATI, A., NELSON, D. & WHITE, E. 2001. TNF-alpha induces Bax-Bak interaction and apoptosis which is inhibited by adenovirus E1B 19K. *Journal of Biological Chemistry*.

SUZUKI, M., YOULE, R. J. & TJANDRA, N. 2000. Structure of Bax: coregulation of dimer formation and intracellular localization. *Cell,* 103**,** 645-654.

TAIT, S. W. & GREEN, D. R. 2013. Mitochondrial regulation of cell death. *Cold Spring Harbor perspectives in biology,* 5**,** a008706.

TAJEDDINE, N., GALLUZZI, L., KEPP, O., HANGEN, E., MORSELLI, E., SENOVILLA, L., ARAUJO, N., PINNA, G., LAROCHETTE, N. & ZAMZAMI, N. 2008. Hierarchical involvement of Bak, VDAC1 and Bax in cisplatin-induced cell death. *Oncogene,* 27**,** 4221.

TEICHNER, A., EYTAN, E., SITRY-SHEVAH, D., MINIOWITZ-SHEMTOV, S., DUMIN, E., GROMIS, J. & HERSHKO, A. 2011. p31comet promotes disassembly of the mitotic checkpoint complex in an ATP-dependent process. *Proceedings of the National Academy of Sciences,* 108**,** 3187-3192.

TERRANO, D. T., UPRETI, M. & CHAMBERS, T. C. 2010. Cyclin-dependent kinase 1-mediated Bcl-xL/Bcl-2 phosphorylation acts as a functional link coupling mitotic arrest and apoptosis. *Molecular and cellular biology,* 30**,** 640-656.

TISCHER, J. & GERGELY, F. 2018. Anti-mitotic therapies in cancer. *J Cell Biol***,** jcb. 201808077.

TODT, F., CAKIR, Z., REICHENBACH, F., EMSCHERMANN, F., LAUTERWASSER, J., KAISER, A., ICHIM, G., TAIT, S. W., FRANK, S. & LANGER, H. F. 2015. Differential retrotranslocation of mitochondrial Bax and Bak. *The EMBO journal,* 34**,** 67-80.

TODT, F., CAKIR, Z., REICHENBACH, F., YOULE, R. & EDLICH, F. 2013. The C-terminal helix of Bcl-x L mediates Bax retrotranslocation from the mitochondria. *Cell death and differentiation,* 20**,** 333.

TOPHAM, C., TIGHE, A., LY, P., BENNETT, A., SLOSS, O., NELSON, L., RIDGWAY, R. A., HUELS, D., LITTLER, S., SCHANDL, C., SUN, Y., BECHI, B., PROCTER, D. J., SANSOM, O. J., CLEVELAND, D. W. & TAYLOR, S. S. 2015. MYC Is a Major Determinant of Mitotic Cell Fate. *Cancer Cell,* 28**,** 129-40.

TOPHAM, C. H. & TAYLOR, S. S. 2013. Mitosis and apoptosis: how is the balance set? *Current opinion in cell biology,* 25**,** 780-785.

TSAI, L.-H., HARLOW, E. & MEYERSON, M. 1991. Isolation of the human cdk2 gene that encodes the cyclin A-and adenovirus E1A-associated p33 kinase. *Nature,* 353**,** 174.

TSE, C., SHOEMAKER, A. R., ADICKES, J., ANDERSON, M. G., CHEN, J., JIN, S., JOHNSON, E. F., MARSH, K. C., MITTEN, M. J. & NIMMER, P. 2008. ABT-263: a potent and orally bioavailable Bcl-2 family inhibitor. *Cancer research,* 68**,** 3421-3428.

TUDOR, G., AGUILERA, A., HALVERSON, D., LAING, N. & SAUSVILLE, E. 2000. Susceptibility to drug-induced apoptosis correlates with differential modulation of Bad, Bcl-2 and Bcl-x L protein levels. *Cell Death & Differentiation,* 7.

UBERSAX, J. A., WOODBURY, E. L., QUANG, P. N., PARAZ, M., BLETHROW, J. D., SHAH, K., SHOKAT, K. M. & MORGAN, D. O. 2003. Targets of the cyclin-dependent kinase Cdk1. *Nature,* 425**,** 859.

UPRETI, M., CHU, R., GALITOVSKAYA, E., SMART, S. K. & CHAMBERS, T. C. 2008a. Key role for Bak activation and Bak-Bax interaction in the apoptotic response to vinblastine. *Molecular cancer therapeutics,* 7**,** 2224-2232.

UPRETI, M., GALITOVSKAYA, E. N., CHU, R., TACKETT, A. J., TERRANO, D. T., GRANELL, S. & CHAMBERS, T. C. 2008b. Identification of the major phosphorylation site in Bcl-xL induced by microtubule inhibitors and analysis of its functional significance. *Journal of Biological Chemistry*.

UPRETI, M., LYLE, C. S., SKAUG, B., DU, L. & CHAMBERS, T. C. 2006. Vinblastine-induced apoptosis is mediated by discrete alterations in subcellular location, oligomeric structure, and activation status of specific Bcl-2 family members. *Journal of Biological Chemistry,* 281**,** 15941-15950.

VAILLANT, F., MERINO, D., LEE, L., BRESLIN, K., PAL, B., RITCHIE, M. E., SMYTH, G. K., CHRISTIE, M., PHILLIPSON, L. J. & BURNS, C. J. 2013. Targeting BCL-2 with the BH3 mimetic ABT-199 in estrogen receptor-positive breast cancer. *Cancer cell,* 24**,** 120-129.

VAN DEN HEUVEL, S. & HARLOW, E. 1993. Distinct roles for cyclin-dependent kinases in cell cycle control. *Science,* 262**,** 2050-2054.

VANOOSTHUYSE, V. & HARDWICK, K. G. 2009. A novel protein phosphatase 1-dependent spindle checkpoint silencing mechanism. *Current Biology,* 19**,** 1176-1181.

VASSILEV, L. T., TOVAR, C., CHEN, S., KNEZEVIC, D., ZHAO, X., SUN, H., HEIMBROOK, D. C. & CHEN, L. 2006. Selective small-molecule inhibitor reveals critical mitotic functions of human CDK1. *Proceedings of the National Academy of Sciences,* 103**,** 10660-10665.

VAUX, D. L. & KORSMEYER, S. J. 1999. Cell death in development. *cell,* 96**,** 245-254.

VELA, L. & MARZO, I. 2015. Bcl-2 family of proteins as drug targets for cancer chemotherapy: the long way of BH3 mimetics from bench to bedside. *Current opinion in pharmacology,* 23**,** 74-81.

VERHAGEN, A. M., COULSON, E. J. & VAUX, D. L. 2001. Inhibitor of apoptosis proteins and their relatives: IAPs and other BIRPs. *Genome biology,* 2**,** reviews3009. 1.

WALCZAK, H. 2013. Death receptor–ligand systems in cancer, cell death, and inflammation. *Cold Spring Harbor perspectives in biology,* 5**,** a008698.

WALLACH, D., KANG, T.-B., DILLON, C. P. & GREEN, D. R. 2016. Programmed necrosis in inflammation: Toward identification of the effector molecules. *Science,* 352**,** aaf2154.

WANG, C., WANG, R., ZHOU, K., WANG, S., WANG, J., SHI, H., DOU, Y., YANG, D., CHANG, L. & SHI, X. 2016. JD enhances the anti-tumour effects of low-dose paclitaxel on gastric cancer MKN45 cells both in vitro and in vivo. *Cancer chemotherapy and pharmacology,* 78**,** 971-982.

WANG, C. & YOULE, R. J. 2012. Predominant requirement of Bax for apoptosis in HCT116 cells is determined by Mcl-1's inhibitory effect on Bak. *Oncogene,* 31**,** 3177.

WANG, H., TAKEMOTO, C., AKASAKA, R., UCHIKUBO-KAMO, T., KISHISHITA, S., MURAYAMA, K., TERADA, T., CHEN, L., LIU, Z.-J. & WANG, B.-C. 2009. Novel dimerization mode of the human Bcl-2 family protein Bak, a mitochondrial apoptosis regulator. *Journal of structural biology,* 166**,** 32-37.

WANG, J., BEAUCHEMIN, M. & BERTRAND, R. 2011. Bcl-xL phosphorylation at Ser49 by polo kinase 3 during cell cycle progression and checkpoints. *Cellular signalling,* 23**,** 2030-2038.

WANG, K., GROSS, A., WAKSMAN, G. & KORSMEYER, S. J. 1998. Mutagenesis of the BH3 domain of BAX identifies residues critical for dimerization and killing. *Molecular and cellular biology,* 18**,** 6083-6089.

WANG, T. H., WANG, H. S. & SOONG, Y. K. 2000. Paclitaxel-induced cell death. *Cancer,* 88**,** 2619-2628.

WANG, Z., FAN, M., CANDAS, D., ZHANG, T.-Q., QIN, L., ELDRIDGE, A., WACHSMANN-HOGIU, S., AHMED, K. M., CHROMY, B. A. & NANTAJIT, D. 2014. Cyclin B1/Cdk1 coordinates mitochondrial respiration for cell-cycle G2/M progression. *Developmental cell,* 29**,** 217-232.

WANI, M. C., TAYLOR, H. L., WALL, M. E., COGGON, P. & MCPHAIL, A. T. 1971. Plant antitumor agents. VI. Isolation and structure of taxol, a novel antileukemic and antitumor agent from Taxus brevifolia. *Journal of the American Chemical Society,* 93**,** 2325-2327.

WATANABE, M., IIZUMI, Y., SUKENO, M., IIZUKA-OHASHI, M., SOWA, Y. & SAKAI, T. 2017. The pleiotropic regulation of cyclin D1 by newly identified sesaminol-binding protein ANT2. *Oncogenesis,* 6**,** e311.

WATANABE, Y. 2005. Sister chromatid cohesion along arms and at centromeres. *TRENDS in Genetics,* 21**,** 405-412.

WEAVER, B. A. 2014. How Taxol/paclitaxel kills cancer cells. *Molecular biology of the cell,* 25**,** 2677-2681.

WEI, M. C., ZONG, W.-X., CHENG, E. H.-Y., LINDSTEN, T., PANOUTSAKOPOULOU, V., ROSS, A. J., ROTH, K. A., MACGREGOR, G. R., THOMPSON, C. B. & KORSMEYER, S.

J. 2001. Proapoptotic BAX and BAK: a requisite gateway to mitochondrial dysfunction and death. *Science,* 292**,** 727-730.

WEI, Y., JIN, J. & HARPER, J. W. 2003. The cyclin E/Cdk2 substrate and Cajal body component p220NPAT activates histone transcription through a novel LisH-like domain. *Molecular and cellular biology,* 23**,** 3669-3680.

WERTZ, I. E., KUSAM, S., LAM, C., OKAMOTO, T., SANDOVAL, W., ANDERSON, D. J., HELGASON, E., ERNST, J. A., EBY, M. & LIU, J. 2011. Sensitivity to antitubulin chemotherapeutics is regulated by MCL1 and FBW7. *Nature,* 471**,** 110.

WESTPHAL, D., DEWSON, G., CZABOTAR, P. E. & KLUCK, R. M. 2011. Molecular biology of Bax and Bak activation and action. *Biochim Biophys Acta,* 1813**,** 521-31.

WHITE, M. & MCCUBREY, J. 2001. Suppression of apoptosis: role in cell growth and neoplasia. *Leukemia,* 15**,** 1011.

WILLIS, S. N. & ADAMS, J. M. 2005. Life in the balance: how BH3-only proteins induce apoptosis. *Current opinion in cell biology,* 17**,** 617-625.

WILLIS, S. N., FLETCHER, J. I., KAUFMANN, T., VAN DELFT, M. F., CHEN, L., CZABOTAR, P. E., IERINO, H., LEE, E. F., FAIRLIE, W. D. & BOUILLET, P. 2007. Apoptosis initiated when BH3 ligands engage multiple Bcl-2 homologs, not Bax or Bak. *Science,* 315**,** 856-859.

WOLTER, K. G., HSU, Y.-T., SMITH, C. L., NECHUSHTAN, A., XI, X.-G. & YOULE, R. J. 1997. Movement of Bax from the cytosol to mitochondria during apoptosis. *The Journal of cell biology,* 139**,** 1281-1292.

WU, M., DING, H. F. & FISHER, D. E. 2001. Apoptosis: molecular mechanisms. *eLS*.

XIE, B., WANG, S., JIANG, N. & LI, J. J. 2018. Cyclin B1/CDK1-regulated mitochondrial bioenergetics in cell cycle progression and tumor resistance. *Cancer letters*.

YAMAGATA, H., SHIMIZU, S., NISHIDA, Y., WATANABE, Y., CRAIGEN, W. & TSUJIMOTO, Y. 2009. Requirement of voltage-dependent anion channel 2 for pro-apoptotic activity of Bax. *Oncogene,* 28**,** 3563.

YAMAGUCHI, H., CHEN, J., BHALLA, K. & WANG, H.-G. 2004. Regulation of Bax activation and apoptotic response to microtubule-damaging agents by p53 transcription-

dependent and-independent pathways. *Journal of Biological Chemistry,* 279**,** 39431-39437.

YAMAGUCHI, H., PARANAWITHANA, S. R., LEE, M. W., HUANG, Z., BHALLA, K. N. & WANG, H.-G. 2002. Epothilone B analogue (BMS-247550)-mediated cytotoxicity through induction of Bax conformational change in human breast cancer cells. *Cancer research,* 62**,** 466-471.

YAMAMOTO, K., ICHIJO, H. & KORSMEYER, S. J. 1999. BCL-2 is phosphorylated and inactivated by an ASK1/Jun N-terminal protein kinase pathway normally activated at G2/M. *Molecular and cellular biology,* 19**,** 8469-8478.

YAMAMOTO, T., YAMADA, A., WATANABE, M., YOSHIMURA, Y., YAMAZAKI, N., YOSHIMURA, Y., YAMAUCHI, T., KATAOKA, M., NAGATA, T. & TERADA, H. 2006. VDAC1, Having a Shorter N-Terminus Than VDAC2 but Showing the Same Migration in an SDS− Polyacrylamide Gel, Is the Predominant Form Expressed in Mitochondria of Various Tissues. *Journal of proteome research,* 5**,** 3336-3344.

YANG, M., LI, B., TOMCHICK, D. R., MACHIUS, M., RIZO, J., YU, H. & LUO, X. 2007. p31 comet blocks Mad2 activation through structural mimicry. *Cell,* 131**,** 744-755.

YANG, Z., KENNY, A. E., BRITO, D. A. & RIEDER, C. L. 2009. Cells satisfy the mitotic checkpoint in Taxol, and do so faster in concentrations that stabilize syntelic attachments. *The Journal of cell biology,* 186**,** 675-684.

YANG, Z. Y., JING, G., NING, L., MIN, Q., WANG, S. N. & ZHU, X. L. 2003. Mitosin/CENP-F is a conserved kinetochore protein subjected to cytoplasmic dynein-mediated poleward transport. *Cell research,* 13**,** 275-283.

YOULE, R. J. & STRASSER, A. 2008. The BCL-2 protein family: opposing activities that mediate cell death. *Nature reviews Molecular cell biology,* 9**,** 47-59.

YU, D., JING, T., LIU, B., YAO, J., TAN, M., MCDONNELL, T. J. & HUNG, M.-C. 1998. Overexpression of ErbB2 blocks Taxol-induced apoptosis by upregulation of p21Cip1, which inhibits p34Cdc2 kinase. *Molecular cell,* 2**,** 581-591.

YU, H. 2002. Regulation of APC–Cdc20 by the spindle checkpoint. *Current opinion in cell biology,* 14**,** 706-714.

YU, H. 2006. Structural activation of Mad2 in the mitotic spindle checkpoint: the two-state Mad2 model versus the Mad2 template model. *The Journal of cell biology,* 173**,** 153-157.

YUAN, S., FU, Y., WANG, X., SHI, H., HUANG, Y., SONG, X., LI, L., SONG, N. & LUO, Y. 2008. Voltage-dependent anion channel 1 is involved in endostatin-induced endothelial cell apoptosis. *The FASEB Journal,* 22**,** 2809-2820.

ZAMORA, M., GRANELL, M., MAMPEL, T. & VIÑAS, O. 2004. Adenine nucleotide translocase 3 (ANT3) overexpression induces apoptosis in cultured cells. *FEBS letters,* 563**,** 155-160.

ZAMZAMI, N. & KROEMER, G. 2001. The mitochondrion in apoptosis: how Pandora's box opens. *Nature Reviews Molecular Cell Biology,* 2**,** 67-71.

ZENG, P.-Y., VAKOC, C. R., CHEN, Z.-C., BLOBEL, G. A. & BERGER, S. L. 2006. In vivo dual cross-linking for identification of indirect DNA-associated proteins by chromatin immunoprecipitation. *Biotechniques,* 41**,** 694-698.

ZHANG, D., YANG, R., WANG, S. & DONG, Z. 2014. Paclitaxel: new uses for an old drug. *Drug design, development and therapy,* 8**,** 279.

ZHANG, L., YU, J., PARK, B. H., KINZLER, K. W. & VOGELSTEIN, B. 2000. Role of BAX in the apoptotic response to anticancer agents. *Science,* 290**,** 989-992.

ZHENG, Y., SHI, Y., TIAN, C., JIANG, C., JIN, H., CHEN, J., ALMASAN, A., TANG, H. & CHEN, Q. 2004. Essential role of the voltage-dependent anion channel (VDAC) in mitochondrial permeability transition pore opening and cytochrome c release induced by arsenic trioxide. *Oncogene,* 23**,** 1239.

ZHOU, J. & GIANNAKAKOU, P. 2005. Targeting microtubules for cancer chemotherapy. *Current Medicinal Chemistry-Anti-Cancer Agents,* 5**,** 65-71.

ZHOU, L., CAI, X., HAN, X., XU, N. & CHANG, D. C. 2014. CDK1 switches mitotic arrest to apoptosis by phosphorylating Bcl-2/Bax family proteins during treatment with microtubule interfering agents. *Cell biology international,* 38**,** 737-746.

ZHOU, L. & CHANG, D. C. 2008. Dynamics and structure of the Bax-Bak complex responsible for releasing mitochondrial proteins during apoptosis. *Journal of cell science,* 121**,** 2186-2196.